University of Alberta

The sedimentology and sequence architecture of the Cathedral Bluffs Tongue of the Wasatch Formation, South Pass, Wyoming

by

Luke Patrick McHugh

A thesis submitted to the Faculty of Graduate Studies and Research
in partial fulfillment of the requirements for the degree of

Master of Science

Earth and Atmospheric Sciences

Fall 2012
Edmonton, Alberta

ABSTRACT

The early Eocene (Gardnerbuttean) Cathedral Bluffs Tongue of the Wasatch Formation near South Pass, Wyoming preserves a succession of continental fluvial deposits, which interfinger with lacustrine strata of the Green River Formation in a basinward direction. This thesis focuses on the sedimentology of the Cathedral Bluffs Tongue and identifies the dominant influences on sediment accumulation. Previous studies focused primarily on the regional (basin-scale) lithostratigraphic architecture of Eocene strata in the Green River Basin. Detailed sedimentological analyses of the study interval have not previously been completed. Using whole-rock geochemistry, gamma spectrometry, outcrop description and petrography, fine-scale correlations were made through the study interval. As climate remained constant throughout the ~ 1. 5 million year study interval, and syndepositional structural influences can be demonstrated in the study area, it is shown that movement of the Wind River Thrust Fault, played a dominant role in Early Eocene sediment accumulation at South Pass.

ACKNOWLEDGMENTS.

There are many people that I need to thank. Without all of their help and support, this thesis would not have been possible. There are too many names to mention here, but I thank all of you that have helped me along the way.

Firstly, I would like to thank my parents, Patrick and Anne McHugh for their support and guidance through my whole life. Their support of my education made all those years of school possible. My girlfriend, Grace Miao, for all of her support and, for lack of a better word, nagging that finally enabled me to complete my thesis. Also, to all of my friends and family for being there for me, and helping me in one way or another through my graduate studies.

I would like to thank Gregg Gunnell of Duke University and Bill Bartels of Albion College. Their support of the field seasons and insights into the geology and paleontology of the area were greatly appreciated. Crawling on my hands and knees to find miniscule mammal teeth was actually fun at times.

Murray Gingras and George Pemberton were great resources for me during my years at the University of Alberta. Their geological knowledge and wide range of research interests continually kept me interested and involved with geology.

All of the Ichnology Research Group members also deserve to be thanked. Curtis Lettley, for hiring me as an undergraduate, which eventually led to my graduate studies. Ryan King was a great help in some of the technical points of this thesis, and his editing and commenting on figures was greatly appreciated. Jesse Schoengut was also a great help in the field, rushing to get gamma readings on a butte as a thunderstorm was rolling in or digging trenches like an animal. Also my field assistant, Bryce Wetthuhn who was with me for the long haul during the 2010 field season. He tolerated long days and bumpy rides in the field, without his help, this much data would not have been collected. There are too many names to mention, but all the good times in the lab, Tim's runs, and extra-curricular activities were fond memories of mine at the U of A.

Lastly, my supervisor, John-Paul Zonneveld. I can not express enough my thanks to JP for his support and the opportunities he allowed me to have. One of the greatest experiences of my time at the U of A was all the conferences and field work I was able to be part of, all due to JP's wide-range of research and support of his students. Trips to the mountains in NE B.C. or walking on the sand flats in Parksville, there was never a dull moment.

TABLE OF CONTENTS

LIST OF TABLES

TABLE **PAGE**

LIST OF FIGURES

FIGURE **PAGE**

Chapter 1

Chapter 2

Chapter 3

LIST OF ABBREVIATIONS

Stratigraphy
LST – Lowstand Systems Tract
TST – Transgressive Systems Tract
HST – Highstand Systems Tract
LSE – Lowstand Surface of Erosion
ITS – Initial Transgressive Surface
MLFS – Maximum Lacustrine Flooding Surface
SPS-1 – South Pass Sequence 1
SPS-2 – South Pass Sequence 2
SPS-3 – South Pass Sequence 3
SPS-4 – South Pass Sequence 4
SPS-5 – South Pass Sequence 5
SPS-6 – South Pass Sequence 6
SPS-7 – South Pass Sequence 7

Minerals
Qtz – Quartz
Afs – Alkali Feldspar
Rf – Rock Fragment
Cal – Calcite
Grt – Garnet
Ms – Muscovite
Ep - Epidote
Chl - Chlorite
Ser - Sericite

Facies
Gmh – Massive to crude horizontally bedded gravel conglomerate
Gt – Trough-cross bedded gravel conglomerate
Sp – Planar-cross bedded sandstone
St – Trough-cross bedded sandstone
Shr – Horizontal bedded to ripple-cross bedded sandstone
Lm – Carbonate mudstone / micrite
Fsh – Organic shale
P1 – Light grey / green mudstone, siltstone, and sandstone
P2 – Dark grey / black mudstone and siltstone
P3 – Red / orange mudstone, siltstone, and sandstone
FA1 – Facies Association 1
FA2 – Facies Association 2
FA3 – Facies Association 3
FA4 – Facies Association 4
FA5 – Facies Association 5

Other
NALMA – North American Land Mammal Ages
COCORP – Consortium for Continental Reflection Profiling
SGR – Spectral-gamma Ray
ICP-MS – Inductively Coupled Plasma Mass Spectrometry
PCA – Principle Component Analysis

<u>Chapter 1</u>

Introduction

1.1. Introduction

The Green River Basin of southwestern Wyoming (Fig. 1.1) records nearly continuous deposition of a continental succession of lacustrine and fluvial sediments deposited during the Eocene (Roehler, 1992a). The Basin fill is a combination of mudstone, siltstone, sandstone, conglomerate, cyanobacterial limestone, bioclastic limestone, evaporite, oil shale, and paleosol units (Zeller and Stephens, 1969). Lacustrine deposits occur throughout the basin while fluvial deposits occur primarily on the basin margins. Lacustrine and fluvial deposits intertongue extensively reflecting numerous fluctuations in the level of the Green River lake system (Roehler, 1992a). Fluctuations in lake level are attributed to tectonic and climatic influences during the early Eocene (Carroll and Bohacs, 1999; Zonneveld *et al.*, 2003). Deposition occurred in and around Paleolake Gosiute, which was a large, shallow lake that covered most of the Greater Green River Basin during its maximum extent (Roehler, 1991a; Zonneveld *et al.,* 2003). With the identification the Godiva Rim Member by Roehler (1991b), there is evidence that during highstand conditions Lake Gosiute connected with Lake Uinta around the eastern margin of the Uinta Mountains, southwest of the study area. The interval of interest for this study consists of the Wasatch and Green River Formations. Each formation contains many different members, tongues, and beds depending on the timing and location of deposition.

The Cathedral Bluffs Tongue of the Wasatch Formation near South Pass, Wyoming is the focus of this study (Fig. 1.2). The Cathedral Bluffs is stratigraphically bound by members of the Green River Formation, with the Tipton Tongue below and the Laney Member above (Roehler 1992a, Pietras and Carroll, 2006). This fluvial tongue also grades basinward into the lacustrine / marginal lacustrine Wilkins Peak member of the Green River

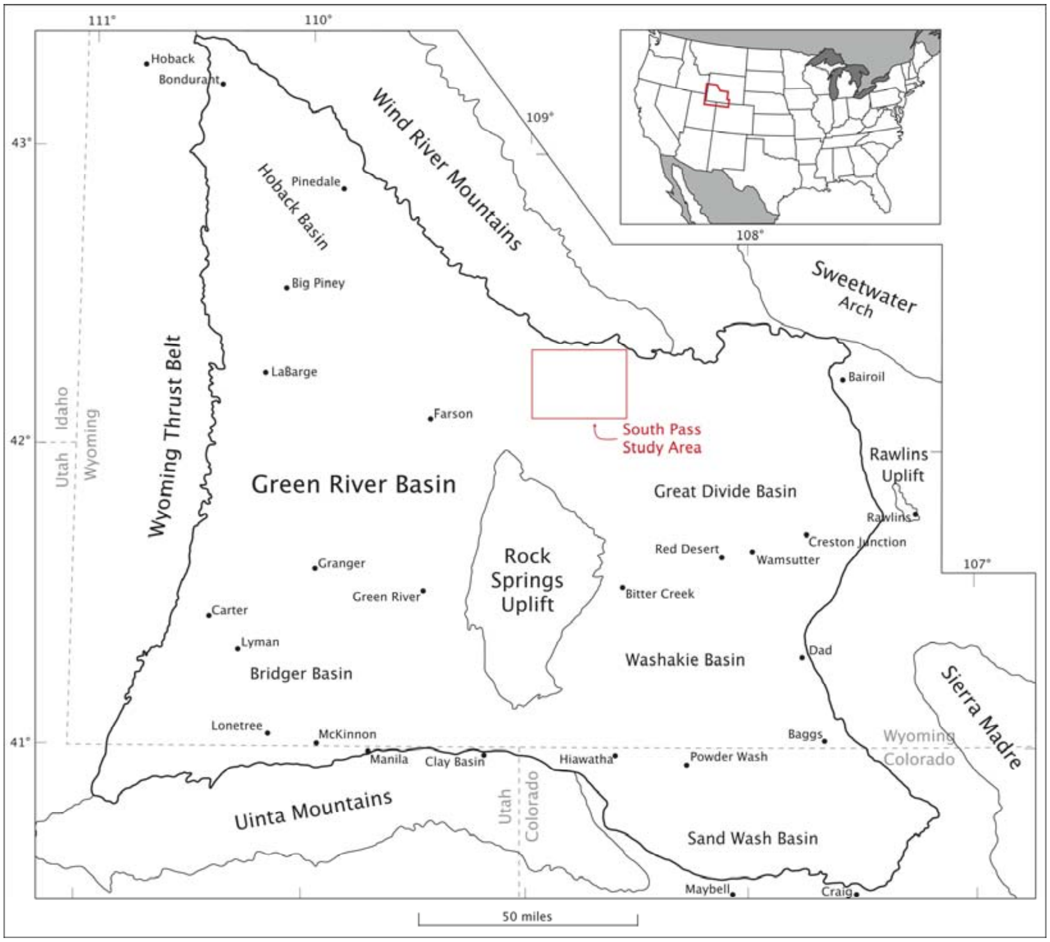

Figure 1.1 – Map of the Green River Basin showing the major structural elements and the location of the South Pass study area on the northern margin.

Formation (Roehler, 1992b; Pietras and Carroll, 2006). The succession exhibits rapid lateral facies changes, sudden thickness variation, and intraformational unconformities (Roehler, 1992a), which can complicate correlation of lithostratigraphic units over short distances. To aid in the correlation of this unit, a variety of methods were used. Detailed facies, thin section, and geochemical analyses along with spectral gamma ray data are utilized to assist with lithologic correlations.

1.2. Geologic Setting

1.2.1. Tectonic Setting

Thrusting was one of the major tectonic processes during the Eocene and contributed to the creation of accommodation space in the Green River Basin due to flexural subsidence (Hall and Chase, 1989; Steidtmann and Middleton, 1991; Johnson and Andersen, 2009). Horizontal compressional forces on the lithosphere led to the development of Laramide-style basins in the continental United States (Brown, 1988; Bird, 1998; Johnson and Andersen, 2009). Understanding of the structure within the Wind River Mountains was helped immensely by study of the COCORP Wind River seismic data (Smithson *et al.*, 1978; Brewer *et al.*, 1980; Lynn *et al.*, 1983). Uplift of the Wind River Mountain Range began ca. 90 Ma, as a positive feature on the sea floor in the Early Cretaceous (Steidtmann and Middleton, 1991). The Laramide orogeny was not a single event. Tectonism occurred intermittently, with thrust faults causing uplift and concomitant subsidence in the basin depocenter, over a period of 30-million years (Roehler, 1992a). Erosion became substantial in the Late Cretaceous and as much as 8 km of sedimentary rocks were shed from the mountains (Steidtmann and Middleton, 1991). Clastic aprons were deposited during the Eocene, as the Wind River Mountains were uplifted and the basement-core of the range was exposed by the early Eocene (Roehler, 1992a; Carroll *et al.*, 2006). Erosion continued to the point where the peaks were nearly buried by their own eroded sediment (Steidtmann and Middleton, 1991). The Laney Member of the Green River Formation is the oldest unit that is not deformed over the Wind River Thrust Fault, indicating that the last movement on the fault occurred before it was deposited, approximately 49 to 50 Ma (Steidtmann and Middleton, 1991).

The Wind River Mountain Range bounds the Green River Basin to the north. The Wyoming Overthrust Belt is to the west, the Uinta Mountains are to the south, and there are a series of uplifts to the east. These uplifts are all part of the Sevier and Laramide orogenies that divided the continental basins of United States during the Paleocene (Dickinson *et al.*, 1988; Carroll *et al.*,

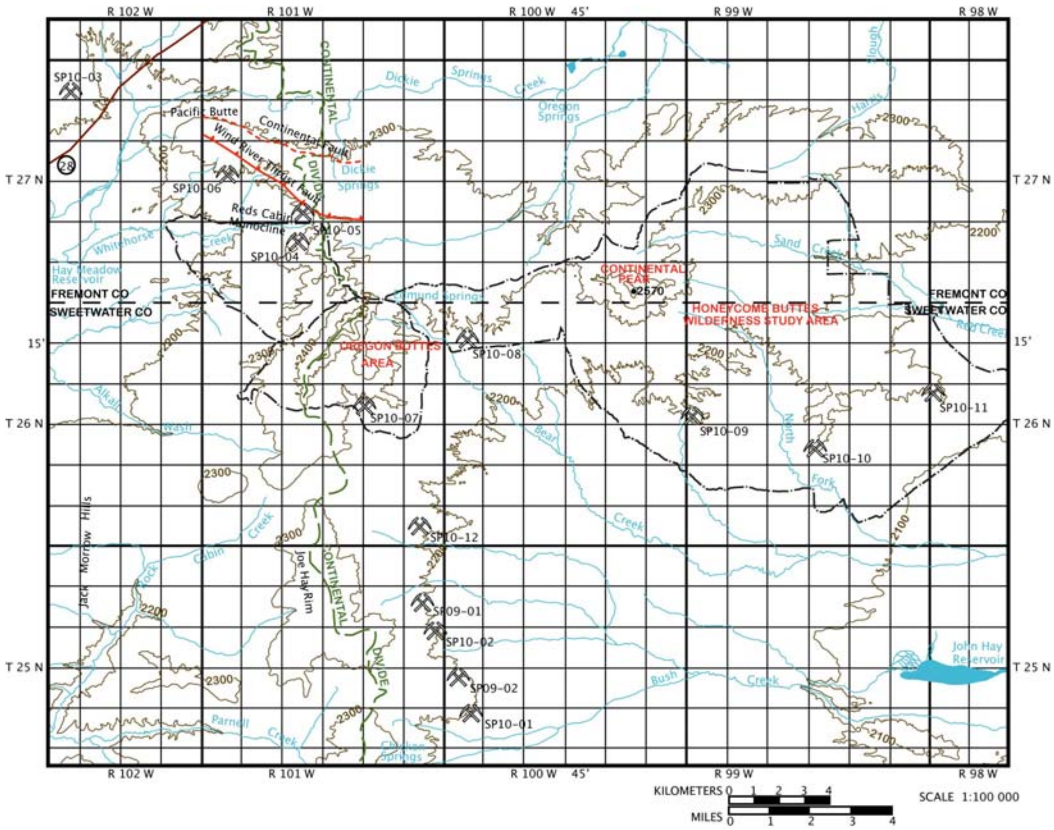

Figure 1.2 – Map of the South Pass Study Area showing major structural elements and the locations of the measured sections.

2006). Structural elements within the basin have led to a series of sub-basins. The largest structural element in the basin, the Rock Springs Uplift, occurs near the center of the basin and divides it into the Bridger Basin to the west and the Great Divide, Washakie, and Sand Wash Basins to the east (Roehler, 1992a). The Great Divide Basin occurs in the northeast corner of the Green River Basin and is separated from the Washakie Basin by the Wamsutter Arch (Roehler, 1992a). Further south, the Cherokee Ridge Anticline partitions the Sand Wash Basin from the Washakie Basin.

In the north, the Green River Basin was formed as a flexural response to the uplift of the Wind River Mountains (Shuster and Steidtmann, 1988; Steidtmann and Middleton, 1991) and the Uinta uplift was responsible for subsidence in the southern part of the basin (Johnson and Andersen, 2009). Also, subsidence on the western margin of the basin was a result of displacement on the Wyoming Overthrust Belt (Clyde *et al.,* 2001). Tectonism during the Eocene played an important role in the deposition of the Wasatch, Green River, and Bridger Formations. Tectonic activity in the area was a result of the interaction of two separate processes. The thin-skinned Sevier Orogeny and the basement involved Laramide Orogeny resulted from the compressional stresses on the interior of the United States (Keighley *et al.*, 2003).

Other structural components of the basin must also be studied to obtain a complete understanding of the tectonics. Reds Cabin Monocline and the Continental Fault are two of the important structural features within the study area. Reds Cabin Monocline is actually an asymmetrical anticline that lies over the trace of the Wind River Thrust Fault, and indicates movement on the fault (Steidtmann and Middleton, 1991; Pietras *et al.*, 2003). The Continental Fault occurs on the northeastern margin of the basin and was an uplifted reverse fault during the Eocene (Steidtmann and Middleton, 1991; Pietras *et al.,* 2003). Since then, the fault has undergone normal movement as the southern end of the Wind River Mountains has collapsed (Zeller and Stephens, 1969; McGee, 1983; Steidtmann and Middleton, 1991).

1.2.2. Regional Stratigraphy

Main Body of the Wasatch Formation

The early Eocene Main Body of the Wasatch Formation is a thick (300-900 m) fluvial unit composed dominantly of variegated lenticular sandstone and grey / green mudstone of floodplain origin (Zeller and Stephens, 1969; Roehler, 1992b). The Main Body is separated from the Cathedral Bluffs Tongue by the Tipton Tongue of the Green River Formation (Fig. 1.3). On the basin margins, where the Tipton Tongue is absent, the Main Body and Cathedral Bluffs Tongue are undifferentiated (Zeller and Stephens, 1969).

Cathedral Bluffs Tongue of the Wasatch Formation

The Cathedral Bluffs Tongue of the Wasatch Formation is the focus of this study. It ranges in thickness from 30 to 200 m in the study area (Zeller and Stephens, 1969; Steidtmann and Middleton, 1991; Roehler, 1992b). The tongue consists of red (oxidized) and green / grey, variegated floodplain mudstone and channel sandstone in the northern part of the basin, grading basinward into darker grey to green (reduced) mudstone with thin beds of oil shale and limestone (Roehler, 1992b). Sandstone units are often calcareous and are poorly sorted and cemented with a grey / green to brown colour (West, 1969). In northernmost outcrop sections, coarse pebble to cobble conglomerate beds occur within a dominantly fine-grained sandstone succession. The Cathedral Bluffs sedimentary succession gets coarser to the north of the study area, indicating a closer proximity to the source of the sediment.

Paleosols are common in the Cathedral Bluffs Tongue and can be identified by their fine-grained nature and pedogenic slickensides. These paleosols were likely developed on the floodplain or overbank region of the fluvial system. Bown and Kraus (1987) worked extensively with paleosols of the Willwood Formation in the Bighorn Basin of northwestern Wyoming. These deposits are similar to the Wasatch Formation. Distinctive colour banding is seen due to the differential concentration and hydration or dehydration of ferric iron compounds (Bown and Kraus, 1987). Purple, maroon, red, pink, green, and grey mudstone packages are observed in outcrop and their colour can be useful to distinguish different soil profiles and identify the extent of pedogenesis. Proximity of the mudstone to the fluvial channel is a major controlling factor in the extent of maturation of the paleosol (Bown and Kraus, 1987). The most mature soils occur farthest away from the channel due to a very slow and periodic sedimentation rate (Bown and Kraus, 1987; Kraus, 1999; Daniels, 2003). Sudden deposition on the floodplain due to a crevasse splay or other flooding event may interrupt soil development and leave the mudstone less altered (Aslan and Autin, 1999).

The relationship between proximity to the channel and soil maturation may partly account for rapid lateral facies changes observed within the Wasatch Formation.

Tipton Tongue of the Green River Formation

The Tipton Shale Member was named by Schultz (1920), and later renamed the Tipton Shale Tongue (Sears and Bradley, 1924) where it is overlain by the Cathedral Bluffs Tongue (Roehler, 1991a). This lacustrine tongue consists of 60 to 75 m of shale, conglomerate, oolitic limestone, claystone, and sandstone (Roehler, 1991a). Two parts of the Tipton Shale Member were identified (Pipiringos, 1961; Bradley, 1969; Roehler, 1991a). The lower unit, designated the Tipton Shale Member, was deposited in freshwater lake and contains abundant shells of *Goniobasis* (Roehler, 1991a). This lower member includes two packages; the freshwater Scheggs Bed (Roehler, 1991a) and the upper saline part of the Tipton Shale, named the Fife Bed (Roehler, 1991a). The upper unit was deposited in a saline lake and named the Wilkins Peak Member of the Green River Formation by Bradley (1969).

The Farson Sandstone Member separates the Scheggs and Fife Beds in the northwest portion of the Green River Basin (Roehler, 1991a; Roehler, 1991b), thinning to the east and to the south. This member is a coarse clastic tongue composed of fine- to coarse-grained sandstone with lenses of conglomerate interpreted as a freshwater, lacustrine delta deposit (Roehler, 1991a). The geometry of this unit indicates that sediments within the Farson Sandstone are derived from the Wind River Mountains to the north (Roehler, 1991a). In the South Pass study area, the Scheggs Bed underlies the Farson Sandstone, but the upper contact of the Farson Sandstone is unconformable with the overlying Cathedral Bluffs Tongue. This unconformity does not reflect the regional stratigraphy of the Green River Basin, but rather it is a local tectonic event which produced Reds Cabin Monocline.

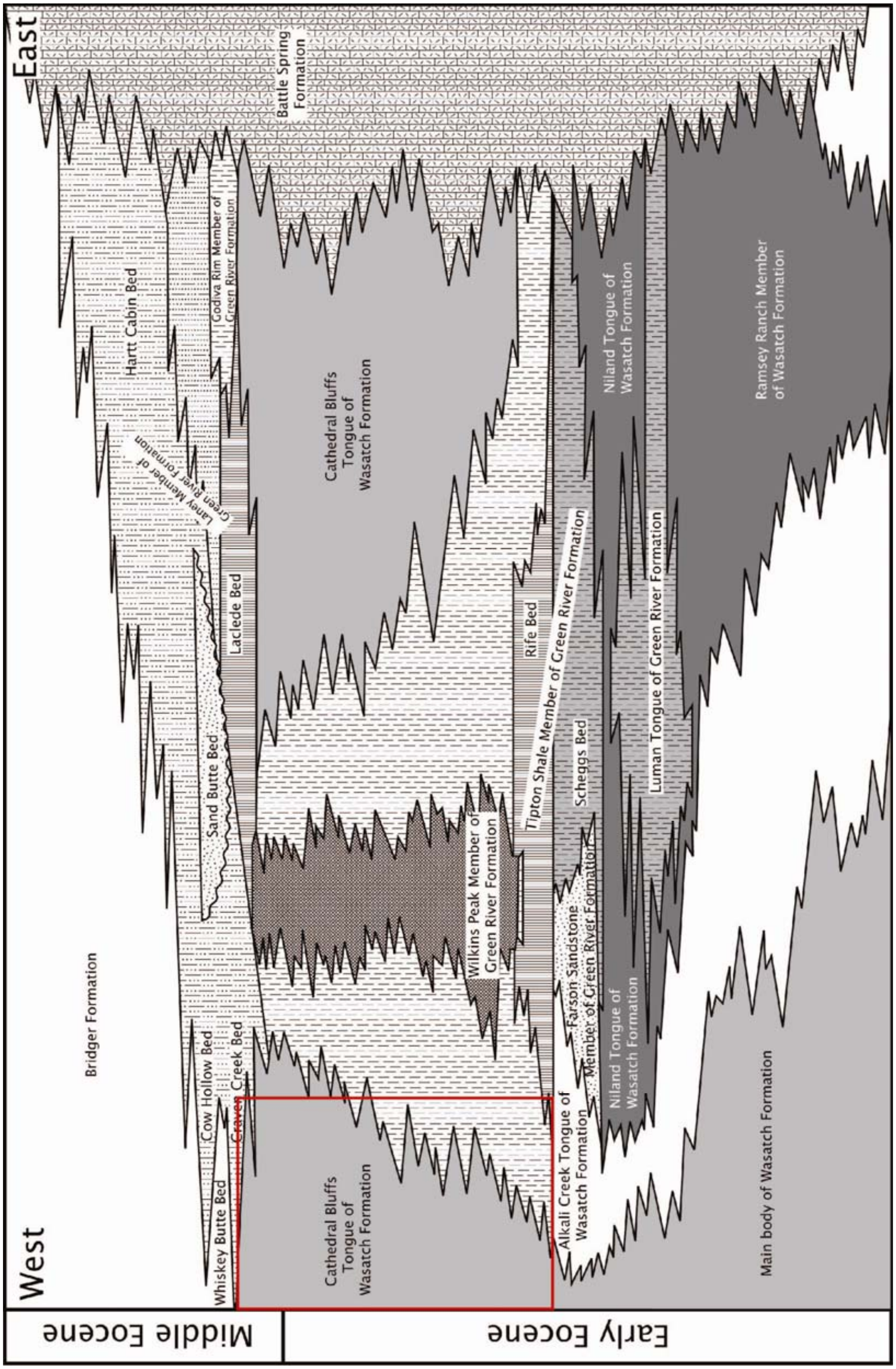

Figure 1.3 – Regional stratigraphy across the Green River Basin from west to east. Modified from Roehler, 1992b. The study interval is highlighted by a red box.

Laney Member of the Green River Formation

The Laney Member can be divided into three units; the LaClede, Hartt Cabin, and Sand Butte Beds (Roehler, 1992b). The Laney Member in the South Pass study area is undifferentiated (Roehler, 1992b) and is composed of basal ostracodal sandstone unit overlain by lacustrine oil shale. Paper shale, limestone, siltstone, and fine-grained sandstone all occur within the Laney Member, which can be more that 69 m thick in the study area (Zeller and Stephens, 1969). The Laney Member caps the study interval conformably, as Cathedral Bluffs Tongue floodplain mud grades upwards into lacustrine margin mudstone and finally grades into Laney Member shale (Zeller and Stephens, 1969). The Laney Member represents the final highstand of Lake Gosiute (Bradley, 1964; Chetel and Carroll, 2010).

1.2.3. Climate and Fauna

The early Eocene was the warmest interval of the Cenozoic (Zachos *et al.*, 1994; Wilf, 2000). The latest Wasatchian and earliest Bridgerian had an intermittently hot and arid to warm temperate climate (Wilf, 2000). The climate in the Green River Basin during the Eocene affected deposition within the basin (Carroll and Bohacs, 1999). According to Carroll and Bohacs (1999), climate mostly controls the sedimentation and water supply rates, and only accounts for small fluctuations in lake level. The authors contend that climate has a subordinate effect on lake deposition to the tectonic influence on the character of the lake sediments. It has also been proposed that Milankovitch cycles that cause climatic changes may account for significant rises and falls in lake level (Keighley *et al.*, 2003), although, this is difficult to demonstrate in the rock record. One problem identifying changes related to climate is that climatic changes may be rapid in comparison to the time required for deposition (Pietras and Carroll, 2006).

The Wasatch Formation contains many mammal, reptile, and bird fossils (Roehler, 1991a; Bartels *et al.,* 2011). The fossil fauna and flora suite is one of the richest assemblages of any other Eocene rocks in the world (Roehler, 1991a). The most common fossils found in the study area are turtle carapace and plastron fragments, but rare mammal fossils are important in the area (Bartels *et al.,* 2011). North American Land Mammal Ages (NALMAs, Fig. 1.4) are used to correlate faunas of similar age across North America (Woodburne, 1987). The Eocene deposits in this area belong to the two earliest Eocene NALMAs, the Wasatchian and Bridgerian (Clyde *et al*., 2001; Zonneveld *et al*., 2003). Due to a diverse mammalian assemblage, many of which have limited biostratigraphic ranges, subdivision of NALMAs into local faunas is possible (Zonneveld *et al.*, 2003). The Cathedral Bluffs Tongue within the study area was deposited during the Gardnerbuttean (BR1a), the first sub-age of the Bridgerian NALMA (Gunnell *et al.,* 2009; Gunnell, pers. comm., 2012).

1.3. Previous Work

The first explorers entered the Green River Basin in the early 1800's and noted the abundance fossils and coal (Roehler, 1992a). Later, in 1867, the discovery of gold on the southeastern end of the Wind River Mountain Range started a gold rush near South Pass, Wyoming (Chadey, 1973; Roehler, 1992a), bringing many people to the area. The first geologic maps were produced by Powell (1876), Hague and Emmons (1877), and King (1878) after the discovery of fossil mammals (Leidy, 1873; Marsh, 1876), fish (Hayden, 1971), and dinosaurs (Cope, 1872) elevated interest in the area. Although the study of the fossils of the Green River Basin began in the mid- to late-1800's, the first geologic study was done by Schultz in 1920 (Roehler, 1992a).

Hayden (1869) named the Wasatch, Green River, and Bridger Formations. Since their inception, there have been many revisions to these

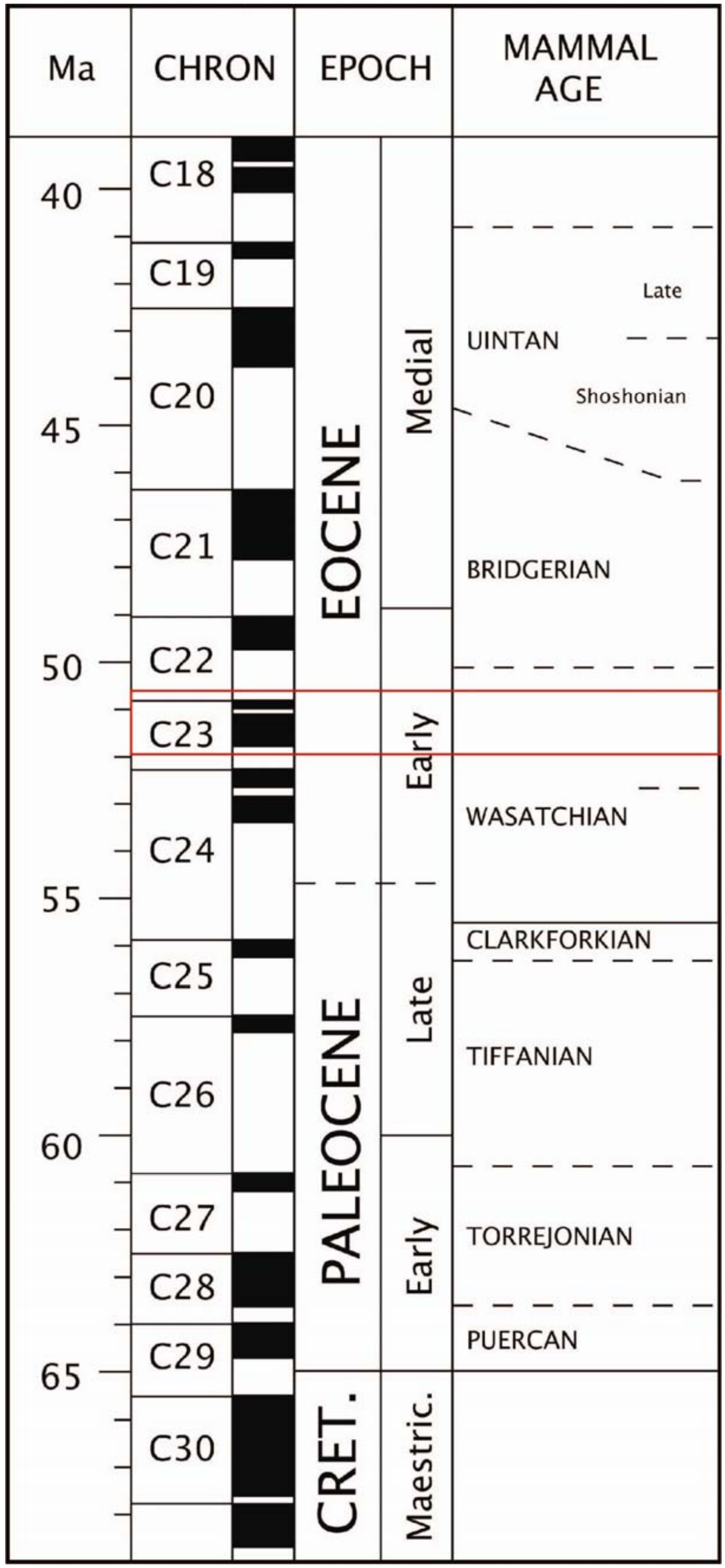

Ma
CHRON
EPOCH
MAMMAL AGE
40
45
50
55
60
65
C18
C19
C20
C21
C22
C23
C24
C25
C26
C27
C28
C29
C30
EOCENE
Medial
Early
PALEOCENE
Late
Early
CRET.
Maestric.
Late
UINTAN
Shoshonian
BRIDGERIAN
WASATCHIAN
CLARKFORKIAN
TIFFANIAN
TORREJONIAN
PUERCAN

Figure 1.4 – The North American Land Mammal Ages for the Paleocene and early Eocene (Modified from Woodburne and Swisher, 1995). Note that this chart places the study interval in chron C22. Recent data, published by Clyde *et al.,* 2001, indicate that the magnetostratigraphic scale in the study interval indicate that this chart should be shifted, extending the Wasatchian-Bridgerian boundary to the C23R-C23N contact and placing the study interval entirely in chron C23.

intertongued units. Several members, tongues, and beds have been named, abandoned, renamed, and revised. It was even suggested that the Green River and Wasatch Formations should be elevated to Group status to accommodate all the different subdivisions (Roehler, 1992a). Schultz (1920) originally assigned the name Cathedral Bluffs Red Bed Member to the variegated red and grey fluvial deposits between the Tipton Shale and Laney Member of the Green River Formation. The Cathedral Bluffs Red Beds Member was later correctly renamed the Cathedral Bluffs Tongue of the Wasatch Formation (Sears and Bradley, 1924; Roehler, 1991a). Through time, there have been many names for the Cathedral Bluffs Tongue and its stratigraphic equivalents throughout the Green River Basin (Roehler, 1991a). Previous designations include the New Fork Tongue (Donavan, 1950), the Upper Tongue (Oriel, 1963; Lawrence, 1963), and the Desertion Point Tongue (Sullivan, 1980). Roehler (1991a) demonstrated that these tongues are all stratigraphically equivalent and part of the Cathedral Bluffs of Schultz (1920).

More recent studies within the Green River Basin have focused on alternative means of correlation across the basin, such as magnetostratigraphy (Clyde, *et al*., 2001), sequence stratigraphy (Zonneveld *et al*., 2003) and biostratigraphy (Gunnell and Yarborough, 2000, Gunnell *et al.*, 2004). Zonneveld *et al.* (2003) focused on a sequence stratigraphic study of the western margin of the basin, near the Little Muddy area of southwestern Wyoming. Determining the phases of the Green River lakes systems has also been the object of much recent study (Carroll and Bohacs, 1999; Smith *et al.*, 2008; Chetel and Carroll, 2010).

1.4. Objectives

A study from a sedimentological standpoint of fluvial and lacustrine strata in the Cathedral Bluffs Tongue in the South Pass area has not previously been undertaken. This thesis seeks to characterize the record of deposition within the context of the fundamental controls on sediment deposition, accumulation and preservation. The comparative effects of tectonic activity and climate on sediment accumulation in the study area are assessed. Division of the Cathedral Bluffs Tongue into sequence stratigraphic, chemostratigraphic, and sedimentological units will facilitate linking the sedimentological evidence to the factors affecting deposition at the time.

1.5. Methods

This study is based on the fieldwork conducted near South Pass, Wyoming in the summer of 2009 and 2010. Fourteen outcrop sections were measured near Oregon Buttes, Continental Peak, and Bush Rim. The base of the Cathedral Bluffs Tongue is very rarely observed in the study area, only in the vicinity of Reds Cabin Monocline where the underlying Farson Sandstone Member outcrops. The upper contact with the Laney occurs near the top of the buttes; however, it is generally recessive and therefore difficult to properly observe. Measured sections were oriented in an approximately NNE to SSW line; approximately sub-parallel to depositional dip of the Cathedral Bluffs Tongue. Detailed outcrop strip logs were constructed at a 1cm = 1m scale including descriptions of the colour, thickness, grain size, sedimentary structures, biogenic structures, and fossils observed in each bed. Beds were measured using a Jacobs Staff, as well as a folding ruler for more precise measurements. The detailed strip logs are presented in Appendix A.

Spectral gamma ray measurements were taken on six of the fourteen sections, all in 2010. Measurements were taken using a hand-held RS-230 BGO Super-SPEC gamma ray scintillometer. Readings were taken at an interval of 0.5 m through the entirety of the section. Each sample was measured for 120 seconds to get a good average value for that bed. Assay readings were taken every 5 readings (2.5m) to aid in correlating the results back to the strip logs. The results are downloaded from the device as counts per million (cpm) and parts per million (ppm) for the radioactive elements uranium, thorium, and potassium (wt %). A total gamma reading is also measured. The results of the gamma ray readings are presented in Appendix D.

Whole-rock geochemical analysis was used to aid in characterization of the Cathedral Bluffs Tongue. Chemostratigraphic characterization is the process of splitting sequences based on their elemental characteristics (Ratcliffe *et al.*, 2007). Three outcrop sections at Bush Rim were sampled for geochemical analysis. Small (50-100g) geochemical samples were taken every meter on these outcrop sections. The samples were crushed and analyzed by Inductively Coupled Plasma Mass Spectrometry (ICP-MS) at the University of Alberta to determine the major and minor element concentrations within the rock. The concentration of each element can be affected by basin redox conditions, facies, weathering, diagenesis, and sediment provenance and may affect the geochemical signature of the strata and can work on a local or regional scale (Ratcliffe *et al.*, 2007). A principle component analysis (PCA) was also conducted on the geochemical data. This analysis was used to reduce the complexity of the dataset to a few underlying factors (Reimann *et al.,* 2002; Svendsen *et al.,* 2007). These factors can be attributed to the aforementioned processes that may affect elemental concentrations. For this study, the effects of sediment provenance and weathering / leaching are two of the primary factors that are determined by the analysis. Analysis of geochemical changes throughout the succession, as well as between outcrop sections, enabled the development of a stratigraphic framework for the study interval. Changes in sediment provenance, as well as climatic and depositional changes were interpreted from the results of this analysis.

Sequence stratigraphic methodologies were also applied to the succession, to determine the viability of this method for fluvial sediments in a lacustrine basin. Previous work on fluvial sequence stratigraphy (Wright and Marriot, 1993; Shanley and McCabe, 1994; Olsen *et al.*, 1995; Kraus and Aslan, 1999; Martinsen *et al.,* 1999; Arnott *et al.*, 2002; Zonneveld *et al.*, 2003; Fanti and Catuneanu, 2010) has developed a multitude of models and frameworks. Common themes were identified in previous analyses and were utilized to facilitate development of an initial sequence stratigraphic framework for the Cathedral Bluffs Tongue at South Pass.

1.6. References

Arnott, R. W. C., Zaitlin, B. A., and Potocki, D. J., 2002. Stratigraphic response to sedimentation in a net-accommodation-limited setting, lower Cretaceous Basal Quartz, south-central Alberta. Bulletin of Canadian Petroleum Geology, v. 50, 92-104.

Aslan, A., and Autin, W. J., 1999. Evolution of the Holocene Mississippi River floodplain, Ferriday, Louisiana: Insights on the origin of fine-grained floodplains. Journal of Sedimentary Research, v. 69, 800-815.

Bartels, W. S., Gunnell, G., Zonneveld, J. -P., McHugh, L. P., Fontana, T. M., 2011. An unusual vertebrate assemblage preserved in distal alluvial fan and lake margin deposits of the Cathedral Bluffs Tongue, Wasatch Formation, Bush Rim, Red Desert, Wyoming. Geological Society of America Abstracts with Programs, v. 43, 264.

Bird, P., 1998. Kinematic history of the Laramide orogeny in latitudes 35°-49°, western United States. Tectonics, v. 17, 780-801.

Bown, T. M., and Kraus, M. J., 1987. Integration of channel and floodplain suites, I. Developmental sequence and lateral relations of alluvial paleosols. Journal of Sedimentary Petrology, v. 57, 587-601.

Bradley, W. H., 1964. Geology of Green River Formation and associated Eocene rocks in southwestern Wyoming and adjacent parts of Colorado and Utah. U. S. Geological Survey Professional Paper, 496-A, 86 pp.

Bradley, W. H., 1969. Geochemistry and paleolimnology of the trona deposits and associated authigenic minerals of the Green River Formation of Wyoming: U.S. Geological Survey Professional Paper 496-B, 71 pp.

Brewer, J. A., Smithson, S. B., Oliver, J. E., Kaufman, S., and Brown, L. D., 1980. The Laramide orogeny: evidence from COCORP deep crustal seismic profiles in the Wind River Mountains, Wyoming. Tectonophysics, v. 62, 165-189.

Brown, W. G., 1988, Deformation style of Laramide uplifts in the Wyoming foreland, *in* Interaction of the Rocky Mountain foreland and Cordilleran thrust belt. Edited by C. J. Schmidt and W. J. Perry, Geological Society of America Memoir 171, 1–25.

Carroll, A. R., and Bohacs, K. M., 1999. Stratigraphic classification of ancient lakes: Balancing tectonic and climatic controls. Geology, v. 27, 99-102.

Carroll, A. R., Chetel, L. M., and Smith, M. E., 2006. Feast to famine: Sediment supply control on Laramide basin fill. Geology, v. 34, 197-200.

Chadey, H. F., 1973. Historical aspects of the Green River Basin, Wyoming. Wyoming Geological Association, 25th Field Conference, on the geology and mineral resources of the Greater Green River Basin, Casper, Wyoming, 27-33.

Chetel, L. M., and Carroll, A. R., 2010. Terminal infill of Eocene Lake Gosiute, Wyoming, U.S.A. Journal of Sedimentary Research, v. 80, 492-514.

Clyde, W. C., Sheldon, N. D., Koch, P. L., Gunnell, G. F., and Bartels, W. S., 2001. Linking the Wasatchian/Bridgerian boundary to the Cenozoic Global Climate Optimum: New magnetostratigraphic and isotopic results from

South Pass, Wyoming. Palaeogeograhpy, Palaeoclimatology, Palaeoecology, v. 167, 175-199.

Clyde, W. C., Bartels, W. S., Gunnell, G. F., Zonneveld, J. -P., 2004. Discussion and reply: 40Ar/39Ar geochronology of the Eocene Green River Formation, Wyoming Discussion. Geological Society of America Bulletin, v. 116, 251-256.

Cope, E. D., 1872. On the existence of dinosauria in the transition beds of Wyoming. American Philosophical Society Proceedings, v. 12, 481-483.

Daniels, J. M., 2003. Floodplain aggradation and pedogenesis in a semiarid environment. Geomorphology, v. 56, 225-242.

Dickinson, W.R., Klute, M.A., Hayes, M.J., Janecke, S.U., Lundin, E.R., McKittrick, M.A., and Olivares, M.D., 1988, Paleogeographic and paleotectonic setting of Laramide sedimentary basins in the central Rocky Mountain region: Geological Society of America Bulletin, v. 100, 1023–1039.

Donavan, J.H., 1950, Intertonguing of Green River and Wasatch Formations in part of Sublette and Lincoln Counties, Wyoming: Wyoming Geological Association Guidebook, 5th Annual Field Conference, Southwest Wyoming, Casper, Wyoming, 59-67.

Fanti, F. and Catuneanu, O., 2010. Fluvial sequence stratigraphy: the Wapiti Formation, west-central Alberta, Canada. Journal of Sedimentary Research, v. 80, 320-338.

Gunnell, G. F., and Yarborough, V. L., 2000. *Brontotheriidae* (*Perissodactyla*) from the late, early, and middle Eocene (Bridgerian), Wasatch and

Bridger Formations, southern Green River Basin, Southwestern Wyoming. Society of Vertebrate Paleontology, v. 20, 349-368.

Gunnell, G. F., Bartels, W. S., Zonneveld, J-P, 2004. A late Wasatchian (late early Eocene) vertebrate assemblage preserved in meandering stream channel deposits, northern Red Desert, Wyoming. Geological Society of America Abstracts with Programs, v. 36, 92.

Hague, A., and Emmons, S. F., 1877. Report of the geological exploration of the Fortieth Parallel, Volume II: Descriptive Geology. U. S. Geological Survey, unnumbered monograph.

Hall, M. K., and Chase, C. G., 1989. Uplift, unbuckling, and collapse: Flexural history and isostacy of the Wind River Range and Granite Mountains, Wyoming. Journal of Geophysical Research, v. 94, 581-593.

Hayden, F. V., 1971. Preliminary report (4th Annual) of the U. S. Geological Survey of Wyoming and contiguous territories. Washington, D. C., 511 pp.

Johnson, P. L., and Andersen, D. W., 2009. Concurrent growth of uplifts with dissimilar orientations in the southern Green River Basin, Wyoming: Implications for Paleocene and Eocene patterns of foreland shortening. Rocky Mountain Geology, v. 44, 1-16.

Keighley D., Flint, S., Howell, J., and Moscariello, A., 2003. Sequence stratigraphy in lacustrine basins: A model for part of the Green River Formation (Eocene), southwest Uinta Basin, Utah, U. S. A. Journal of Sedimentary Research, v. 73, 987-1006.

King, C., 1878. Annual Report of the geological exploration of the fortieth parallel from the Sierra Nevada to the eastern slope of the Rocky Mountains. U. S. Government Printing Office, 6 pp.

Kraus, M. J., 1999. Paleosols in clastic sedimentary rocks: their geologic applications. Earth-Science Reviews, v. 47, 41-70.

Kraus, M. J. and Aslan, A., 1999. Paleosol sequences in floodplain environments; a hierarchical approach. Special Publication of the International Association of Sedimentologists, v. 27, 303-321.

Lawrence, J. C., 1963. Origin of the Wasatch Formation, Cumberland Gap area, Wyoming. *in* Contributions to Geology: University of Wyoming, v. 2, 151-158.

Leidy, J. L., 1873. Contributions to the extinct vertebrate fauna of the Western Territories. U. S. Geographical and Geological Survey of the Territories Report, v. 1, 14-358.

Lynn, H. B., Quam, S., and Thompson, G. A., 1983. Depth migration and interpretation of the COCORP Wind River, Wyoming, seismic reflection data. Geology, v. 11, 462-469.

Marsh, O. C., 1876. On some characters of the genus *Coryphodon*. American Journal of Science, 3rd Series, v. 11, 425-428.

Martinsen, O. J., Ryseth, A., Helland-Hansen, W., Flesche, H., Torkildsen, and Idil, S., 1999. Stratigraphic base level and fluvial architecture: Ericson Sandstone (Campanian), Rock Springs Uplift, SW Wyoming, USA. Sedimentology, v. 46, 235-259.

McGee, L. C., 1983. Laramide sedimentation, folding and faulting southern Wind River Range, Wyoming. PhD Diss., University of Wyoming, Laramie, 92 pp.

Olsen, T., Steel, K., Hogseth, K., Skar, T., and Roe, S. L., 1995. Sequential architecture in a fluvial succession: sequence stratigraphy in the upper Cretaceous Mesaverde Group, Price Canyon, Utah. Journal of Sedimentary Research, v. B65, 265-280.

Oriel, S. S., 1963. Preliminary geologic map of the Fort Hill Quadrangle, Lincoln County, Wyoming. U. S. Geological Survey Oil and Gas Investigations Map OM-212, scale 1:48000.

Pietras, J. T., Carroll, A. R., and Rhodes, M. K., 2003. Lake basin response to tectonic drainage diversion: Eocene Green River Formation, Wyoming. Journal of Paleolimnology, v. 30, 115-125.

Pietras, J. T., and Carroll, A. R., 2006. High-resolution stratigraphy of an underfilled lake basin: Wilkins Peak Member, Eocene Green River Formation, Wyoming, U.S.A. Journal of Sedimentary Research, v. 76, 1197-1214.

Pipiringos, G. N., 1961. Uranium-bearing coal in the central part of the Great Divide Basin. U. S. Geological Survey, Bulletin 1099-A, 104 pp.

Powell, J. W., 1876. Report on the geology of the eastern portion of the Uinta Mountains and a region of country adjacent thereto. U. S. Geological and Geographical Survey of the Territories, 2nd division, 157.

Ratcliffe, K. T., Morton, A. C., Ritcey, D. H., Evenchick, C.A., 2007. Whole-rock geochemistry and heavy mineral analysis as petroleum exploration tools in the Bowser and Sustut basins, British Columbia, Canada. Bulletin of Canadian Petroleum Geology, v. 55, 320-336.

Reimann, C., Filzmoser, P., Garrett, R. G., 2002. Factor analysis applied to regional geochemical data: problems and possibilities. Applied Geochemistry, v. 17, 185-206.

Roehler, H. W., 1991a. Revised stratigraphic nomenclature for the Wasatch and Green River Formations of Eocene age, Wyoming, Utah, and Colorado. United States Geological Survey Professional Paper 1506-B, 38pp.

Roehler, H. W., 1991b. Godiva Rim Member – A new stratigraphic unit of the Green River Formation in southwest Wyoming and northwest Colorado. United States Geological Survey Paper 1506-C. 17pp.

Roehler, H. W., 1992a. Introduction to Greater Green River Basin geology, Physiography, and history of investigations. United States Geological Survey Professional Paper 1506-A, 14pp.

Roehler, H. W., 1992b. Correlation, composition, areal distribution, and thickness of Eocene stratigraphic units, Greater Green River Basin, Wyoming, Utah, and Colorado. United States Geological Survey Professional Paper 1506-E, 49pp.

Schultz, A.R., 1920, Oil possibilities in and around Baxter Basin, in the Rock Springs uplift, Sweetwater County, Wyoming: U.S. Geological Survey Bulletin 702, 107 pp.

Sears, J. D., and Bradley, W. H., 1924. Relations of the Wasatch and Green River Formations in northwestern Colorado and southern Wyoming, with notes on oil shale in the Green River Formation. U. S. Geological Survey Professional Paper 132, 93-107.

Shanley, K.W. and McCabe, P. J., 1994. Perspectives on the sequence stratigraphy of continental strata. AAPG Bulletin, v. 78, 544-568.

Shuster, M. W., and Steidtmann, J. R., 1988. Tectonic and sedimentary evolution of the northern Green River Basin, western Wyoming, in Schmidt, C. J., and Perry, W. J., eds. Interaction of the Rocky Mountain foreland and the Cordilleran thrust belt. Geological Society of America Memoir, v. 171, 515-530.

Smith, M. E., Carroll, A. R., Singer, B. S., 2008. Synoptic reconstruction of a major ancient lake system: Eocene Green River Formation, western United States. Geological Society of American Bulletin, v. 120, 54-84.

Smithson, S. B., Brewer, J., Kaufman, S., Oliver, J., and Hurich, C., 1978. Nature of the Wind River thrust, Wyoming, from COCORP deep-reflection data and from gravity data. Geology, v. 6, 648-652.

Steidtmann, J. R., and Middleton, L. T., 1991. Fault chronology and uplift history of the southern Wind River Range, Wyoming: Implications for Laramide and post-Laramide deformation in the Rocky Mountain foreland. Geological Society of America Bulletin, v. 103, 472-485.

Sullivan, R., 1980. A stratigraphic evaluation of the Eocene rocks of southwestern Wyoming. The Geological Survey of Wyoming, Report of Investigations, v. 20, 50 pp.

Svendsen, J. B., Friis, H., Stollhoffen, H., Hartley, N., 2007. Facies discrimination in a mixed fluvio-eolian setting using elemental whole-rock geochemistry – Applications for reservoir characterization. Journal of Sedimentary Research, v. 77, 23-33.

West, R. M., 1969. Biostratigraphy of fluvial sediments of the upper Wasatch Formation in the northern Green River Basin, Wyoming. Rocky Mountain Geology, v. 8, 184-196.

Wilf, P., 2000. Late Paleocene-early Eocene climate changes in southwestern Wyoming: Paleobotanical analysis. Geological Society of America Bulletin, v. 112, 292-307.

Woodburne, M. O. (editor), 1987. Cenozoic mammals of North America: geochronology and biostratigraphy. University of California Press, Berkeley and Los Angeles, California, 336 pp.

Woodburne, M. O., and Swisher, C. C. III, 1995. Land Mammal high-resolution geochronology, intercontinental overland dispersals, sea level, climate, and vicariance. Geochronology Time Scales and Global Stratigraphic Correlation, SEPM Special Publication, No. 54.

Wright, P. V., and Marriott, S. B., 1993. The sequence stratigraphy of fluvial depositional systems: the role of floodplain sediment storage. Sedimentary Geology, v. 86, 203-210.

Zachos, J. C., Stott, L. D., Lohmann, K. C., 1994. Evolution of early Cenozoic marine temperatures. Paleoceanography, v. 9, 353-387.

Zeller H. D., and Stephens, E.V., 1969. Geology of the Oregon Buttes area, Sweetwater, Sublette and Freemont Counties, southwestern, Wyoming. U. S. Geological Survey Bulletin No. 1256, 60pp.

Zonneveld, J. -P., Bartels, W. S., and Clyde, W. C., 2003. Stratal architecture of an Early Eocene fluvial-lacustrine depositional system, Little Muddy Creek area, southwestern Green River Basin, Wyoming. Cenozoic Systems of the Rocky Mountain Region: Rocky Mountain SEPM, 253-287.

Chapter 2

Fluvial architecture and facies model for the Cathedral Bluffs Tongue, southwestern Wyoming.

2.1. Introduction

Fluvial sediments are deposited in a wide range of environmental settings. Fluvial channels are generally high-energy environments, but energy within the channel is strongly dependent on the fluvial gradient (often related to proximity to an uplifted area) (Martinsen *et al*., 1999; Miall, 2010). Conglomerate and coarse sandstone may be deposited in high-energy mountain streams or alluvial fans at the farthest upstream reaches of a river system. Farther downstream sediment may be trapped in braided or meandering channels, crevasse splays, lakes, or floodplains. These environments are generally lower energy, where very fine-grained sand, silt and mud may be deposited. As sediment travels through a sediment routing system, auto- and allogenic processes may remobilize the sediment and move it further downstream (Allen and Heller, 2012). Sediment preserved in the rock record represents only a fraction of the sediment that at one time was deposited in a given area.

River systems commonly start at a continental uplift and run down a graded longitudinal profile with a decreasing gradient downstream (Miall, 2010). Rivers that occur in front of orogenic belts can preserve fluvial deposits over long geologic time scales due uplift and concomitant subsidence in the basin (Johnson and Andersen, 2009; Miall, 2010). Analyses of thick packages of fluvial strata can provide evidence of the tectonic and climatic history of a sedimentary basin.

The Cathedral Bluffs Tongue of the Wasatch Formation is a strictly continental, mudstone-dominated fluvial succession that occurs within the Green River Basin of southwestern Wyoming (Fig. 2.1) (Roehler, 1992a).

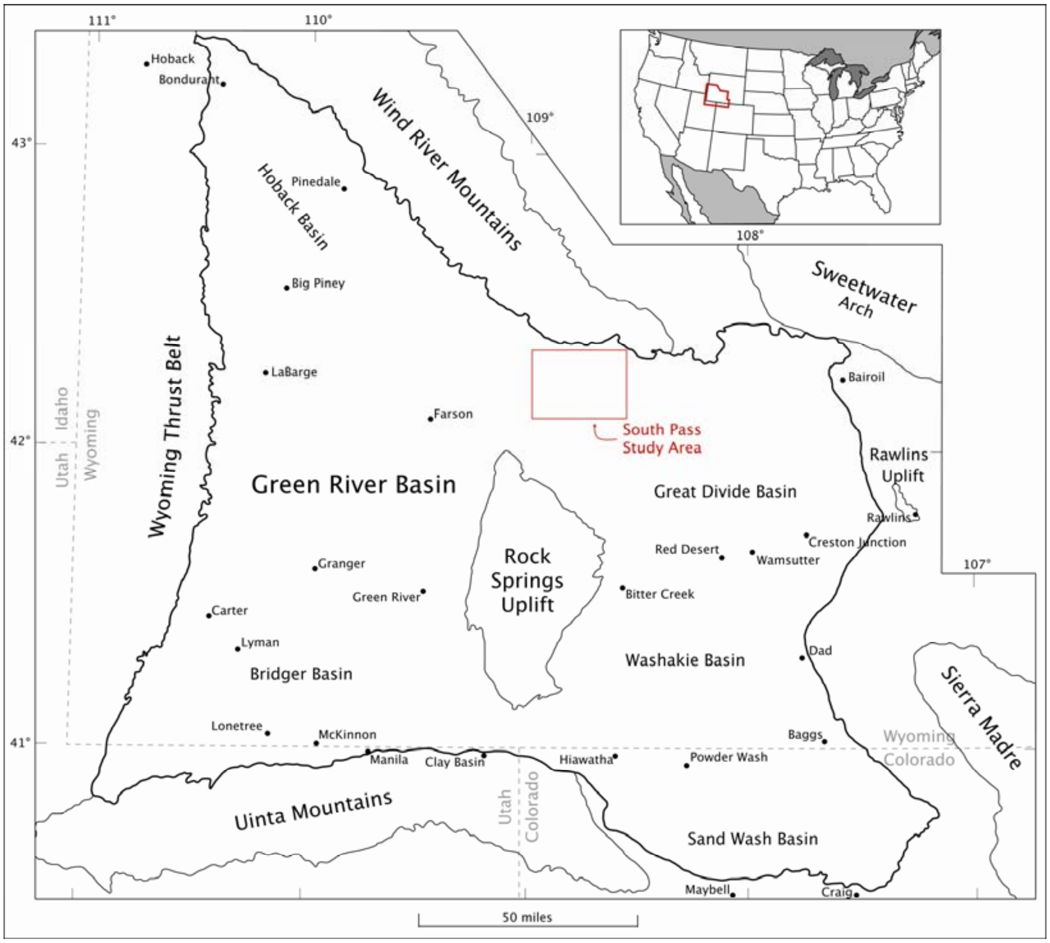

Figure 2.1 – Map showing the position of the Green River Basin within the continental United States. The study area occurs on the northeastern margin of the basin, along the southwestern flank of the Wind River Mountains. Modified from Roehler, 1991.

There was no marine influence within the Green River Basin during the early Eocene (Roehler, 1991; 1992a; Zonneveld *et al*., 2003). While there are many factors that affected deposition, climate and tectonics were the two dominant factors that controlled the evolution of the Green River Basin (Carroll and Bohacs, 1999; Bohacs *et al.,* 2000; Zonneveld *et al*., 2003). Together, these two processes directly controlled deposition of the Cathedral Bluffs Tongue. This study focuses on describing the architecture and determining the depositional patterns that occur in this basin margin succession and consequently assessing the relative effects of tectonic and climate influences in the evolution of the northeastern Green River Basin, in the region of South Pass, Wyoming (Fig. 2.2).

2.2. Geological Setting

The Green River basin was created by Sevier and Laramide uplift along the periphery of the basin (Hall and Chase, 1989; Steidtmann and Middleton, 1991; Roehler, 1992a). This created accommodation space within the basin, allowing for the deposition of late Cretaceous through Oligocene sediment (Zeller and Stephens, 1969; Roehler, 1991). On the northeastern margin of the basin, movement on the Wind River Thrust Fault uplifted the basement-cored Wind River Mountains during the late Cretaceous (Brewer *et al*., 1980; Hall and Chase, 1989; Steidtmann and Middleton, 1991). The range is 220 km long and 70 km wide with a northwest trending structure (Hall and Chase, 1989). Substantial erosion began soon after. As much as 8 km of sedimentary cover was removed, exposing the basement core of the range before the end of the early Eocene (Steidtmann and Middleton, 1991). Lacustrine deposition in Paleolake Gosiute dominated the basin fill during the early Eocene, with subordinate fluvial deposits interfingering along the basin margins (Roehler, 1991; 1992a).

This study is focused on fluvial deposits of the Cathedral Bluffs Tongue on the northeastern margin Green River Basin. Outcrop of the Cathedral Bluffs Tongue occurs near the northeastern margin of the Green River Basin between the Wind River Mountains and the Rock Springs Uplift. The study area is on the southwestern flank of the Wind River Mountain Range in the Red Desert near South Pass, Wyoming (Fig 2.3). Sediment derived from the topographically high Wind River Range supplied sediment to alluvial fans proximal to the uplift (Steidtmann and Middleton, 1991). Coarse conglomerate beds and sandstone were deposited within these

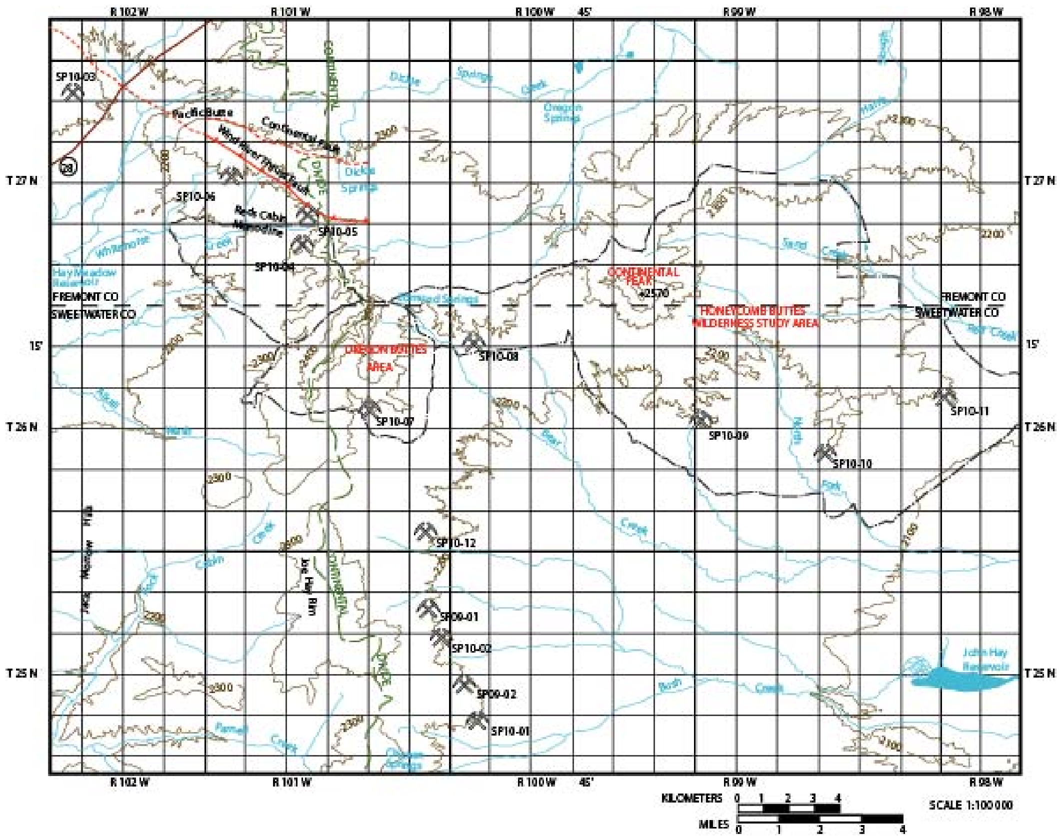

Figure 2.2 – Map of the South Pass study area on the northeastern margin of the basin. The Continental Fault and trace of the Wind River Thrust Fault are marked in the northwestern part of the map area.

proximal areas, while further basinward, finer-grained sand and mud dominate the succession (Fig. 2.3).

2.3. Facies Analysis

Facies are intervals or packages of rock that are distinguished from other intervals by a distinct set of features (Anderton, 1985; Reading, 1996; Miall, 1999). Grain size, colour, geometry, primary structures, biogenic structures, and chemical makeup are all characteristics of rock that can be used to characterize facies. Separating these packages of rock with similar characteristics (facies) and determining how they relate to each other is the heart of the discipline of facies analysis. The meaning of the term facies, and its use for describing sedimentary rocks, has often been debated (Selley,

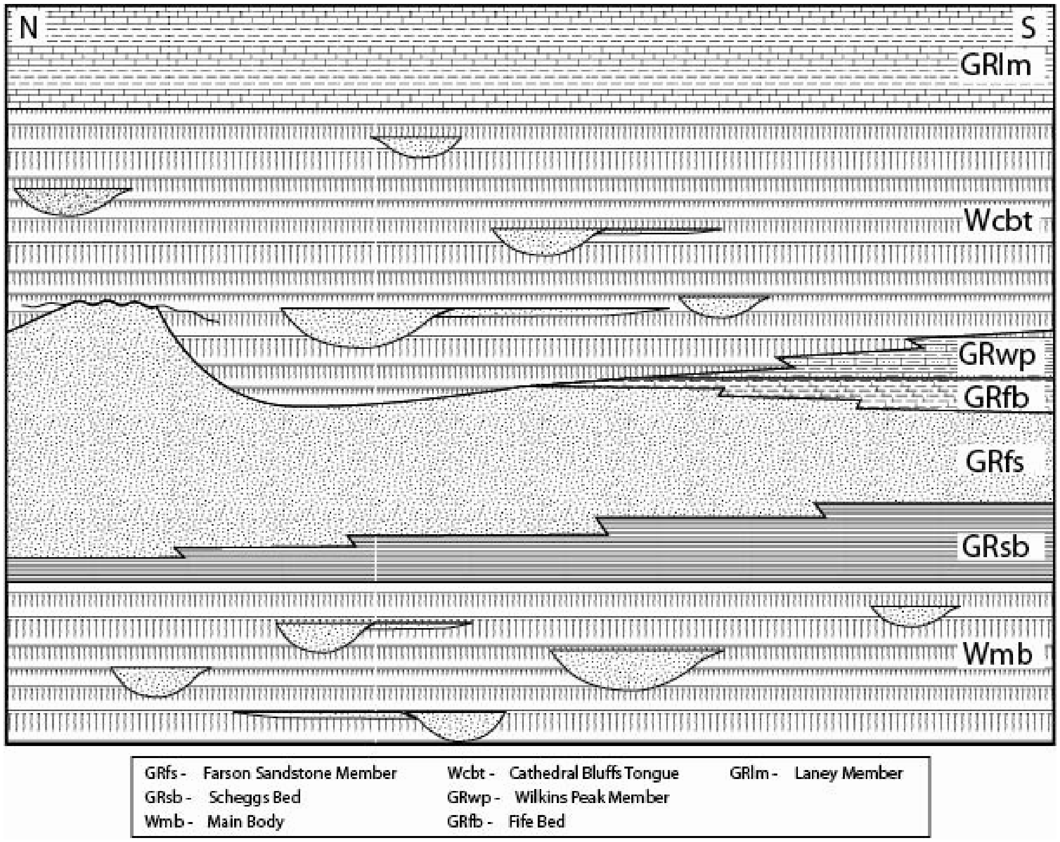

Figure 2.3 – Lithostratigraphic relationships between the lacustrine Green River and fluvial Wasatch Formations in the study area. The interval of interest is the Cathedral Bluffs Tongue of the Wasatch Formation. Modified from Roehler, 1992b.

1982; Anderton, 1985; Miall, 1996). Additionally, using facies models in fluvial settings resulted in the creation of a plethora of models, each established for a specific study area (Reading, 1978; Dott and Bourgeois, 1983; Miall, 1985). The use of architectural elements has been proposed to solve the problems associated with the proliferating number of fluvial facies models (Friend, 1983; Allen, 1982; Ramos and Sopena, 1983; Miall, 1985). Although the validity of fluvial facies models is questionable, as they do not always correctly represent reality, a facies model is created here to create a greater understanding of the system.

Detailed measurements and notes were taken on 14 outcrop sections, mainly on a southeast to northwest trend from Bush Rim in the south to northwest of Oregon Buttes. This trend is approximately parallel to depositional dip as the sediments in this part of the basin originated from the

Wind River Mountains (McGee, 1983; Steidtmann and Middleton, 1991). Three additional sections were measured in an E-W orientation along the Honeycomb Buttes outcrop belt. 'Badland-like' weathering of the outcrop allows for good 3-D exposure of the succession, however, the weathering of the fine-grained deposits generally covers the outcrops. Trenches were dug approximately 20 to 40 cm deep and 40 to 80 cm wide to expose solid rock. The cover over the outcrop made it difficult to identify architectural elements, so lithofacies are utilized to carry out a facies analysis.

Miall (1977) named gravel and sand facies in braided-river deposits with a two-letter code. Although developed for braided-river deposits, the naming scheme is applicable to a wide range of fluvial deposits. The naming scheme has been revised over the years (Miall, 1978; 1996) to include additional minor facies such as coal and paleosols (Miall, 2010). The gravel and sand facies from Miall's original work is used here. However, for the fine-grained clastic facies, new classifications have been constructed. Miall's fine-grained classification of P (paleosol carbonate), C (coal, carbonaceous mud), and Fr (mud, silt, incipient soil) is regarded as inadequate for this study as the fine-grained fraction of the Cathedral Bluffs Tongue constitutes the bulk of the succession. The facies analysis presented herein is a combination of Miall's fluvial sand and gravel facies and a modified version of Bown and Kraus (1987) pedofacies (Table 2.1). Each facies has been modified to more accurately portray the sediments contained in the Cathedral Bluffs Tongue. Three pedofacies, and seven gravel, sand, and fine-grained facies are identified within the Cathedral Bluffs Tongue.

2.3.1. Gravel, Sand, and Fine-grained Facies

The Cathedral Bluffs Tongue in the study area is subdivided into two gravel facies, three sand facies, and two fine-grained facies that are not pedogenically-altered. Gravel facies are only observed in the most proximal

Facies Code	Lithofacies	Structures / Textures	Interpretation
Gmh	Gravel conglomerate, Clast-supported massive to crudely stratified	Crude horizontal bedding, weak grading	Longitudinal bars, pseudoplastic debris flows
Gt	Gravel conglomerate, matrix supported, stratified	Trough crossbeds, normal grading	Chute channel fills
Sp	Sandstone, fine to medium	Planar crossbeds	2-D dunes, transverse bars
St	Sandstone, fine to coarse, may be pebbly	Trough crossbeds, normai grading	Linguoid 3-D dunes
Shr	Sandstone, v. fine to fine	Horizontal and ripple crosslaminae, parting lineation	Plane-bed flow, current ripples
Lm	Lime mudstone / micrite	Horizontal laminae	Pond, lagoon, or sheltered lacustrine deposits, settle from suspension
Fsh	Organic rich shale	Horizontal laminae	Stratified lacustrine, settle from suspension
P1	Light grey / green v. fine sandstone, siltstone, and mudstone	Horizontal and ripple laminae, rootlets	Proximal overbank, abandoned channel, incipient soil
P2	Dark grey / black siltstone and mudstone	Horiontal laminae, rootlets, plant material	Shallow pond, swamp, gleyed soil
P3	Red / orange siltstone and mudstone	Churned (B.I.=5-6), rootlets	Distal overbank, prolonged sub-aerial exposure, mature soil

Table 2.1 – Characteristics of the facies for the Cathedral Bluffs Tongue. The gravel and sand facies are modified from Miall's fluvial facies models. The fine-grained facies are subdivided into more detailed facies as the succession is dominated by the fine-grained facies.

(northern) sections (SP10-03, SP10-06, and SP10-04). Even in these proximal settings, gravel conglomerate is fairly rare.

Sand facies are common throughout the study area, but tend to decrease in thickness and abundance to the south (basinward). Facies St is very common, but often does not show well-defined trough crossbeds. Only crude troughs and normal grading are observed in many locations. Primary sedimentary structures may have been destroyed during diagenesis.

Fine-grained facies are only observed in the most basinward sections (SP10-01, SP09-02, SP10-02, SP09-01, and SP10-12). Facies Lm and Fsh are very rare, even in distal sections, and account for a very small portion of the preserved record in the study area. Facies Fsh is not a characteristic Wasatch Formation facies and if it was to be traced basinward, it would likely thicken rapidly and become a tongue of the Green River Formation.

2.3.2. Pedofacies

The Cathedral Bluffs Tongue is dominated by pedogenically-altered floodplain silt and mudstone. The degree of pedogenic alteration is an important component of the facies analysis. The pedofacies concept (Bown and Kraus, 1987) was introduced to describe the lateral variation of cumulative paleosols in an alluvial setting (Fig. 2.4). The term *pedofacies* is described as "…*laterally contiguous bodies of sedimentary rock that differ in their contained laterally contiguous paleosols as a result of their distance (during formation) from areas of relatively high sediment accumulation*" (Bown and Kraus, 1987, p. 599). Paleosol patterns can give insights into climate, tectonics, and sedimentation rates at the time of deposition (Kraus, 1999; Daniels, 2003). A more detailed description of the overbank architectural element will create a greater understanding of the depositional system, especially in strata where this is the dominant element. Pedofacies are separated according to their grain size, colour, horizon thickness, profile thickness, ichnology, and sedimentary structures. The pedofacies model of Bown and Kraus (1987) is directly related to channel proximity and in turn, sedimentation rate (Fig. 2.5). The model includes five pedofacies, separated by paleosol maturity; however, in the Cathedral Bluffs Tongue only three distinct types of paleosol were identified as distinct facies. Facies P1 through P3 roughly correspond to the Bown and Kraus (1987) pedofacies model, with

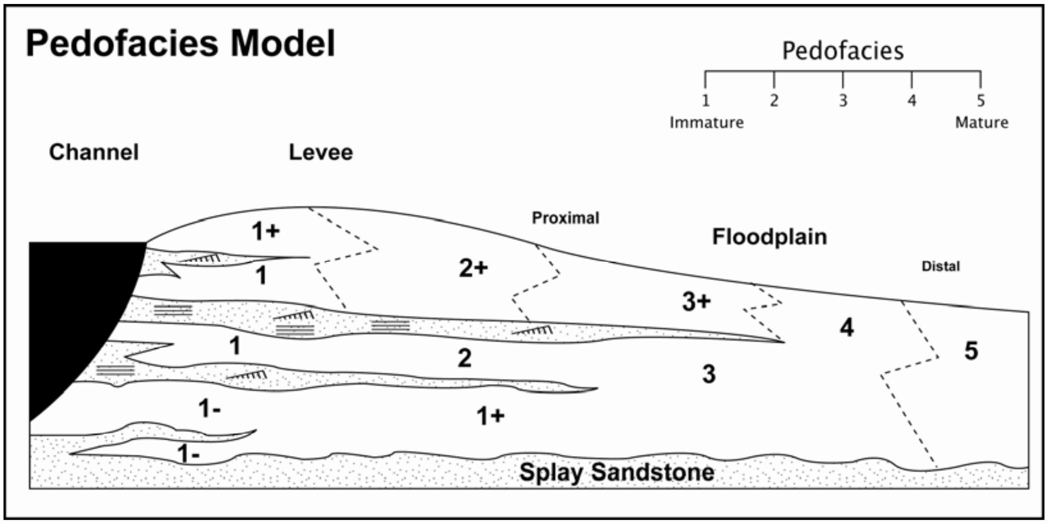

Figure 2.4 - The pedofacies concept (modified from Kraus and Bown, 1993). Since it's inception, pedofacies have evolved to include more factors than just distance from a channel. Sedimentation rate, temperature, precipitation, time, drainage conditions, vegetation, and bioturbation all affect the pedogenic process. Assuming similar climatic conditions, distance from the channel (~sedimentation rate) has the greatest effect on paleosol maturity.

facies P1 as the least mature (closest to the channel) and facies P2 as more mature (farther from the channel). Facies P3 is the most mature, but could be any distance from a channel as the pedogenesis is interpreted to include secondary overprinting of the original fabric.

2.3.3 Facies

Facies Gmh – Massive to Crude Horizontally Bedded Gravel

Description

Facies Gmh (Fig. 2.6B-D) is composed of massive or crudely bedded, clast-supported gravel conglomerate. Clast sizes range from 0.5 to 20 cm. Beds are typically between 1 to 2 m thick, or occur as rare thin (approximately 10 to 50 cm) gravel lenses. The basal contact is frequently erosional and the top contact gradational. Crude horizontal bedding is occasionally observed demarcated by both normal and reverse grading. Imbricated clasts are observed locally within this facies. No traces or fossils

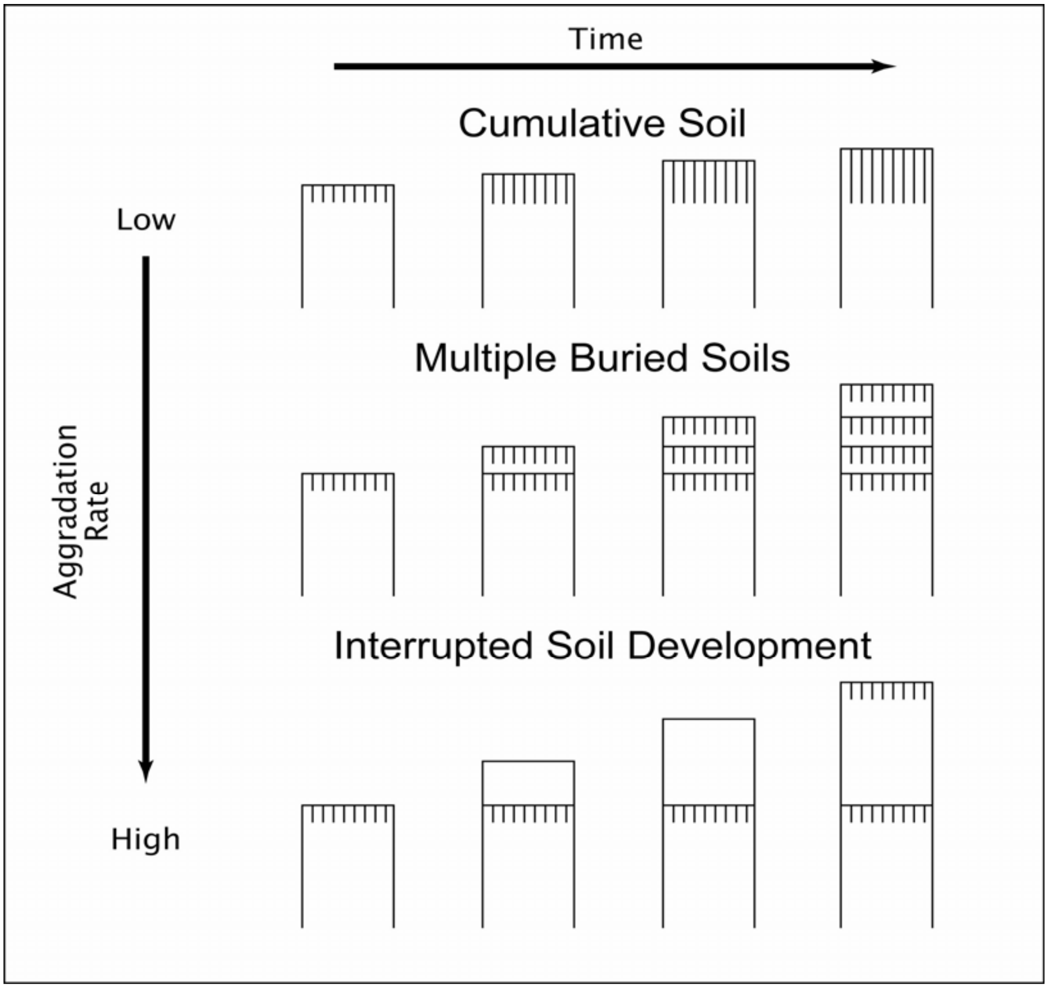

Figure 2.5 – Different paleosol types form based on the relationship between the two most important factors controlling paleosol development; time and aggradation rate. A relationship exists between these two factors that affects paleosol maturity and profile thickness. Modified from Daniels (2003).

are included within this facies. Clast lithology is dominantly composed of quartzite, granite, and low-grade schist. Facies Gmh occurs erosionally over facies P1 through P3 and less commonly erosionally over facies St.

Interpretation

Due to the massive or crudely bedded nature of facies Gmh, it is interpreted to represent the accretion of gravel in longitudinal bars. Longitudinal bars are the most common type of gravel bedform and they form as the coarsest grains are deposited during waning flow (Rust, 1972;

Smith, 1974; Gustavson, 1978; Miall, 1977). Formation of these bars begins with the largest clasts as diffuse gravel sheets (Hein and Walker, 1977), and eventually formed into longitudinal bars as bar growth continued (Miall, 1977). Grain size within longitudinal bars generally diminishes upwards as well as downstream in modern gravel-dominated braided rivers (Smith, 1974; Miall, 1977). Therefore, normal grading occurs as flow wanes and reverse grading would be caused by the downstream migration of the bedform, as coarse material migrated over the finer gravel.

Facies Gt – Trough-cross Bedded Gravel

Description

Facies Gt (Fig. 2.6A) consists of trough-cross bedded, clast-supported gravel conglomerate with clast sizes ranging from 0.5 to 10 cm along the longest axis. The beds range from 25 cm up to approximately 2 m thick within the study area. Lens-shaped bodies commonly amalgamate together to form more continuous beds. The bottom contacts are erosional, causing undulatory, concave up bases while the tops of the beds are commonly gradational into facies St, Sp, and rarely into P2 or P3. Crude trough-cross stratification, common clast imbrication, and normally graded beds are the dominant sedimentary features observed. No traces or fossils are included within this facies. Clast lithology is dominantly composed of quartzite, granite, and low-grade schist. This facies occurs erosionally over P1 through P3 (relatively immature paleosols).

Interpretation

This facies is interpreted as channel and pool fills within a braided river system. Trough-cross bedded gravel can result from the migration of non-linear transverse bars or the infill of small channels (Miall, 1996). The troughs observed in the Cathedral Bluffs Tongue are relatively small and

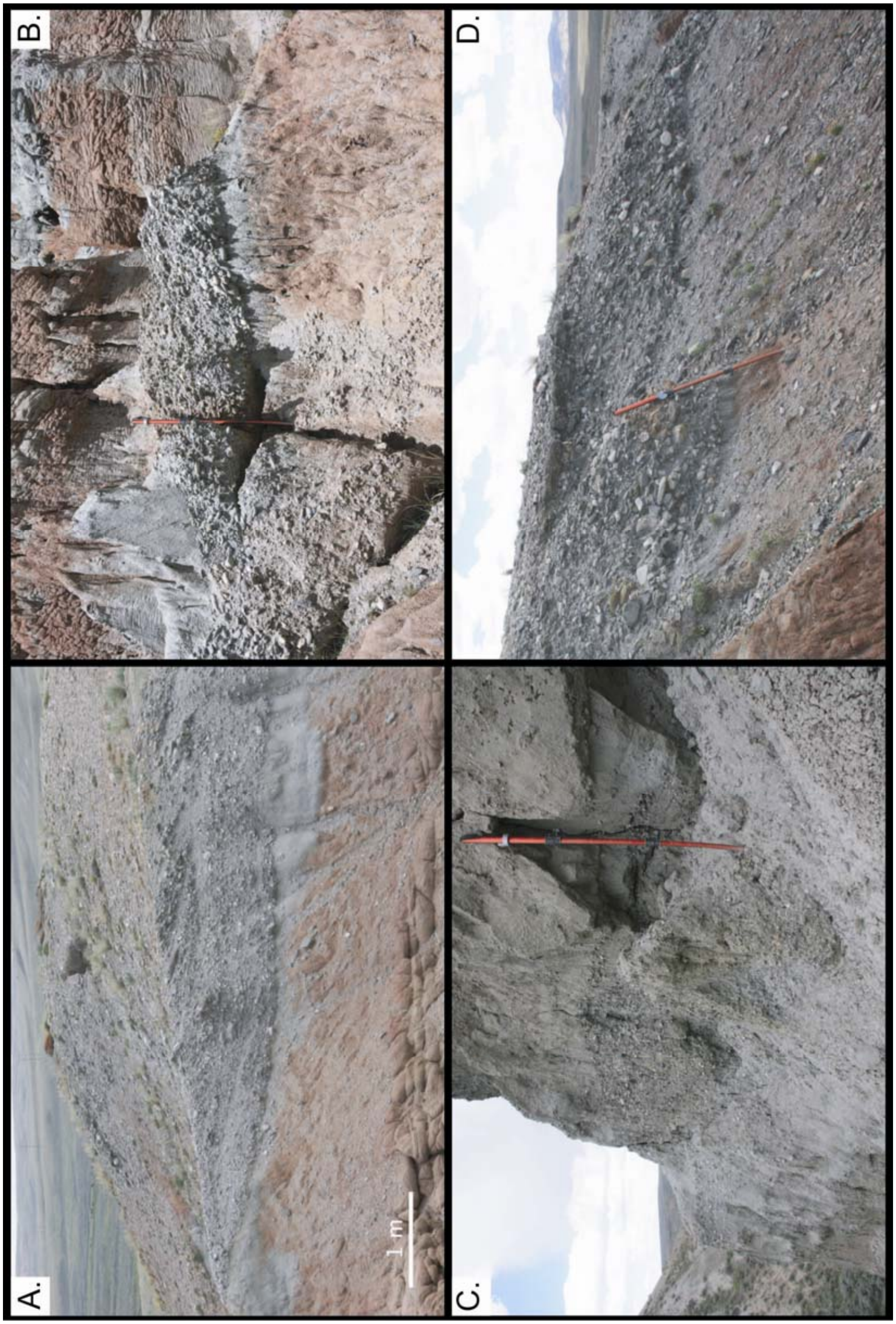
A.
B.
C.
D.
1 m

Figure 2.6 - The fine gravel to cobble conglomerates observed within the Cathedral Bluffs Tongue. **A.** SP10-03. Facies Gt – Trough-cross bedded gravel. This facies is interpreted as minor channel fills. **B.** SP10-06 - Average clast size is approximately 5 cm. This bed is not as laterally extensive as the in SP10-03. As in SP10-03 there seems to be two periods of uplift and concomitant deposition of two intervals of coarse gravel conglomerate. Pogo for scale is 1.5 m long. **C.** SP10-04 - This fine-gravel conglomerate is located near the top of the section. The bed is variable laterally, being present on some of the buttes, but not others. Pogo for scale is 1.5 m long **D.** SP10-03 - approximately 16 meters from the base of the section a thick coarse gravel to cobble conglomerate bed cuts into the underlying grey fine sandstone. The maximum clast size is ~20 cm in the longest direction with average clast size approximately 10 cm. The scoured bases of these beds can range in height by approximately 2 meters. Cross bedding dipping towards the southwest was also observed. Pogo for scale is 1.5 m long.

occur within lens-shaped bodies; therefore, deposition likely occurred as small channel infills.

Facies Sp – Planar-cross Bedded Sand

Description

Facies Sp (Fig. 2.7C) is composed of a planar-cross bedded, well sorted medium sandstone with rare coarser grains. Bed thickness ranges from 20 to 60 cm and contacts are generally sharp. These beds are tabular in nature and occur as far as at least one hundred meters laterally. The base of these beds is often massive to planar laminated and grades upwards into planar-cross bedded sand. Amplitude on the planar-cross beds is approximately 20 cm. No traces or fossils were observed in these beds. This facies occurs erosionally over facies P3.

Interpretation

Planar-cross bedded sand is formed by the migration of 2-D dunes (Miall, 1996). In medium sand, the grains would be transported by traction up the stoss side of the dune and deposited on the lee side. Slightly curved toesets and flattening out of the foresets indicates flows at near plane-bed conditions as separation eddies are smaller (Miall, 1996).

Facies St – Trough-cross Bedded Sand

Description

Facies St (Fig. 2.7D) is comprised of poorly to moderately sorted, fine- to very coarse-grained sandstone and commonly displays trough-cross bedding. Bed thickness ranges from 25 to 150 cm and commonly occurs as amalgamated beds. Bases are sharp and grade normally upwards to gradational contact with facies Sp or Shr, or a repeated trough-cross bedded sand. In addition to trough-cross bedding, normally graded couplets on the order of ~5 cm occur within the troughs. Small mud clasts (0.5 to 1.5 cm) are observed within laminae while rare larger mud clasts (up to 11cm) are found scattered throughout the facies. Gravel clasts are also commonly observed in this facies, especially in sections more proximal to the sediment source. Ichnofossils are rare, but large (up to 24 cm vertically) *Arenicolites*-like burrows have been observed as well as cf. *Edaphichnium*. Thin (~25 cm) troughs occasionally contain abundant fossil and crocodilian fossils as well as large stromatolitic clasts. This facies occurs erosionally over facies P1 and P2 as well as occasionally gradationally over facies Gt.

Interpretation

Trough-cross bedding is created by the migration of 3-D dunes (Miall, 1996). Curved foresets and basal lags consisting of gravel and mud clasts distinguish this facies from facies Sp. The concave up nature of the troughs indicate erosional scour from each of the dunes as it migrated.

Facies Shr – Horizontal Bedded to Ripple-Cross Bedded Sand

Description

Facies Shr (Fig. 2.7A-B) is composed of well sorted, fine to medium grain sandstone. Beds range from 10 – 50 cm in thickness with sharp bases and gradational tops. The horizontal bedded sandstone has been observed grading upwards into ripple-cross bedded sandstone. The areal extent of these beds can be from 100's of meters to a kilometer or two. Current ripples


A.
B.
C.
D.
2cm

Figure 2.7 – Sand facies of the Cathedral Bluffs Tongue. **A.** Facies Shr - ripple cross-laminated sandstone bed from SP10-01. **B.** Facies Shr - planar-horizontal laminae in a. Hammer for scale is 28 cm long. **C.** Facies Sp – Planar tabular cross-bedded sandstone from SP10-10. Pogo for scale has ~60 cm showing and has 10 cm divisions. **D.** Facies St – trough cross-bedded sandstone with gravel lenses at SP10-07. Pogo for scale has ~1 m showing and has 10 cm divisions.

with amplitudes of 1-1.5cm are the dominant sedimentary feature. Horizontal planar-laminated sand beds are also observed with parting lineation along the bedding planes. There is a range of trace fossils included within this facies, including *Ancorichnus, Planolites, Skolithos*, and *Camborygma*. Commonly this facies is highly bioturbated (B.I. 5-6) is high and shows large traces (*Ancorichnus* 7 to 15 mm). Less commonly these beds have rare bioturbation (B.I. 1-2) and display very small traces (*Ancorichnus* 1.5 to 3 mm). Fragments of turtle and crocodilian bone are found in varying amounts scattered throughout this facies. Commonly occurs over any of the pedofacies and less commonly over facies St.

Interpretation

Horizontal plane bedded sand can be created by two processes, upper plane bed conditions or with coarse to very coarse sand at low flow conditions (Miall, 1996; Prothero and Schwab, 2004). Due to the grain size (fine- to medium-grained sand) this facies may be deposited from laminar flow conditions. The presence of a subtle primary-current lineation and the well-sorted nature are both in keeping with this interpretation. Ripple cross-bedded sand is deposited under similar conditions, but at lower flow velocities or in deeper water (Prothero and Schwab, 2004).

Facies Fsh – Organic-rich Shale

Description

Facies Fsh (Fig. 2.8C-D) is composed of fine-grained, organic-rich shale. Beds are 1 to 10 mm thick and are characterized by sharp contacts both at the base and the top. The beds are extensive, ranging up to at least 4 km. This shale sometimes occurs interbedded with facies Lm, where the shale beds are mm scale and the carbonate is cm scale. Horizontal laminae are observed within the shale. No bioturbation or fossils are observed. This facies occurs as discrete beds and occurs with facies P1 over and underlying the beds. Facies Lm has also been observed underlying the shale beds.

Interpretation

This facies is interpreted to be from a deep (profundal) lacustrine environment, with deposition due silt and mud settling from suspension. The high organic content and lack of biogenic mixing leads to the interpretation that this shale was deposited in a dysoxic to anoxic environment within a stratified lake setting (Bradley, 1926). The occurrence of this facies leads to the interpretation of a lake transgression, depositing the shale in quiet waters. These beds are very thin; therefore, making their preservation potential low. The interbedding of facies Fsh with facies Lm may represent intermittent clastic input into the lacustrine basin. Thin clay-rich clastic layers may have been deposited during periods of high fluvial discharge, such as in the spring. During periods of no clastic input, carbonate mud slowly accumulated until the next influx of clastic sediment into the lake. The organic component of the shale is likely derived predominantly from the remains of planktonic organisms from the surface waters of the lake (Bradley, 1926).

Facies Lm – Carbonate Mud / Micrite

Description

Facies Lm (Fig. 2.8A-B) is composed of tan-white lime mudstone or micrite. Contacts are sharp both at the base and top and bed thickness is bimodal, ranging from 1 to 3 mm or 3 to 5 cm. This facies almost always occurs interbedded with facies Fsh or P1, either in mm scale beds or in cm scale beds. These beds often show wavy to horizontal planar laminae, which are observable due to thinly interbedded mudstone. Commonly bioturbated

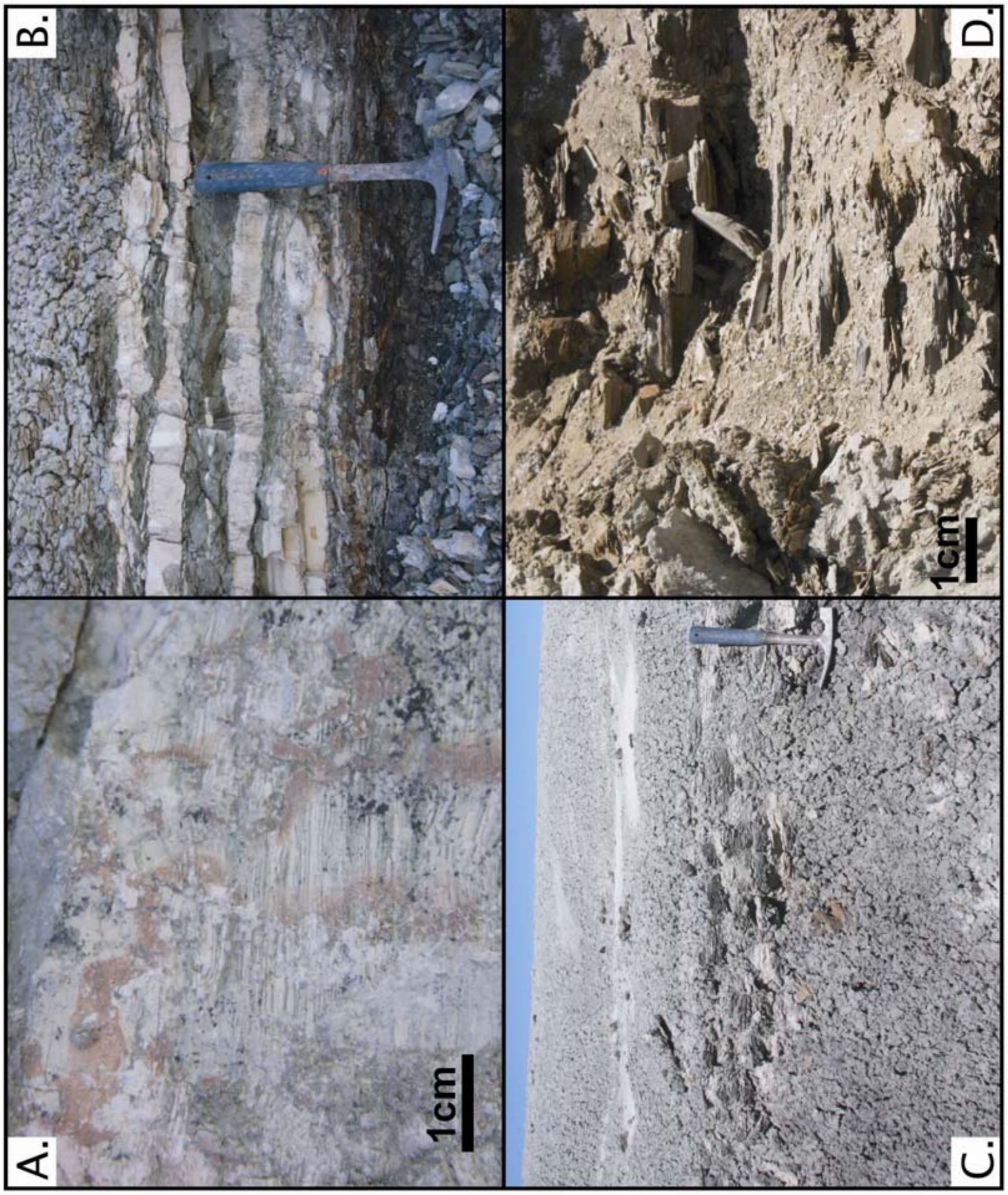

Figure 2.8 – The fine-grained facies of the Cathedral Bluffs Tongue **A.** facies Lm and P1 interbedded at millimeter scale with some wavy bedding. *Planolites* and *Skolithos*-like burrows are observed in this facies. **B.** Centimeter-scale interbeds of facies Lm and P1. Facies Lm usually does not occur alone, but interbedded with either P1 or Fsh. Hammer for scale is 28 cm long. **C.** Oil-shale beds of facies Fsh that become convoluted with exposure to the sun. Hammer for scale is 28 cm long. **D.** Planar-horizontal laminated lacustrine shale of the Laney Member, directly overlying the Cathedral Bluffs Tongue.

when interbedded in mm scale beds with facies Fsh, including *Planolites* and some horizontal, sub-vertical, and vertical back-filled burrows (*c.f. Naktodemasis*). The cm scale beds show no observable bioturbation and no body fossils are observed within this facies. Facies Lm commonly occurs over immature pedofacies, and less commonly over facies Shr or thin coal beds. Overlying this facies is usually facies Fsh or more immature pedofacies.

Interpretation

One of the major controls on carbonate deposition is the amount of siliciclastic input into the system. Clastic input not only dilutes the carbonate during deposition, but it inhibits carbonate production (Tucker *et al.,* 1990). The lack of clastic material in this facies leads to the interpretation of deposition in isolated, standing bodies of water. Thin (<5 cm), tabular marlstone beds have previously been interpreted as deposition from flood ponds or shallow lacustrine conditions (Eberth and Miall, 1991). The lack of bioturbation observed within the cm scale beds is troubling, and inhibits the ability to distinguish ponded deposits with shallow lacustrine. However, the presence of coal underlying these beds indicates floodplain pond or swamp deposition.

Facies P1 – Light Grey / Green Sand, Silt, and Mud

Description

This facies (Fig. 2.9B) is composed of light green to grey mudstone, siltstone, and very fine-grained sandstone with or without minor yellow, orange, or red mottling. Individual profiles range from 10 to 100 cm. Pedogenic slickensides and soil horizons are absent to very poorly developed. Horizontal planar laminae are commonly observed, with rare asymmetrical ripple cross stratification in the silty to sandy beds. Bioturbation is present (B.I. 0-1), typically with a *Naktodemasis* monospecific trace fossil assemblage. However, *Camborygma* have also been observed within this facies. This facies commonly overlies facies St and Shr. Typically this facies is sharply topped by facies Shr or St, but other pedofacies (P2 and P3) can conformably overlie this facies.

Interpretation

The incipient nature of pedogenesis leads to an interpretation of high sedimentation rates proximal to the trunk channel. This pedofacies is commonly found associated with avulsion-belt deposits. The rate of pedogenesis was unable to keep up wit the sedimentation rate, resulting in poor soil development. In relation to avulsion, these paleosols could be deposited as thick packages very quickly (Aslan and Autin, 1999), as opposed to sporadic influxes of thin packages of sediment.

Facies P2 – Dark Grey / Black Silt and Mud

Description

Facies P2 (Fig. 2.9A,C) is characterized by dark grey to black mudstone, siltstone, and very fine-grained sandstone. Thicknesses are highly variable, ranging from 20 cm to nearly 2 m. Pedogenic slickensides are often present and occur only within the finer grained (mudstone to siltstone) beds. Primary sedimentary structures, such as horizontal planar laminae, are rare and discontinuous if observed. Desiccation cracks are observed within this facies, and are often observed associated with facies Lm. Soil horizons are apparent, yet colour contacts are still relatively diffuse. Mottling is extensive throughout all the beds. Small (<1 cm) carbonate and siderite concretions are sometimes present throughout. Small (~1 mm diameter), vertical traces are observed, and are often highlighted by sandy interbeds within the black mudstone. Organic (plant) material is observed within this facies. This facies generally lies above facies Fsh or P1. Minor coal deposits as well as facies Lm occur above and below this facies as well.

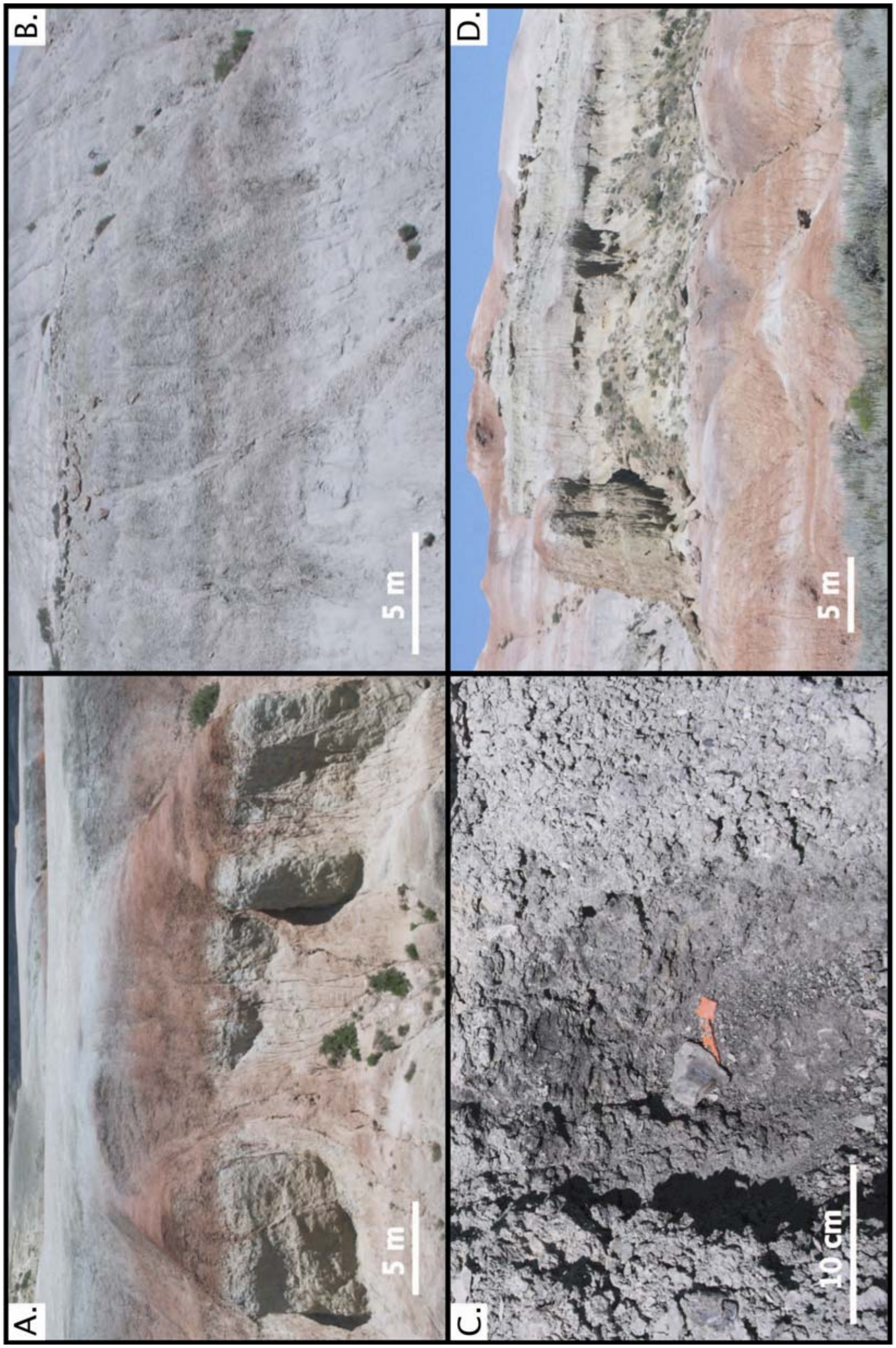
A.
5 m
B.
5 m
C.
10 cm
D.
5 m

Figure 2.9 – Fine-grained, pedogenically-altered facies of the Cathedral Bluffs Tongue. **A.** Bright red paleosols of facies P3 underlying the dark grey to black paleosols of facies P2. This is near the top of the Cathedral Bluffs section, and the lacustrine margin mudflats of facies P2 grade upwards into lacustrine shales of the Laney Member. **B.** Poorly developed paleosols of facies P1 that occur within the avulsion-belt deposits (DS2) of Bush Rim. **C.** The recessive dark grey mudstones of facies P2. Desiccation cracks and limestone beds commonly occur in this facies. **D.** A thick, amalgamated channel package overlying the bright red to purple paleosol of facies P3. Sub-aerial exposure allowed the paleosols to become well-drained and oxidized.

Interpretation

The black to dark grey colour of this facies is attributed to the high amount organic material preserved within the sediment. Evidence of wetting and drying in the form of pedogenic slickensides and desiccation cracks leads to the interpretation that this facies was periodically inundated by water (Kraus and Aslan, 1993). This facies is interpreted to represent the lake margin mudflats. The presence of coal and limestone sediment indicates a high water table, and deposition within ponds and swamps (Eberth and Miall, 1991). This facies only occurs in the most distal sections, as well as near the contact between the Cathedral Bluffs Tongue and the Laney Member of the Green River Formation.

Facies P3 – Red / Orange Silt and Mud

Description

Light to dark red, purple, and pink mudstone, siltstone and very fine-grained sandstone characterize facies P3 (Fig. 2.9 A,D). Horizon thickness shows a large variation, but can be up to 5 m thick, much thicker than P1 and P2. No sedimentary structures are observable and pedogenic slickensides are common and moderately extensive. Soil horizons are well developed. Ichnofossils such as *Naktodemasis* and *Camborygma* (Fig. 2.10A-B) are observed, as well as rhizoliths. Bioturbation indices are very high (B.I.=6). This facies occurs commonly above other pedofacies, and together are typically bounded by facies Shr. This facies is often erosionally overlain by facies St, Shr, and rarely Gt.

Interpretation

The red colouration of these paleosols indicates high oxidation state of iron. This may indicate long periods of sub-aerial exposure and well-drained conditions. The high thickness of these paleosols is attributed to pedogenesis overprinting previous paleosol horizons into one thick well-drained paleosol horizon. The high degree of bioturbation indicates that sedimentation rates were very low. It is possible that the top of this facies represents an erosional or non-depositional surface, where pedogenesis may have occurred during a period of sediment bypass. The presence of sandy facies sharply above (St, Shr, and Gt) would indicate an erosional event. Other pedofacies and facies Shr conformably overly this facies and indicate periods of non-deposition.

2.4. Facies Associations

2.4.1. Facies Association 1 (FA1): Fluvial Channel Association

Description

Facies Association 1 (FA1) occurs as laterally confined, lenticular bodies composed of sand and gravel facies (St, Sp, Gmh, and Gt). The basal contact is erosional and commonly displays a poorly sorted, conglomeratic base. Individual channel bodies are often amalgamated to form larger channel belt deposits. The morphology is highly variable, ranging from small (~1.5 meters thick, ~50-100 meters wide) to large (~8 meters thick, 100's meters wide) bodies of channelized sandstone. Fining upward sequences occur in beds 20 to 100 cm thick. Smaller fining upwards sequences, on the order of 5 cm, are observed in laminae within the beds. For facies Gmh and Gt it is difficult to determine the bedding thicknesses, as there is no distinct

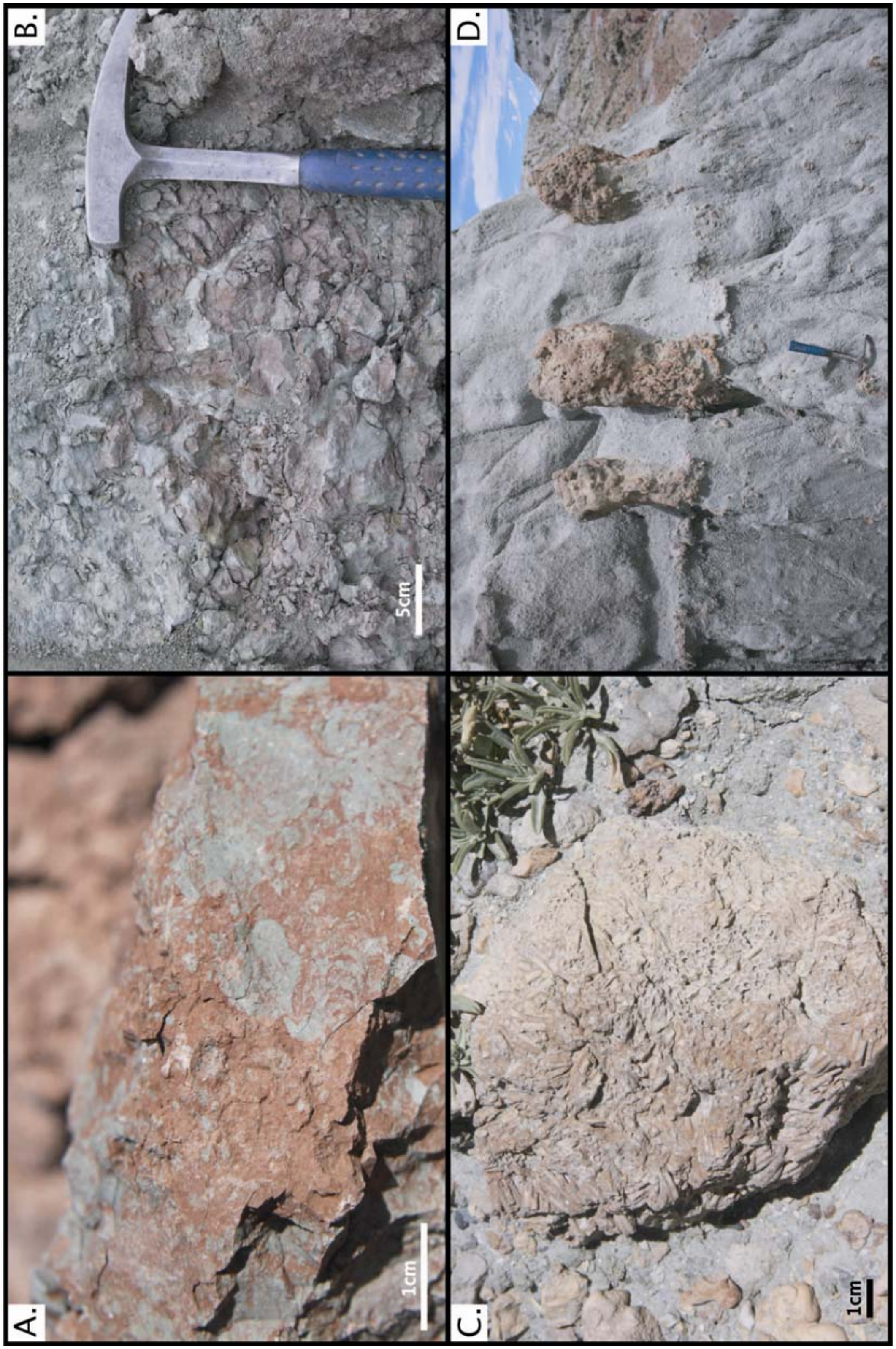
A.
1cm
B.
5cm
C.
1cm
D.

Figure 2.10 – Trace fossils observed within the fine-grained facies and paleosols of the Cathedral Bluffs Tongue. **A.** *Naktodemasis* burrow in a red and green mottled mudstone. This is a backfilled meniscate trace, interpreted to be formed by burrowing insects (Smith, 2007). **B.** *Camborygma* in a mottled, but dominantly green mudstone. **C.** Caddisfly pupal cases. This is a broken piece of carbonate mounds constructed of the pupal cases that can reach up to 60 cm thick in the study area. **D.** Nest-like features within very fine-grained sandstone to siltstone beds. Hammer for scale is 33 cm long.

bedding. For facies Gt, the trough depth looks to be approximately 1 to 2 meters, with widths of approximately 4 m. Some troughs occur as solitary lens-shaped bodies quickly fining up into sandstone, but more commonly they are amalgamated, with upper troughs cutting into lower troughs.

This association commonly overlies FA3 (overbank fines) and is generally overlain by FA2. Ichnofossils within this association are quite rare due to the coarse grained, conglomeratic nature of the sediment. There are occurrences of ichnofossils, however, in the fine- to medium-grained sandstone observed at some locations. Traces observed include large (>20cm) cf. *Arenicolites* (Fig. 2.11D), cf. *Edaphichnium* (Fig. 2.11E), and one *Glossifungites*-like surface (SP10-10) was observed at a basal unit contact.

At the most northern section (SP10-03), at an approximate distance of 25 km from the base of the Wind River Mountains, the coarsest beds are gravel / pebble conglomerate with clasts up to 20 cm in diameter. Moving 10 km south to an intermediate section (SP10-04), the coarsest units are coarse- to very coarse-grained sandstone with rare clasts up to 5 cm in diameter. At the southern-most measured section (SP10-01) located around 50 km south of the Wind River Mountains, the coarsest sediments are fine- to coarse-grained sandstone, rarely displaying very coarse sand to fine gravel bases.

Interpretation

FA1 is interpreted to represent channelized fluvial flow changing from gravel-dominated braided rivers (in proximal settings), with sandy overbank deposits, to sandy meandering rivers further away from the Wind River uplift (i.e. in distal settings). FA1 corresponds to the channel (CH) architectural element. The sedimentary structures, as well as the geometry and breadth of the beds, leads to a fluvial interpretation. The presence of trough cross-stratified sands and fining upwards sequences with mud rip-up clasts at the base of the channels are consistent with fluvial sedimentation (Miall, 1996; Blum and Aslan, 2006). Floodplain erosion probably occurred during channel avulsion, which created the rip-up mud clasts (Bridge, 1984). Cut-bank erosion during lateral channel migration is another process that can erode floodplain deposits and include the rip-up clasts within FA1.

Intermittent movement along the Wind River Thrust Fault caused uplift in the source area and subsidence in the basin, therefore increasing the gradient of stream-profile (Steidtmann and Middleton, 1991; Roehler, 1992a). This resulted in a change in channel morphology and increase in grain size carried by the river system. Channel morphology is interpreted to change from gravel-braided rivers in proximal settings (such as sections SP10-03 and SP10-06) to sandy meandering rivers in settings distal to the Wind River uplift (such as sections SP10-07 through SP10-01). Gravel beds are preserved by the migration of longitudinal bars, transverse bars, and small chute-fill gravels during maximum discharge in the rivers (Hein and Walker, 1977; Gustavson, 1978; Miall, 1996). Gravel beds eventually pinch out basinward and are not present within more distal sections such as those along Bush Rim. Trough-cross bedded sandstone (St) is the most common facies within FA1, preserved by the migration of linguoid 3-D dunes along the streambed (Miall, 1996). The basal surface of this facies association can erode down many meters into the underlying sediment.

2.4.2. Facies Association 2 (FA2): Crevasse Splay Association

Description

This facies association is composed of sandstone facies (Shr, Sp, and St) and occurs as extensive (100's of meters to a few kilometers) sheet-like sandstone bodies or as thin (50 cm to 2 m thick), restricted channels (3 to 15

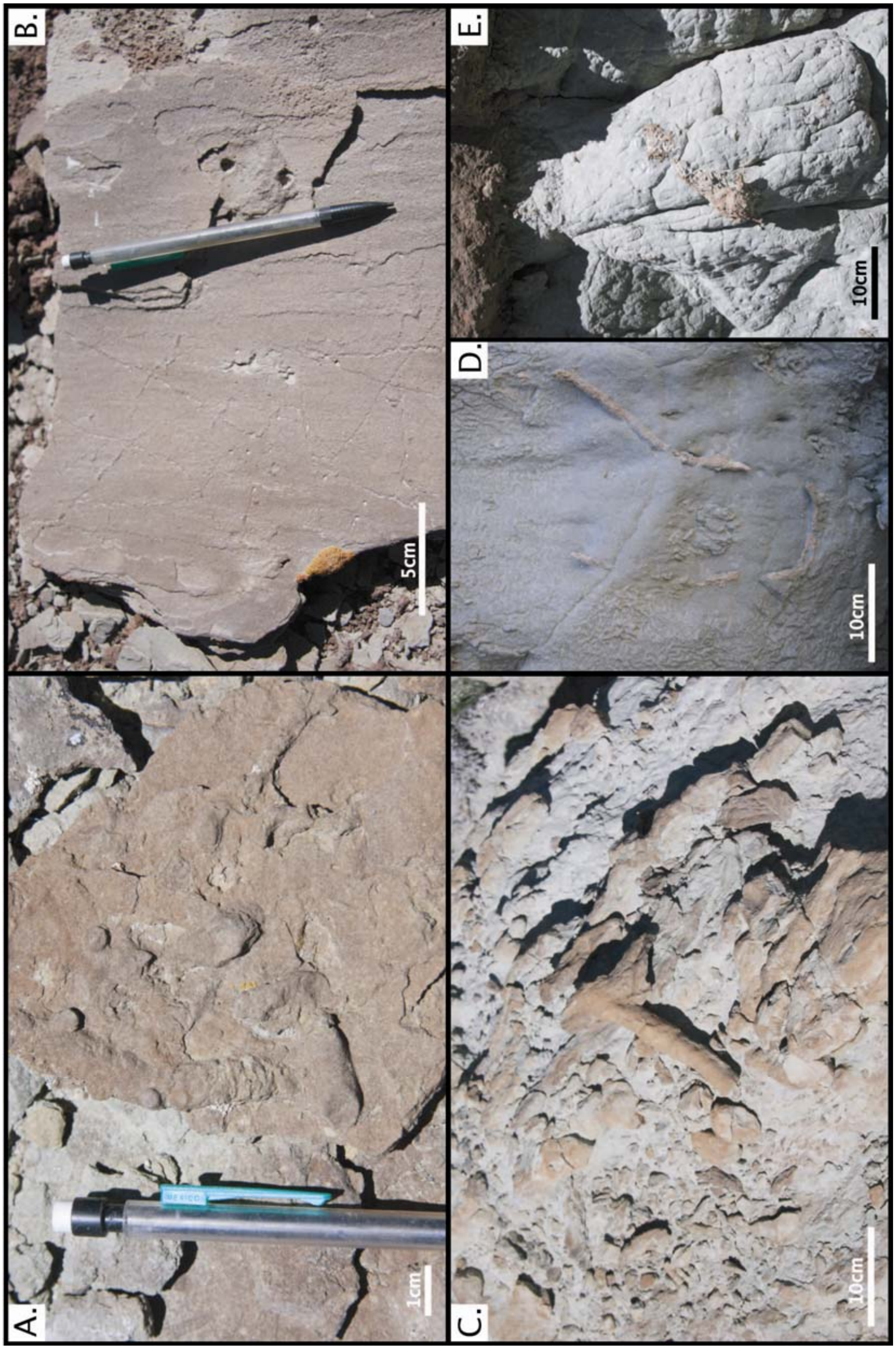
A.
1cm
B.
5cm
C.
10cm
D.
10cm
E.
10cm

Figure 2.11 – Ichnofossils within the sandstones of the Cathedral Bluffs Tongue. **A.** Dominantly horizontal to subvertical backfilled traces, belonging to either *Ancorichnus* or *Scoyenia* ichnogenus occurring on the upper surface of a crevasse splay sandstone. **B.** Thin (1-2 mm) backfilled horizontal traces on the parting lineation of a crevasse splay sandstone. **C.** Root traces on the upper surface of a crevasse splay sandstone. **D.** Large *Arenicolites*-like burrow within a very fine- to fine-grained channel sandstone. **E.** A large *c.f. Edaphichnium* burrow within very fine- to fine-grained channel sandstone.

m wide). Horizontal plane-bedded (with parting lineation), tabular cross-bedded, and ripple cross-bedded sandstone occurs within sheet-like beds. Small-scale trough cross-bedding is observed in the small channelized sandstone bodies. The tops of these sandstone units are often highly bioturbated (B.I. 5-6) and rework any primary sedimentary structures. Traces observed include *Ancorichnus, Skolithos, Lockia, Edaphichnium* and *Camborygma,* as well as fossil roots and branches. Abundant disarticulated fossil material (turtle, crocodilian, mammalian), and occasionally reworked stromatolitic material is found within this association. FA2 commonly bounds packages of FA3, and is also found overlying FA1. The basal contacts of these beds are sharp and in some instances erosional, while the upper contact can be sharp to gradational.

Interpretation

Facies association 2 is interpreted to represent crevasse splay (architectural element CS) and crevasse channel (architectural element CR) deposits. Extensive sheet-like splays may occur during large flood occurrences (Smith *et al*., 1989; Kraus and Aslan, 1993; Rhee and Chough, 1993). The crevasse channel deposits occur within the crevasse splay, distributing water and sediment across the splay. Planar-horizontal bedding is interpreted to be the result of upper flow regime laminar (super-critical) flow in unconfined sheetflows, with Froude numbers greater than 1 (Boggs, 2001; Prothero and Schwab, 2004). As flow wanes or the water becomes deeper, the Froude number drops below 1 and turbulent flow produces current-rippled sand (Prothero and Schwab, 2004). As flow continues to wane, the very fine- to fine-grained sandstone may grade upward into silt or show a sharp top contact. Less commonly planar-cross bedded sand is observed, interpreted as 2-D dune migration within small crevasse channels. This association is most often associated with avulsion deposits and occurs with relatively immature paleosols (Aslan and Autin, 1999; Davies-Vollum and Kraus, 2001). Sedimentation rates will be highest near the channel, where crevasse splay and overbank deposits are rapidly deposited (Bown and Kraus, 1987; Davies-Vollum and Kraus, 2001; Blum and Aslan, 2006).

The ichnofossil suite observed in this facies association indicates rapid deposition and subsequent non-deposition. The sandstone beds show low bioturbation through the beds, with thoroughly bioturbated tops (Fig. 2.11A). Often *c.f. Edaphichnium* burrows (Fig. 2.11E) occur below these sheet-like sandstone beds, but it is indeterminate whether they were present before the splay, or were formed afterwards. The presence of *Camborygma* indicates that the environment was sub-aerially exposed, at least temporarily, after deposition (Smith, 2007).

2.4.3. Facies Association 3 (FA3): Pedogenically-altered Overbank Fines Association

Description

Facies Association 3 (FA3) is composed of mudstone, siltstone, and very fine-grained sandstone. This facies association dominates the preserved succession within the study area, especially in the southern and eastern sections. It includes all of the pedofacies (P1-P3) and generally overlies FA2 (crevasse splay). FA3 is also capped by FA2 or incised by FA1. Purple, red, green, and grey to black variegated bands characterize this association. The thickness of these bands can range from 10 cm to over 2 m. Distinct beds containing abundant carbonate (1 to 10 cm) and siderite (mm to 3 cm) concretions are observed and weather out of the outcrop. Bed thicknesses vary from 30 cm to over 1 meter. Packages of FA3 can be tens of meters thick, or thinner with FA2 interbedded throughout. Small (5 to 40 cm) slickenside surfaces are observed with lustrous clay coats along the surface. FA3 commonly lies gradationally over FA2. The top contact of this association is always sharp, commonly with FA2 or erosional overlain by FA1. Less commonly FA4 and FA5 overly this association, but the top contact is still sharp. Typically, the thicker the package of FA2 underlying FA3, the less mature the paleosols will be. It has been observed that P3 paleosols may overly thin (<10cm) packages of FA2. Paleosol profiles tend to overly one another, and their pedofacies tend to change upwards to less mature paleosols before FA2 caps the package.

Paleosol profiles can range in thickness from 20 cm to over 3 m. Specific soil horizons also have wide range of thicknesses. The A-horizon can be green, grey, or dark grey to black. Typically the A horizon is thin (5 to 30 cm) or completely absent creating a 'naked' B-horizon (Kraus and Gwinn, 1997). The B-horizon has a wide range of thicknesses, ranging from 20 cm to approximately 2 meters. It is generally red, but can range from orange to deep purple in facies P3. The C-horizon is commonly green to light grey, regardless of pedofacies and ranges in thickness from 15 to 75 cm.

These beds are variably bioturbated and are dominated by the traces *Naktodemasis* and *Camborygma,* with subordinate amounts of *Planolites*- and *Skolithos*-like traces. Facies P1 is generally less bioturbated that facies P2 and P3. Fossils are relatively rare compared to FA2, but those fossils that are present are commonly better articulated. Emydid turtles have been discovered with the plastron and the carapace articulated. Rhizoliths with preserved organic material and other plant material are commonly observed in this association (especially P1). A thin (10 cm) lignitic bed caps this association at SP10-01.

Interpretation

The variegated beds of FA3 are interpreted to represent ancient soil horizons (paleosols). This facies association is interpreted to represent the overbank areas of an alluvial plain. Although in a broad geological sense the system may be considered to have continually aggraded, considering sedimentation rates for this facies association to be continuous is specious. Sedimentation was episodic, depending on the frequency of flooding or splaying of the trunk channel. The variable stages of paleosol maturity indicate variable, episodic sedimentation rates that are primarily dependent on proximity to a main channel (Bown and Kraus, 1987; Daniels, 2003). Pedogenic alteration occurred as the sediment was sub-aerially exposed for long periods of time. Depending on the amount of sediment introduced to the floodplain during a flood event, it may have been incorporated into the soil profile, or alternatively may have buried the previous profile and initiated a new sediment package that would subsequently undergo pedogenic alteration (Daniels, 2003).

Paleosol profiles commonly overly one another, until they are interrupted either by FA1 or FA2. The maturity of the paleosol sets commonly decreases upwards to a point in which a crevasse splay sheet or channel incises into it. This implies gradual movement of fluvial channels towards a given point during deposition of individual paleosol sets. The degree of pedogenic-alteration of mudstone successions is due primarily due to the proximity to the trunk channel (Bown and Kraus, 1987, Kraus, 1999). The controlling process for deposition of paleosol sets is sedimentation rate and time (Daniels, 2003).

Ichnological evidence is consistent with the interpretations made from pedogenic and sedimentary features. The presence of *Camborygma* within these soils indicates sub-aerial exposure at least temporarily on the floodplain surface (Smith, 2007). These were likely open burrows coming down from a relatively stable paleo-surface (Smith, 2007). *Naktodemasis* also indicates relatively dry conditions at the top of paleosol profiles. These traces were likely produced by terraphilic to hygrophilic (living above the water table) burrowing insects (Smith, 2007; Smith *et al.,* 2008).

2.4.4. Facies Association 4 (FA4): Palustrine to Lacustrine Margin Association

Description

Facies association 4 (FA4) is composed of white lime mudstone (facies Lm), green mudstone with minimal pedogenic alteration (facies P1), and dark grey to black mudstone (facies P2). Facies Lm and P1 occur as interlaminated (mm scale) or interbedded (cm-dm scale) deposits ranging from 50 cm to 1.5 meters in thickness. The extent of these deposits is relatively unknown due to the recessive and mostly covered nature of these beds in outcrop. Correlations across Bush Rim have connected these deposits over several kilometers. Facies P2 commonly displays desiccation cracks and vertical tube-like traces. Mottling and siderite nodules are common within this facies association. *In situ* stromatolites occur infrequently within FA4. Commonly stromatolitic material is remobilized and deposited within other facies associations. Caddis-fly pupal case carbonate mounds were also observed at section SP10-12. FA4 is frequently overlain by FA5 or FA3, and less commonly FA2. Underlying this facies association is generally FA5 or FA3.

Interpretation

This facies association is interpreted to represent deposition in floodplain ponds, lagoonal lacustrine settings, and lacustrine margin mudflats. Ponds are interpreted to represent periods of relatively high water table or regional lacustrine transgression. This is reinforced by the association of FA4 above or below with FA5, which indicates the maximum extent of lacustrine transgression in the Green River Basin. Although the lithologies of this facies association can be traced for several kilometers, they are not interpreted to be connected as one floodplain pond, but rather reflect a period where the water table was high, which allowed multiple ponds to form on the floodplain. The interbedding within this facies association is interpreted to represent seasonal variation or flood frequency. Carbonate deposition occurs when clastic input is restricted / terminated (during dry periods), and silt and mud are brought into the system by heavy rainfall or flooding. Thin oil shale beds are commonly observed over and underlying these deposits. The presence of desiccation cracks and mottles within this facies association indicates periods of wetting and drying (Kraus and Aslan, 1993; Kraus, 1999), consistent with a lacustrine margin mudflat interpretation. Stromatolites and caddisfly carbonate mounds strongly indicate a lacustrine margin environment (Leggit *et al*., 2007).

2.4.5. Facies Association 5 (FA5): Lacustrine Shale Association

Description

This facies association is abundant within the overlying Laney Member of the Green River Formation. However, in the Cathedral Bluffs Tongue, only thin (5 to 20 cm), continuous (over a few kms) beds of organic-rich oil shale (facies Fsh) occur in the most basinward (southern) sections. Organic-rich shale (facies Fsh) and lime mudstone (facies Lm) are often interbedded in mm to cm scale beds. The organic rich beds are fissile and easily recognizable in outcrop as they distort into convolute laminae when they are exposed to sun and air. Contacts with the over- and underlying strata are generally quite sharp. Small coprolites and scattered fish bone are common in this facies association. FA5 is commonly bound both above and below by FA4. Less regularly, FA3 may occur above or below this facies association.

Interpretation

FA5 is likely deposited within the deep (profundal) stratified water column of Lake Gosiute during an interval of maximum lacustrine transgression. This is the only true lacustrine facies observed within the Cathedral Bluffs Tongue. Facies Fsh must be deposited in quiet, dysoxic water conditions to preserve the amount of organic material within it (Bohacs *et al.,* 2000; Dypvik and Harris, 2001). Planar laminae, preservation of both small and moderate-sized coprolites and an absence of scour surfaces all support the interpretation of deposition within a quiescent setting (Wells *et al.,* 1993). The scattered fish skeletal debris observed on many bedding planes likely attests to the activity of scavengers although taphonomic analyses have not been conducted to support this interpretation (Wilson, 1987; Wells *et al.,* 1993). Therefore, this association indicates periods of lacustrine transgression. The interbedding of Fsh and Fm may be attributed to seasonal runoff bringing fine-grained clastic sediment into the lake. Seasonal runoff would also bring nutrients into the lake, increasing the amount of organic material present. During periods with no clastic input to inhibit carbonate production (Tucker *et al.,* 1990), carbonate mud (facies Lm) slowly accumulated until the next influx of clastic sediment.

Lake level is determined by a complex interplay of subsidence, sedimentation rate, and climate. Due the size of Lake Gosiute, it is unlikely that high rates of precipitation could have had much affect on lake level. However, it is interpreted that a low gradient near the lakeshore could have accounted for large scale flooding of the alluvial plain with only a slight increase in base level. Also, it is unknown whether the effect of tectonics and subsidence would not have such a quick, acute effect on the lake level.

2.5. Discussion

2.5.1. Provenance

The provenance of the Cathedral Bluffs Tongue of the Wasatch Formation can be determined by identifying the mineral components and their relative abundances. Sediment within the Cathedral Bluffs Tongue was derived from the nearby Wind River Mountain Range (Fig. 2.12). Initial uplift

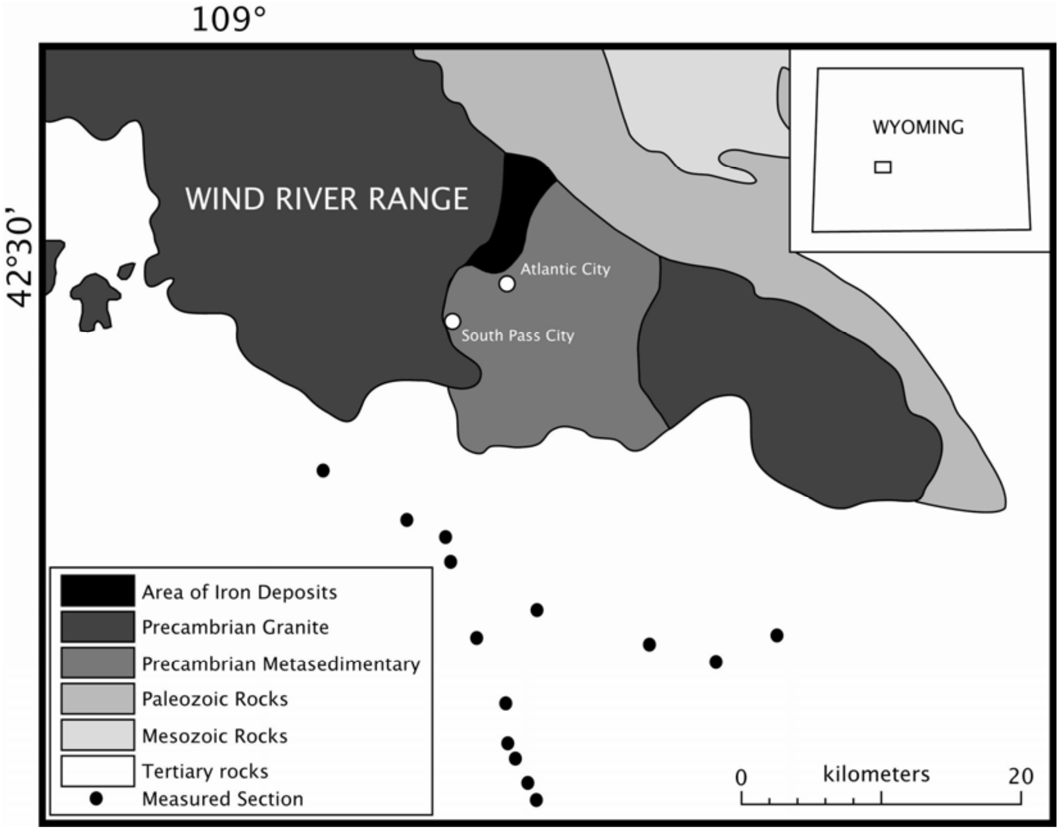

Figure 2.12 – Lithologies of the basement-core of the Wind River Mountain Range, showing the positions of all measured outcrop sections. Modified from McGee, 1983.

of the range began in the early Cretaceous with sediment shed into the basin by the late Cretaceous (Hall and Chase, 1989; Steidtmann and Middleton, 1991). The basement-core of the Wind River Mountains is mainly composed of Archean gneiss, supracrustal rocks, intrusive granites, and granodiorites (McGee, 1983; Hall and Chase, 1989). The southern end of the range consists of a belt of low-grade metasedimentary and metavolcanic rocks (McGee, 1983; Hall and Chase, 1989). Near Atlantic City (Fig. 2.12), a Precambrian banded iron formation outcrops, sourcing large amounts of epidote and magnetite to the sediments in the Green River Basin (McGee, 1983). The grain lithologies observed in the Cathedral Bluffs sediments are indicative of this source to the northeast of the study area (McGee, 1983).

Conglomerate clasts observed in the Cathedral Bluffs Tongue include low-grade schist, quartzite, and low-grade metamorphosed fine-grained sandstone. Thin section analyses have led to the identification of significant amounts of epidote, garnet, and opaque minerals dominated by magnetite (Fig. 2.13C-D). The lithology of the conglomerate clasts, as well as the identification of epidote and magnetite in thin section, indicates that the source of sediment comes from the belt of Precambrian metasedimentary rocks east from South Pass City and Atlantic City. Quartz and alkali feldspar are the dominant components of the sandstone units, with subordinate lithic fragments. Using Dott (1964) classification scheme, the sandstone of the Cathedral Bluffs Tongue is classified as an arkosic arenite. However, the sandstone commonly has a fine-grained matrix composed of sericite, chlorite, and other clay minerals suggesting classification as arkosic wackestone (Fig. 2.13B).

McGee (1983) reported bimodal paleoflow orientations from the Main Body of the Wasatch through the Tipton Tongue and into the Cathedral Bluffs Tongue depocentre. Southwestern and southeastern flow orientations were observed, indicating that changes in the drainage patterns occurred through time (McGee, 1983). Differential faulting within the Wind River Mountains likely caused the change in drainage. Uplift occurred as a series of events along with the post-Laramide orogeny during the Eocene and Oligocene (Steidtmann *et al*., 1989; Roehler, 1991). The importance of this is that the source of sediments changed with changing drainage patterns after intermittent tectonic events. Evidence for this occurs at the sections along the Continental Fault in the study area. The Continental Fault is now a normal fault that collapsed along the southern end of the Wind River Range (Hall and Chase, 1989). However, during the Eocene the fault was a positive feature. The large (~3 m diameter) granite boulders observed on the surface of Pacific Butte are sourced from the Continental Fault. Boulder conglomerate facies occur all along the southwestern margin of the Wind River Mountains, adjacent to the trace of the Continental Fault (Steidtmann and Middleton, 1991; Pietras *et al.,* 2003). The boulders in the study area were not observed *in situ*, but are interpreted to be sourced from above the

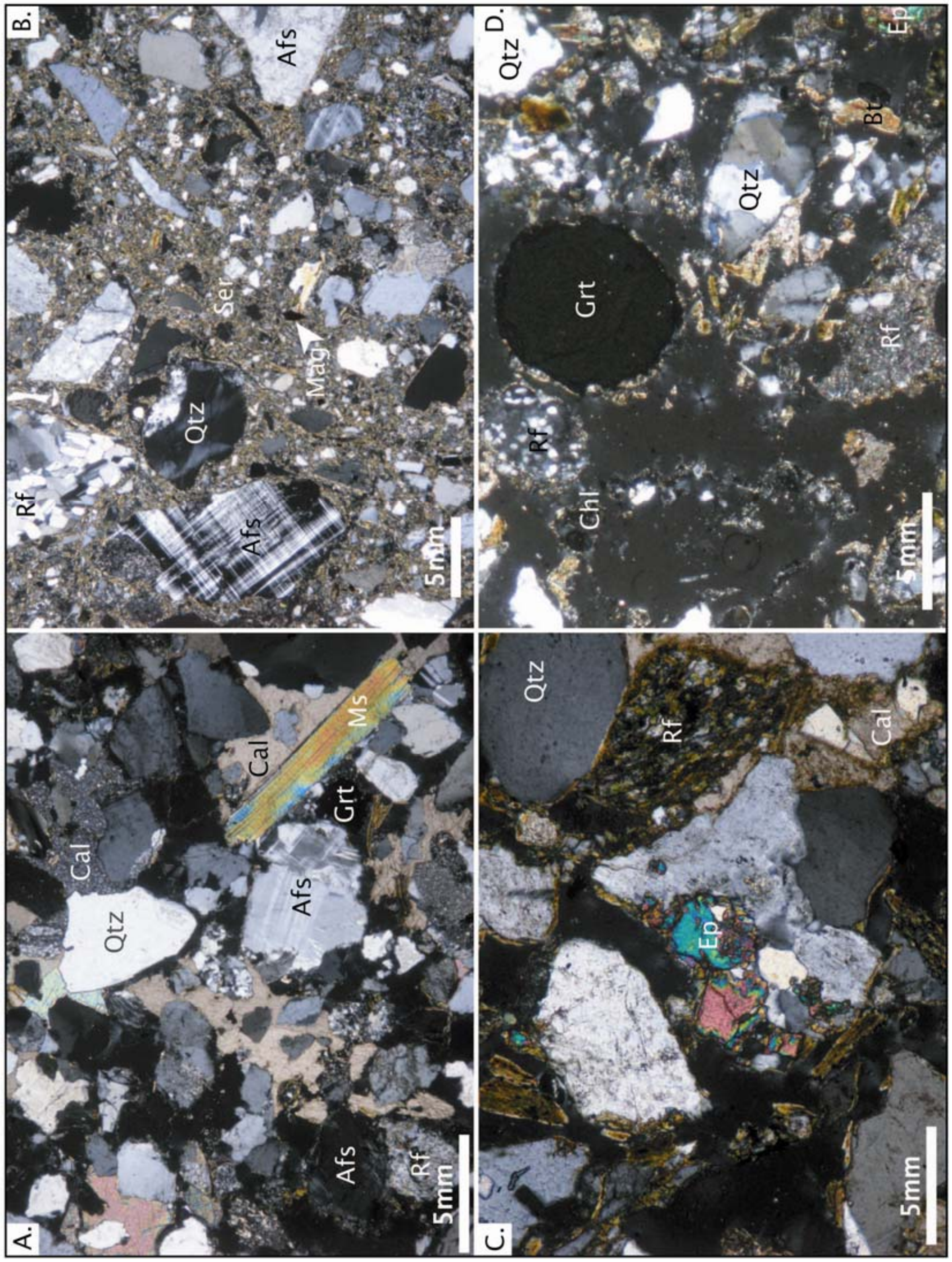
A.
Qtz
Cal
Afs
Grt
Ms
Rf
5mm
B.
Rf
Afs
Qtz
Ser
Mag
5mm
C.
Qtz
Rf
Cal
Ep
5mm
D.
Qtz
Bt
Ep
Grt
Rf
Chl
5mm

Figure 2.13 – Thin sections of sandstone beds within the Cathedral Bluffs Tongue. Qtz = quartz, Afs = alkali feldspar, Rf = rock fragment, Cal = calcite, Grt = garnet, Ms = muscovite, Ep = epidote, Chl = chlorite, Ser = sericite. **A.** Thin section of SP10-07 at 36.2m showing subangular quartz, feldspar, and muscovite grains with a poikilotopic calcite cement. **B.** Thin section of SP10-07 at 1.4m. Grains are still very immature, but a fine-grained sericite (clay) matrix is displayed. **C.** Thin section of SP10-09 at 5.1m showing the presence of epidote within the study area. **D.** Thin section of SP10-03 at 18.45m showing large a large subhedral, rounded garnet grain. There is no matrix or cement in this sample, only epoxy between grains.

measured section at SP10-06. These boulder conglomerate beds have been interpreted to be exhumed alluvial fans (Pietras *et al*., 2003).

2.5.2. Avulsion Stratigraphy

Channel avulsion is a common process in fluvial sedimentology that contributes significant amounts of sediment to the floodplain (Aslan and Autin, 1999; Davies-Vollum and Kraus, 2001; Aslan *et al*., 2005). Avulsion stratigraphy has been studied extensively in modern environments (Smith *et al.,* 1989; Kraus and Aslan, 1993; Aslan *et al.,* 2005) to help identify and classify avulsion deposits in the rock record (Kraus, 1996; Davies-Vollum and Kraus, 2001; Blum and Aslan, 2006). Channel reoccupation (slow creation of accommodation, gradual aggradation) and aggradational avulsion (rapid creation of accommodation, high aggradation rates) are the two main avulsion types identified in modern and ancient environments (Aslan and Blum, 1999; Morozova and Smith, 1999; Davies-Vollum and Kraus, 2001).

The cause of avulsion is a complex interplay between many autogenic (levee development, substrate cohesiveness, sinuosity, local topography) and allogenic (tectonics, climate, base level) factors (Bride and Leeder, 1979; Aslan and Autin, 1999; Kraus and Davies-Vollum, 2004). It has been shown from experimental data that cross-valley (S_c) to down-valley slope (S_d) ratio may be a controlling factor for river avulsion (Mackey and Bridge, 1995). Ratios of >8 (Slingerland and Smith, 1998) or 3 to 5 (Tornqvist and Bridge, 2002) have been proposed as thresholds for avulsion. For the modern

Mississippi River, ratios ranging from 16 to 110 have been recorded (Aslan *et al.*, 2005). These high ratios indicate that other factors, such as substrate composition and distribution of floodplain channels may make the channel more resistant to avulsion (Aslan *et al.*, 2005). It has also been suggested that avulsion may be a two-part process. First the necessary conditions must be created, and then a trigger event is needed to initiate the avulsion (Aslan *et al*., 2005).

The Cathedral Bluffs Tongue contains an especially heterogeneous interval containing sheet-like splay deposits (FA2) interbedded with poorly developed paleosols (FA3, facies P1). This 20 to 25 meter interval is exposed through the southernmost sections along Bush Rim and is interpreted to represent aggradational avulsion-belt deposits, similar to those of Davies-Vollum and Kraus (2001). The package is constrained above and below by deposits of mature, well-drained paleosols, representing more stable conditions on the floodplain. During periods of high accommodation, aggradational channel avulsion occurred. This resulted in the deposition of thick packages of poorly developed paleosols and splay sandstone beds. Above and below the avulsion-belt, accommodation space was likely low, and lateral channel migration across the floodplain would be more common. This can lead to interpretations about the position of base level as well as the other factors causing creation of accommodation space, namely tectonics. The abundance of splay deposits indicates that flow within trunk channels often breached the banks of the channel. The immaturity and thickness of the paleosols leads to the interpretation of rapid fine-grained sedimentation on the floodplain. Crevasse splay sandstone beds occur more commonly in this avulsion-belt than in the surrounding sediment. The splay deposits are also thicker through this interval, indicating a closer proximity to the trunk channel. At the top of the northernmost Bush Rim section (SP09-01) a large channel, interpreted to be a trunk channel, is present. This channel caps the avulsion-belt, possibly indicating the final position of the channel, as the fluvial gradient leveled out.

The thick, confined nature of this avulsion-belt leads to the interpretation of allogenic processes causing the avulsions. This can be attributed to many factors, such as movement along the Wind River Thrust Fault, uplift along the Continental Fault, or a climate change that increased the discharge from the rivers. Evidence of movement along the Wind River Fault during the deposition of the Cathedral Bluffs Tongue is shown at the Reds Cabin Monocline (Fig 2.14A). The lower beds of the Cathedral Bluffs Tongue have been folded, but the upper 15 to 20 m of the Cathedral Bluffs Tongue and the overlying Laney Member are not folded. This indicates that movement on the fault occurred during the latter stages of Cathedral Bluffs Tongue deposition. Additionally, fault scarp boulders within the Cathedral Bluffs Tongue show that the Continental Fault was a positive, likely mobile, feature at the time. At Pacific Butte and near Dickie Springs, both along the trace of the Continental Fault, fault scarp boulders are present, indicating alluvial fans coming off of the upthrown Continental Fault (McGee, 1983; Pietras *et al.,* 2003). Compressional forces at the time would have caused uplift of the source area, as well as possible increased subsidence rates in the basin (with increased sediment supply and discharge from uplifted source area). These factors may have caused a rapid increase in accommodation space leading to a thick package of aggradational avulsion deposits (Smith *et al*., 1989, Davies-Vollum and Kraus, 2001).

2.5.3. Alluvial Fan Architecture

The Cathedral Bluffs Tongue was deposited by fluvial processes on the distal portion of an alluvial fan system and the proximal portion of an alluvial plain. Proximal alluvial fan deposits are not preserved within the study area, likely due to post-depositional uplift and erosional removal (Pietras *et al.,* 2003). An overall decrease in grain size from north to south confirms that the source of sediment for the Cathedral Bluffs Tongue is to the north. Depositional style within the study interval changes with increased distance


A.
B.
C.
D.

Figure 2.14 – Structural elements and lithology of clasts within boulder and cobble conglomerate of the Cathedral Bluffs Tongue. **A.** Reds Cabin Monocline along the trace of the Wind River Thrust Fault. The resistant sandstone cliff is approximately 20 m thick. **B.** Coarse-pebble to cobble conglomerate observed at SP10-03. Clast lithologies are dominantly quartzite, low-grade metamorphic sandstone, and low-grade schist. Pogo for scale is showing 70 cm with 10cm divisions. **C.** Large ~3m diameter granite boulder observed along the Continental Fault. Boulders are not in place, but are interpreted to be part of the upper Cathedral Bluffs Tongue. Hammer for scale is 33 cm long. **D.** Precambrian banded iron formation boulder observed along the Continental Fault with the granite boulders. Hammer for scale is 33 cm long.

from the source area. The proximal portions of the fan at the northernmost part of the study area are interpreted to represent braided river deposits. Coarse-grained gravel conglomerate, along with fault scarp boulders and some potential debris flow deposits, occur encased within very fine- to fine-grained sandstone. These sandstone units are interpreted to indicate proximal overbank deposits, since evidence of pedogenic alteration is clear. Farther from the source area, the maximum grain size decreases significantly and depositional processes differed. In the distal part of the study area, overbank mudstone (FA3) dominates the succession with varying amounts of crevasse splay (FA2) and channel deposits (FA1). The fluvial style changed from braided to meandering as the fluvial gradient decreased basinward. This change occurred within a relatively short distance (~20-25 kms) indicating narrow depositional belts along the fringe of the Wind River Mountains.

The most distal sections in the study area occur near Bush Rim. The succession has been split into three main depositional sequences, labeled as depositional sequences 1 through 3 (Fig. 2.15).

Depositional Sequence 1 (DS1)

The first depositional sequence starts at the base of Bush Rim. It is dominated by overbank fines (FA3) and contains mature paleosols. A thick, dark red paleosol (facies P3) caps this depositional sequence and is very extensive across the buttes in the southeastern margin of the study area. It thickens to the north, and quickly grades into less mature paleosols. Interbedded claystone and marlstone, small channel sandstone units, stromatolite-encrusted logs, and desiccation cracks have all been observed in this depositional sequence. This indicates a lacustrine margin lowland environment. The base of the Cathedral Bluffs Tongue occurs at the base of the outcrop sections. Regional correlations indicate that lacustrine margin deposits occur at the base of Bush Rim. The thick, red paleosol capping this depositional sequence likely represents a depositional hiatus and prolonged sub-aerial exposure, suggesting that accommodation space was low and sediment bypassed the study area whilst being transported towards the basin centre.

Depositional Sequence 2 (DS2)

The second depositional sequence begins as a thick, continuous splay sandstone succession, or in some cases as the base of a channel sandstone bedset. Crevasse splay sandstone units and poorly developed paleosol successions dominate this depositional sequence. In some sections, channels are abundant. Stromatolite encrusted logs and stumps have also been observed. Reworked fragments of stromatolite occur commonly within the splay sandstone units. The abundance of splay sandstone and poorly developed paleosols leads to the interpretation that channel avulsion was common during the deposition of this depositional sequence.

Depositional Sequence 3 (DS3)

The last depositional sequence below the Laney Member of the Green River Formation is composed of mature paleosols with subordinate limestone and splay sandstone. The base of this depositional sequence occurs at a sharp change to dark grey muddy paleosols. There are three subunits within this depositional sequence. 1) Depositional sequence 3a is composed of dark grey / purple paleosol units with subordinate amounts of finely laminated lime mudstone and oil shale. This unit weathers to dark grey with

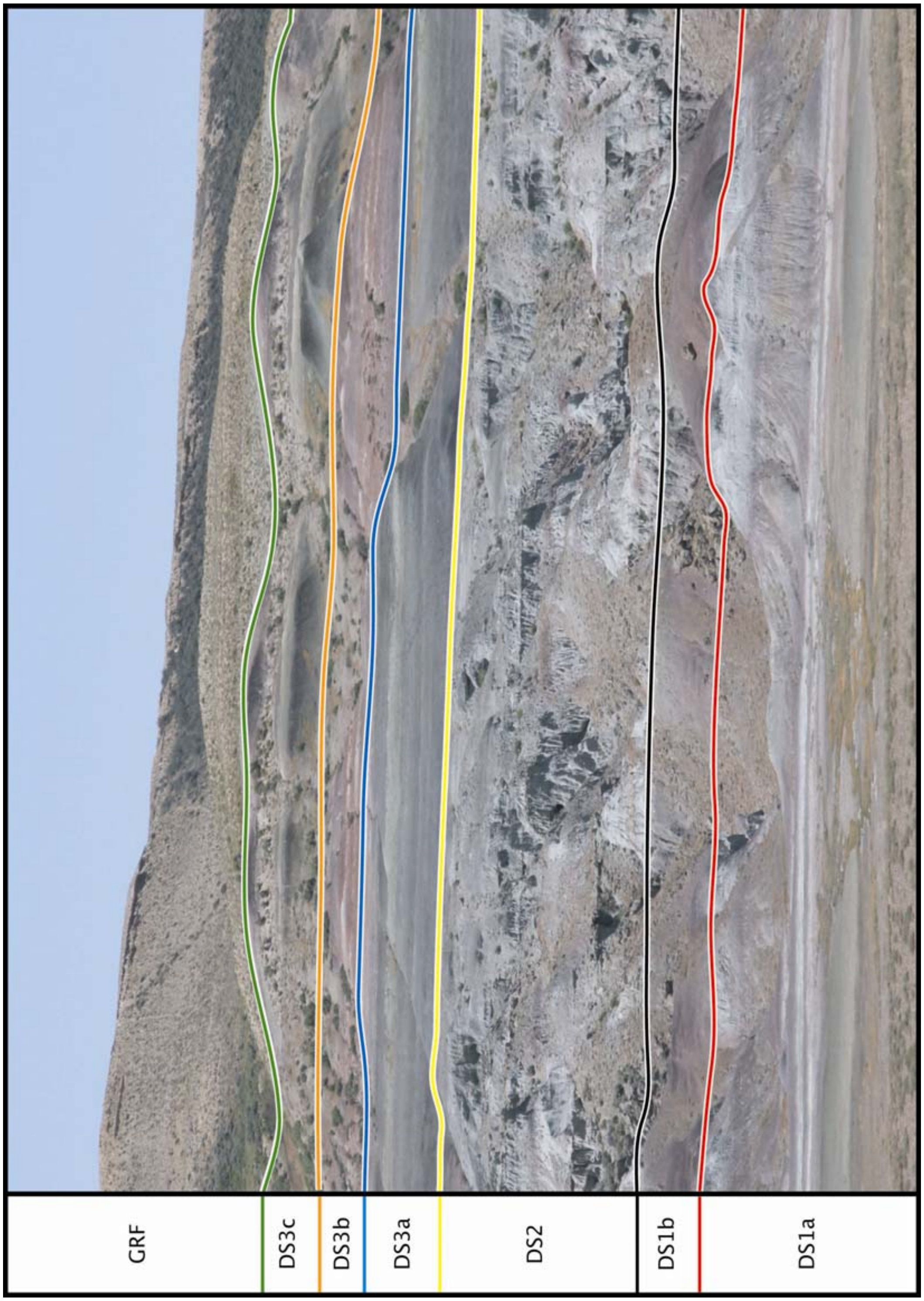

Figure 2.15 – Sedimentological architecture of the Bush Rim area. The light grey band in the middle (DS2) is interpreted to represent an avulsion belt. The section from the base to the Laney Member (green line) is approximately 60 meters.

a popcorn-like texture. In the distal sections, there is an absence of any sandstone beds in the unit. 2) Depositional sequence 3b is composed of thick, bright red paleosols with subordinate splay sandstone. The splay sandstone successions in this unit show ripple- and planar-laminae. 3) Depositional sequence 3c is also composed of dark grey mudstone, but also contains red and green mudstone as well. Bedded marlstone and oil shale also occur within this unit. Desiccation cracks, root traces, and planar laminae are also observed within the mudstone successions. Depositional sequence 3 was deposited as lake level was rising. The paleosol units exhibit hydromorphic features, which indicate that water table levels were high (Kraus and Aslan, 1993). The presence of FA4 in this depositional sequence indicates that the water table was high, as ponds were common on the floodplain during this interval. As well, emplacement of the overlying lacustrine Laney Member suggests that Paleolake Gosiute may have been rising during the latest stages of Cathedral Bluffs deposition.

2.6. Conclusions

The Cathedral Bluffs Tongue of the Wasatch Formation preserves early Eocene sediments deposited on alluvial fans and plains. Braided fluvial systems in the northwestern part of the study area segue into meandering channel successions to the southeast (Fig. 2.16). The study interval is dominated by overbank deposition suggesting that accommodation space was high to preserve this proportion of fine-grained sediment. Evidence of tectonic perturbations within Wind River Mountains Range concurrent with deposition of the Cathedral Bluffs Tongue, supports the interpretation that this was the controlling influence on facies association architecture. Abundant accommodation space is herein attributed to this active tectonism on the northern margin of the basin, causing high rates of flexural subsidence in the study area.

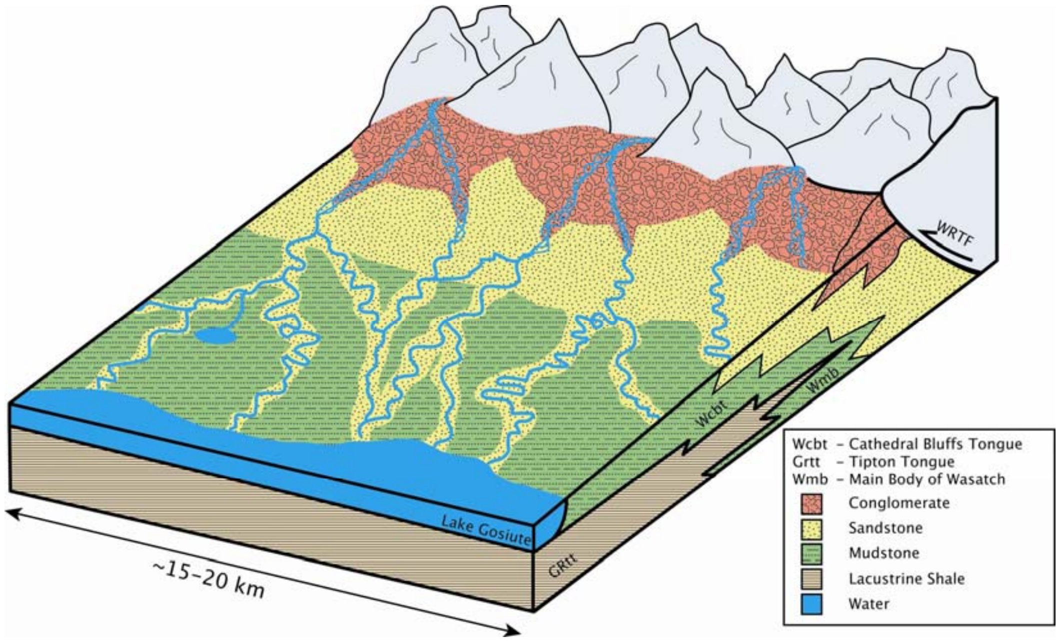

Figure 2.16 – Schematic diagram of the depositional environment for the Cathedral Bluffs Tongue. Alluvial fans were located very close to the orogenic belt, as braided rivers carried gravel-sized sediment basinward. Eventually the braided channels graded into meandering channels that were dominantly sandy. Downstream, the overbank areas were much finer grained, and sandstone lithologies are restricted to channel and channel associated processes.

The abundance of thick, poorly developed paleosols in the heart of the Cathedral Bluffs Tongue can be attributed to relatively high down valley gradients, causing channel avulsion to occur. Channel avulsion processes can deposit thick packages of overbank mudstone in a relatively quick time interval (Aslan *et al.*, 2005) and is common in areas with high depositional gradients. This was likely caused by uplift in the hinterlands. Identification of these avulsion deposits may aid future studies in the recognition of avulsion-belts in outcrop.

The depositional sequences observed and described indicate a simple model for Cathedral Bluffs deposition. DS1 indicates a period of lake level regression and ultimately base level fall. The thick, red paleosol cap of this depositional sequence indicates a period of low accommodation sediment bypass, which often occurs as base level is falling (Shanley and McCabe, 1994). DS2 indicates a progradation of fluvial units basinward, with frequent avulsion events. This depositional sequence is the coarsest package within the distal sections, and represents the time of furthest basinward extent of the Cathedral Bluffs Tongue. The base of DS3 demarcates the retrogradation of the Cathedral Bluffs Tongue. There is some variation in this deposition sequence, but generally the level of Lake Gosiute was rising up to the overlying Green River Formation.

2.7. References

Allen, J. R. L., 1982. Sedimentary structures: Their character and physical basis. v. I and II: Elsevier, Amsterdam, 594 pp.

Allen, P. A., and Heller, P. L., 2012. Dispersal and preservation of tectonically generated alluvial gravels in sedimentary basins, *in* Tectonics of Sedimentary Basins: Recent Advances. Edited by C. Busby and A. A. Perez, 111-130.

Anderton, R., 1985. Clastic facies models and facies analysis. The Geological Society Special Publication, v. 18, 31-47.

Aslan, A., and Autin, W. J., 1999. Evolution of the Holocene Mississippi River floodplain, Ferriday, Louisiana: Insights on the origin of fine-grained floodplains. Journal of Sedimentary Research, v. 69, 800-815.

Aslan, A., and Blum, M. D., 1999. Contrasting styles of Holocene avulsion, Texas Gulf Coastal Plain, U.S.A., *in* Fluvial Sedimentology VI. Edited by N. D. Smith and J. Rogers, International Association of Sedimentologists, Special Publication 28, 293–308.

Aslan, A., Autin, W. J., Blum, M. D., 2005. Causes of river avulsion: Insights from the late Holocene avulsion history of the Mississippi River, U.S.A. Journal of Sedimentary Research, v. 75, 650-664.

Blum, M. D., and Aslan, A., 2006. Signatures of climate vs. sea-level change within incised valley-fill successions: Quaternary examples from the Texas Gulf Coast. Sedimentary Geology, v. 190, 177-211.

Boggs, S., 2001, Principles of Sedimentology and Stratigraphy (third edition), Prentice-Hall, New Jersey, 726 pp.

Bohacs, K. M., Carroll, A. R., Neal, J. E., Mankiewicz, P. J., 2000. Lake-basin type, source potential, and hydrocarbon character: an integrated-sequence stratigraphic– geochemical framework, *in* Lake basins through space and time. Edited by E. H. Gierlowski- Kordesch and K. R. Kelts, AAPG Studies in Geology, v. 46, 3–34.

Bown, T. M., and Kraus, M. J., 1987. Integration of channel and floodplain suites, I. Developmental sequence and lateral relations of alluvial paleosols. Journal of Sedimentary Petrology, v. 57, 587-601.

Bradley, W. H., 1926. Shore phases of the Green River Formation in northern Sweetwater County, Wyoming. United States Geological Survey Professional Paper 140, 121-131.

Brewer, J. A., Smithson, S. B., Oliver, J. E., Kaufman, S., and Brown, L. D., 1980. The Laramide orogeny: evidence from COCORP deep crustal seismic profiles in the Wind River Mountains, Wyoming. Tectonophysics, v. 62, 165-189.

Bridge, J. S., 1984. Large-scale facies sequences in alluvial overbank environments. Journal of Sedimentary Petrology, v. 54, 583-588.

Bridge, J. S., and Leeder, M. R., 1979. A simulation model of alluvial stratigraphy. Sedimentology, v. 26, 617-644.

Carroll, A. R., and Bohacs, K. M., 1999. Stratigraphic classification of ancient lakes: Balancing tectonic and climatic controls. Geology, v. 27, 99-102.

Daniels, J. M., 2003. Floodplain aggradation and pedogenesis in a semiarid environment. Geomorphology, v. 56, 225-242.

Davies-Vollum, K. S., and Kraus, M. J., 2001. A relationship between alluvial backswamps and avulsion cycles: an example from the Willwood Formation of the Bighorn Basin, Wyoming. Sedimentary Geology, v. 140, 235-249.

Dott, R. H., JR., 1964. Wacke, greywacke and matrix; what approach to immature sandstone classification? Journal of Sedimentary Petrology, v. 43, 625-632.

Dott, R. H., J. R., and Bourgeois, J., 1983. Hummocky stratification: significance of its variable bedding sequences: reply to discussion by R.G. Walker et al.: Geological Society of America, Bulletin, v. 94, 1245–1251.

Dypvik, H., and Harris, N. B., 2001. Geochemical facies analysis of fine-grained siliciclastics using Th/U, Zr/Rb, and (Zr+Rb)/Sr ratios. Chemical Geology, v. 181, 131-146.

Eberth, D. A., and Miall A. D., 1991. Stratigraphy, sedimentology and evolution of a vertebrate-bearing, braided to anastomosed fluvial system, Cutler Formation (Permian-Pennsylvanian), north-central New Mexico. Sedimentary Geology, v. 72, 225-252.

Friend, P. F., 1983. Towards the field classification of alluvial architecture or sequence, *in* Modern and Ancient Fluvial Systems. Edited by J. D. Collinson and J. Lewin. International Association of Sedimentology Special Publication, v. 6, 345-354.

Gustavson, T. C., 1978. Bed forms and stratification types of modern gravel meander lobes, Nueces River, Texas. Sedimentology, v. 25, 401-426.

Hall, M. K., and Chase, C. G., 1989. Uplift, unbuckling, and collapse: Flexural history and isostacy of the Wind River Range and Granite Mountains, Wyoming. Journal of Geophysical Research, v. 94, 581-593.

Hein, F. J. and Walker, R. G., 1977. Bar evolution and development of stratification in the gravelly, braided, Kicking Horse River, British Columbia. Canadian Journal of Earth Sciences, v. 14, 562-570.

Johnson, P. L., and Andersen, D. W., 2009. Concurrent growth of uplifts with dissimilar orientations in the southern Green River Basin, Wyoming: Implications for Paleocene and Eocene patterns of foreland shortening. Rocky Mountain Geology, v. 44, 1-16.

Kraus, M. J., 1996. Avulsion deposits in lower Eocene alluvial rocks, Bighorn Basin, Wyoming. Journal of Sedimentary Research, v. 66, 354-363.

Kraus, M. J., 1999. Paleosols in clastic sedimentary rocks: their geologic applications. Earth-Science Reviews, v. 47, 41-70.

Kraus, M. J., and Aslan, A., 1993. Eocene hydromorphic paleosols: Significance for interpreting ancient floodplain processes. Journal of Sedimentary Petrology, v. 63, 53-463.

Kraus, M. J., and Bown, T. M., 1993. Short-term sediment accumulation rates determined from Eocene alluvial paleosols. Geology, v. 21, 743-746.

Kraus, M. J., and Gwinn, B., 1997. Facies and facies architecture of Paleogene floodplain deposits, Willwood Formation, Bighorn Basin, Wyoming, USA. Sedimentary Geology, v. 114, 33-54.

Kraus, M. J., and Davies-Vollum, S., 2004. Mudrock-dominated fills formed in avulsion splay channels: examples from the Willwood Formation, Wyoming. Sedimentology, v. 51, 1127-1144.

Leggit, V. L., Biaggi, R. E., Buchheim, H. P., 2007. Palaeoenvironments associated with caddisfly-dominated microbial-carbonate mounds from the Tipton Shale Member of the Green River Formation: Eocene Lake Gosiute. Sedimentology, v. 54, 661-669.

Mackey, S. D., and Bridge, J. S., 1995. Three-dimensional model of alluvial stratigraphy: Theory and application. Journal of Sedimentary Research, v. B65, 7-31.

Martinsen, O. J., Ryseth, A., Helland-Hansen, W., Flesche, H., Torkildsen, and Idil, S., 1999. Stratigraphic base level and fluvial architecture: Ericson Sandstone (Campanian), Rock Springs Uplift, SW Wyoming, USA. Sedimentology, v. 46, 235-259.

McGee, L. C., 1983. Laramide sedimentation, folding and faulting southern Wind River Range, Wyoming. PhD Diss., University of Wyoming, Laramie, 92 pp.

Miall, A. D., 1977. A review of the braided-river depositional environment. Earth Science Reviews, v. 13, 1-62.

Miall, A. D., 1978. Lithofacies types and vertical profile models in braided river deposits: a summary, *in* Fluvial Sedimentology. Edited by A. D. Miall, Canadian Society of Petroleum Geologists Memoir, v. 5, 597-604.

Miall, A. D., 1985. Architectural-element analysis: a new method of facies analysis applied to fluvial deposits, Earth Science Reviews, v.22, 261-308.

Miall, A. D., 1996. The geology of fluvial deposits; sedimentary facies, basin analysis, and petroleum geology. Spinger-Verlag: Berlin, 582 pp.

Miall, A. D., 1999. In defense of facies classification and models. Journal of Sedimentary Research, v. 69, 2-5.

Miall, A. D., 2010. Alluvial Deposits, *in* Facies Models 4. Edited by N. P. James and R. W. Dalrymple, 586 pp.

Morozova, G. S., and Smith, N. D., 1999. Holocene avulsion history of the lower Saskatchewan fluvial system, Cumberland Marshes, Saskatchewan Manitoba, Canada, *in* Fluvial Sedimentology VI. Edited by N.D. Smith and J. Rogers, International Association of Sedimentologists, Special Publication 28, 231–249.

Pietras, J. T., Carroll, A. R., and Rhodes, M. K., 2003. Lake basin response to tectonic drainage diversion: Eocene Green River Formation, Wyoming. Journal of Paleolimnology, v. 30, 115-125.

Prothero, D.R., and Schwab, F., 2004, Sedimentary Geology (second edition), W.H. Freeman and Company, New York, 557 pp.

Ramos, A. and Sopena, A., 1983. Gravel bars in low-sinuosity streams (Permian and Triassic, central Spain), *in* Modern and Ancient Fluvial Systems. Edited by J.D. Collinson and J. Lewin, International Association of Sedimentologists Special Publication, v. 6, 301-312.

Reading, H. G. (Editor), 1978. Sedimentary Environments and Facies. Blackwell, Oxford, 557 pp.

Reading, H. G., 1996. Sedimentary Environments and Facies (third edition), Blackwell Scientific Publications, Boston, 615pp.

Rhee, C. W., and Chough, S. K., 1993. The Cretaceous Pyonghae Basin, southeastern Korea: sequential development of crevasse splay and avulsion in a terminal alluvial fan. Sedimentary Geology, v. 83, 37-52.

Roehler, H. W., 1991. Revised stratigraphic nomenclature for the Wasatch and Green River Formations of Eocene age, Wyoming, Utah, and Colorado. United States Geological Survey Professional Paper 1506-B, 38pp.

Roehler, H. W., 1992a. Introduction to Greater Green River Basin geology, Physiography, and history of investigations. United States Geological Survey Professional Paper 1506-A, 14pp.

Roehler, H. W., 1992b. Correlation, composition, areal distribution, and thickness of Eocene stratigraphic units, Greater Green River Basin, Wyoming, Utah, and Colorado. United States Geological Survey Professional Paper 1506-E, 49pp.

Rust, B., 1972. Structure and process in a braided river. Sedimentology, v. 18, 221-245.

Selley, R. C., 1982. An Introduction to Sedimentology, 2nd edition. Academic Press, London 417 pp.

Shanley, K.W. and McCabe, P. J., 1994. Perspectives on the sequence stratigraphy of continental strata. AAPG Bulletin, v. 78, 544-568.

Slingerland, R., and Smith, N. D., 1998. Necessary conditions for a meandering-river avulsion. Geology, v. 26, 435-438.

Smith, N. D., 1974. Sedimentology and bar formation in the upper Kicking Horse River, a braided outwash stream. Journal of Geology, v. 82, 205-223.

Smith, N. D., Cross, T. A., Dufficy, J. P., Clough, S. R., 1989. Anatomy of an avulsion. Sedimentology, v. 36, 1-23.

Smith, J. J., 2007. Ichnofossils of the Paleogene Willwood Formation and the Paleocene-Eocene Thermal Maximum (PETM): Response of an ancient soil ecosystem to transient global warming. Ph D. Thesis, University of Kansas, 184 pp.

Smith, M. E., Carroll, A. R., Singer, B. S., 2008. Synoptic reconstruction of a major ancient lake system: Eocene Green River Formation, western United States. Geological Society of American Bulletin, v. 120, 54-84.

Steidtmann, J. R., Middleton, L. T., Shuster, M. W., 1989. Post-Laramide (Oligocene) uplift in the Wind River Range, Wyoming. Geology, v. 17, 38-41.

Steidtmann, J. R., and Middleton, L. T., 1991. Fault chronology and uplift history of the southern Wind River Range, Wyoming: Implications for

Laramide and post-Laramide deformation in the Rocky Mountain foreland. Geological Society of America Bulletin, v. 103, 472-485.

Tornqvist, T. E., and Bridge, J. S., 2002. Spatial variation of overbank aggradation rate and its influence on avulsion frequency. Sedimentology, v. 49, 891-905.

Tucker, M. E., Wright, P., Dickson, J. A. D., 1990. Carbonate depositional systems; I, marine shallow-water and lacustrine carbonates. United Kingdom: Blackwell Scientific Publishing.

Wells, N. A., Ferber, C. T., Ohman, J. C., 1993. Discriminate analysis of fish-bearing deposits in the Eocene Green River Formation of Utah and Wyoming. Palaios, v. 8, 81-100.

Wilson, M. V. H., 1987. Predation as a source of fish fossils in Eocene lake sediments. Palaios, v. 2, 497-504.

Zeller, H. D., and Stephens, E.V., 1969. Geology of the Oregon Buttes area, Sweetwater, Sublette and Freemont Counties, southwestern, Wyoming. U. S. Geological Survey Bulletin No. 1256, 60pp.

Zonneveld, J. -P., Bartels, W. S., and Clyde, W. C., 2003. Stratal architecture of an Early Eocene fluvial-lacustrine depositional system, Little Muddy Creek area, southwestern Green River Basin, Wyoming. Cenozoic Systems of the Rocky Mountain Region: Rocky Mountain SEPM, 253-287.

Chapter 3

Defining the stratigraphy of the Cathedral Bluffs Tongue utilizing spectral-gamma ray, sequence stratigraphy, and chemostratigraphy

3.1. Introduction

Sequence stratigraphy, a discipline that focuses on stratigraphic correlation of temporally equivalent, unconformity bound stratigraphic units, was first developed for coastal marine strata (Posamentier *et al.*, 1988; Van Wagoner *et al.*, 1990). Sequence stratigraphy works best in these settings because changes in sea-level affected depositional patterns the most in these areas. Small changes in sea-level can be recognized in coastal areas, whereas, small changes would not necessarily change the depositional conditions of deeper water or continental areas. The concept of sequence stratigraphy works on the basis of depositional patterns being affected by changes in base-level (Vail *et al.*, 1977; Posamentier *et al.*, 1988; Shanley and McCabe, 1991). Base-level is an "equilibrium surface… above which a particle can not come to rest and below which deposition and burial is possible" (Sloss, 1962, p. 416). The movement of this hypothetical surface controls the rate of creation or destruction of accommodation space. The amount of accommodation space and its rate of change are controlled by tectonic subsidence and eustacy (Posamentier *et al.*, 1988; Shanley and McCabe, 1991; Martinsen *et al.*, 1999).

The study of sequence stratigraphy has expanded into fluvial successions (e.g. Wright and Marriot, 1993; Shanley and McCabe, 1994; Olsen *et al.*, 1995; Kraus and Aslan, 1999; Martinsen *et al.*, 1999; Arnott *et al.*, 2002; Zonneveld *et al.*, 2003; Fanti and Catuneanu, 2010). Applying the concepts of sequence stratigraphy to continental, fluvial successions has proven somewhat problematic (Olsen *et al.*, 1995; Martinsen *et al.*, 1999; Arnott *et al.*, 2002; Catuneanu, 2006). In the fluvial realm, systems tracts and stratal surfaces have different expressions than their marine counterparts and remain poorly understood (Bohacs *et al.*, 2000). This is especially true for strictly continental basins, with absolutely no marine influence. Global eustacy has no direct effect on these basins; thus, other factors control sequence development. Climate and tectonics are the primary factors that control base-level, and therefore, the architecture of lacustrine basin margin successions (Carroll and Bohacs, 1999). Base-level in non-marine settings may be thought of as equivalent to the graded stream profile (Shanley and McCabe, 1991; Wright and Marriot, 1993).

This study focuses on the stratigraphic architecture of the Cathedral Bluffs Tongue along the northern margin of the Green River Basin in the vicinity of South Pass, Wyoming (Fig. 3.1). The Cathedral Bluffs Tongue is a fluvial wedge within the dominantly lacustrine Green River Basin (Roehler, 1991). Lithostratigraphic correlation of strata within this unit is difficult, due to rapid lateral facies changes and intraformational unconformities (Roehler, 1992a). Alternative correlation methods, such as biostratigraphy or magnetostratigraphy, have been applied to this basin before (Clyde *et al.*, 2001; Gunnell and Yarborough, 2000; Zonneveld *et al.*, 2003). North American Land Mammal Ages (NALMAs) provide a biostratigraphic framework for Cenozoic strata in North America (i.e. Woodburne, 1987). The Cathedral Bluffs Tongue was deposited during the Bridgerian NALMA (Zonneveld, 1994; Clyde *et al*., 1997; Zonneveld *et al*., 2000), which has been subdivided into smaller subdivisions (Br0, Br1a, Br1b; Gunnell and Yarborough, 2000; Zonneveld *et al*., 2000; Bartels *et al.*, 2004). Although these subdivisions have been well established on the western margin of the basin (Gunnell and Yarborough, 2000; Zonneveld *et al*., 2000), the subdivisions remain poorly constrained in the study area. Magnetostratigraphy has also proven to be an effective correlation method for the Cathedral Bluffs Tongue across the Green River Basin (Clyde *et al.*, 2001, Zonneveld *et al.*, 2003). This type of correlation is useful for regional studies, but does not allow for development of a higher resolution

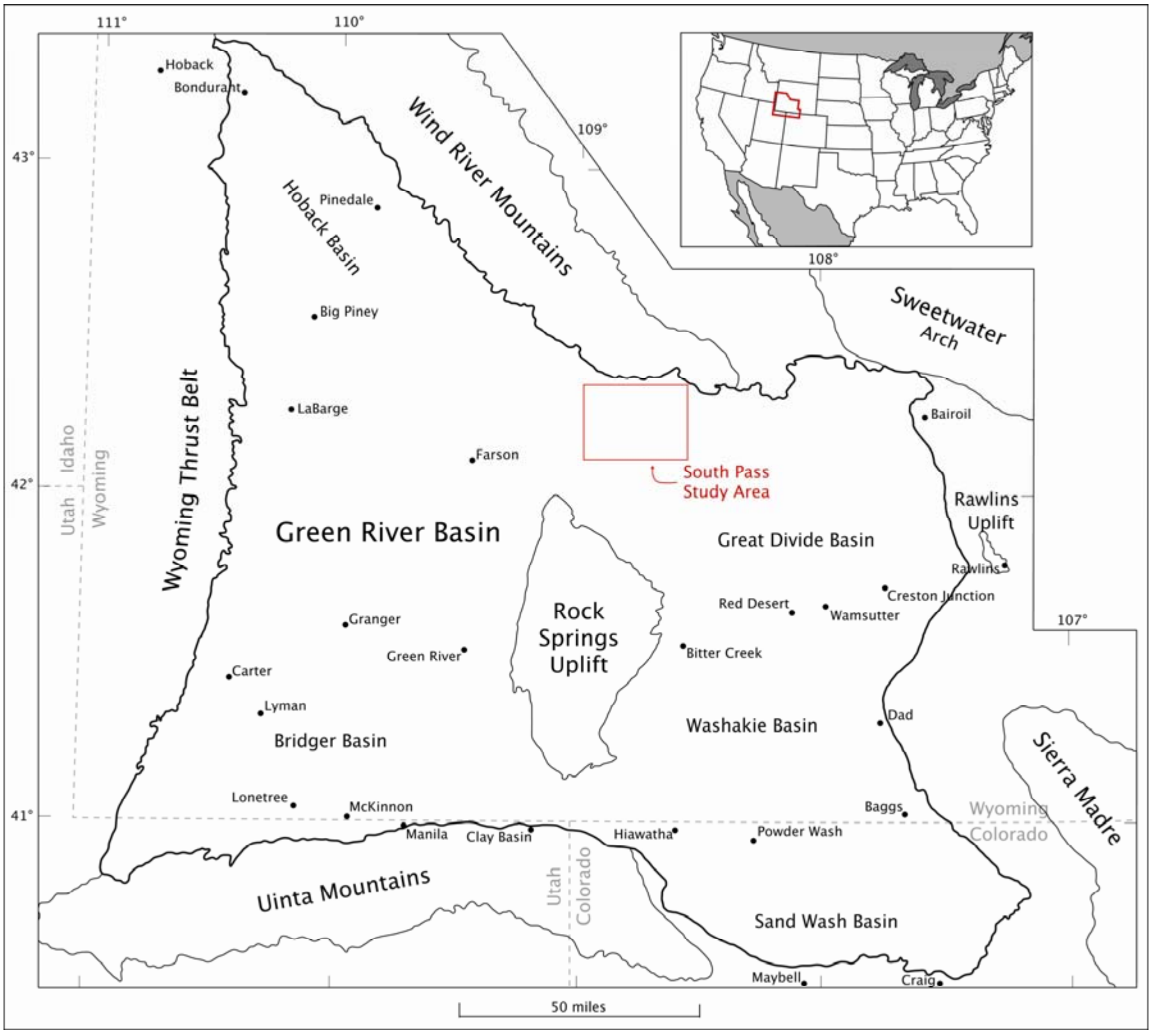

Figure 3.1 – Map of the Green River Basin of southwestern Wyoming showing the study area on the northeastern margin of the basin.

framework within the study interval. Subdivision of the study interval falls below both biostratigraphic and magnetostratigraphic resolution. Lithostratigraphic surfaces, although useful, are generally not continuous enough to provide confident correlation beyond single outcrop exposures.

The stratigraphic terminology used for this study will be identical to that for marine and marginal marine sequence stratigraphy (Posamentier *et al.,* 1988; Van Wagoner *et al.,* 1990). Lowstand, transgressive, and highstand systems tracts are used herein to describe the characteristic packages of sediment deposited within a sequence. The marine sequence stratigraphic terms are applied to this lacustrine basin for a few reasons. Firstly, for large lakes, changes in lake level exert similar influences on deposition in lacustrine basins as sea-level controls shallow marine stratigraphy in marine basins (Shanley and McCabe, 1994; Zonneveld *et al.,* 2003). Also, major sedimentary units of lacustrine basins are primarily controlled by lake level, climate, and tectonics, which are similar controls as for marine settings (Baltzer, 1991; Shanley and McCabe, 1994; Carroll and Bohacs, 1999; Zonneveld *et al.,* 2003). While the term transgression is more appropriately applied in marine settings, large lakes can also move towards the basin margin in a similar way to a transgression. The term base-level transit (Wheeler, 1964) has been used to describe changes in base-level, but is rarely used in modern literature; therefore, not used herein.

Development of a high-resolution stratigraphic architecture for the Cathedral Bluffs Tongue will provide the requisite framework for developing early Eocene paleoecological models at South Pass and constrain local subdivisions within the Bridgerian NALMA. In order to define stratigraphic units across the study area, a variety of techniques were utilized: 1) A detailed facies analysis was performed to gain a greater understanding of the sedimentology and how it relates to stratigraphy; 2) Sequence stratigraphic concepts are applied to the succession with assistance from spectral gamma ray logs through the study interval; and finally 3) whole-rock geochemistry was used to determine the utility of chemostratigraphy for correlating thin, heterogeneous fluvial deposits.

3.2. Geological Setting

The Cathedral Bluffs Tongue of the Wasatch Formation outcrops extensively near South Pass, Wyoming. The study area lies along the southeastern flank of the Wind River Mountains; a basement cored Laramide Uplift (Hall and Chase, 1989; Steidtmann and Middleton, 1991). Deposition of the Cathedral Bluffs Tongue occurred during the early Eocene within the dominantly lacustrine Green River Basin (Roehler, 1991; Roehler, 1992a).

The climate was globally warm and supported some of the earliest mammal faunas (Wilf, 2000; Zonneveld *et al*., 2003; Smith *et al*., 2008). Lake Gosiute dominated deposition within the Green River Basin for approximately 4 million years, (Surdam and Wolfbauer, 1975). Numerous fluctuations in lake-level resulted in extensive intertonguing of fluvial and lacustrine deposits on the basin margins. This study focuses on the Cathedral Bluffs Tongue, a fluvial clastic wedge that thickens north towards the Wind River Mountains. The Cathedral Bluffs Tongue is part of the Wasatch Formation and is separated from the Main Body of the Wasatch by the Tipton Tongue of the Green River Formation (Fig. 3.2) (Roehler, 1991). Towards the basin margin, the Tipton Tongue pinches out and the Wasatch Formation is undifferentiated.

The Cathedral Bluffs Tongue is up to 100m thick in the study area (Fig 3.3), but can be over 600m thick in the Washakie and Sand Wash Basins (Roehler, 1991). The Tipton Tongue is present within the study area, and occurs as far north as sec. 21, T. 27N, R. 101 at Reds Cabin Monocline (Zeller and Stephens, 1969). Movement along the Wind River Thrust Fault and recent erosion has allowed the Farson Sandstone Member of the Tipton Tongue to outcrop at this location. This member is a lacustrine delta that prograded into the basin during regression of Lake Gosiute (Roehler, 1991; Pietras *et al.*, 2003). Magnetostratigraphic studies (Clyde *et al.*, 2001) identified the C23n.2n-C23n.1r-C23n.1n magnetochrons within the upper portion of the Cathedral Bluffs Tongue within the study area (~SP10-11). This provides an approximate temporal range for the Cathedral Bluffs Tongue from 52 to 50.5 Ma.

Initial movement on the Wind River Thrust Fault occurred during the late Cretaceous, and intermittent tectonism occurred over a period of 30 million years (Roehler, 1991; Steidtmann and Middleton, 1991). By the Paleocene, montane uplift had resulted in unroofing of ~8000 meters of sedimentary cover (Steidtmann and Middleton, 1991). Periodic movement along the Wind River Thrust Fault occurred during deposition of the Cathedral Bluffs

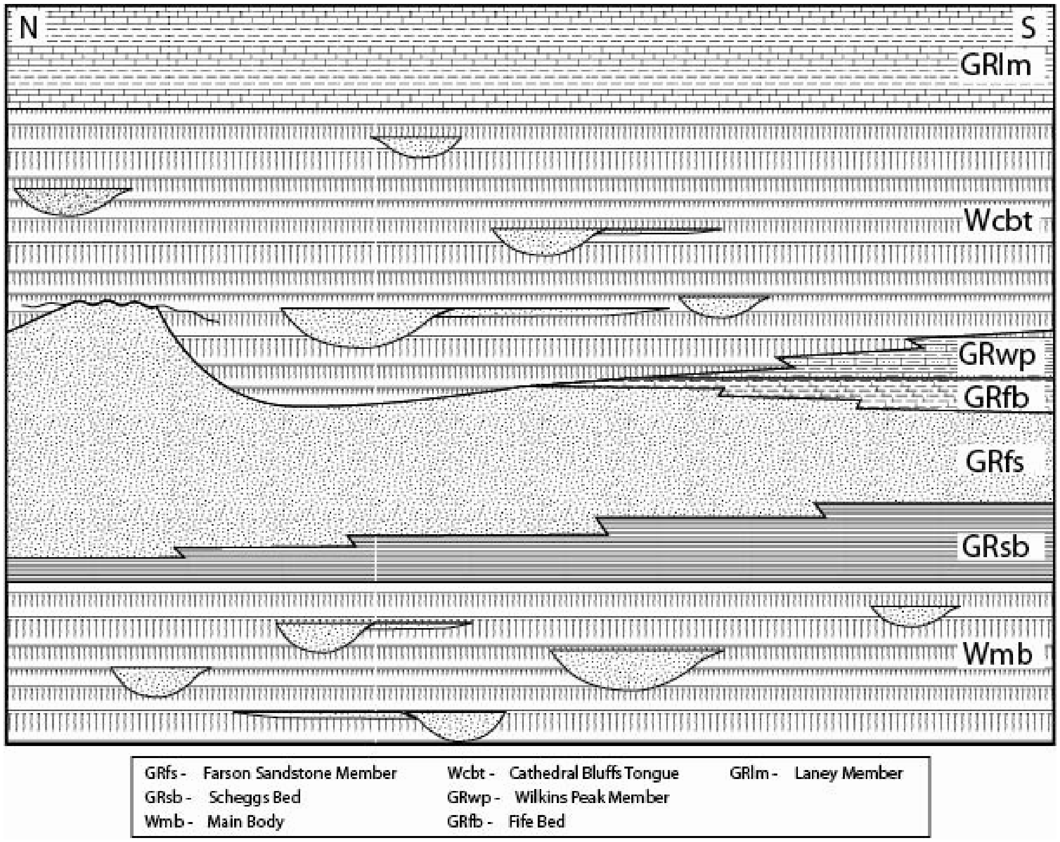

Figure 3.2 – Generalized lithostratigraphy of the Green River Basin showing the interfingering of the lacustrine Green River Formation and the fluvial Wasatch Formation. The local unconformity on the northern edge is due to Reds Cabin Monocline. Modified from Roehler, 1992b.

Tongue. Reds Cabin Monocline and the Continental Fault are two structural features in the study area that indicate syndepositional tectonic activity (Fig. 3.3) (McGee, 1983; Steidtmann and Middleton, 1991; Pietras *et al.*, 2003). The sedimentary fabric of the Cathedral Bluffs Tongue also reflects strong structural influences. Conglomerate and sandstone dominate the succession proximal to the range and pedogenically-altered mudstone dominates the distal areas. Coarser lenses within the Cathedral Bluffs Tongue are likely related to active periods of tectonism.

3.3. Methods

A total of 14 outcrop sections were measured during the 2009 and 2010 field seasons. Detailed notes were taken on the grain size, sedimentary and biological structures, paleosol colour and fracture patterns, and lateral extent / geometry of lithological units. Detailed lithological logs were constructed and used for correlation (Appendix A).

3.3.1. Chemostratigraphy

Chemostratigraphy is the process of using bulk elemental chemistry for characterization and correlation of a sedimentary succession (Ratcliffe *et al.*, 2007; Pearce *et al.*, 2010). Changes in the abundance of major elements, trace elements, and rare earth elements are utilized within a chemostratigraphic framework to differentiate between separate sedimentary packages. Variable source composition, facies, paleoclimate, weathering, and diagenesis all contribute to the varying elemental composition through a section (Ratcliffe *et al.*, 2007). Chemostratigraphic studies are typically conducted on large-scale (100's of meters) homogeneous, barren successions (Dypvik and Harris, 2001; Jenkyns *et al.*, 2002; Pearce *et al.*, 2010). The lack of datable fossils and distinct surfaces makes correlation within these successions difficult. Chemostratigraphy is useful because it can be performed on any succession, regardless of its other characteristics. Another advantage of this method is that it can be applied to outcrop, core or drill cuttings, or any combination thereof (Dypvik and Harris, 2001; Pearce *et al.,* 2010).

The purpose of this study is to test the validity of this method for small-scale (~60 meters) outcrop sections to facilitate high-resolution stratigraphic models of within a single fluvial-dominated succession bound by lacustrine successions. The Cathedral Bluffs Tongue contains many different facies and is abundantly fossiliferous. Chemostratigraphy may be necessary for the Cathedral Bluffs Tongue due to rapid lateral facies changes, and intraformational unconformities (Roehler, 1992a). The purpose is to identify if there were any significant changes in provenance or paleoclimate during the deposition of the Cathedral Bluffs Tongue. Surfaces demarcated by distinct chemical signatures can aid in the interpretation of synchronous slices through each outcrop section.

Chemostratigraphic analyses were performed for three sections along Bush Rim (Fig. 3.3). Samples were taken at intervals of one-meter, regardless of facies or lithology. A representative 50-100g piece of each sample was broken off and crushed into a fine powder using a SPEX CertiPrep Shatterbox 8515. A tungsten carbide bowl was used to prevent contamination of the samples with geochemically important elements. Each powdered sample

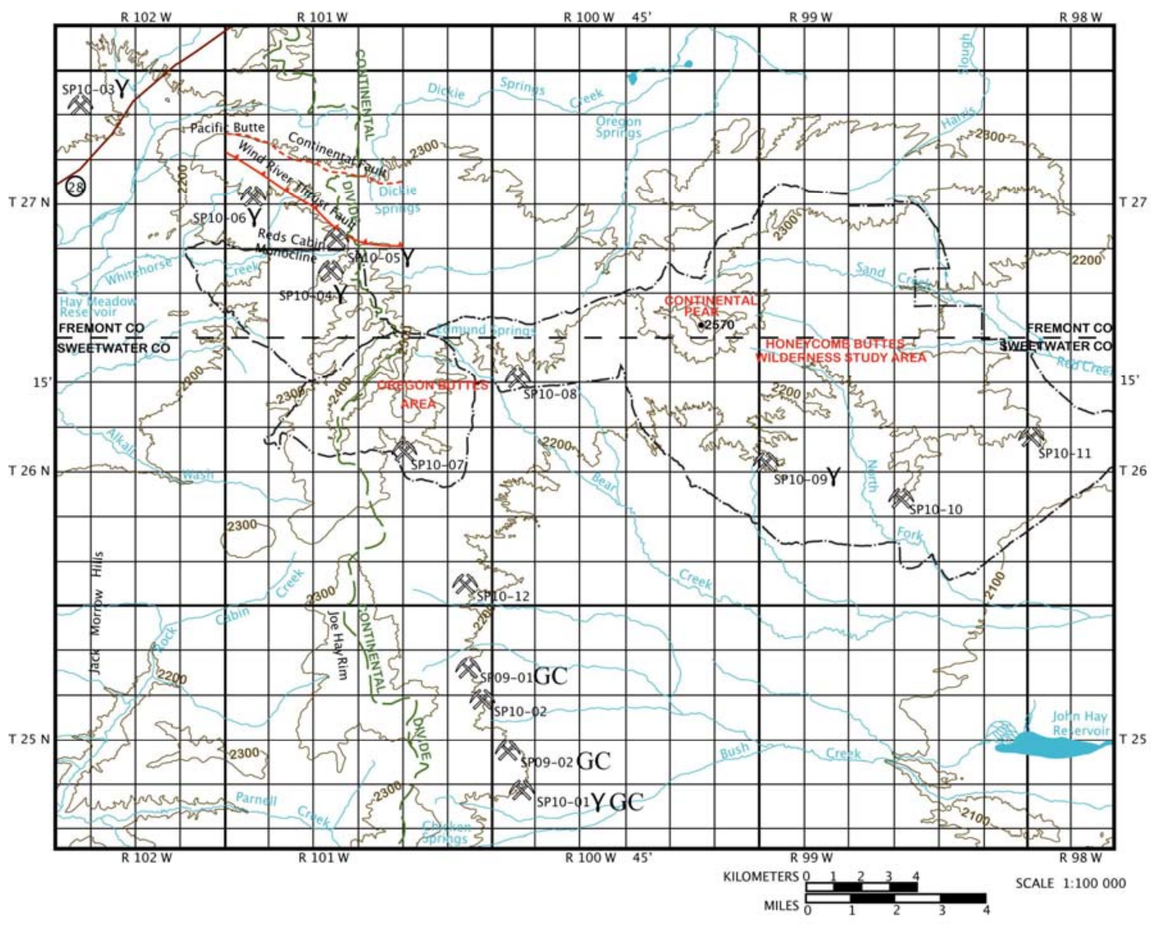

Figure 3.3 – Map of the South Pass study area showing the locations of the measured sections and pertinent structural features. Most sections are measured along an approximately N-S orientation roughly parallel to depositional dip. Sections with spectral gamma ray or geochemical data are indicated by the symbols γ (gamma ray data) and GC (geochemical data).

(n=179) was then analyzed for 57 elements (Appendix C) using ICP-MS at the University of Alberta. Each sample was run against the United States Geological Survey (USGS) SGR-1 standard to correct for long-term instrument drift. The reference material is from the Mahogany zone of the Green River Formation. It was chosen as the reference material because it is from the same basin, therefore, likely contains broadly similar elemental abundances. However, lithologic differences due to the very different depositional environments between the standard and the Cathedral Bluffs Tongue may introduce error. There is no simple way to choose an internal standard but it should be based on similar elemental mass between the analyte and standard (Finley-Jones *et al.,* 2008).

Furthermore, the ICP-MS results were analyzed using a principal component analysis. Advanced statistical methods are used to simplify the dataset and determine element associations and principal component analysis is one of the primary methods used to evaluate the raw geochemical data (Zhang *et al.,* 2002; Pearce *et al.,* 2005; Ali *et al.,* 2006; Svendsen *et al.,* 2007; Pe-Piper *et al.,* 2008; Ogala *et al.,* 2009). It is a mathematical process used to reduce the dimensionality of large, complex datasets. The intent of the procedure is to explain the variance within a multivariate dataset using only a few underlying factors. It is also possible to find hidden structures in the dataset that would not have otherwise been recognized (Reimann *et al.,* 2002). Variables that behave similarly will be grouped into the same factor and thus reduce the dimensionality of the dataset.

Advanced statistical methods, such as principal component analysis, are not suited for geochemical datasets (Reimann *et al.,* 2002); however, the results may show important trends within the dataset. For the purpose of this study, the results of the statistical analyses were used to identify elemental associations and their relation to depositional and weathering processes. Proper processing of the dataset before undertaking a principal component analysis can greatly improve the results. Care must be taken to follow strict guidelines as one small change in the data processing can greatly change the results (Reimann *et al*., 2002).

Firstly, all data outliers were removed from the dataset. Outlier data points were determined as any elemental concentration that was greater than two standard deviations from the mean value of the element over the outcrop section. An example of an outlier removed would be the sample at 56 m from SP10-01. The Sr concentration was 1585.8 ppm while the average (331.6 ppm) plus two standard deviations (213.1) was only 757.7 ppm. Since outliers can affect the outcome of advances statistical analyses, they must be removed prior to analysis (Pison *et al.*, 1999; Reimann *et al.*, 2002). As well as outliers, data that is below the detection limits of the measuring method must be removed. In the case of a certain element constantly being below detection limits, it was removed from the analysis. For elements that were rarely below the detection limit, the value was set to half of the detection limit (Reimann *et al.*, 2002).

Secondly, advanced statistical analysis works best on data that is normally distributed, which it is now know that geochemical datasets rarely do (Pison *et al.*, 1999; Reimann and Filzmoser, 2000; Reimann *et al.*, 2002). The data from the Cathedral Bluffs Tongue was normalized using a logarithmic transformation and then transformed to have a mean of 0 and a standard deviation of 1. The equation $x' = (x-\mu)/\sigma$, where x = log normalized value, μ = mean, and σ = the standard deviation for each element. This allowed the dataset to approach a normal distribution and yield more stable results for the principal component analysis. Within the principal component analysis an orthogonal Varimax rotation was used, as it is simpler than the oblique rotation methods (Kaiser, 1958; Reimann *et al.*, 2002).

3.3.2. Spectral Gamma Ray Logs

Natural gamma ray radiation was measured for six of the sections through the South Pass study area in the 2010 field season. Measurements were taken using a hand-held RS-230 BGO Super-SPEC gamma ray scintillometer. The outcrops were sampled at an interval of 0.5 m with each sample run for 120 seconds. Assay recordings were taken at 2.5 m intervals to assist matching the readings to the outcrop log. A hand-held spectral gamma tool generally has a sample area of 30 to 50 cm, but the area varies among devices (Myers and Wignall, 1987; Slatt *et al.*, 1992). To minimize errors associated with contamination of a sample by adjacent beds, the held gamma ray scintillometer w as held as parallel to bedding as possible, so the volume of rock being sampled is in the same bed (Davies and Elliott, 1996). The results are total gamma counts (ppm, cpm) and spectral gamma results for K (wt %), Th, and U ppm and cpm.

3.4. Dataset

3.4.1. Whole-rock Geochemistry

Whole-rock geochemical analyses are complicated by a number of factors including diagenesis, weathering, sediment provenance, element mobility, and mineral leaching (Ratcliffe *et al.*, 2007). Changes within some of these factors allow recognition of different intervals. Chemical changes due to a change in sediment provenance can provide a signal to a specific point in basin evolution, but may not be completely synchronous across a study area. Weathering and leaching may be related to the climatic conditions at the time of deposition and have been used to determine the mean annual temperature and precipitation (Sheldon and Tabor, 2002). Elements that should show a primary depositional signal are those elements that are immobile and will be preserved where they were deposited (Preston *et al.*, 1998). Elements such as Cr, Nb, Th, and Zr are relatively immobile and may give an indication of the sediment provenance of a sample (Fig. 3.4). Elemental concentrations from

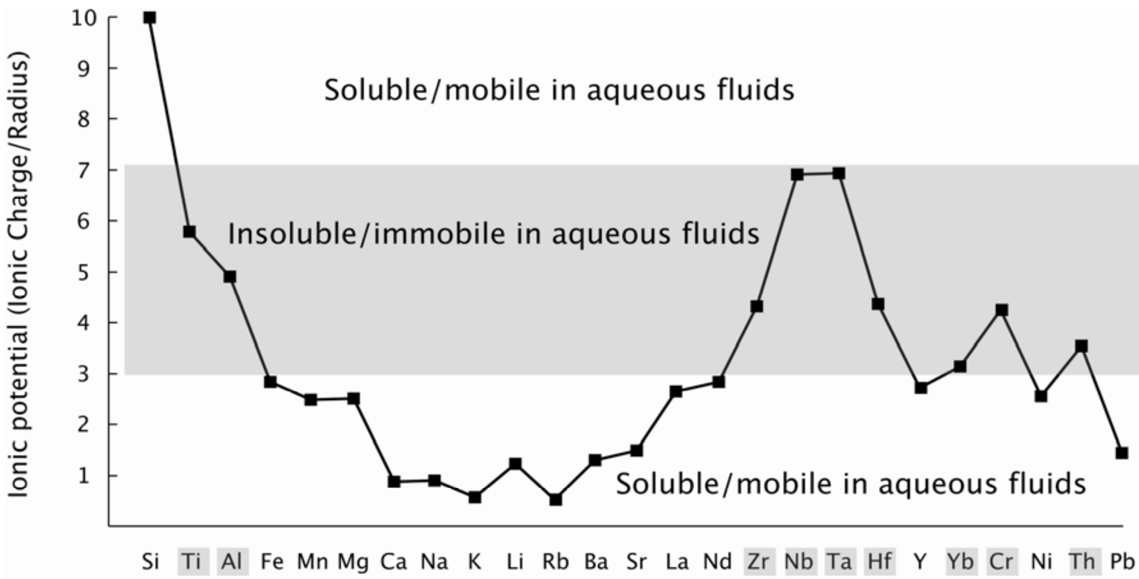

Figure 3.4 – Graph showing the mobility of certain elements. Note that K falls in the range of mobile, while Th is considered to be immobile (after Preston *et al.,* 1998). Both mobile and immobile elements are useful for correlation in geochemical studies. Immobile elements give a signal of the primary depositional chemical characteristics such as sediment provenance, while mobile elements can track weathering or diagenetic changes.

the Cathedral Bluffs Tongue only show very vague trends in the variance of these elements (Fig. 3.5). The elemental ratio of Th/Cr is apparently low in the lower half of the succession, while the Cr/Nb ratio shows an inverse relationship that can best be observed in SP09-02. This is likely caused by the variance of Cr, which may be related to Cr-spinel or other heavy minerals (Svendsen and Hartley, 2002; North *et al.*, 2005; Ratcliffe *et al.*, 2010). Surfaces that demarcate chemical changes are roughly equivalent to some of the sequence stratigraphic surfaces picked from lithologic and gamma ray analysis. The absence of any diagnostic trends within the immobile elements may indicate that no significant change in sediment provenance occurred during deposition of the Cathedral Bluffs Tongue.

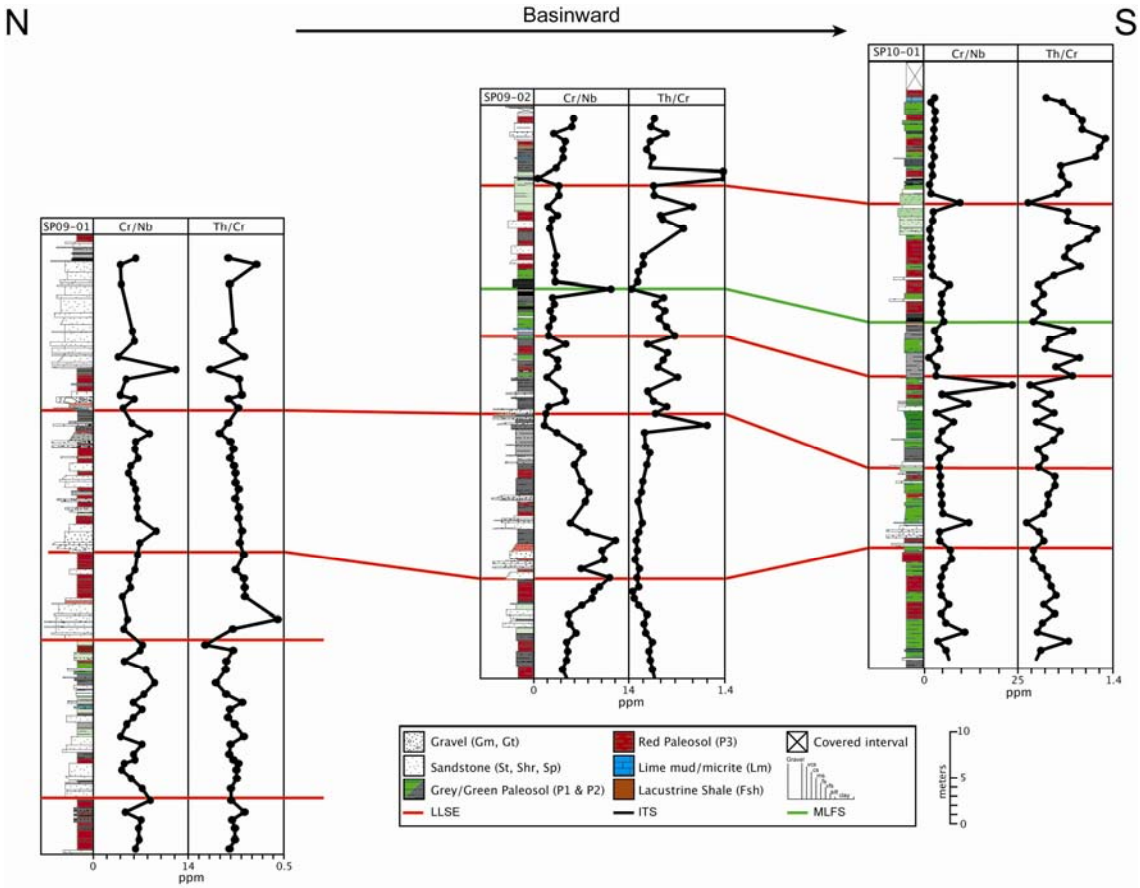

Figure 3.5 – Ratios of immobile elements Cr, Nb, and Th. These elemental ratios should give some indication of the sediment provenance for the Cathedral Bluffs Tongue. The stratigraphic surfaces marked roughly correspond to sequence stratigraphic surfaces in figure 3.14.

Principal Component Analysis

Advanced statistical methods are useful tools to elucidate geochemical datasets (Siegel *et al.*, 1995; Reimann *et al.*, 2002; Svendsen *et al.*, 2007). The datasets are commonly very large and therefore difficult to comprehend without the aid of statistical analysis. Two types of analysis are generally used within geochemical studies, principal component analysis and factor analysis. These analyses reduce the dimensionality of the dataset and allow for trends within the dataset to become apparent. There are many problems associated with advanced statistical analysis being used on geochemical datasets (Reimann *et al.,* 2002). Regardless, a principal component analysis was completed on the geochemical dataset from the Cathedral Bluffs Tongue.

The principal components and mineral associations from the analyses are shown in figure 3.6. Principal component 1 (PC1) accounts for 45.00% of the variance in the dataset. It contains high positive loadings for Al, Ti, V, Fe, Cu, Zn, Ga, Rb, Nb, Cs, and the REE. This suite of elements is interpreted to represent the clay content of the sediment. Therefore, this component can be used as a proxy for grain size. The component scores for each sample support this interpretation. At outcrop SP10-01 only four samples were sandstone, and these samples show strong negative scores for PC1 (Fig. 3.7).

Principal component 2 (PC2), accounting for 12.49% of the variance, shows high positive loadings for Mg, P, and Ca and is interpreted to represent the carbonate component of the rocks. This is somewhat equivocal, as geochemical datasets do not discern between carbonate cements and depositional carbonate. In figure 7, a negative loading for PC1 and a high positive loading for PC2 within generally low values likely indicates carbonate-cemented sandstone.

Principal component 3 (PC3) displays high positive loadings for Co, Sr, and Ba and accounts for 9.33% of the variance in the dataset. This component is somewhat ambiguous. Strontium is most commonly associated with carbonates as it is a common replacement element for Ca (North *et al.*, 2005). It has also noted that Sr is strongly correlated with phosphorites, possible replacing Ca in apatite. However, other carbonate-associated elements (Ca, Mg) do not show significant correlation with this component. Therefore, Sr is not associated with the carbonate component and must be related to some other process, possibly weathering as Sr is a mobile element (Preston *et al.*, 1998). Variance in Ba is also problematic, as processes related to barium concentrations are poorly understood in continental settings.

Variable	PC 1	PC 2	PC 3	PC 4	PC 5
Be	0.646	-0.044	0.242	-0.338	0.238
Mg	0.543	**0.547**	-0.016	0.185	-0.350
Al	**0.854**	-0.393	-0.009	0.044	0.081
P	0.243	**0.711**	0.149	0.086	0.164
K	0.523	-0.310	0.315	-0.530	-0.252
Ca	-0.537	**0.738**	0.074	0.014	-0.088
Ti	**0.919**	-0.015	0.224	0.097	-0.040
V	**0.869**	0.142	0.062	-0.246	-0.015
Cr	0.590	0.372	0.440	0.029	-0.178
Fe	**0.910**	0.152	0.069	-0.009	-0.180
Mn	-0.324	0.721	0.360	0.088	-0.271
Co	-0.084	-0.166	**0.734**	-0.132	0.096
Cu	**0.820**	0.334	0.040	0.032	0.143
Zn	**0.875**	0.057	-0.086	0.060	-0.171
Ga	**0.932**	-0.254	-0.054	0.025	0.031
Rb	**0.781**	-0.151	0.045	-0.465	-0.248
Sr	-0.357	0.372	**0.665**	0.037	0.212
Y	0.599	0.438	-0.254	0.111	**0.338**
Zr	0.434	-0.300	0.390	**0.682**	0.119
Nb	**0.894**	-0.067	-0.172	0.031	0.018
Mo	0.225	0.338	-0.070	-0.363	**0.504**
Sn	0.661	-0.032	0.094	0.299	-0.167
Cs	**0.928**	0.034	0.091	-0.075	-0.259
Ba	-0.216	-0.286	**0.725**	-0.239	0.253
La	**0.865**	0.178	-0.229	-0.053	0.279
Ce	**0.824**	0.218	-0.215	-0.028	0.280
Hf	0.505	-0.369	0.247	**0.658**	0.143
Eigenvalue	12.419	3.372	2.518	1.957	1.308
% of Var.	45.996	12.490	9.327	7.247	4.844
Cum. %	45.996	58.486	67.813	75.060	79.904
Controlling Elements	Al, Ti, V, Fe, Cu, Zn, Ga, Rb, Nb, Cs, REE	Mg, P, Ca	Co, Sr, Ba	Zr, Hf	Y, Mo,
Controlling Minerals	Clay Minerals	Carbonate, Siderite	Adsorption on Kaolinite	Zircon	?
Controlling Process	Weathering/ Textural Maturity	Pedogenesis/ Leaching	Weathering, Leaching	Heavy Minerals/ Provenance	?

Figure 3.6 – Results of the Principal Component Analysis. High positive loadings represent good correlation with the component, while strong negative loadings indicate an inverse relationship with that component.

In marine settings, barium concentration is related to biogenic productivity and bathymetry (Dehairs *et al.*, 1980). The Ba/Sr ratio has been used by others (Retallack, 1990; Sheldon *et al.,* 2002) as a proxy for weathering as Sr is mobile and Ba is immobile. However, this ratio shows no significant relationship with the paleosols of the Cathedral Bluffs Tongue.

The last component considered to be significant is principal component 4 (PC4), which explains for 7.25% of the variance. This component shows high loadings for Zr and Hf. Zirconium is the main component of the mineral zircon and Hf is the most common substitution element in zircon. This component is therefore associated with the heavy mineral component. This may be related to provenance, but likely has some relation to grain size as well.

The result of the PCA is a small number of components that can be compared throughout and between outcrop sections. Each sample has case-wise scores for each principal component. A high case-wise score value means that a sample correlates well with the component, while a low value indicates a poor correlation. Therefore, rather than comparing the abundance of Al or K between sections, comparing the case-wise scores for PC1 between sections accounts for Al, K, and any other elements that varies similarly with those elements. The components of this PCA have output variables related to grain size, weathering / leaching, and heavy minerals. If there are any significant changes through a vertical section, plotting the case-wise scores will show the variance trends. Once diagnostic trends are determined, the trends can be correlated between outcrop sections. Also, elements may group together on binary plots (Fig. 3.8) and will show relationships between elements that may not be expected, such as K grouping with Zr and Hf.

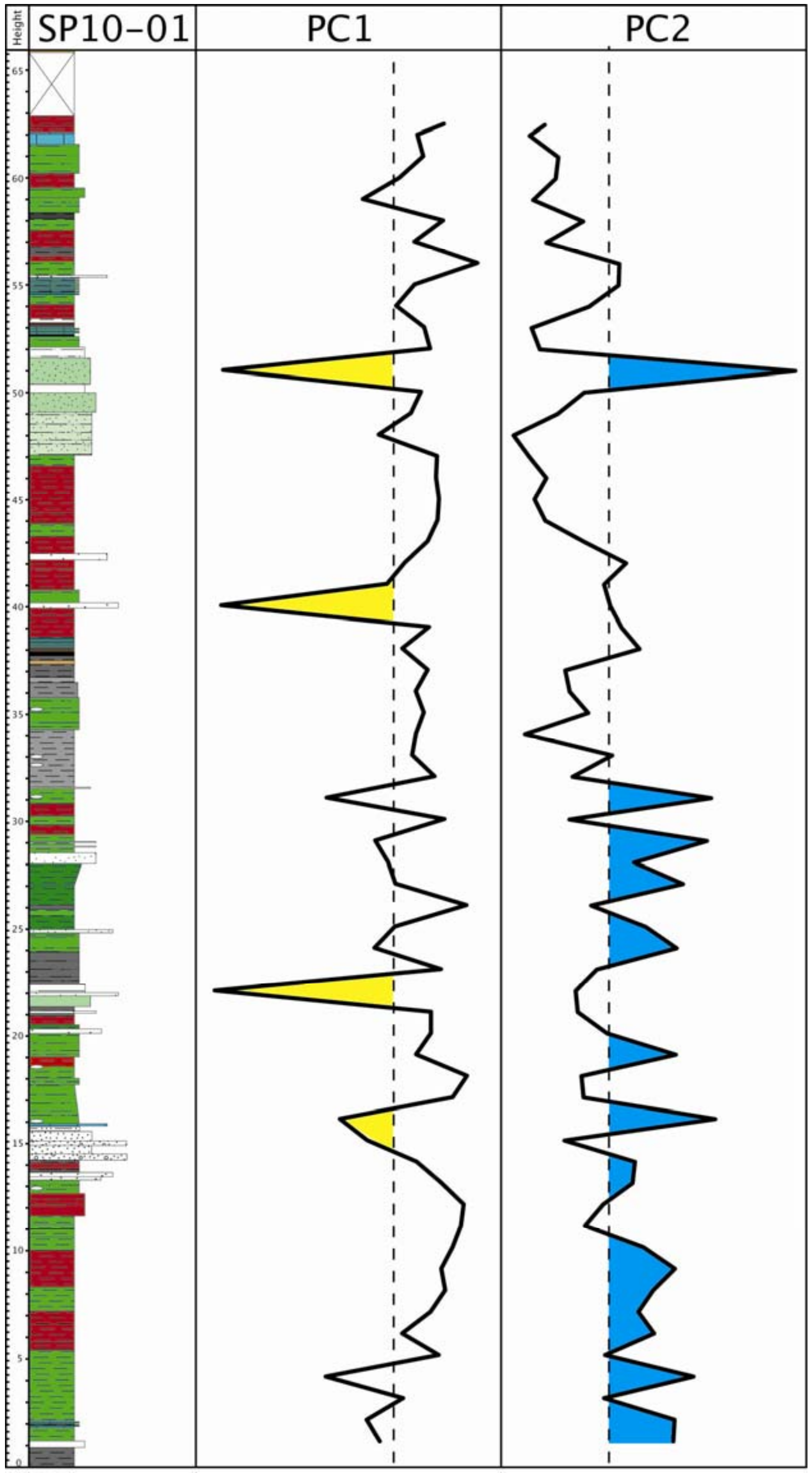

Figure 3.7 – Case-wise scores for PC1 and PC2 plotted with the striplog for SP10-01. The interpreted attributes of the principal components (PC1 – grain size, PC2 – carbonate) seems to hold fairly true for this section.

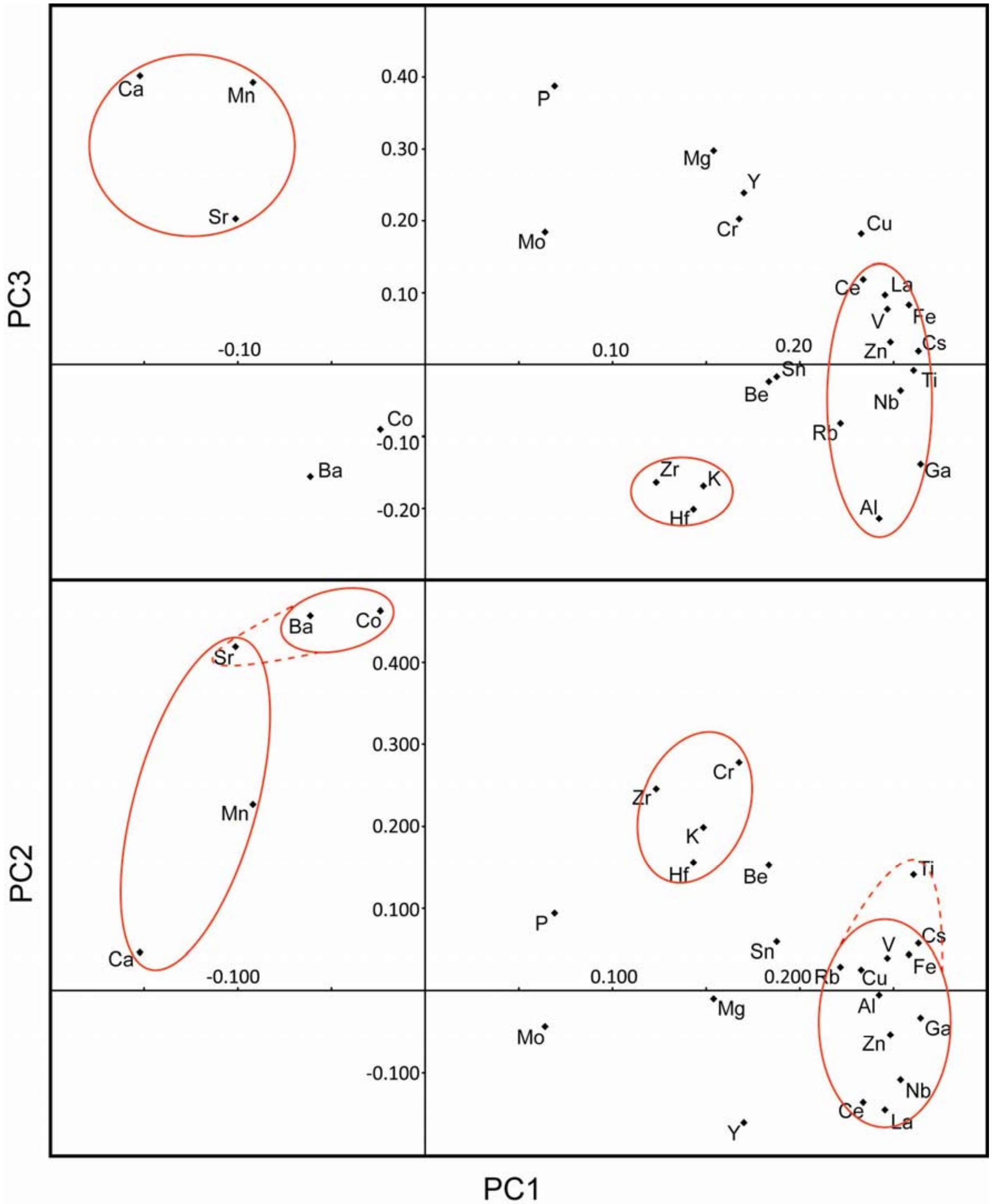

Figure 3.8 – Eigenvector plots from the Principal Component Analysis showing the grouping of certain elements into groups. An interesting result is that K (usually associated with clays and feldspars) groups closely with Zr and Hf (generally associated with the heavy element suite, specifically within zircon).

3.4.2. Spectral Gamma Ray

Spectral gamma ray (SGR) curves allow for easy visualization and interpretation of sedimentary successions. The hand-held SGR device measures the radioactivity of ^{40}K, ^{232}Th, and U (mostly ^{238}U) and converts the counts per second (cps) to a concentration in parts per million (ppm) or weight percent (wt %). The radioactive signatures of the elements, along with the Th/K and Th/U ratios, are used to subdivide each section into packages. Measurements taken on non-planar surfaces will affect the volume of rock included in the measurement and can cause significant changes in the radioelement abundance (Davies and Elliott, 1996). Using ratios, such as Th/U and Th/K, renders this type of error insignificant as the relative abundances for each sample should remain equal (Davies and Elliott, 1996). The average values for these elements from the gamma data are 2.07 wt% potassium, 5.00 ppm uranium, and 11.05 ppm thorium. With these average concentrations, the amount of error associated with each element can be calculated from experimental results. The errors for each element using the RS-230 BGO Super-Spec at the sigma 1 level are: 0.181 wt% for K, 0.417 ppm for U, and 0.437 ppm for Th (Radiation Solutions, 2008).

Sequence stratigraphic surfaces and systems tract boundaries tend to have diagnostic concentrations of specific radioactive elements (Davies and Elliott, 1996; Hampson *et al.*, 2005). Sequence boundaries are important stratigraphic surfaces, and in continental strata can be identified on SGR logs. Strong depletions in K (<0.05 wt %) are observed underlying sequence boundaries. The low concentration of K can be attributed to leaching of K out of the paleosols during soil formation (Davies and Elliott, 1996). Potassium is easily soluble in meteoric waters as the K^+ cation due to its low ionic potential (Preston *et al.*, 1998). This allows K to be readily leached from soils as they are sub-aerially exposed. Most authors (Davies and Elliott, 1996; Hampson *et al.*, 2005) identify interfluvial sequence boundaries where the

Th/K ratio is high (>12), as K is depleted (<0.04 wt %) due to leaching. Thorium is not as mobile (soluble) as potassium (Preston *et al.*, 1998); thus, a high Th/K ratio is due intense weathering and the presence of kaolinitic clays.

These diagnostic gamma ray patterns are observed in many of the sections within the study area (Fig. 3.9). However, within the Cathedral Bluffs Tongue, sequence boundaries are picked at the top of K and Th depleted packages. The concentration of K and Th correlate well to each other, even in areas of paleosol development. This is problematic because K is mobile and should be depleted in paleosols, while Th is essentially immobile under all environmental conditions (Preston *et al.,* 1998). However, some studies have shown that Th can be relatively mobile and leached from the top of the soil column (Kurtz *et al.*, 2000). The correlation between the two elements is higher towards the basin margin (R^2=0.78, 0.89), and lower towards the basin centre (R^2=0.66, 0.47). Depletion in both elements causes a more variable Th/K ratio at sequence boundaries. It is also observed that the Th/K ratios are much lower (<10) than reported elsewhere for interfluve sequence boundaries (Davies and Elliott, 1996; Hampson *et al.*, 2005). It is apparent that the highest Th/K ratios increase as you move basinward, and in the most distal section the ratio is generally >10 and can reach up to 25. The high ratios observed in this distal section are attributed to higher Th concentrations, rather than K depletion, which discount these Th/K spikes as sequence boundaries. Thorium-potassium cross-plots show two distinct populations. The first population (Th<4 ppm and K<1 wt %) is depleted in both elements, and is attributed to leaching in well-drained, mature sequence bounding paleosols. The second population (Th>4 ppm and K>1 wt %) consists of sediment with normal concentrations of the elements.

Thorium occurs within the heavy mineral suite (Davies and Elliott, 1996; Hampson *et al.*, 2005; Pearce *et al.*, 2010) and thus is enriched directly above sequence boundaries, in channel sandstone lags. This high Th lag deposit is why some authors attribute high Th/K ratios to sequence

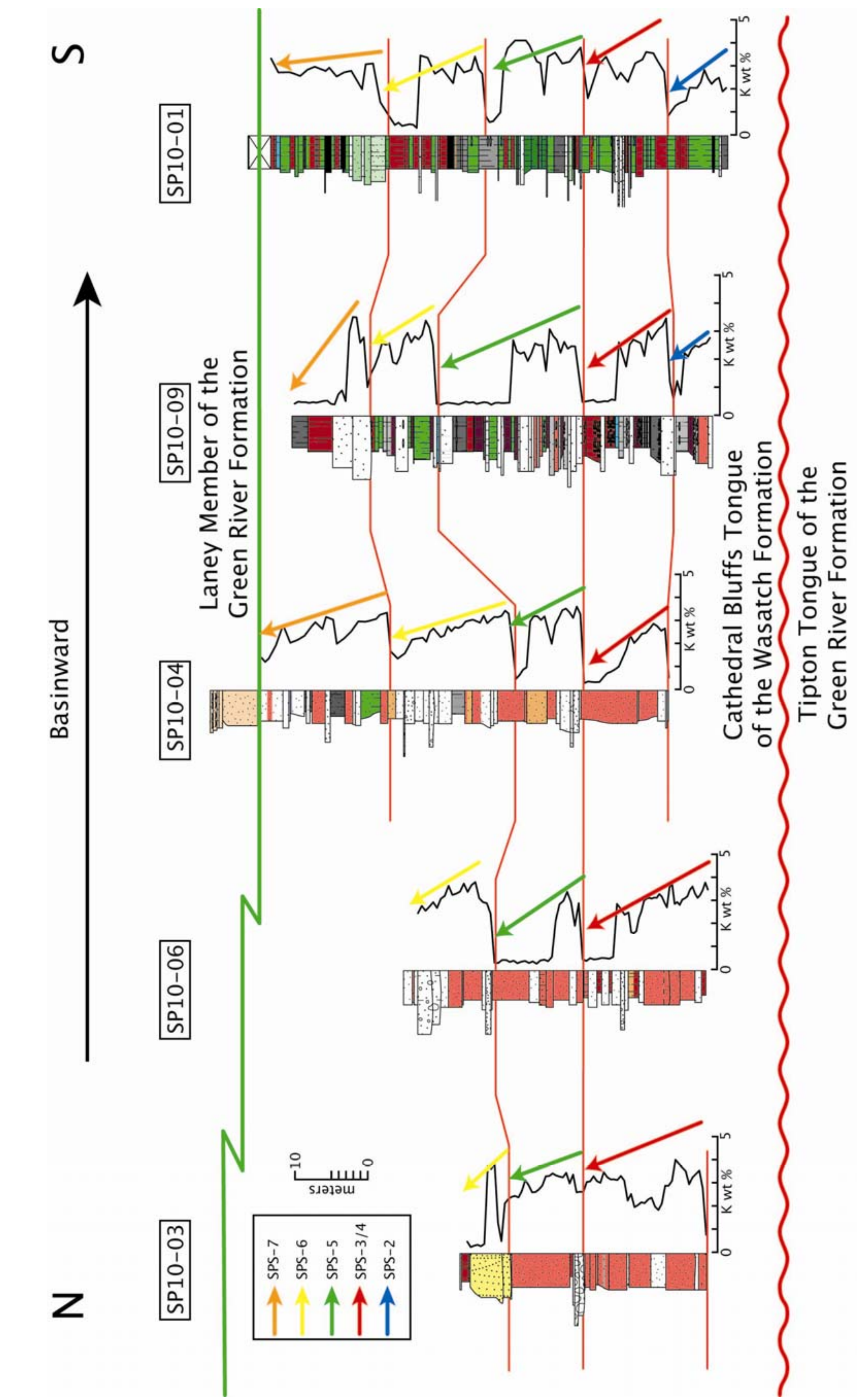
N
S
Basinward
SP10-03
SP10-06
SP10-04
SP10-09
SP10-01
SPS-7
SPS-6
SPS-5
SPS-3/4
SPS-2
meters
10
0
K wt %
0
5
Laney Member of the Green River Formation
Cathedral Bluffs Tongue of the Wasatch Formation
Tipton Tongue of the Green River Formation

Figure 3.9 – Correlation based on the spectral-gamma results. The K wt% shows diagnostic patterns with relation to weathering.

boundaries. However, within the Cathedral Bluffs Tongue, the sediment is very immature and contains high amounts of feldspars and micas within these channels. This leads to both the Th and the K concentrations spiking directly over a sequence boundary, and consequently no change in the Th/K ratio. In beds where Th spikes without a similar K spike, Th appears to be associated with the U concentration and organic material or subaqueous dysoxic / anoxic conditions.

The concentration of U within the Cathedral Bluffs Tongue is associated with the heavy mineral suite, as well as potentially anoxic lacustrine sediments. Thus, the presence of U on the basin margins is due more to the heavy minerals, while towards the basin center U is associated more with lacustrine deposits. Moderate U spikes (5 to 8 ppm) are observed at the base of some channel sandstone beds. This U spike is accompanied by a Th spike as well, and is likely associated with heavy mineral lags at the base of channel sandstone scours.

Previous studies (Davies and Elliott, 1996) have used the presence of high concentrations of U, as well as a low Th/U ratio, to pick maximum flooding surfaces. A high concentration of U is related to deposition under dysoxic / anoxic conditions and is thus associated with basinward facies. This is true of both marine basins, wherein organic detritus is preferentially preserved in oxygen-deficient basin floor settings, as well as continental basins wherein organic material may be preserved on the floors of stratified lakes. For the distal areas of the Cathedral Bluffs Tongue, this assumption seems to hold true, whereas the proximal deposits do not show U peaks associated with flooding surfaces. This is likely due to the fact that flooding surfaces do not necessarily indicate subaqueous conditions on the basin margin. It has been observed that U is a highly mobile element potentially causing uneven distribution of U concentration (Kurtz *et al.*, 2000; Hampson *et al.*, 2005).

3.4.3. Lithology

The Green River Basin is a continent-interior lacustrine basin (Roehler, 1991; 1992a). Thus, global eustacy had no influence on the depositional evolution of the Cathedral Bluffs Tongue. Climate and tectonics are the two main factors that influence depositional patterns and sequence development within lacustrine basins (Carroll and Bohacs, 1999; Zonneveld *et al.*, 2003). Tectonic activity controls base-level changes through uplift and concomitant subsidence, changes in drainage areas, and changing sediment supply. Climate principally controls precipitation and evaporation, subsequently causing changes in sediment supply and fluvial discharge (Carroll and Bohacs, 1999; Bohacs *et al.*, 2000). Facies of the Cathedral Bluffs Tongue are displayed in table 1 and 2.

Some studies (Martinsen *et al*., 1999; Arnott *et al*., 2002; Catuneanu, 2006) have divided successions into proximal and distal areas based on the relative influence of upstream and downstream controls. In this method, distal areas are named using traditional marine systems tracts, but the proximal deposits are subdivided into high- and low-accommodation systems tracts (Martinsen *et al.,* 1999). However, it is noted that the influence of geomorphic base-level affected only the most distal sections (Fig. 3.10). Neither lacustrine interbeds nor evidence of high water table levels was observed at proximal (upland) sections in the study area. The proximal areas are subdivided solely into lowstand and transgressive systems tracts, as identification of the maximum lacustrine flooding surface (MLFS) or its

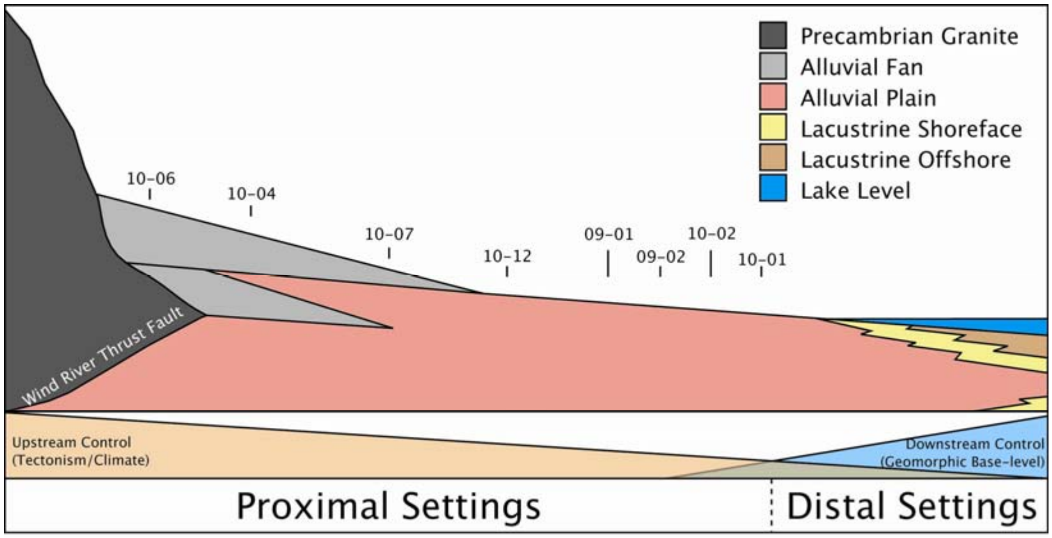

Figure 3.10 – Schematic cross section showing the location of measured sections and the controls on sequence development. Tectonics and climate are thought to have the most direct impact on deposition of the Cathedral Bluffs Tongue. Geomorphic base-level has very little effect any distance upstream.

landward equivalent did not prove possible. Difficulty in identifying the MLFS could be a result of the diminutive effect of base-level changes towards the basin margin, or the comparably poor vertical exposure of the unit in the proximal sections (i.e. ~40 m exposure of 60-100m unit thickness; Zeller and Stephens, 1969; Roehler, 1991; Pietras *et al.*, 2003).

Using the fluvial sequence stratigraphic concepts developed by previous workers (Wright and Marriot, 1993; Shanley and McCabe, 1994; Olsen *et al.*, 1995; Kraus and Aslan, 1999; Martinsen *et al.*, 1999; Arnott *et al.*, 2002; Zonneveld *et al.*, 2003; Fanti and Catuneanu, 2010), the Cathedral Bluffs Tongue can be subdivided into a chronostratigraphic framework. The succession can be split into 7 depositional sequences (SPS-1 through SPS-7; Fig. 3.11), all bounded by erosional unconformities. The sequences identified within the Cathedral Bluffs Tongue are higher frequency (lower order) sequences than previously identified within the Green River Basin (Bohacs *et al.*, 2000; Zonneveld *et al.*, 2003).

Facies Association	Facies Code	Facies Name
FA1 Channel	**Gm**	Massive gravel conglomerate
	Gt	Trough-cross bedded gravel conglomerate
	St	Trough-cross bedded sandstone
FA2 Crevasse Splay	**Sp**	Planar-cross bedded sandstone
	St	Trough-cross bedded sandstone
	Shr	Planar-horizontal to ripple-cross laminated sandstone
FA3 Pedogenically-altered Overbank Fines	**P1**	Light grey / green v. fine sandstone, siltstone, and mudstone
	P2	Dark grey / black siltstone and mudstone
	P3	Red / orange siltstone and mudstone
FA4 Palustrine to Lacustrine Margin	**Lm**	Lime mudstone / micrite
	P1	Mudstone w/ no pedogenic alteration
FA5 Lacustrine	**Fsh**	Organic-rich shale
	Lm	Lime mudstone / micrite

Table 3.1 – Facies Associations of the Cathedral Bluffs Tongue.

Facies Association	Description / Interpretation
FA1 Channel	Channel morphology is interpreted to change from braided (proximal) to meandering (distal) as we move away from the Wind River uplift. Gravel beds are preserved by the migration of longitudinal bars, transverse bars, and small channel fill gravels during maximum discharge in the rivers. Gravel beds eventually pinch out basinward and are not present within the Bush Rim sections. Trough-cross bedded sandstone (St) is the most common facies observed in the more distal sections, preserved by the migration of linguiod 3-D dunes along the streambed. The basal surface of this facies association can scour down many meters into the underlying sediment.
FA2 Crevasse Splay	Occurs as extensive sheet-like sandstone bodies or as small, restricted channels. Planar-horizontal bedding is interpreted to be the result of upper flow regime sheetflood-type flow. As flow wanes, current-rippled sand is deposited and grades upwards into silt/mud deposits. Less commonly planar-cross bedded sand is observed, interpreted as 2-D dune migration within small crevasse channels. This facies association often contains abundant fossil (turtle, crocodilian, mammalian) material, and occasionally reworked stromatolitic material. This facies is most often associated with avulsion deposits and occurs with relatively immature paleosols.
FA3 Pedogenically-altered Overbank Fines	This is the most abundant facies association observed within the Cathedral Bluffs Tongue. Paleosol development is observed in many stages of maturity and generally consists of alternating red and grey-green mudstones. The maturity and thickness of paleosol profiles is dependant on many factors such as floodplain elevation, temperature, precipitation, drainage conditions, and sedimentation rate (determined by flood frequency and distance from channel). Paleosol profile thickness can range anywhere between 20 cm to over 3 m. While these facies are dominantly composed of mudstone, there are occasions where the overbank deposits are predominantly very fine- to fine-grained sand creating sandy paleosols.
FA4 Palustrine to Lacustrine Margin	Palustrine deposits generally occur as interlaminated (mm scale) or interbedded (cm-dm scale) lime mud/micrite and green mudstone. Ponds are interpreted to represent periods of relatively high water table or lake transgression. The interbedding is interpreted to represent seasonal variation or flood frequency. Carbonate deposition occurs when there is no clastic input (during dry periods), and silt and mud are brought into the system by heavy rainfall or flooding. Thin oil shale beds are commonly observed over and underlying these deposits.
FA5 Lacustrine	This facies association in mainly contained within the overlying Laney Member of the Green River Formation. However, thin, continuous beds of organic-rich oil shale (facies Fsh) occur in the most basinward sections indicating periods of ephemeral lake transgression. Interpreted to be deposited in quiet, stratified lacustrine conditions due to the preservation of organic material.

Table 3.2 – Facies association descriptions for the Cathedral Bluffs Tongue.

Sequences within the Cathedral Bluffs Tongue show a large variation in the expression of surfaces and systems tracts between the proximal and distal areas. Generally, the sequence boundaries can be picked either below coarse-grained, amalgamated channel deposits, or above thick, well-drained paleosols. The LST commonly consists of sharp-based sandstone channel deposits. However, in distal sections, the LST did not display such coarse-grained material in several examples (Fig. 3.12; sections SP09-01, SP09-02, SP10-01).

Following lowstand conditions, lacustrine transgressions occurred leading to deposition of the next systems tract. The TST is dominated by isolated channel and crevasse-splay sandstone encased in floodplain mudstone. The mudstone shows only incipient pedogenesis, and is typically a dull grey-green colour. The transgressive deposits are thickest in a basinward direction and thin towards the basin margins.

Highstand systems tracts are easily identified in the distal region of the study area. The highstand deposits overly the MLFS, which are commonly expressed as thin, micritic oil shale beds, *in situ* stromatolites or stromatolite encrusted stumps, or paludal facies. These thin (2 to 20 cm) lacustrine interbeds record the maximum transgression of Lake Gosiute. The sediments within this systems tract range from dark grey to black mudstone at the base to generally thick, red paleosol units at the top. Minor amounts of sheet-like crevasse-splay sandstone beds occur in increasing abundance upwards.

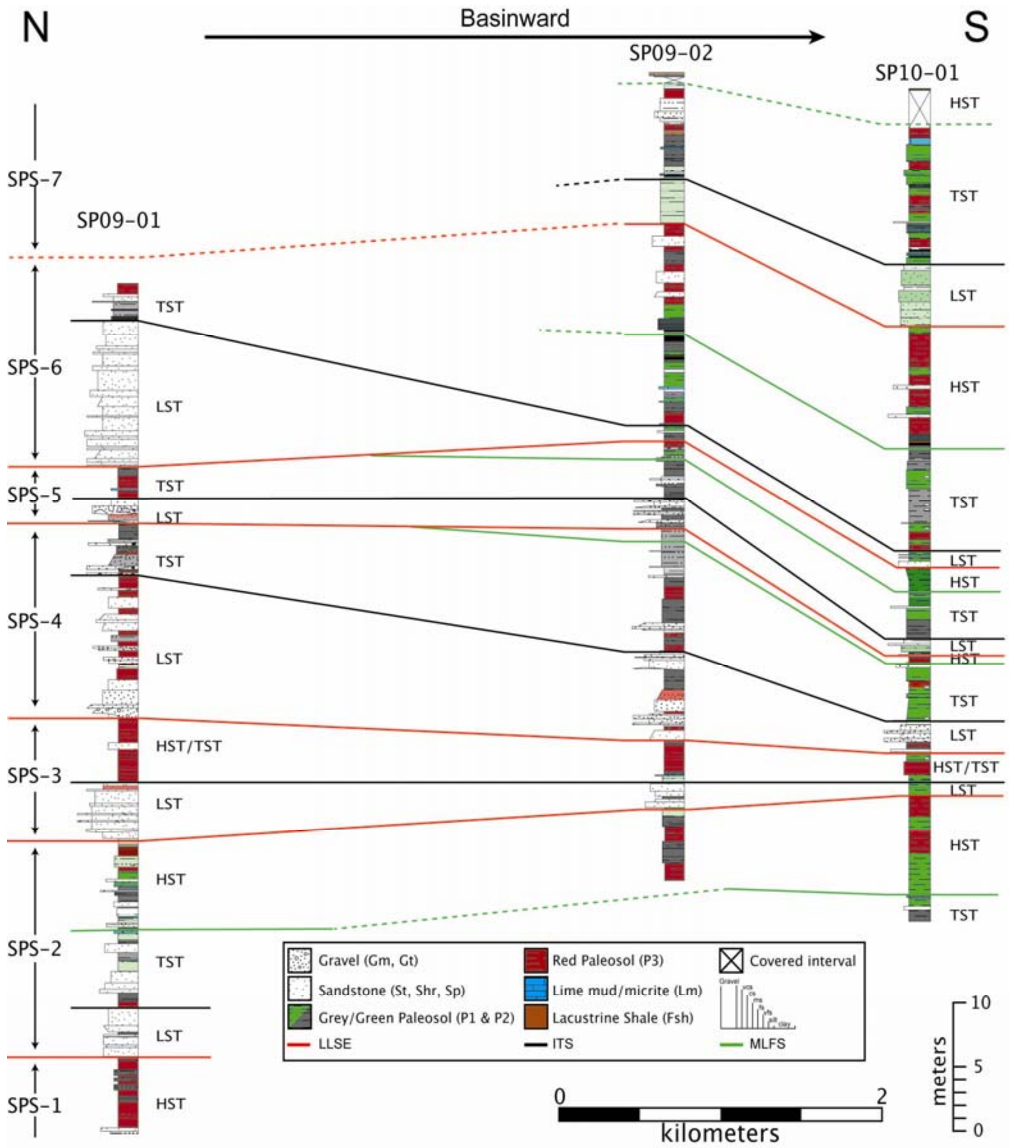

Figure 3.11 – Cross section showing the seven depositional sequences identified within the Cathedral Bluffs Tongue. These are some of the most distal sections in the study area. Notice how the Maximum Lacustrine Flooding Surfaces are eroded away as you move towards the basin margin. LST: Lowstand Systems Tract, TST: Transgressive Systems Tract, HST: Highstand Systems Tract, LSE Lowstand Surface of Erosion, ITS: Initial Transgressive Surface, MLFS: Maximum Lacustrine Flooding Surface.

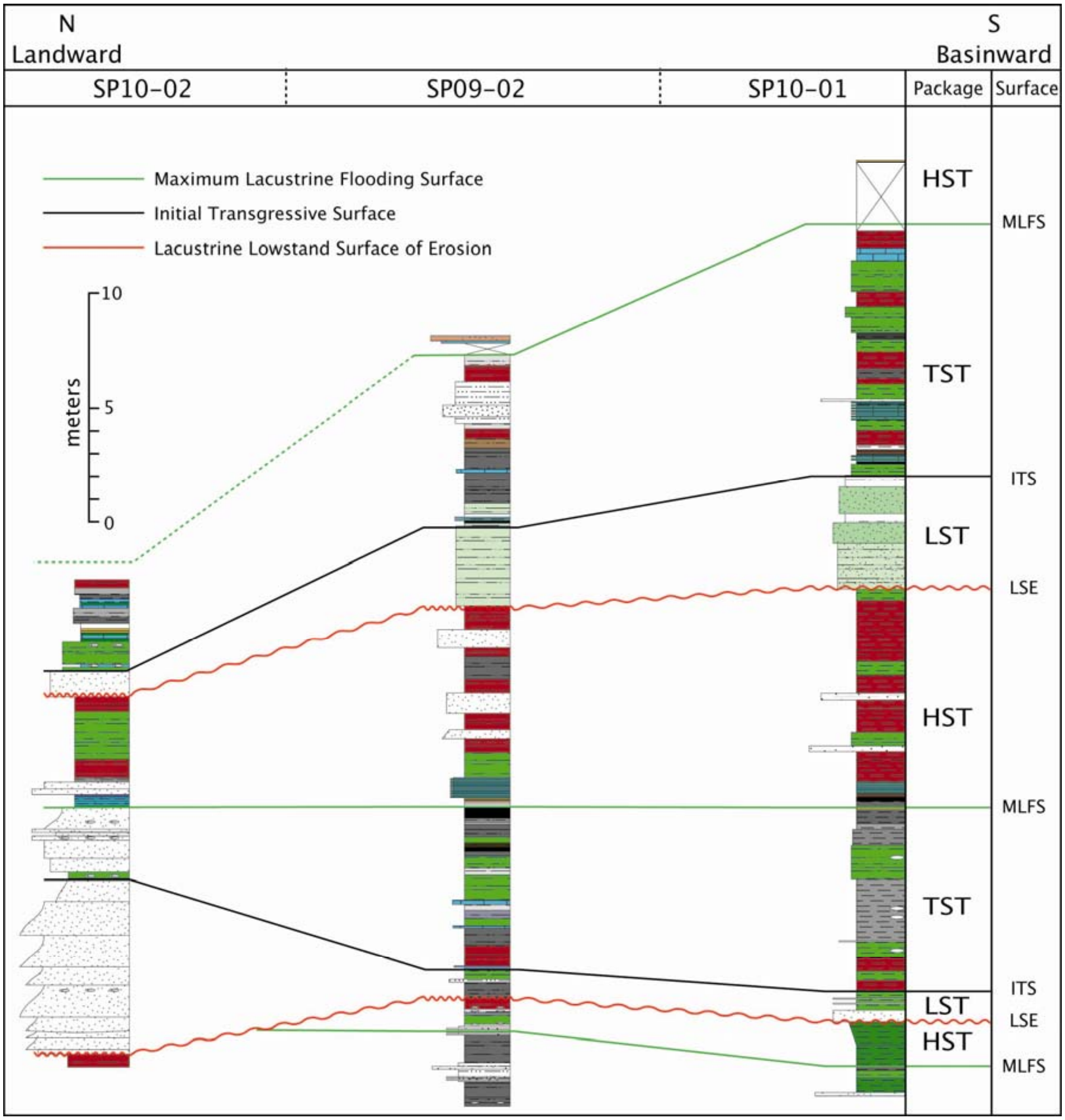

Figure 3.12 – The upper part of Bush Rim showing good sequence development. The basinward sections show terraces or interfluvial sequence boundaries above the red, well-drained paleosols. Section SP10-02 shows a thick, amalgamated channel unit belonging to the LST at the base of the sequence.

3.5. Discussion

Applying sequence stratigraphic principles to fully continental settings is more complex than applying these principles in mixed marine-continental and fully marine settings in that identification of key surfaces is typically more problematic and the artifacts of autocyclic processes may be difficult to differentiate from the products of more regional, allocyclic processes (Bohacs *et al.*, 2000; Zonneveld *et al.*, 2003). As well, the expression of key surfaces differs dramatically between proximal and distal settings and thus correlation between the two may be difficult.

3.5.1. Stratal Surfaces

Sequence boundaries within the Cathedral Bluffs Tongue can be picked based on either the sediment over- or underlying the boundary. Above the boundary, coarse-grained, amalgamated channel sandstone units (FA1, Fig. 3.13A-D) representing LST deposits may demarcate a sequence boundary. Below this surface, often bright red, well-drained paleosol profiles (FA3, Fig. 3.14C) may occur. These paleosols formed during base-level fall, and are well-drained due to the low water table level. They are interpreted to represent sequence boundaries on interfluve or terrace areas. Sequence-bounding unconformities were formed on the alluvial plain in response to base-level fall. As base-level dropped, sediment bypass and erosion occurred, which produced a depositional hiatus and possibly resulted in local fluvial incision. Valley incision may not occur in areas with low gradients during base-level fall. Planar unconformities associated with sheet sandstone bodies may form instead (Shanley and McCabe, 1991; Posamentier *et al.*, 1992; Schumm, 1993; Koss *et al.*, 1994). If valleys are cut, the sequence boundary will also overly interfluve and terrace deposits. Thick, well-drained paleosols form on these interfluve areas due to prolonged sub-aerial exposure and pedogenesis. In these cases, there is

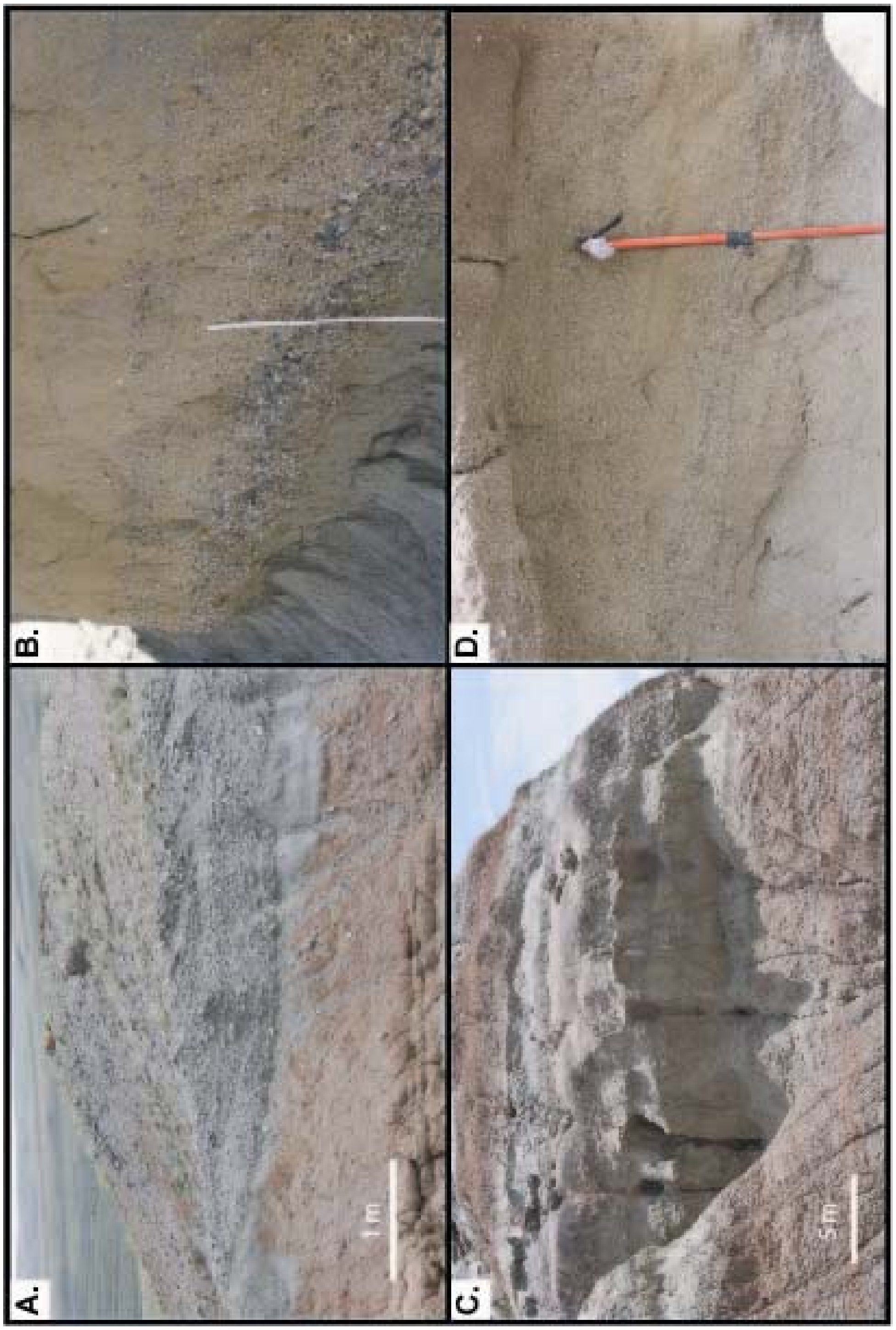

Figure 3.13 – Facies Association 1(FA1) – Fluvial Channel. **A.** SP10-03: Trough-cross bedded gravel eroding into sandy overbank facies. This is the most proximal area and the gravel is the base of a braided channel. **B.** SP10-08: Sandy channel with a coarse-gravel lag at the base. This channel is cutting into facies P1 and shows strong normal grading in the bottom 40 cm of the channel. Ruler for scale is showing ~ 60 cm. **C.** SP10-10: Isolated lenticular channel sandstone encased within facies P3. **D.** SP10-07: Trough-cross bedded sandstone with pebbly crossbeds. Pogo for scale is showing ~1m with 10 cm divisions.

Figure 3.14 – A. Facies Association 2 (FA2) – Crevasse Splay. The thin, sheet-like sandstone body in the center of the photograph is typical of FA2 in the study area. On the right side of the photograph, a small crevasse channel is observed. **B. – D.** Facies Association 3 (FA3) – Pedogenically-altered Overbank Fines. **B.** Light grey paleosols (facies P1) showing faint profile development, only incipient pedogenesis has occurred. **C.** Dark grey paleosol (facies P2). This unit is often recessive making it difficult to get a proper photograph. **D.** Bright red paleosols (P3) overlain by very thick channel sandstone.

generally an absence of coarse-grained, amalgamated channel deposits above the sequence boundary. During the early part of base-level rise channel deposits were confined to valleys cut during the previous interval of base-level fall.

Identification of sequence boundaries in the study area may be aided by the presence of abundant stromatolitic and fossil material at the base of channel sandstone successions. The presence of reworked laminar and bulbous stromatolites clasts indicates erosion of previously underlying lake margin sediments. In this case, the lowstand systems tract has cut down through the previous maximum lacustrine flooding surface including rip up clasts and stromatolitic material into the deposit. Additionally, incision on the floodplain may have processed previously deposited sediment, thereby, distilling fossil material into much higher abundances directly above sequence boundaries. The presence of specific basin-centre and lake margin turtle (trionychids, *Baptemys*, and *Echmatemys*), alligatorid (*Procaimanoidea utahensis*), and crocodilian taxa also strongly suggest incision and reworking of underlying lake margin deposits (Bartels *et al*., 2011).

Glossifungites surfaces in the marine realm are interpreted to represent stratigraphic discontinuities (Pemberton and Frey, 1985; Pemberton and MacEachern, 1995; MacEachern *et al.*, 2006). This type of surface is observed in the study area (Fig. 3.15), but is not interpreted to represent an unconformable surface. The firmground surfaces occur at the base of channel sandstone packages and are interpreted to represent autocyclic processes rather than allocyclic processes (Pemberton and Frey, 1985; Pemberton and MacEachern, 1995; Zonneveld *et al.*, 2003; Zonneveld *et al.,* 2006). Channel incision and lateral migration resulted in exposure of firm, compacted floodplain mudstone that was subsequently colonized by invertebrates within the channel. Applying the name *Glossifungites* to this type of surface in continental settings is questionable, as firmground substrates are part of the ambient condition of paleosols (MacEachern *et al.,* 2006).

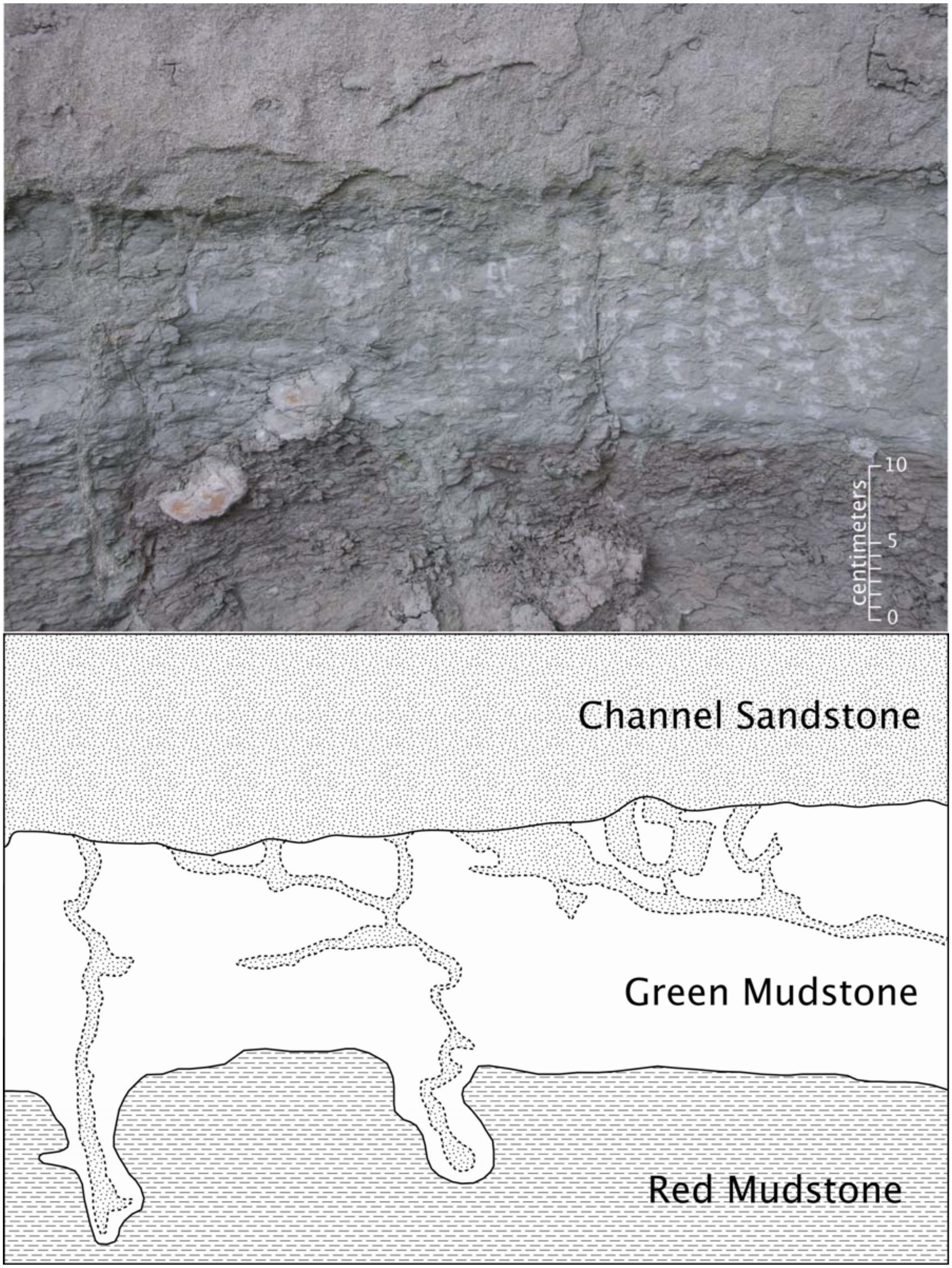

Figure 3.15 – *Glossifungites*-like surface from SP10-10. Autogenic channel avulsion, rather than a regional allogenic process produced this surface.

Channel incision, amalgamation of coarse-grained channel fill successions, and sediment bypass associated with lowstand conditions occur below the initial transgressive surface (ITS). The ITS is picked where the preserved sedimentary succession indicates that accommodation rates increased, allowing for more rapid sedimentation rates. A change from coarse-grained, amalgamated channels to thick mudstone packages with isolated channels and extensive crevasse-splay sandstone beds (potentially with reworked floodplain stromatolite clasts) demarcates this surface. A rapid increase in accommodation space resulted in deposition and preservation of mudstone-dominated floodplain successions with subordinate crevasse-splay and channel sandstone beds (Pedersen and Steel, 1999; Zonneveld *et al.*, 2003). The floodplain mudstone units generally show only incipient or low-grade pedogenesis, and primary laminae are commonly preserved. The immaturity of the paleosols is due to the relatively rapid sedimentation rates, thus preventing clear pedogenic profiles from being differentiated before the succession is buried.

Maximum lacustrine flooding surfaces are clearly demonstrable only in the more distal sections of the study area. Thin intervals of micritic oil shale (10 to 15 cm, Fig. 3.16C-D) overlying poorly drained paleosol successions demarcate maximum lacustrine transgression in the most distal sections. These thin beds rapidly pinch out, or were erosionally removed by subsequent fluvial processes in basin margin settings. The micritic oil shale is the most distal lacustrine facies observed. Towards the basin margin, more proximal lacustrine facies are observed, such as bedded stromatolites or tree stumps in growth position encrusted by stromatolites. Although lacustrine sediments were not directly observed, the presence of laminar and bulbous stromatolites indicates lacustrine margin conditions. Further towards the basin margin, encrusting stromatolites (commonly on logs and standing trees) are observed and, in several examples, were post-depositionally reworked in fluvial channels. Thin section analysis has revealed the presence of ooids within the sediment included in the stromatolite structure (Fig.

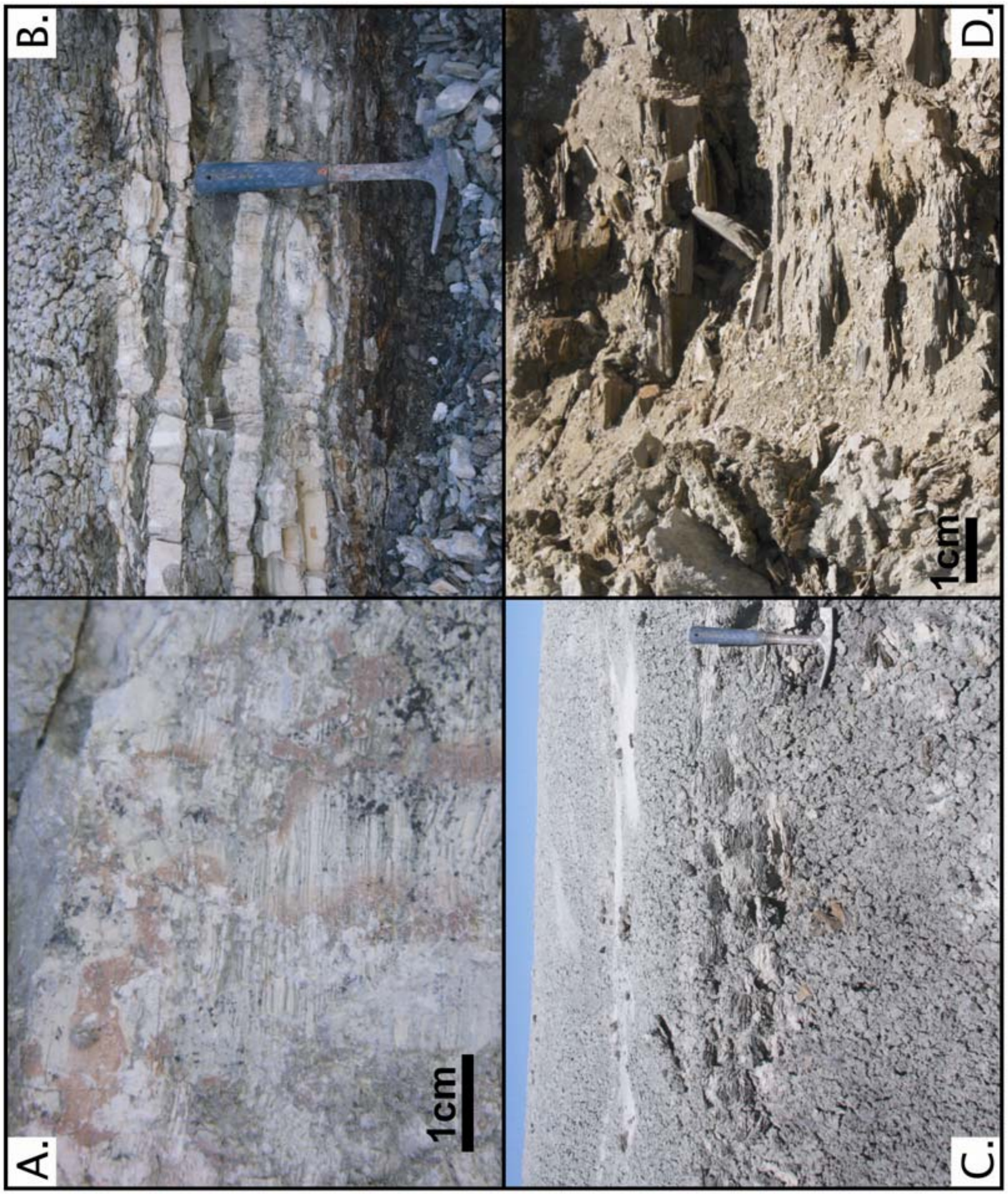

Figure 3.16 – Facies Association 4 (FA4) – Palustrine to Lacustrine Margin. **A.** SP10-01: Millimeter scale interlaminae of facies Lm and P1. Laminae are wavy, possibly indicating a shallow water depositional setting. **B.** SP10-01: Centimeter scale interbedding of facies Lm and P1. FA4 is overlying a lignitic layer, indicating a swampy / pond-like depositional setting. Hammer for scale is 28 cm long. **C.** Facies Association 5 (FA5) – Lacustrine. SP10-01: Facies Fsh after weathering by exposure to sun and air. The bedding become convolute as the oil-shale-like sediment is dried. Hammer for scale is 28 cm long. **D.** SP10-10: Laney Member lacustrine shale (facies Fsh) overlying the Cathedral Bluffs Tongue.

3.17B). This reinforces the interpretation that these stromatolites were indeed lacustrine in origin and provides evidence of a lacustrine transgression, followed by erosion of the HST and MLFS. In peripheral areas, where the lacustrine transgression did not reach, the MLFS can be identified by interbedded mudstone and marlstone (Fig. 3.16A-B), indicating paludal deposits caused by the elevated water table. At the northern margin of Bush Rim (SP10-12), a MLFS in section SP10-12 contains stromatolitic caddisfly pupal-case mounds (Fig. 3.17C). These mounds are indicative of lake margin settings (Leggit *et al.,* 2007).

In the most proximal (upland) sections of the Cathedral Bluffs Tongue, it is not possible to identify the MLFS. It is possible that either fluctuating lake-level applied only subtle or no influence to these proximal deposits, or erosion associated with overlying sequence boundaries eroded basin-margin expressions of the MLFS.

3.5.2. Stratal Packages

The Cathedral Bluffs Tongue can be separated into transgressive-regressive (T-R) stratal packages based on fluctuations in lake level. These packages have been identified in other alluvial successions with no marine influence (Olsen *et al.*, 1995; Petersen *et al.*, 1999; Arnott *et al.*, 2002; Zonneveld *et al.*, 2003; Fanti and Catuneanu, 2010). The stratal packages are split into systems tracts identical to those of marine deposits (Posamentier and Allen, 1999). However, marine and lacustrine sequences have very different expressions. Additionally lacustrine sequences show a wide variety of depositional types based on the type of lake depositional system (Bohacs *et al.,* 2000).

The lowstand systems tract occurs between the lacustrine lowstand surface of erosion (sequence boundary) and the initial transgressive surface (maximum regressive surface). Erosion and valley incision occurred on the basin margins as base-level began to fall and accommodation space was

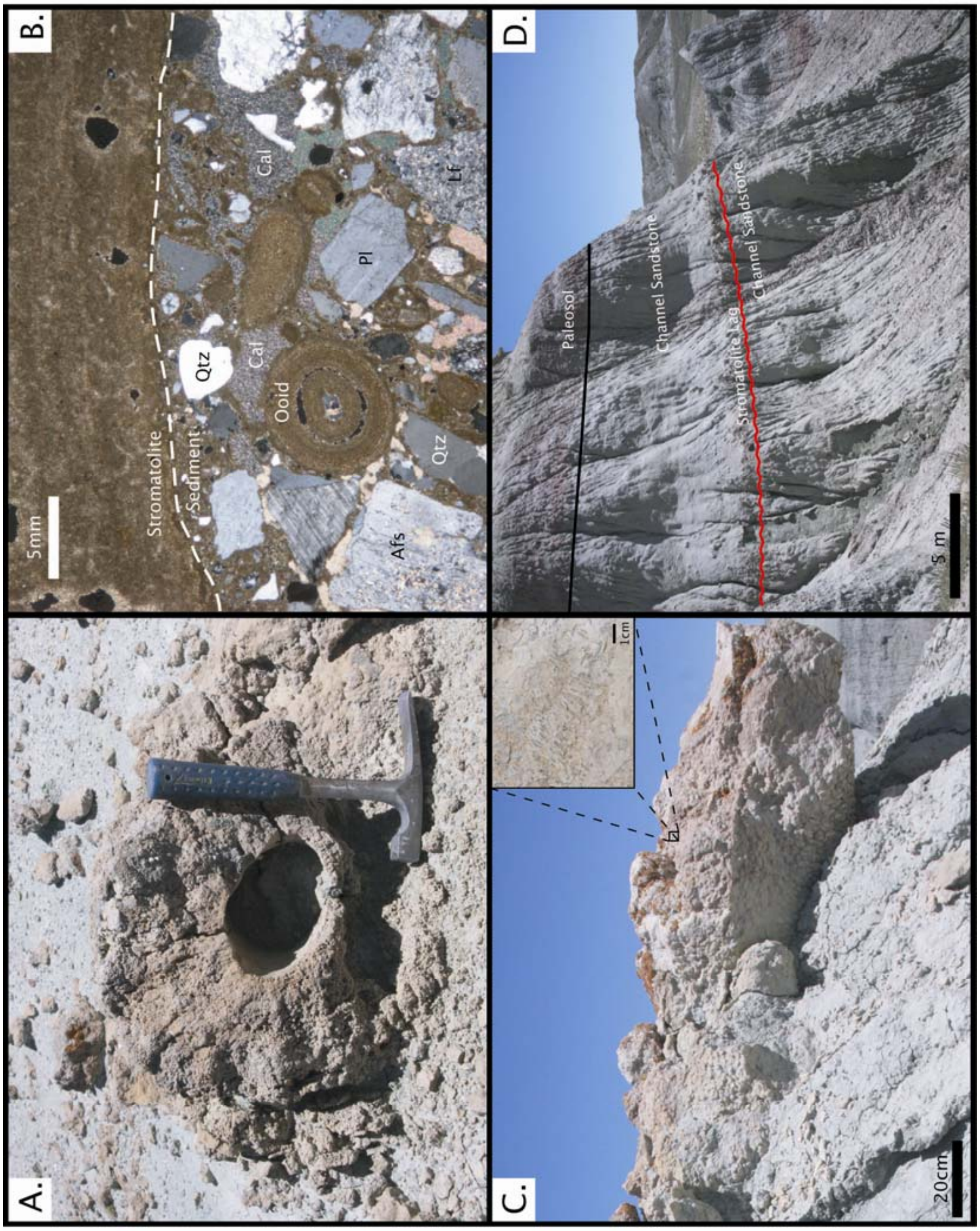

Figure 3.17 – Indication of lacustrine transgressions. **A.** SP10-02: A stromatolite encrusted log. Hammer for scale is 28 cm long. **B.** SP09-02: Thin section through a similar, sediment infilled stromatolitic log mold. Note the presence of ooids within the sediment, indicating lacustrine conditions during time of deposition. **C.** SP10-12: Caddisfly pupal mounds indicative of a lacustrine margin setting. **D.** SP10-12: A stromatolitic lag at the base of a sequence boundary. The upper channel has cut down into another channel sandstone; they are only distinguished by the lacustrine stromatolite lag in between.

negative. As base-level began to rise again, accommodation space slowly increased, allowing for deposition in the LST.

Coarse-grained, amalgamated channel sandstone units (FA1, Fig. 3.13A-D) of the LST mark the base of each sequence. The base of the channel fill often contains granule to pebble lags, and in some cases contain reworked vertebrate fossil and stromatolitic material. On spectral gamma logs, these coarse lags may show high concentrations of radioactive Th and U due to the abundance of heavy minerals and fossil bone in the channel lags. The presence of stromatolites at the base of the channels indicates that the valleys must have incised into transgressive or highstand lacustrine deposits. Due to the low accommodation space during deposition, preservation of floodplain fines (FA3, Fig. 3.14B-D) is rare in this interval.

Low total gamma radiation is often used to identify lowstand sediments, as lowstand deposits are generally coarse-grained in nature (Davies and Elliott, 1996), However, this not the case for the Cathedral Bluffs Tongue as a result of the immaturity of the sediment. An abundance of mica and feldspar produce high potassium (2 to 3 wt %) readings, while the aforementioned heavy minerals result in high thorium (18 to 20 ppm) and intermediate uranium (5 to 8 ppm) concentrations at the bases of amalgamated LST channel successions.

The deposits of the transgressive systems tract occur above the LST, between the ITS and the MLFS. During this interval, base-level rose at a faster rate than it did during lowstand conditions, which resulted in the rapid creation of accommodation space. During the TST, the creation of accommodation space outpaced the input of sediment, which resulted in a lacustrine transgression that produced diagnostic depositional patterns on the alluvial plain.

Floodplain-dominated, overall fine-grained, heterolithic sediments characterize TST successions within the Cathedral Bluffs Tongue. Thick, light grey-green mudstone units with incipient pedogenesis (FA3, Fig. 3.14B), isolated channel sandstone beds (FA1, Fig. 3.13), and extensive, thin crevasse-splay sheet sandstone beds (FA2, Fig. 3.14A) are the most common facies within the TST. Due to the heterolithic nature of the systems tract, a variable natural gamma response is observed. Concentrations of K and Th tend to be relatively high and may decrease upwards to the next sequence boundary. However, some sections (SP10-09, SP10-06) show high values of K and Th in the TST and a sharp decrease at the MLFS. A subtle increase in the U concentration upwards is also observed in some sections.

This type of heterolithic succession is herein attributed to rapid base-level rise creating abundant accommodation space, concomitantly capturing high proportions of overbank fines within the system and isolating channel sandstone beds within dominantly fine-grained intervals. High accommodation space resulted in both common crevassing and channel avulsion and is interpreted to account for much of the mudstone deposition within these intervals (Aslan and Autin, 1999; Aslan *et al.*, 2005). The apparent thickening of the TST towards the basin centre is consistent with existing sequence stratigraphic models (Plint *et al*., 2006; Keighley *et al*., 2003; Catuneanu, 2006).

The highstand systems tract occurs above the TST, between the MLFS and the next sequence boundary. During deposition of the HST, base-level rise slowed. The rate of accommodation space creation was outpaced by the sedimentation rate, which resulted in negative net accommodation. All available accommodation space was utilized and some sediment bypass occurred. In other successions it has been observed that channel abundance increases upwards through the HST (Olsen *et al.*, 1995; Arnott *et al.*, 2002; Catuneanu, 2006), however this has not been observed in the Cathedral Bluffs Tongue.

The basal portion of the HST often contains poorly-drained paleosols, as well as black and dark grey mudstone (FA3, Fig. 3.12C). Interbedded marl and claystone (FA4, Fig. 3.13A-B) are also commonly observed in the early HST. The MLFS is the lower boundary of the HST and demarcates both the highest lake levels within the study area, as well as the farthest landward point that lacustrine facies occur. Thus, water table levels were high resulting in paludal facies and poorly-drained paleosols (FA3, Fig. 3.14C).

Paleosol maturity levels increase upwards through the HST. This maturity trend may be attributed to the decreased sedimentation rate, as accommodation space is less available. Thick, well-drained paleosols with dark red colouration and thin, sheet-like sandstone lenses (FA2, Fig. 3.14A) may cap the HST. Sediments deposited during the latest stages of base-level rise are overprinted by weathering related to sub-aerial exposure and to secondary pedogenic alteration during base-level fall. In many sections, these distinctive red paleosols were eroded during base-level fall, which resulted in coarse LST deposits overlying the dark grey, immature paleosols or paludal facies.

The highstand systems tract can be easily distinguished on spectral gamma logs. The HST is characterized by low concentrations of both K and Th. The low K values are attributed to the leaching of K during sub-aerial exposure and pedogenesis. Thorium depletion is unexpected because it is an immobile element, and should not leach out of paleosols. The low concentration of Th is attributed to the absence of heavy minerals in the finer grained fraction of floodplain mudstone.

The proximal deposits of the Cathedral Bluffs Tongue show thick, distinct packages that exhibit very low levels of radioactive K. This is attributed to the presence of a sequence bounding unconformity overlying the low-K paleosols. In more distal sections (SP10-04, SP10-01), the K concentration does not show such a complete leaching through an entire zone. The K concentration decreases upwards towards the sequence boundary and at the boundary increases dramatically. This allows for a quick and easy way to identify some sequence boundaries although it must be noted that not all sequence boundaries overlie intervals with such depleted K concentrations, as these deposits are often erosionally removed.

3.5.3. Sequence Controls

Sequences in marine settings are dominantly controlled by fluctuations in sea-level (Vail *et al.*, 1977; Posamentier *et al.*, 1988). The Green River Basin is a continental lacustrine basin located at a great distance from the nearest ocean and thus, global eustacy had no direct affect on sequence development. For the Cathedral Bluffs Tongue, base-level rise or fall was dependent mainly upon tectonic activity and climatic change (Carroll and Bohacs, 1999; Bohacs *et al.*, 2000; Zonneveld *et al.*, 2003). Variations in climate affect precipitation, evaporation, sediment supply, and fluvial discharge. All of these factors had a significant effect on the level of Lake Gosiute. Tectonic influences may change drainage areas, drainage patterns, spillway elevations, fluvial gradient, and control local subsidence rates. Tectonic influences in the study area during the Eocene are attributed primarily to intermittent movement on the Wind River Thrust Fault (Steidtmann and Middleton, 1991; Carroll *et al*., 2006; Johnson and Anderson, 2009).

The Cathedral Bluffs Tongue in the study area is a coarse clastic wedge, emanating from the Wind River Mountains. Deposition of the tongue is thought to have occurred during a relatively short interval, approximately 1.0 to 1.5 Ma (Clyde *et al.,* 2001). The period of deposition occurred during the early Eocene Climactic Optimum (ECO), from about 52 to 50 Ma (Lowenstein and Demicco, 2006; Smith *et al.*, 2008). Paleobotanical evidence has shown that during the early Bridgerian, southwestern Wyoming was warm (MAT ~20°C) with low temperature seasonality, and dry with seasonal precipitation (Wilf, 2000). Mean annual rainfall decreased from approximately 140 cm to 80 cm between the Wasatchian and earliest Bridgerian NALMAs (Wilf, 2000), which may have partly caused the regression of Lake Gosiute. The climate during the Bridgerian NALMA is assumed to be warm and relatively constant, due to the short timeframe of Cathedral Bluffs deposition.

Due to the relative stability of the climate, tectonic activity was likely the dominant control on higher-order sequence development. There is clear evidence of syndepositional tectonic movement in the Cathedral Bluffs Tongue in study area. Reds Cabin Monocline (sec. 20-21, T. 27N, R. 101W) is a 3 km long asymmetrical anticline, with a shallowly dipping northern limb and steeply dipping southern limb (Fig. 3.18A-B). The monocline follows the trace of the Wind River Thrust Fault and is likely associated with movement along the fault during the late stages of Cathedral Bluffs deposition (Steidtmann and Middleton, 1991). Sedimentological evidence and thickness relationships from this study reinforce the timing of this structural event to before the end of Cathedral Bluffs Deposition. Uplift on the Continental Fault also occurred during deposition of the Cathedral Bluffs Tongue. Large (3 to 4 m diameter) boulders of granite and iron formation (Fig. 3.18C-D) occur strewn along the surface adjacent to the Continental Fault (Zeller and Stephens, 1969; McGee, 1983; Steidtmann and Middleton, 1991; Pietras *et al.*, 2003). The boulders were originally deposited within or above the upper part or the Cathedral Bluffs Tongue (Love and Christiansen, 1985; Steidtmann and Middleton; 1991). These remnants of boulder conglomerate beds are thought to represent exhumed alluvial fans (Pietras *et al.*, 2003) emplaced along the Continental Fault (an uplifted reverse fault) during the latest Early Eocene (McGee, 1983; Steidtmann and Middleton, 1991; Pietras *et al.* 2003). The fault has since undergone normal movement as the southern margin of the Wind River Mountains has collapsed (Hall and Chase, 1989).

The result of tectonic uplift is primarily increased erosion in the hinterlands leading to increased sediment supply. However, if uplift outpaces erosion, tectonic loading will cause subsidence adjacent to the orogen. Therefore, coarse-grained sediment is trapped in the proximal areas by a rapid increase in accommodation space. Progradation of the coarse-grained

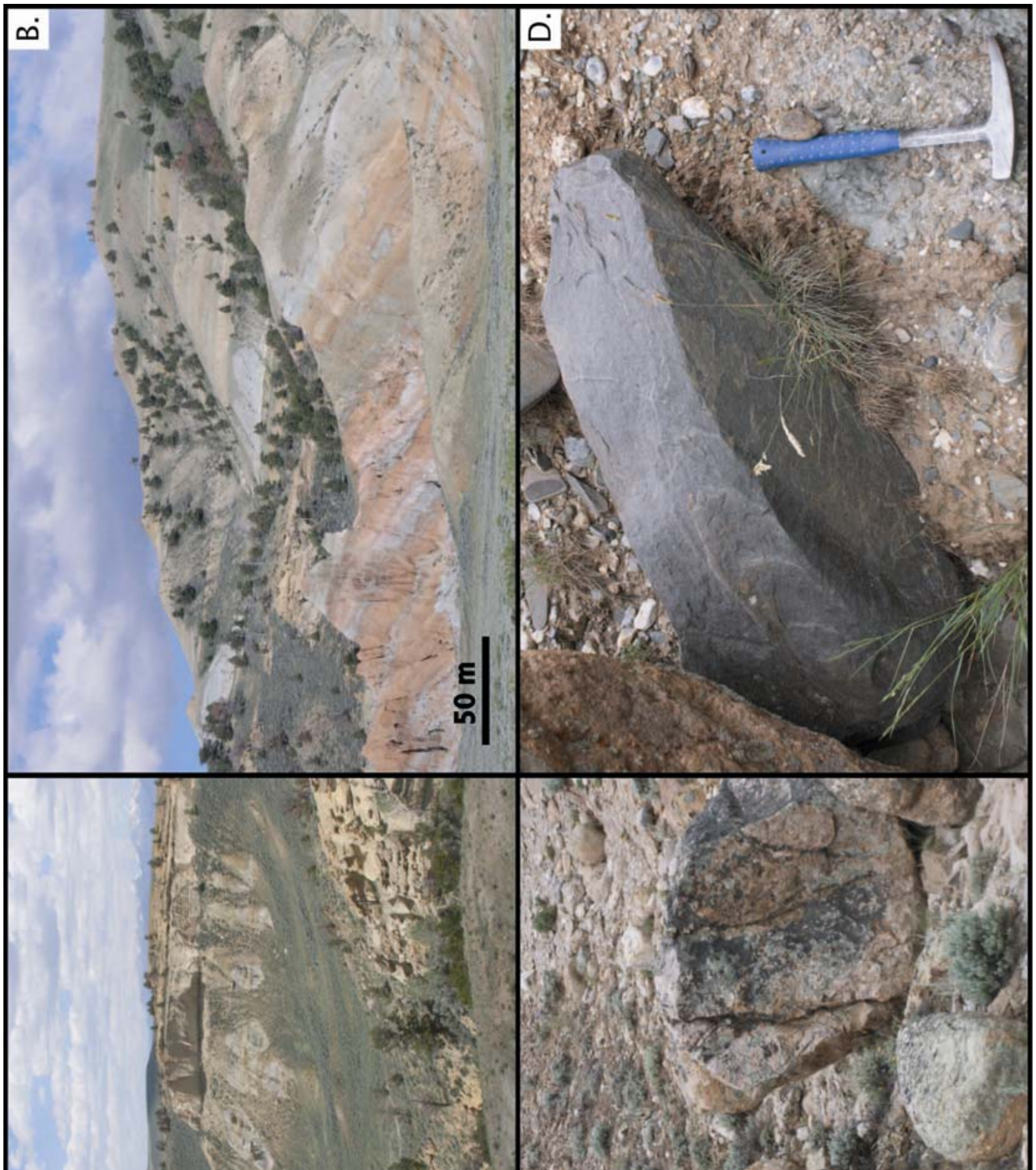
A.
B.
50 m
C.
D.

Figure 3.18 - Evidence of active tectonism during deposition of the Cathedral Bluffs Tongue. **A.** The Reds Cabin Monocline looking northwest, with the steeply dipping beds on the left side of the photo. The resistant sandstone is the Farson Sandstone Member of the Green River Formation. Underlying the deltaic sand is the Scheggs Bed, the Tipton Shale, and at the base of the section the Main Body of the Wasatch Formation. Measured section SP10-05. Resistant sandstone cliff is approximately 20 m thick. **B.** The southeastern end Reds Cabin Monocline. Notice the dipping red and grey variegated beds of the Cathedral Bluffs Tongue. The thick light grey unit capping the alternating red and grey bands is the last package of CBT deposition. Notice how this band and the overlying Laney Member are not deformed over the monocline. **C.** Granite boulders observed near the Continental Fault. Hammer for scale is 33 cm long. These boulders are not in place, but come from somewhere above measured section SP10-06. Hammer for scale is 33 cm long. **D.** Precambrian iron formation boulders that occur with the granite boulders near Pacific Butte. Hammer for scale is 33 cm long.

sediment will not occur until subsidence rates decrease or available accommodation space is filled. This means that the episode of greatest gravel progradation indicates a period of relative tectonic quiescence (Allen and Heller, 2012). The episodic tectonic perturbations in the Cathedral Bluffs Tongue are likely on the order of 10^4 to 10^5 years, as there are at least at least two, and likely more, significant events in the study area over approximately 1.5 Ma (Clyde *et al.,* 2001). Numerical models (Paola *et al.,* 1992; Allen and Heller, 2012) have shown that typically the equilibrium time or landscape evolution response times are on the order of 10^6 years. With the uplift times less than the equilibrium times, the Cathedral Bluffs Tongue likely never reached equilibrium state.

3.6. Conclusions

Outcrop of the Cathedral Bluffs Tongue near South Pass, Wyoming was examined to determine stratigraphic relationships. The deposits of the Cathedral Bluffs Tongue occur in five facies associations: fluvial channel (FA1), crevasse splay (FA2), pedogenically-altered overbank fines (FA3), palustrine to lacustrine margin (FA4), and lacustrine offshore (FA5). These associations were analyzed within a sequence stratigraphic and chemostratigraphic framework. Each approach was tested for its applicability to the floodplain-dominated fluvial succession. Comparison of the two approaches has allowed for identification of deficiencies for each method.

Detailed outcrop analyses and spectral gamma ray data were used to identify stratal packages and surfaces. The result of the study is a high-resolution chronostratigraphic framework containing seven depositional sequences (SPS-1 through SPS-7). The sequences are bound by erosional unconformities (Fig. 3.19) and generally display systems tracts similar to other fluvial sequence stratigraphic models (Wright and Marriot, 1993; Shanley and McCabe, 1994; Olsen *et al.*, 1995; Kraus and Aslan, 1999; Martinsen *et al.*, 1999; Arnott *et al.*, 2002; Zonneveld *et al.*, 2003). Identification and correlation of sequences throughout the study area is significantly improved by integration of SGR data with lithological analysis.

Above sequence boundaries, K and Th concentrations increase substantially due to the high abundance of feldspars / micas and heavy minerals, respectively. These minerals are observed in abundance within the immature lowstand sediments of the Cathedral Bluffs Tongue. Spikes in the Th and U concentrations, attributed the heavy mineral lags, occur at the base of these lowstand channels. Uranium spikes in channel lags have intermediate concentrations (between 5 to 8 ppm) and Th spikes are at their highest point (~18-20 ppm).

Maximum flooding surfaces can be identified by high U concentrations (>10 ppm) in the most distal sections. These uranium spikes are observed in the most distal sections due to deposition under dysoxic / anoxic lacustrine conditions. Lacustrine transgressions did not reach the absolute margins of the basin and thus anoxic signatures of radioactive elements do not occur in the most proximal sections.

Within the study area, well-drained, mature paleosols underlie sequence boundaries and can be identified on SGR logs by very low K (<0.05 wt %) and Th (<5 ppm) concentrations. Potassium is a soluble, and therefore

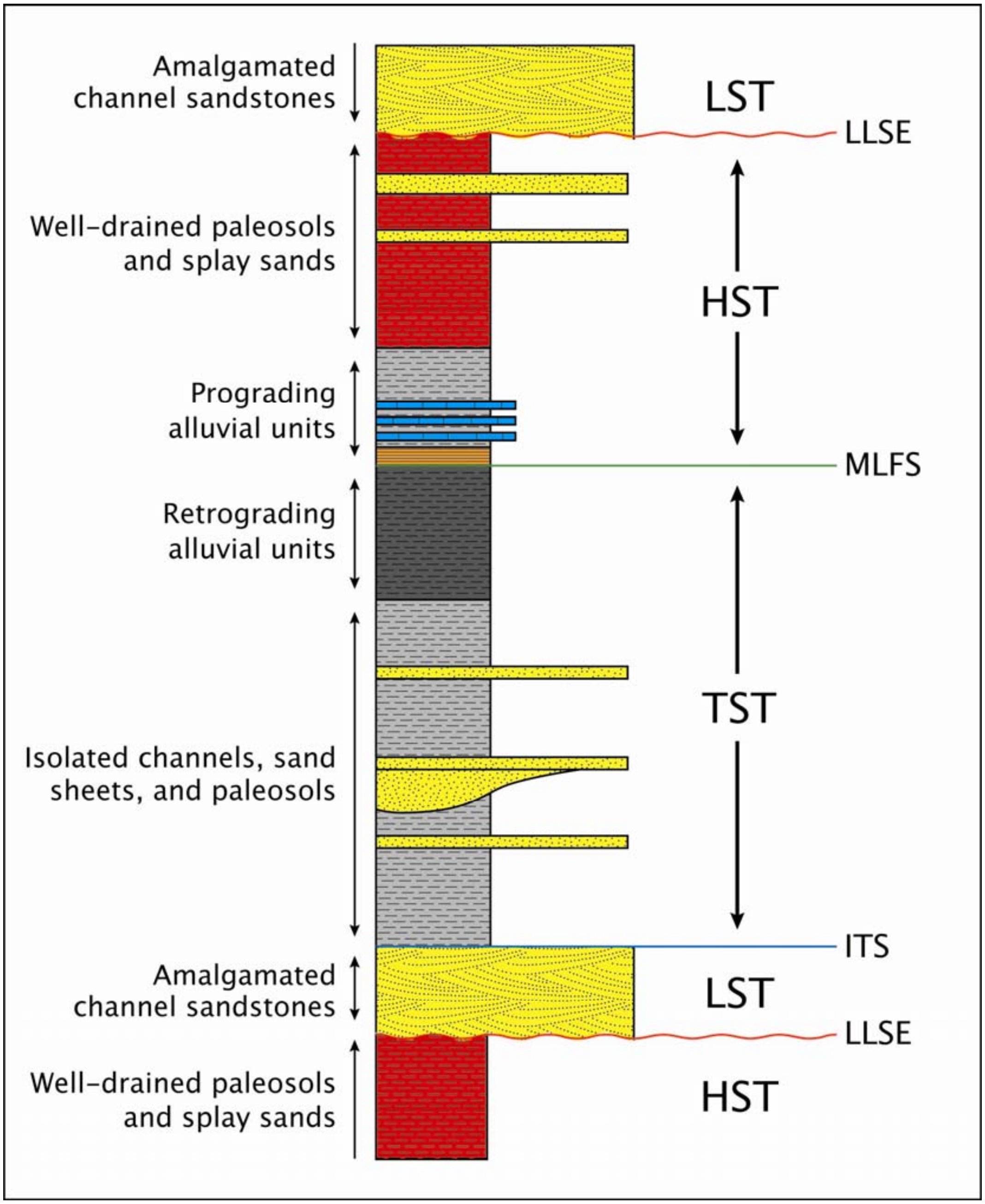

Figure 3.19 – An idealized schematic of the sequence stratigraphic architecture within the Cathedral Bluffs Tongue.

mobile element, and depletions are attributed to leaching K during sub-aerial exposure and pedogenesis. Although Th is generally considered an immobile element, it is also strongly depleted within these sequence boundary paleosols. Thorium concentrations correlate well with variations in potassium concentration. This is unexpected, as Th is considered to be immobile relative to K (Preston *et al.,* 1998).

Sequence development within the Cathedral Bluffs Tongue is attributed primarily to tectonic influences. Fault-scarp boulders from the Continental Fault and movement on the Wind River Thrust fault causing the Reds Cabin Monocline are both evidence of syndepositional movements during deposition of the Cathedral Bluffs Tongue. Cobble / pebble conglomerate within sandy deposits proximal to the Wind River Range are also interpreted to indicate syndepositional movement along the Wind River Thrust Fault. Uplift, and concomitant flexural subsidence in the basin, controlled the creation and destruction of accommodation space in the basin. The subsidence in the basin trapped all coarse material in the most proximal areas, where subsidence was greatest (Allen and Heller, 2012).

3.7. References

Ali, K., Cheng, Q., Li, W., Chen, Y., 2006. Multi-element association analysis of stream sediment geochemistry data for predicting gold deposits in south-central Yunnan Province, China. Geochemistry: Exploration, Environment, Analysis, v. 6, 341-348.

Allen, P. A., and Heller, P. L., 2012. Dispersal and preservation of tectonically generated alluvial gravels in sedimentary basins, *in* Tectonics of Sedimentary Basins: Recent Advances. Edited by C. Busby and A. Azor, 111-130.

Arnott, R. W. C., Zaitlin, B. A., and Potocki, D. J., 2002. Stratigraphic response to sedimentation in a net-accommodation-limited setting, lower Cretaceous Basal Quartz, south-central Alberta. Bulletin of Canadian Petroleum Geology, v. 50, 92-104.

Aslan, A., and Autin, W. J., 1999. Evolution of the Holocene Mississippi River floodplain, Ferriday, Louisiana: Insights on the origin of fine-grained floodplains. Journal of Sedimentary Research, v. 69, 800-815.

Aslan, A., Autin, W. J., Blum, M. D., 2005. Causes of river avulsion: Insights from the late Holocene avulsion history of the Mississippi River, U.S.A. Journal of Sedimentary Research, v. 75, 650-664.

Baltzer, F., 1991. Late Pleistocene and Recent detrital sedimentation in the deep parts of northern Lake Tanganyika (East African rift), *in* Lacustrine facies analysis, Edited by P. Anadon, L. Cabrera, and K. Kelts. International Association of Sedimentologists Special Publication 13, 147-173.

Bartels, W. S., Zonneveld, J. -P., and Gunnell, G. F., 2004. Early fluvial (Cathedral Bluffs) deposition into a lacustrine basin (Green River) and the resulting preservation of an unusual terrestrial vertebrate assemblage, Honeycomb Buttes, Wyoming. Abstracts with Programs - Society of America, v. 36, 527.

Bartels, W. S., Gunnell, G., Zonneveld, J. -P., McHugh, L. P., Fontana, T. M., 2011. An unusual vertebrate assemblage preserved in distal alluvial fan and lake margin deposits of the Cathedral Bluffs Tongue, Wasatch Formation, Bush Rim, Red Desert, Wyoming. Geological Society of America Abstracts with Programs, v. 43, 264.

Bohacs, K. M., Carroll, A. R., Neal, J. E., Mankiewicz, P. J., 2000. Lake-basin type, source potential, and hydrocarbon character: an integrated-sequence stratigraphic– geochemical framework, *in* Lake basins through space and time. Edited by E. H. Gierlowski- Kordesch and K. R. Kelts, AAPG Studies in Geology, v. 46, 3–34.

Carroll, A. R., and Bohacs, K. M., 1999. Stratigraphic classification of ancient lakes: Balancing tectonic and climatic controls. Geology, v. 27, 99-102.

Carroll, A. R., Chetel, L. M., and Smith, M. E., 2006. Feast to famine: Sediment supply control on Laramide basin fill. Geology, v. 34, 197-200.

Catuneanu, O., 2006. Principles of sequence stratigraphy. Elsevier Science, 386 pp.

Clyde, W. C., Zonneveld, J. -P., Stamatakos, J., Gunnell, G. F., and Bartels, W. S., 1997. Magnetostratigraphy across the Wasatchian/Bridgerian NALMA boundary (early to middle Eocene) in the western Green River Basin, Wyoming. Journal of Geology, v. 105, 657-669.

Clyde, W. C., Sheldon, N. D., Koch, P. L., Gunnell, G. F., and Bartels, W. S., 2001. Linking the Wasatchian/Bridgerian boundary to the Cenozoic Global Climate Optimum: New magnetostratigraphic and isotopic results from South Pass, Wyoming. Palaeogeograhpy, Palaeoclimatology, Palaeoecology, v. 167, 175-199.

Davies, S.J., and Elliott, T., 1996. Spectral gamma ray characterisation of high resolution sequence stratigraphy: examples from Upper Carboniferous fluviodeltaic systems, *in* High Resolution Sequence Stratigraphy: Innovations and Applications. Edited by J. A. Howell and J. F. Aitken, Geological Society, London, Special Publications, v. 104, 25–35.

Dehairs, F., Chesselet, R., Jedwab, J., 1980. Discrete suspended particles of barite and the barium cycles in the open ocean. Earth Planetary Science Letters, v. 49, 528-550.

Dypvik, H., and Harris, N. B., 2001. Geochemical facies analysis of fine-grained siliciclastics using Th/U, Zr/Rb, and (Zr+Rb)/Sr ratios. Chemical Geology, v. 181, 131-146.

Fanti, F. and Catuneanu, O., 2010. Fluvial sequence stratigraphy: the Wapiti Formation, west-central Alberta, Canada. Journal of Sedimentary Research, v. 80, 320-338.

Finley-Jones, H. J., Molloy, J. L., Holcombe, J. A., 2008. Choosing internal standards based on a multivariate approach with ICP(TOF)MS. Journal of Analytical Atomic Spectrometry, v. 23, 1169-1316.

Gunnell, G. F., and Yarborough, V. L., 2000. *Brontotheriidae* (*Perissodactyla*) from the late, early, and middle Eocene (Bridgerian), Wasatch and Bridger Formations, southern Green River Basin, Southwestern Wyoming. Society of Vertebrate Paleontology, v. 20, 349-368.

Hall, M. K., and Chase, C. G., 1989. Uplift, unbuckling, and collapse: Flexural history and isostacy of the Wind River Range and Granite Mountains, Wyoming. Journal of Geophysical Research, v. 94, 581-593.

Hampson, G. J., Davies, W., Davies, S. J., Howell, J. A., Adamson, K. R., 2005. Use of spectral gamma-ray data to refine subsurface fluvial stratigraphy: late Cretaceous strata in the Book Cliffs, Utah, USA. Journal of the Geological Society, v. 162, 603-621.

Jenkyns, H. C., Jones, C. E., Grocke, D. R., Hesselbro, S. P., Parkinson, D. N., 2002. Chemostratigraphy of the Jurassic System: application, limitations, and implications for palaeoceanography. Journal of the Geological Society, v. 159, 351-378.

Johnson, P. L., and Andersen, D. W., 2009. Concurrent growth of uplifts with dissimilar orientations in the southern Green River Basin, Wyoming: Implications for Paleocene and Eocene patterns of foreland shortening. Rocky Mountain Geology, v. 44, 1-16.

Kaiser, H. F., 1958. The Varimax criterion for analytic rotation in factor analysis. Psychometrika, v. 23, 187–200.

Keighley D., Flint, S., Howell, J., and Moscariello, A., 2003. Sequence stratigraphy in lacustrine basins: A model for part of the Green River Formation (Eocene), southwest Uinta Basin, Utah, U. S. A. Journal of Sedimentary Research, v. 73, 987-1006.

Koss, J. E., Ethridge, F. G., Schumm, S. A., 1994. An experimental study of the effects of base-level change on fluvial, coastal and shelf systems. Journal of Sedimentary Research, v. B64, 90–98.

Kraus, M. J. and Aslan, A., 1999. Paleosol sequences in floodplain environments; a hierarchical approach. Special Publication of the International Association of Sedimentologists, v. 27, 303-321.

Kurtz, A. C., Derry, L. A., Chadwick, O. A., Alfano, M. J., 2000. Refractory element mobility in volcanic soils. Geology, v. 28, 683-686.

Leggit, V. L., Biaggi, R. E., Buchheim, H. P., 2007. Palaeoenvironments associated with caddisfly-dominated microbial-carbonate mounds from the Tipton Shale Member of the Green River Formation: Eocene Lake Gosiute. Sedimentology, v. 54, 661-669.

Love, J. D., and Christiansen, A. C., 1985. Geologic map of Wyoming: U.S. Geological Survey, 3 sheets, scale 1:500,000.

Lowenstein, T. K., and Demicco, R. V., 2006. Elevated Eocene atmospheric CO_2 and its subsequent decline. Science, v. 313, 1928.

MacEachern, J. A., Gingras, M. K., Bann, K. L., Dafoe, L. T., and Pemberton, S. G., 2006. Application of ichnology to petroleum exploration and production. SEPM Special Publication.

Martinsen, O. J., Ryseth, A., Helland-Hansen, W., Flesche, H., Torkildsen, and Idil, S., 1999. Stratigraphic base-level and fluvial architecture: Ericson Sandstone (Campanian), Rock Springs Uplift, SW Wyoming, USA. Sedimentology, v. 46, 235-259.

McGee, L. C., 1983. Laramide sedimentation, folding and faulting southern Wind River Range, Wyoming. PhD Diss., University of Wyoming, Laramie, 92 pp.

Myers, K. J., and Wignall, P. B., 1987. Understanding Jurassic organic-rich mudrocks; new concepts using gamma-ray spectroscopy and palaeo-ecology; examples from the Kimmeridge Clay of Dorset and the Jet Rock of Yorkshire, *in* Marine Clastic Sedimentology; Concepts and Case Studies. Edited by J. K. Leggett and G. G. Zuffa, Graham & Trotman, London, 172–189.

North, C. P., Hole, M. J., Jones, D. G., 2005. Geochemical correlation in deltaic successions: A reality check. Geological Society of America Bulletin, v. 117, 620-632.

Ogala, J. E., Akaegbobi, M. I., Omo-Irabor, O. O., Finkelman, R. H., 2009. Statistical analysis of geochemical distribution of major and trace elements of the Maastrichtian Coal Measures in the Anambra Basin, Nigeria. Petroleum and Coal, v. 4, 260-269.

Olsen, T., Steel, K., Hogseth, K., Skar, T., and Roe, S. L., 1995. Sequential architecture in a fluvial succession: sequence stratigraphy in the upper Cretaceous Mesaverde Group, Price Canyon, Utah. Journal of Sedimentary Research, v. B65, 265-280.

Paola, C., Heller, P. L., and Angevine, C. L., 1992. The large scale dynamics of grain-size variations in alluvial basins, 1: theory. Basin Research, v. 4, 73-90.

Pearce, T. J., Wray, D., Ratcliffe, K., Wright, D. K., and Moscariello, A., 2005. Chemostratigraphy of the upper Carboniferous Schooner Formation, southern North Sea, *in* Carboniferous hydrocarbon geology: the southern North Sea and surrounding onshore areas. Edited by J. D. Collinson, D. J., Evans, D. W. Holliday, N. S. Jones. Yorkshire Geological Society.

Pearce, T. J., Martin, J. H., Cooper, D., Wray, D. S., 2010. Chemostratigraphy of upper Carboniferous (Pennsylvanian) sequences from the southern North Sea (United Kingdom). SEPM Special Publication no. 94, 109-127.

Pedersen, P. K., and Steel, R., 1999. Sequence stratigraphy and alluvial architecture of the Upper Cretaceous Ericson Sandstone, Glades-Clay Basin area, Wyoming-Utah border. The Mountain Geologist, v. 36, 71-84

Pemberton, S. G., and Frey, R. W., 1985. The Glossifungites Ichnofacies; modern examples from the Georgia coast, U.S.A. Society of Economic Paleontologists and Mineralogists Special Publication, v. 35, 237-259.

Pemberton, S. G., and MacEachern, J. A., 1995. The sequence stratigraphic significance of trace fossils: examples from the Cretaceous Foreland Basin of Alberta, Canada, *in* Sequence Stratigraphy of Foreland Basins. Edited by J. C. Van Wagoner and G. T. Bertram, American Association of Petroleum Geologists Memoir 64, 429-475.

Pe-Piper, G., Triantafyllidis, S., Piper, D. J. W., 2008. Geochemical identification of clastic sediment provenance from known sources of similar geology: The Cretaceous Scotian Basin, Canada. Journal of Sedimentary Research, v. 78, 595-607.

Petersen, H. I., Nielsen, L. H., Bojesen-Koefoed, J. A., Mathiesen, A., Kristensen, L., Dalhoff, F., 1999. Evaluation of the quality, thermal maturity, and distribution of potential source rocks in the Danish part of the Norwegian-Danish Basin. Geological Survey of Denmark and Greenland Bulletin, v. 16, 66 pp.

Pietras, J. T., Carroll, A. R., and Rhodes, M. K., 2003. Lake basin response to tectonic drainage diversion: Eocene Green River Formation, Wyoming. Journal of Paleolimnology, v. 30, 115-125.

Pison, G., Rousseeuw, P. J., Filzmoser, P., Croux, C., 1999. Factor analysis in a robust way. University of Antwerp, Belgium.

Plint, A. G., McCarthy, P. J., Faccini, U. F., 2006. Nonmarine sequence stratigraphy: Updip expression of sequence boundaries and systems tracts in a high-resolution framework, Cenomanian Dunvegan Formation, Alberta foreland basin, Canada. American Association of Petroleum Geologists Bulletin, v. 85, 1967-2001.

Posamentier, H. W., Jervey, M. T., and Vail, P. R., 1988. Eustatic controls on clastic deposition I – Conceptual framework. Special Publication - Society of Economic Paleontologists and Mineralogists, v. 42, 109-124.

Posamentier, H. W., Allen, G. P., James, D. P., Tesson, M., 1992. Forced regressions in a sequence stratigraphic framework: Concepts, examples, and exploration significance. American Association of Petroleum Geologists Bulletin, v. 76, 1687-1709.

Posamentier, H. W., and Allen, G. P., 1999. Siliciclastic sequence stratigraphic concepts and applications. SEPM Concepts in Sedimentology and Paleontology, no. 7, 210 pp.

Preston, J., Hartley, A., Hole, M., Buch, S., Bond, J., Mange, M., Still, J., 1998. Integrated whole-rock trace element geochemistry and heavy mineral chemistry studies: aids to the correlation of continental red-bed reservoirs in the Beryl Field, UK North Sea. Petroleum Geoscience, v. 4, 7-16.

Radiation Solutions, 2008. RS-125 Super-Spec/RS-230 BGO Super-Spec Users Manual, revision 1.7, version v5.04, 35 pp.

Ratcliffe, K. T., Morton, A. C., Ritcey, D. H., Evenchick, C.A., 2007. Whole-rock geochemistry and heavy mineral analysis as petroleum exploration tools in the Bowser and Sustut basins, British Columbia, Canada. Bulletin of Canadian Petroleum Geology, v. 55, 320-336.

Ratcliffe, K. T., Wright, A. M., Montgomery, P., Palfrey, A., Vonk, A., Vermeulen, J., Barrett, M., 2010. Application of chemostratigraphy to the Mungaroo Formation, the Gorgon Field, offshore northwester Australia. APPEA Journal, 50th Anniversary issue.

Reimann, C., and Filzmoser, P., 2000. Normal and lognormal data distribution in geochemistry: death of a myth. Consequences for the statistical treatment of geochemical and environmental data. Environmental Geology 39, 1001–1014.

Reimann, C., Filzmoser, P., Garrett, R. G., 2002. Factor analysis applied to regional geochemical data: problems and possibilities. Applied Geochemistry, v. 17, 185-206.

Rettallack, G. J., 1990. Soils of the past; an introduction to paleopedology. Unwin Hyman, Boston, MA, 520 pp.

Roehler, H. W., 1991. Revised stratigraphic nomenclature for the Wasatch and Green River Formations of Eocene age, Wyoming, Utah, and Colorado. United States Geological Survey Professional Paper 1506-B, 38pp.

Roehler, H. W., 1992a. Introduction to Greater Green River Basin geology, Physiography, and history of investigations. United States Geological Survey Professional Paper 1506-A, 14pp.

Roehler, H. W., 1992b. Correlation, composition, areal distribution, and thickness of Eocene stratigraphic units, Greater Green River Basin, Wyoming, Utah, and Colorado. United States Geological Survey Professional Paper 1506-E, 49pp.

Schumm, S. A., 1993. River response to baselevel change: Implications for sequence stratigraphy. The Journal of Geology, v. 101, 279-294.

Shanley, K. W. and McCabe, P. J., 1991. Predicting facies architecture through sequence stratigraphy – An example from the Kaiparowits Plateau, Utah. Geology, v. 19, 742-745.

Shanley, K.W. and McCabe, P. J., 1994. Perspectives on the sequence stratigraphy of continental strata. AAPG Bulletin, v. 78, 544-568.

Sheldon, N. D., and Tabor, N. J., 2002. Quantitative paleoenvironmental and paleoclimatic reconstruction using paleosols. Earth-science Reviews, v. 95, 1-52.

Sheldon, N. D., Retallack, G. J., and Tanaka, S., 2002. Geochemical climofunctions from North American Soils and application to paleosols across the Eocene-Oligocene boundary in Oregon. The Journal of Geology, v. 110, 687-696.

Siegel, F. R., Gupta, N., Shergill, B., Stanley, D. J., Gerber, C., 1995. Geochemistry of Holocene sediments from the Nile Delta. Journal of Coastal Research, v. 11, 415-431.

Slatt, R. M., Jordan, D. W., D'Agostino, A. E., Gillespie, R. H., 1992. Outcrop gamma-ray logging to improve understanding of subsurface well log correlations, *in* Geological Applications of Wireline Logs II. Edited by A. Hurst, C. M. Griffiths, P. F. Worthington, Geological Society Special Publication, no. 65, 3-19.

Sloss, L. L., 1962. Stratigraphic models in exploration. Journal of Sedimentary Petrology, v. 32, 415-422.

Smith, M. E., Carroll, A. R., Singer, B. S., 2008. Synoptic reconstruction of a major ancient lake system: Eocene Green River Formation, western United States. Geological Society of American Bulletin, v. 120, 54-84.

Steidtmann, J. R., and Middleton, L. T., 1991. Fault chronology and uplift history of the southern Wind River Range, Wyoming: Implications for Laramide and post-Laramide deformation in the Rocky Mountain foreland. Geological Society of America Bulletin, v. 103, 472-485.

Surdam, R. C., and Wolfbauer, C. A., 1975, Green River Formation, Wyoming: A playa-lake complex: Geological Society of America Bulletin, v. 86, p. 335–345.

Svendsen, J. B., and Hartley, N.R., 2002. Synthetic heavy mineral stratigraphy: applications and limitations. Marine and Petroleum Geology, v. 19, 389-405.

Svendsen, J. B., Friis, H., Stollhoffen, H., Hartley, N., 2007. Facies discrimination in a mixed fluvio-eolian setting using elemental whole-rock geochemistry – Applications for reservoir characterization. Journal of Sedimentary Research, v. 77, 23-33.

Vail, P. R., Mitchum, R. M., Jr., Todd, R. G., Widmier, J. M., Thompson, S. III, Songree, J. B., Bubb, J. N., Hatelid, W. G., 1977. Seismic stratigraphy-applications to hydrocarbon exploration: American Association of Petroleum Geologists Memoir, v. 26, 49-212.

Van Wagoner, J. C., Mitchum, R. M. Jr., Campion, K. M., and Rahmanian, V. D., 1990. Siliciclastic sequence stratigraphy in well logs, cores, and outcrops: concepts for high-resolution correlation of time and facies. American Association of Petroleum Geologists Methods in Exploration Series, v. 7, 55 pp.

Wheeler, H. E., 1964. Baselevel, lithosphere surface, and time-stratigraphy. Geological Society of America Bulletin, v. 75, 599-610.

Wilf, P., 2000. Late Paleocene-early Eocene climate changes in southwestern Wyoming: Paleobotanical analysis. Geological Society of America Bulletin, v. 112, 292-307.

Woodburne, M. O. (editor), 1987. Cenozoic mammals of North America: geochronology and biostratigraphy. University of California Press, Berkeley and Los Angeles, California, 336 pp.

Wright, P. V., and Marriott, S. B., 1993. The sequence stratigraphy of fluvial depositional systems: the role of floodplain sediment storage. Sedimentary Geology, v. 86, 203-210.

Zeller H. D., and Stephens, E.V., 1969. Geology of the Oregon Buttes area, Sweetwater, Sublette and Freemont Counties, southwestern, Wyoming. U. S. Geological Survey Bulletin No. 1256, 60pp.

Zhang, C., Wang, L., Li, G., Dong, S., Yang, J., Wang, X., 2002. Grain size effect on multi-element concentrations in sediments from the intertidal flats of Bohai Bay, China. Applied Geochemistry, v. 17, 59-68.

Zonneveld, J. -P., 1994. The Wasatchian-Bridgerian Land Mammal Age boundary (early to middle Eocene) in the southwestern Green River Basin, Wyoming. Abstract: Journal of Vertebrate Paleontology, v. 14, 54.

Zonneveld, J. -P., Gunnell, G. F., and Bartels, W. S., 2000. Early Eocene fossil vertebrates from the southwestern Green River Basin, Lincoln and Uinta counties, Wyoming. Journal of Vertebrate Paleontology, v. 20, 369-386.

Zonneveld, J. -P., Bartels, W. S., and Clyde, W. C., 2003. Stratal architecture of an Early Eocene fluvial-lacustrine depositional system, Little Muddy Creek area, southwestern Green River Basin, Wyoming. Cenozoic Systems of the Rocky Mountain Region: Rocky Mountain SEPM, 253-287.

Zonneveld, J. -P., Lavigne, J. M., Bartels, W. S., Gunnell, G. F., 2006. *Lunulichnus Tuberosus Ichnogen*. and *Ichnosp. Nov*. from the early Eocene Wasatch Formation, Fossil Butte National Monument, Wyoming: An arthropod-constructed trace fossil associated with alluvial firmgrounds. Ichnos, v. 13, 87-94.

Chapter 4

Conclusions

4.1 Conclusions

The early Eocene Cathedral Bluffs Tongue of the Wasatch Formation is a heterolithic fluvial tongue on the northern margin of the Green River Basin. The tongue is bounded by, and interfingers with, the lacustrine Green River Formation (Roehler, 1992). A combination of tectonic and climatic influences caused an overall regression of Lake Gosiute and created accommodation space and sediment supply, which allowed the Cathedral Bluffs to prograde into the basin. The succession is dominated by overbank deposition; therefore, accommodation space was likely abundant and, concomitantly, thick packages of this architectural element were preserved (Aslan and Autin, 1999). Lenticular channel sandstones and sheet-like splay sandstones occur intermittently within the overall fine-grained succession.

A detailed facies analysis identified five sandstone and gravel conglomerate facies, two non-pedogenically altered fine-grained facies, and three pedogenically altered fine-grained facies. These facies were then arranged into five facies associations. FA3 was the most common facies association including all the pedogenically-altered sandstone, siltstone, and mudstone. FA1 and FA2 are dominantly sandstone and gravel conglomerate that correspond to fluvial channel and crevasse splay association, respectively. The last two facies associations, FA4 and FA5, are associated with paludal, lacustrine margin, and lacustrine deposition and only account for a very small proportion of the sediment in the succession.

An overall fining trend is observed in an approximately north to south direction. The northern part of the study area displays 3 m diameter fault scarp boulders and gravel / pebble conglomerate beds with clasts up to 15 cm in diameter. These conglomerate packages quickly pinch out. In the southern part of the study area the coarsest grain size observed is coarse-grained sand to fine gravel. This fining trend supports the hypothesis that the sediment source was to the north, from the Wind River Mountain Range. A proximal to distal change, from alluvial fans, to braided rives, to meandering rivers is apparent. The grain size trends, along with analyses of sedimentary structures and channel morphologies confirm a gradation from braided to meandering rivers basinward.

Detailed outcrop observation, supported by petrographic analyses, determined that the lithologies, including iron formation and metasedimentary rocks, within conglomerate and sandstone beds of the Cathedral Bluffs Tongue are consistent with those found in the core of the Wind River Mountains (McGee, 1983; Hall and Chase, 1989). In thin section the presence of minerals such as epidote, garnet, and iron formation support a source in the vicinity of Atlantic City, Wyoming (McGee, 1983). The mineralogical suite observed through each section does not significantly change from the base to the top of the Cathedral Bluffs Tongue. Whole-rock geochemical data supports this observation, as no significant change was observed in the immobile elements through any of the sections. This would indicate the sediment source did not change substantially over the period of Cathedral Bluffs deposition.

The study of fully continental fluvial deposits allows for observation of fluvial processes without interference from tidal or eustatic influences (Zonneveld *et al.,* 2003). For fluvial settings within a marine basin, it is unknown how far upstream tidal and eustatic influences occur; however, it has been suggested that sea level may affect fluvial processes up to 300 km upstream (Aslan and Autin, 1999). With no eustatic influence, the level of ancient lakes was controlled primarily by climate and tectonics (Carroll and Bohacs, 1999; Bohacs *et al.*, 2000; Zonneveld *et al.*, 2003). In lacustrine basins, such as the Green River Basin, lake level may have a similar effect on depositional patterns as relative sea level in marginal marine settings (Shanley and McCabe, 1994; Zonneveld *et al.,* 2003). Therefore, sequence stratigraphic concepts developed for marginal marine settings can be applied to lacustrine settings.

The Cathedral Bluffs Tongue is an alluvial succession with highly complex stratigraphic relationships due to the absence of extensive regional markers. However, lithologic evidence, used in conjunction with geochemical and gamma ray data, has allowed for a subdivision of this unit into seven distinct unconformity-bounded sequences. These units, designated SPS-1 through SPS-7, reflect fluctuations in the level of Lake Gosiute in the study area. Each sequence is an unconformity-bounded package of sediment with a characteristic sedimentary character. Within this high-resolution stratigraphic framework, identification of the sequences is based on a combination of these methods. Spectral-gamma ray logs show distinctive patterns with respect to the K wt%, allowing for correlation across many kilometers. The base of each sequence is generally coarse-grained and may display a sharp increase in K concentration. Sequences are commonly capped by mature, well-drained paleosols that have been leached of mobile elements, specifically potassium (Preston *et al.,* 1998; Hampson *et al.,* 2005). This accounts for the sharp increase in K concentration at sequence boundaries.

Structural features in the area indicate that tectonics played a dominant role in influencing depositional patterns. Fault scarp boulders along the Continental Fault indicate that the fault was a positive feature during the Eocene (Steidtmann and Middleton, 1991; Pietras *et al.,* 2003). The other prominent structural element in the study area is Reds Cabin Monocline, which overlies the trace of the Wind River Thrust Fault. Both of these features indicate that deposition of the Cathedral Bluffs Tongue occurred during the latest stages of the Laramide orogeny. These syndepositional tectonic movements likely had a significant impact on the deposition of the Cathedral Bluffs Tongue. Uplift of the range created accommodation space by loading and flexural subsidence, thereby, trapping coarse sediments close the mountain range (Johnson and Andersen, 2009; Allen and Heller, 2012)

4.2. References

Allen, P. A., and Heller, P. L., 2012. Dispersal and preservation of tectonically generated alluvial gravels in sedimentary basins, *in* Tectonics of Sedimentary Basins: Recent Advances. Edited by C. Busby and A. A. Perez, 111-130.

Aslan, A., and Autin, W. J., 1999. Evolution of the Holocene Mississippi River floodplain, Ferriday, Louisiana: Insights on the origin of fine-grained floodplains. Journal of Sedimentary Research, v. 69, 800-815.

Bohacs, K. M., Carroll, A. R., Neal, J. E., Mankiewicz, P. J., 2000. Lake-basin type, source potential, and hydrocarbon character: an integrated-sequence stratigraphic– geochemical framework, *in* Lake basins through space and time. Edited by E. H. Gierlowski- Kordesch and K. R. Kelts, AAPG Studies in Geology, v. 46, 3–34.

Carroll, A. R., and Bohacs, K. M., 1999. Stratigraphic classification of ancient lakes: Balancing tectonic and climatic controls. Geology, v. 27, 99-102.

Hall, M. K., and Chase, C. G., 1989. Uplift, unbuckling, and collapse: Flexural history and isostacy of the Wind River Range and Granite Mountains, Wyoming. Journal of Geophysical Research, v. 94, 581-593.

Hampson, G. J., Davies, W., Davies, S. J., Howell, J. A., Adamson, K. R., 2005. Use of spectral gamma-ray data to refine subsurface fluvial stratigraphy: late Cretaceous strata in the Book Cliffs, Utah, USA. Journal of the Geological Society, v. 162, 603-621.

Johnson, P. L., and Andersen, D. W., 2009. Concurrent growth of uplifts with dissimilar orientations in the southern Green River Basin, Wyoming:

Implications for Paleocene and Eocene patterns of foreland shortening. Rocky Mountain Geology, v. 44, 1-16.

McGee, L. C., 1983. Laramide sedimentation, folding and faulting southern Wind River Range, Wyoming. PhD Diss., University of Wyoming, Laramie, 92 pp.

Pietras, J. T., Carroll, A. R., and Rhodes, M. K., 2003. Lake basin response to tectonic drainage diversion: Eocene Green River Formation, Wyoming. Journal of Paleolimnology, v. 30, 115-125.

Preston, J., Hartley, A., Hole, M., Buch, S., Bond, J., Mange, M., Still, J., 1998. Integrated whole-rock trace element geochemistry and heavy mineral chemistry studies: aids to the correlation of continental red-bed reservoirs in the Beryl Field, UK North Sea. Petroleum Geoscience, v. 4, 7-16.

Roehler, H. W., 1992. Introduction to Greater Green River Basin geology, Physiography, and history of investigations. United States Geological Survey Professional Paper 1506-A, 14pp.

Shanley, K.W. and McCabe, P. J., 1994. Perspectives on the sequence stratigraphy of continental strata. AAPG Bulletin, v. 78, 544-568.

Steidtmann, J. R., and Middleton, L. T., 1991. Fault chronology and uplift history of the southern Wind River Range, Wyoming: Implications for Laramide and post-Laramide deformation in the Rocky Mountain foreland. Geological Society of America Bulletin, v. 103, 472-485.

Zonneveld, J. -P., Bartels, W. S., and Clyde, W. C., 2003. Stratal architecture of an Early Eocene fluvial-lacustrine depositional system, Little Muddy Creek area, southwestern Green River Basin, Wyoming. Cenozoic Systems of the Rocky Mountain Region: Rocky Mountain SEPM, 253-287.

APPENDIX A

Outcrop Striplogs

Ichnofossil Symbols

- *Ancorichnus*
- *Arenicolites*
- *Camborygma*
- *Glossifungites* surface
- *Lockeia*
- *Macaronichnus*
- *Naktodemasis*
- *Planolites*
- Root Traces
- *Scoyenia*
- *Siphonichnus*
- *Skolithos*
- *Treptichnus*
- *Terebellina*
- Undifferentiated Bioturbation
- Horizontal branching trace

Physical Sedimentary Structures

- Flaser Bedding
- Shrinkage/Dessication cracks
- Planar bedding
- Ripple Laminae (wave/current)
- Low angle cross-stratification
- Trough cross-stratification
- Over steepened beds
- Pedogenic slickensides
- Wavy bedding (homogeneous)

- Maximum Lacustrine Flooding Surface
- Initial Transgressive Surface
- Lacustrine Lowstand Surface of Erosion

HST	Highstand Systems Tract
TST	Transgressive Systems Tract
LST	Lowstand Systems Tract

Fossil Symbols

- Gastropod
- Bivalved pelecypods
- Ostracod
- Bioclastic debris
- Vertebrate skeletal elements
- Wood
- Leaves
- Carbonaceous matter
- Carbonaceous laminae
- Stromatolites
- Full turtle fossil
- Turtle Fragments
- Reworked Stromatolite
- Stromatoporoid
- Caddisfly Mound
- Stromatolite encrusted log
- Coprolites

Extras

- Mud clasts
- Pebble lag
- Outcrop locality
- Imbricated clasts
- Carbonate concretion

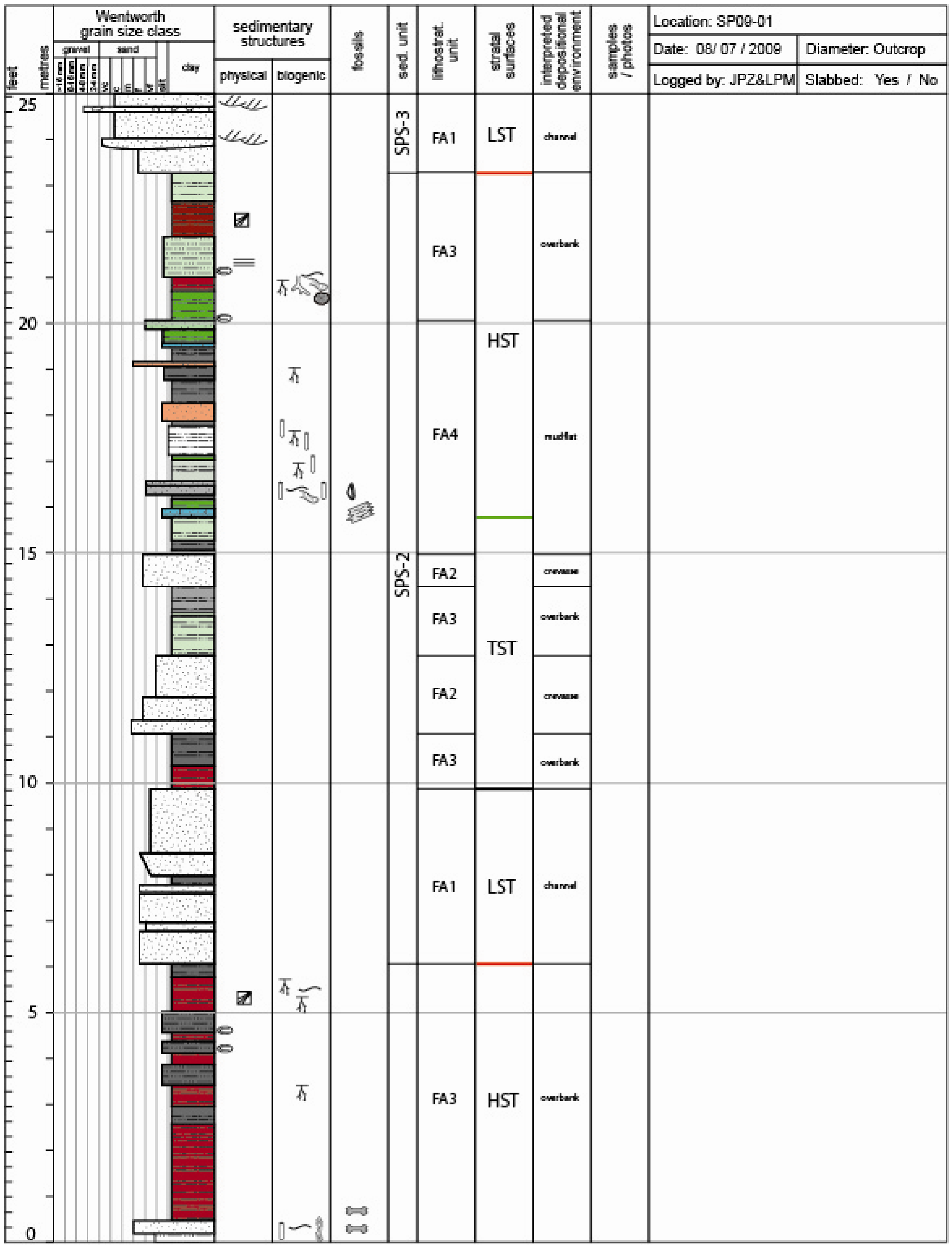

feet
metres
Wentworth grain size class
gravel
sand
clay
sedimentary structures
physical
biogenic
fossils
sed. unit
lithostrat. unit
stratal surfaces
interpreted depositional environment
samples / photos
Location: SP09-01
Date: 08/ 07 / 2009
Diameter: Outcrop
Logged by: JPZ&LPM
Slabbed: Yes / No
25
20
15
10
5
0
SPS-3
SPS-2
FA1
FA3
FA4
FA2
FA3
FA2
FA3
FA1
FA3
LST
HST
TST
LST
HST
channel
overbank
mudflat
crevasse
overbank
crevasse
overbank
channel
overbank

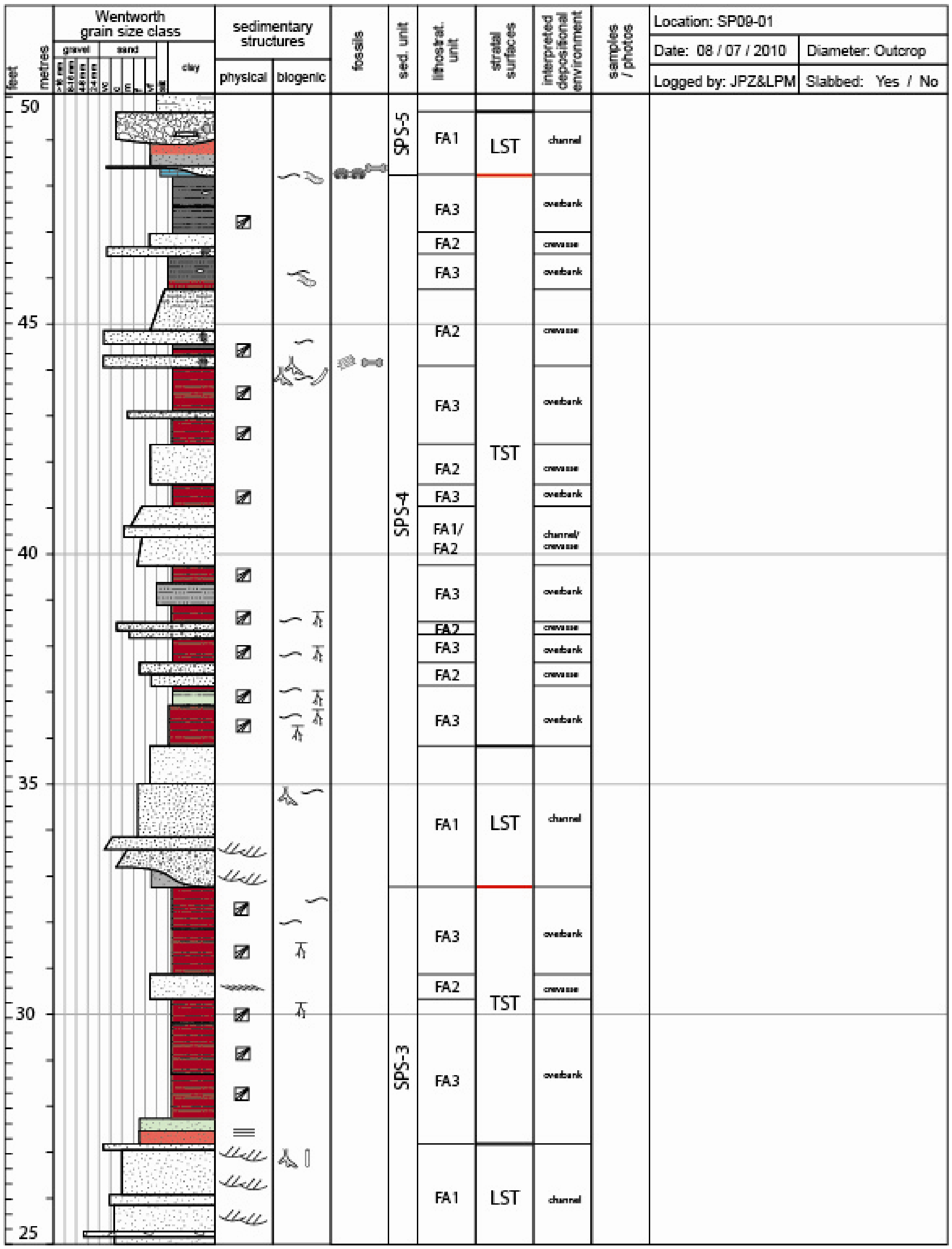

Wentworth grain size class
gravel
sand
clay
sedimentary structures
physical
biogenic
fossils
sed. unit
lithostrat. unit
stratal surfaces
interpreted depositional environment
samples / photos
Location: SP09-01
Date: 08 / 07 / 2010
Diameter: Outcrop
Logged by: JPZ&LPM
Slabbed: Yes / No
feet
metres
50
45
40
35
30
25
SPS-5
SPS-4
SPS-3
FA1
FA3
FA2
FA3
FA2
FA3
FA2
FA3
FA1/ FA2
FA3
FA2
FA3
FA2
FA3
FA1
FA3
FA2
FA3
FA1
LST
TST
LST
TST
LST
channel
overbank
crevasse
overbank
crevasse
overbank
crevasse
overbank
channel/ crevasse
overbank
crevasse
overbank
crevasse
overbank
channel
overbank
crevasse
overbank
channel

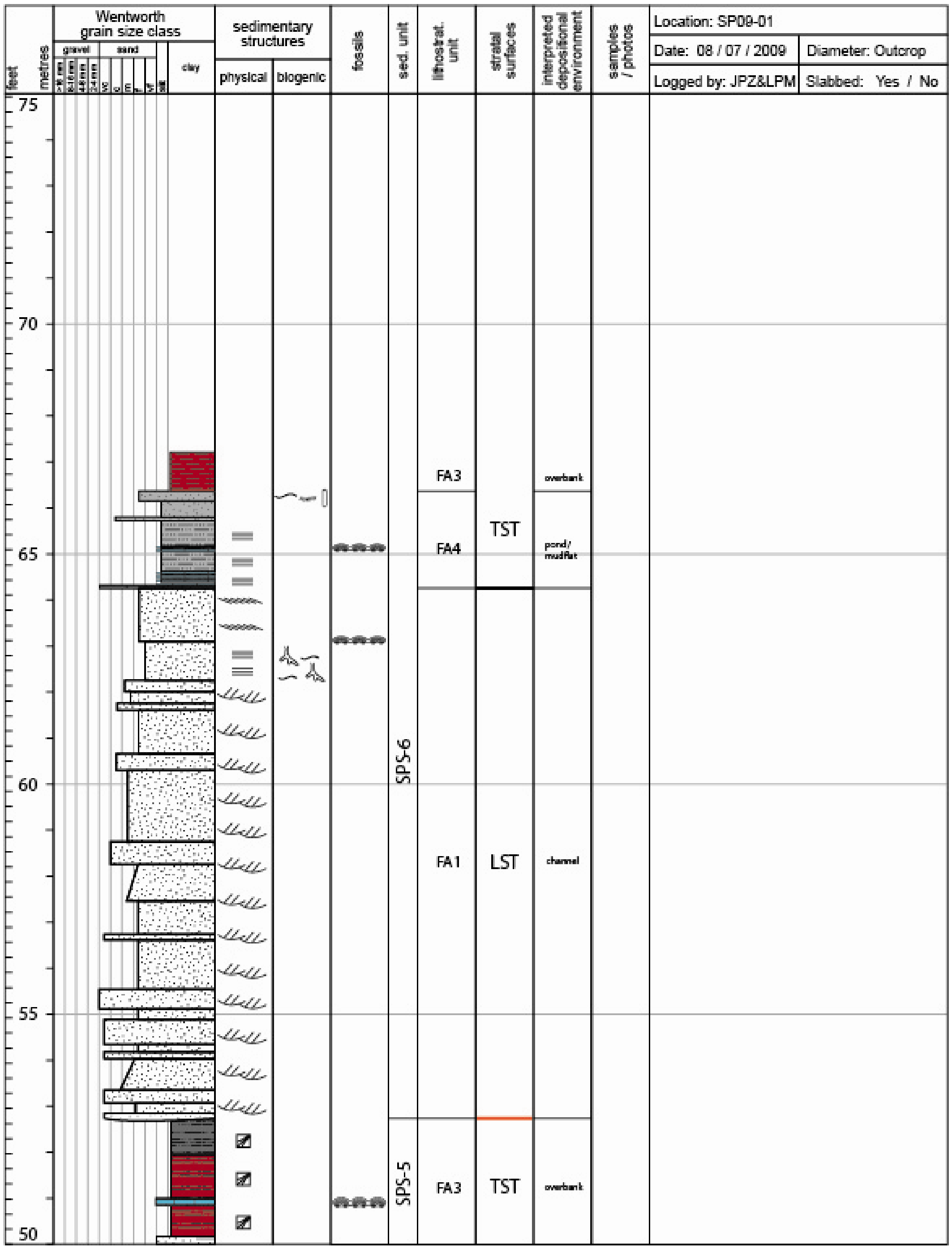

Wentworth grain size class
gravel
sand
clay
sedimentary structures
physical
biogenic
fossils
sed. unit
lithostrat. unit
stratal surfaces
interpreted depositional environment
samples / photos
Location: SP09-01
Date: 08 / 07 / 2009
Diameter: Outcrop
Logged by: JPZ&LPM
Slabbed: Yes / No
feet
metres
75
70
65
60
55
50
FA3
overbank
TST
FA4
pond/ mudflat
SPS-6
FA1
LST
channel
SPS-5
FA3
TST
overbank

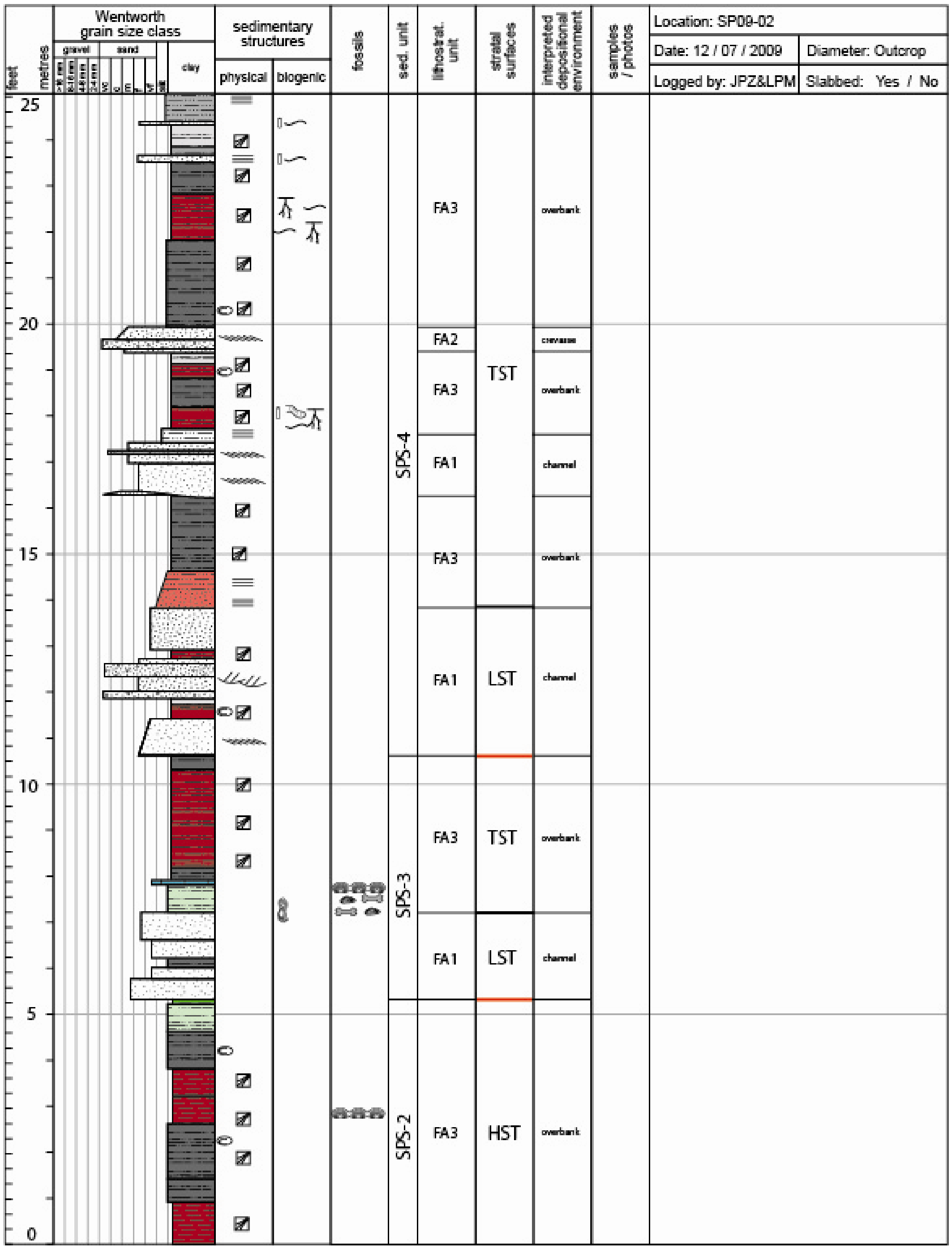
Location: SP09-02
Date: 12 / 07 / 2009
Diameter: Outcrop
Logged by: JPZ&LPM
Slabbed: Yes / No
Wentworth grain size class
sedimentary structures
physical
biogenic
fossils
sed. unit
lithostrat. unit
stratal surfaces
interpreted depositional environment
samples / photos
feet
metres
SPS-4
SPS-3
SPS-2
FA3
FA2
FA3
FA1
FA3
FA1
FA3
FA1
FA3
TST
LST
TST
LST
HST
overbank
crevasse
overbank
channel
overbank
channel
overbank
channel
overbank
25
20
15
10
5
0

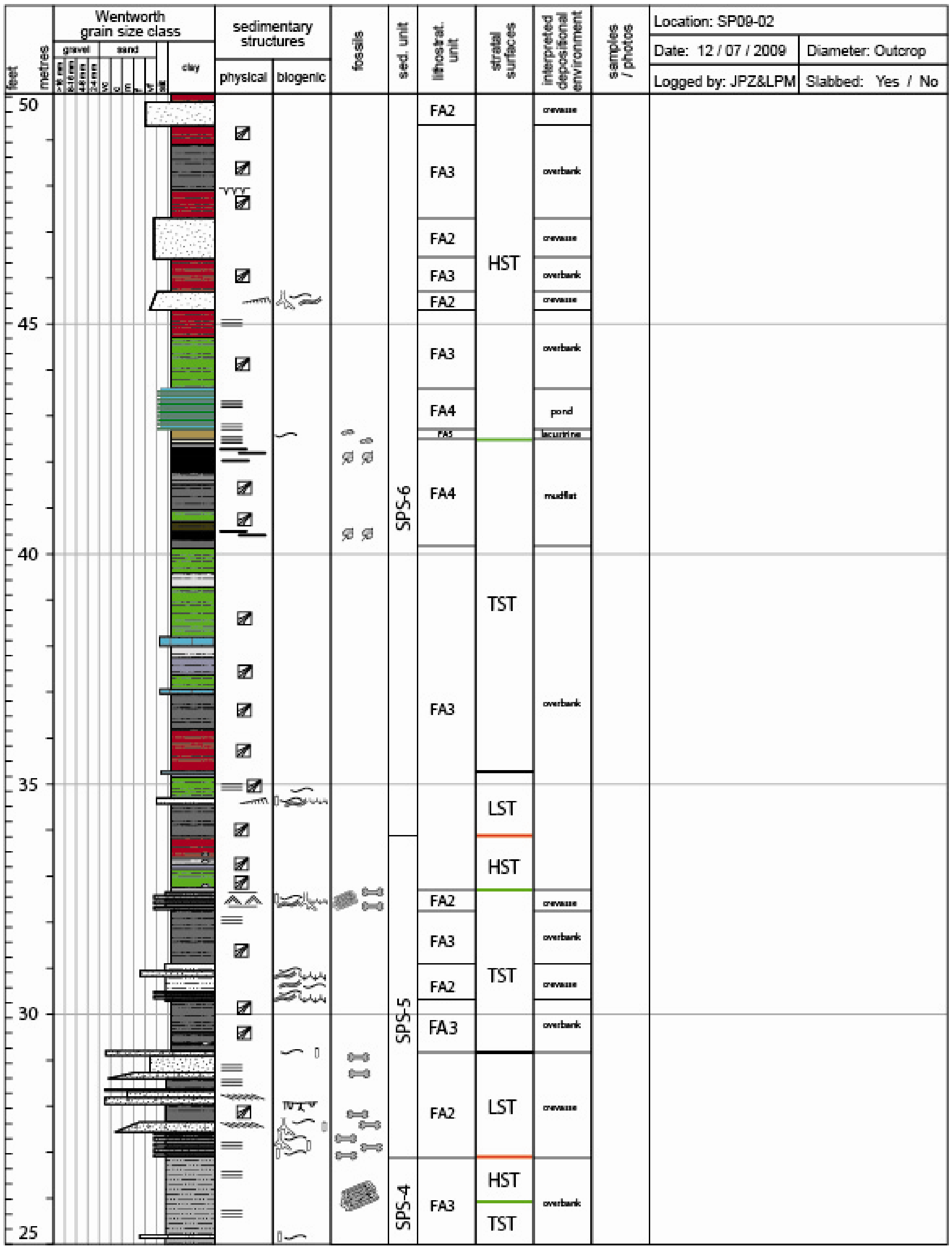

Location: SP09-02
Date: 12 / 07 / 2009
Diameter: Outcrop
Logged by: JPZ&LPM
Slabbed: Yes / No
feet
metres
Wentworth grain size class
gravel
sand
clay
sedimentary structures
physical
biogenic
fossils
sed. unit
lithostrat. unit
stratal surfaces
interpreted depositional environment
samples / photos
SPS-6
SPS-5
SPS-4
FA2
FA3
FA4
FA5
HST
TST
LST
crevasse
overbank
pond
lacustrine
mudflat
50
45
40
35
30
25

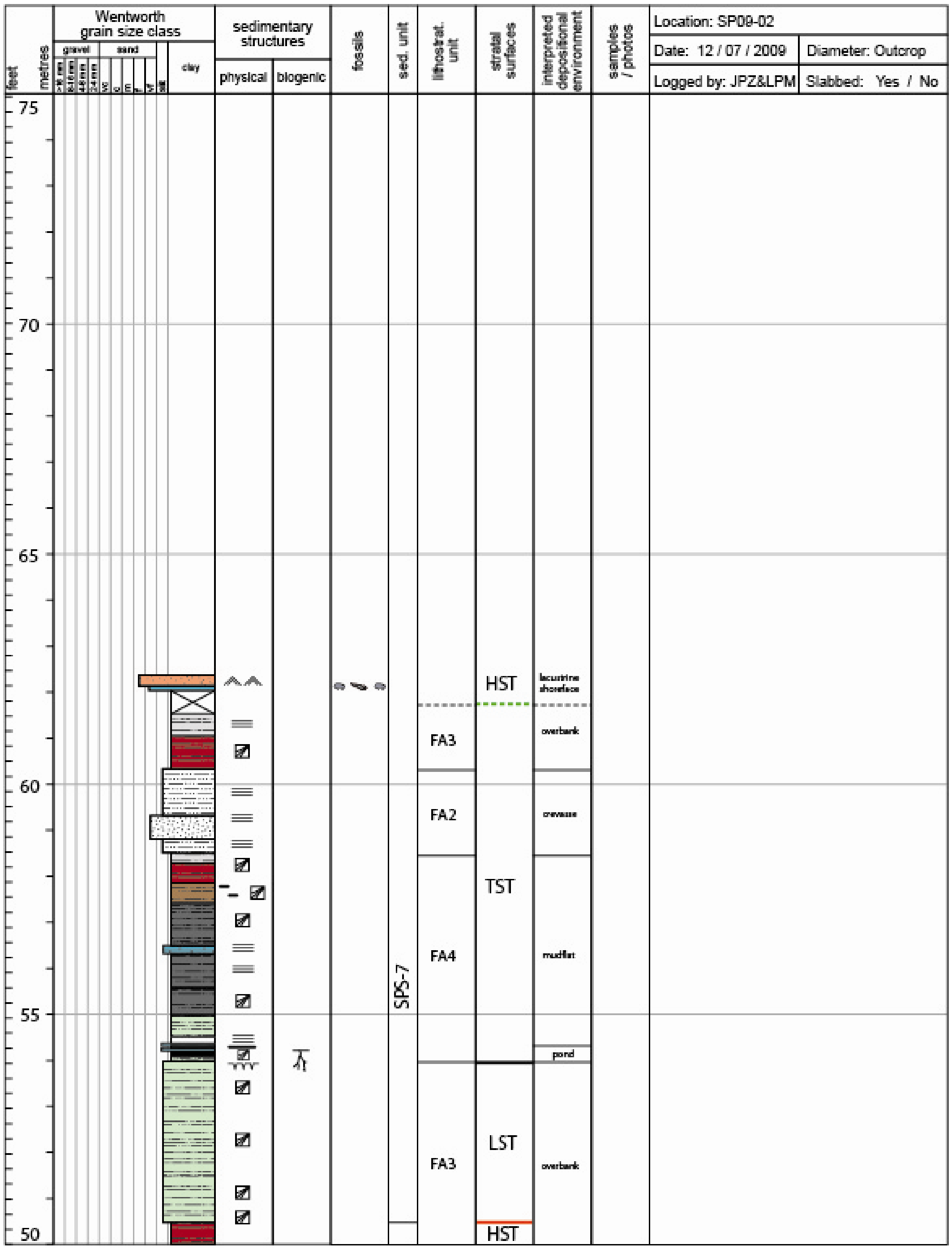

Wentworth grain size class
gravel
sand
clay
feet
metres
sedimentary structures
physical
biogenic
fossils
sed. unit
lithostrat. unit
stratal surfaces
interpreted depositional environment
samples / photos
Location: SP09-02
Date: 12 / 07 / 2009
Diameter: Outcrop
Logged by: JPZ&LPM
Slabbed: Yes / No
75
70
65
60
55
50
HST
lacustrine shoreface
FA3
overbank
FA2
crevasse
TST
FA4
mudflat
SPS-7
pond
LST
FA3
overbank
HST

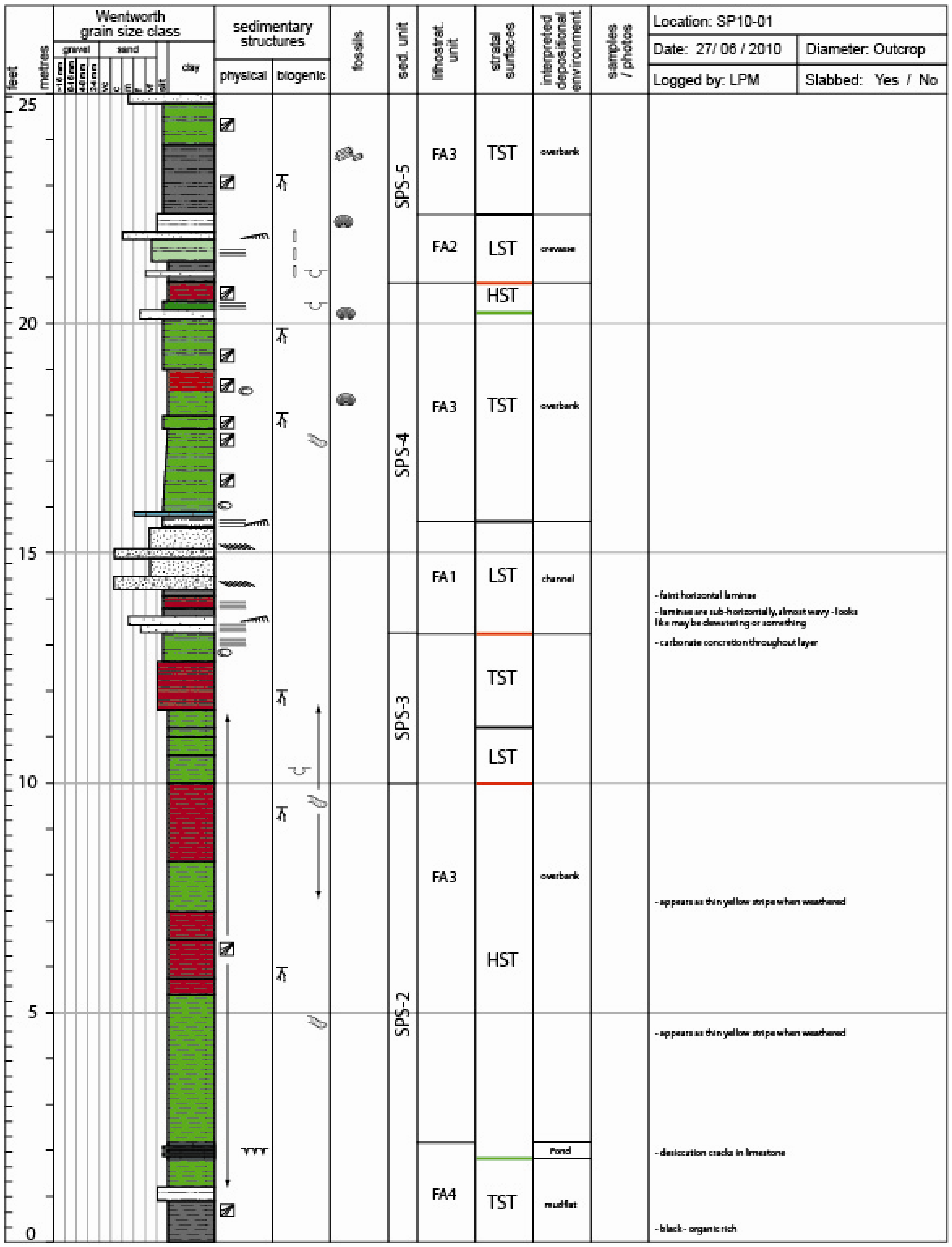
Location: SP10-01
Date: 27/ 06 / 2010
Diameter: Outcrop
Logged by: LPM
Slabbed: Yes / No
feet
metres
Wentworth grain size class
gravel
sand
clay
sedimentary structures
physical
biogenic
fossils
sed. unit
lithostrat. unit
stratal surfaces
interpreted depositional environment
samples / photos
SPS-5
SPS-4
SPS-3
SPS-2
FA3
FA2
FA3
FA1
FA3
FA4
TST
LST
HST
TST
LST
TST
LST
HST
TST
overbank
crevasse
overbank
channel
overbank
Pond
mudflat
- faint horizontal laminae
- laminae are sub-horizontally, almost wavy - looks like may be dewatering or something
- carbonate concretion throughout layer
- appears as thin yellow stripe when weathered
- appears as thin yellow stripe when weathered
- desiccation cracks in limestone
- black - organic rich
25
20
15
10
5
0

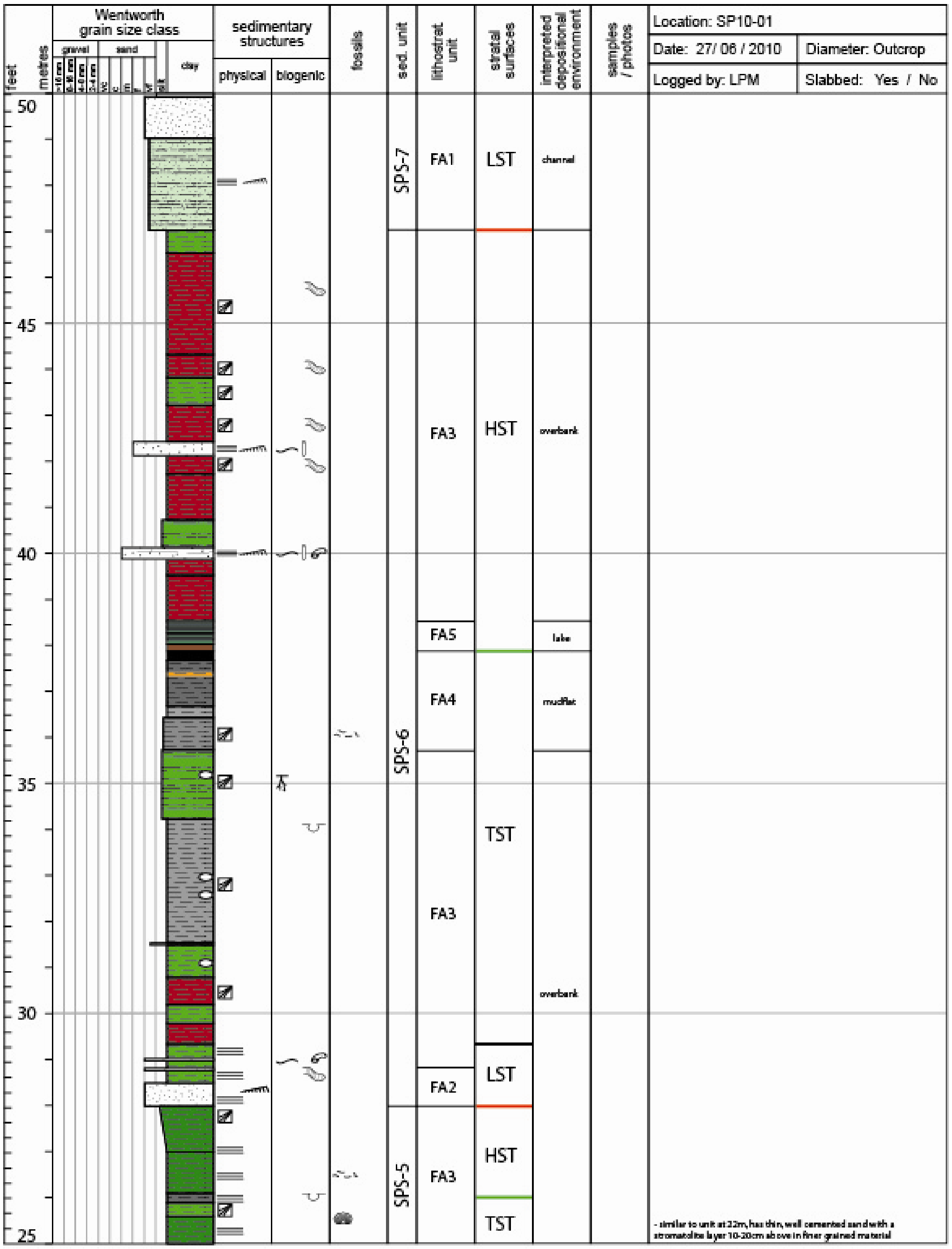
Wentworth grain size class
gravel
sand
clay
sedimentary structures
physical
biogenic
fossils
sed. unit
lithostrat unit
stratal surfaces
interpreted depositional environment
samples / photos
Location: SP10-01
Date: 27/ 06 / 2010
Diameter: Outcrop
Logged by: LPM
Slabbed: Yes / No
feet
metres
50
45
40
35
30
25
SPS-7
SPS-6
SPS-5
FA1
FA3
FA5
FA4
FA3
FA2
FA3
LST
HST
TST
LST
HST
TST
channel
overbank
lake
mudflat
overbank
- similar to unit at 22m, has thin, well cemented sand with a stromatolite layer 10-20cm above in finer grained material

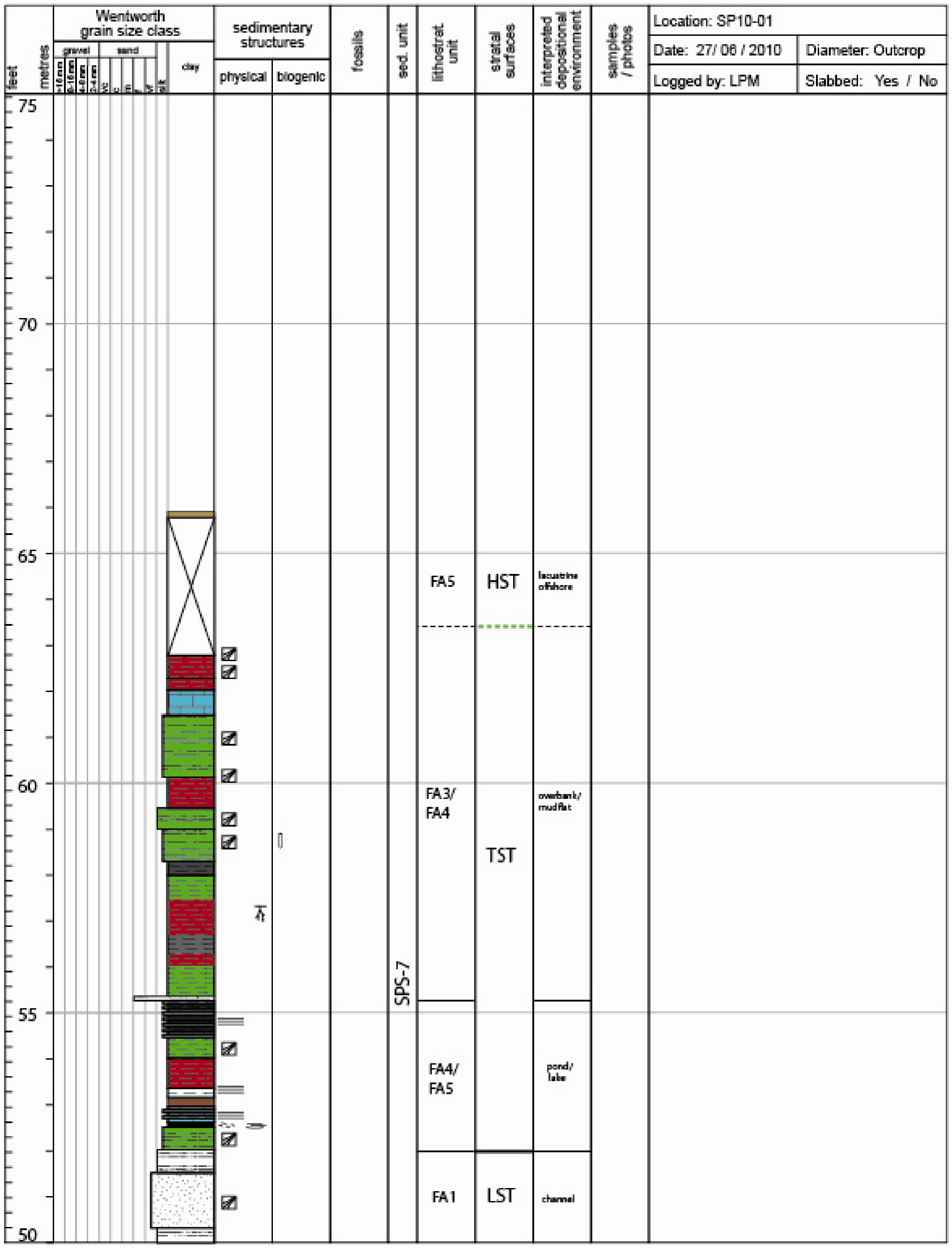
Wentworth grain size class
gravel
sand
clay
feet
metres
sedimentary structures
physical
biogenic
fossils
sed. unit
lithostrat unit
stratal surfaces
interpreted depositional environment
samples / photos
Location: SP10-01
Date: 27/ 06 / 2010
Diameter: Outcrop
Logged by: LPM
Slabbed: Yes / No
75
70
65
60
55
50
FA5
HST
lacustrine offshore
FA3/ FA4
overbank/ mudflat
TST
SPS-7
FA4/ FA5
pond/ lake
FA1
LST
channel

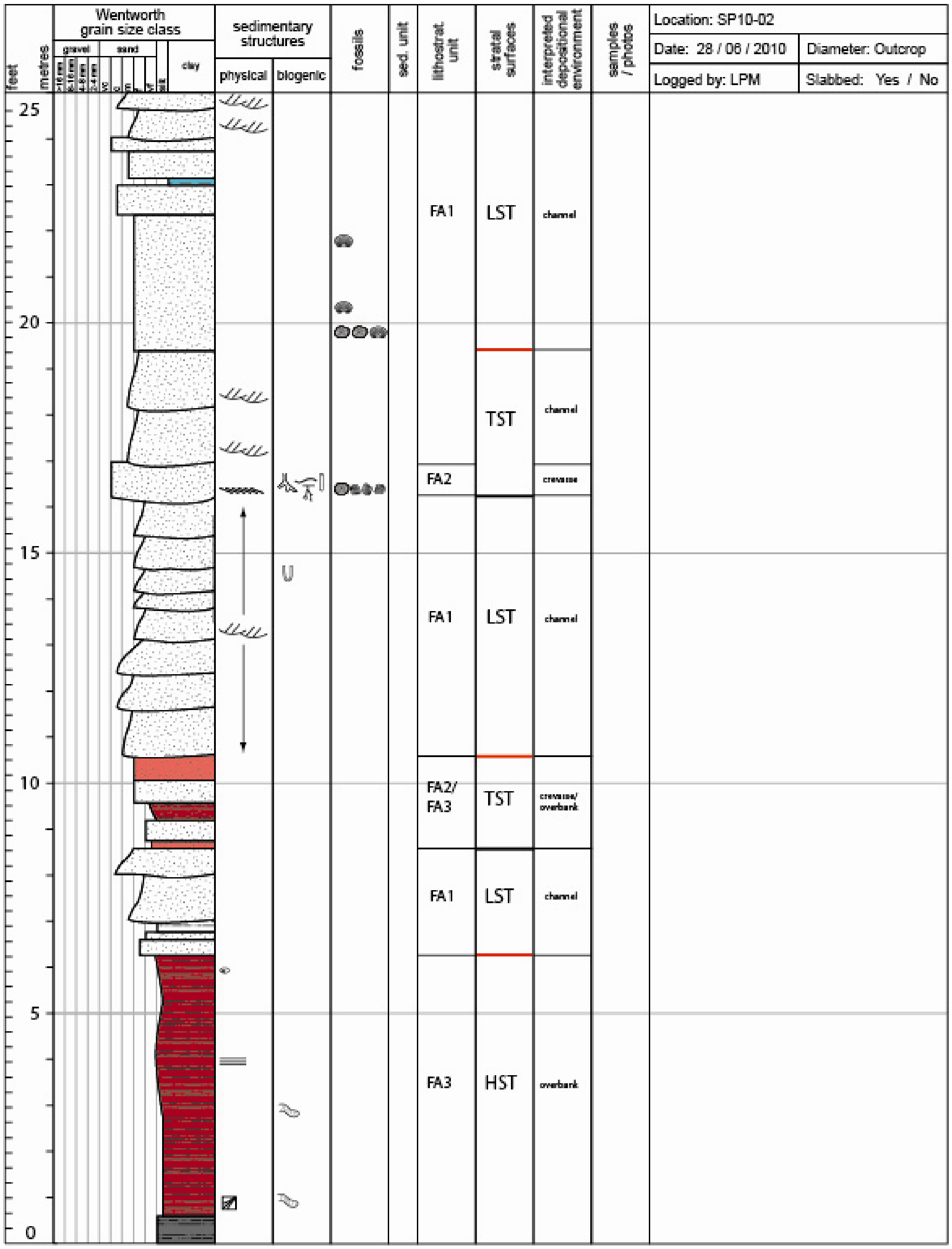
Location: SP10-02
Date: 28 / 06 / 2010
Diameter: Outcrop
Logged by: LPM
Slabbed: Yes / No
feet
metres
Wentworth grain size class
gravel
sand
clay
sedimentary structures
physical
biogenic
fossils
sed. unit
lithostrat. unit
stratal surfaces
interpreted depositional environment
samples / photos
FA1
LST
channel
TST
channel
FA2
crevasse
FA1
LST
channel
FA2/ FA3
TST
crevasse/ overbank
FA1
LST
channel
FA3
HST
overbank
25
20
15
10
5
0

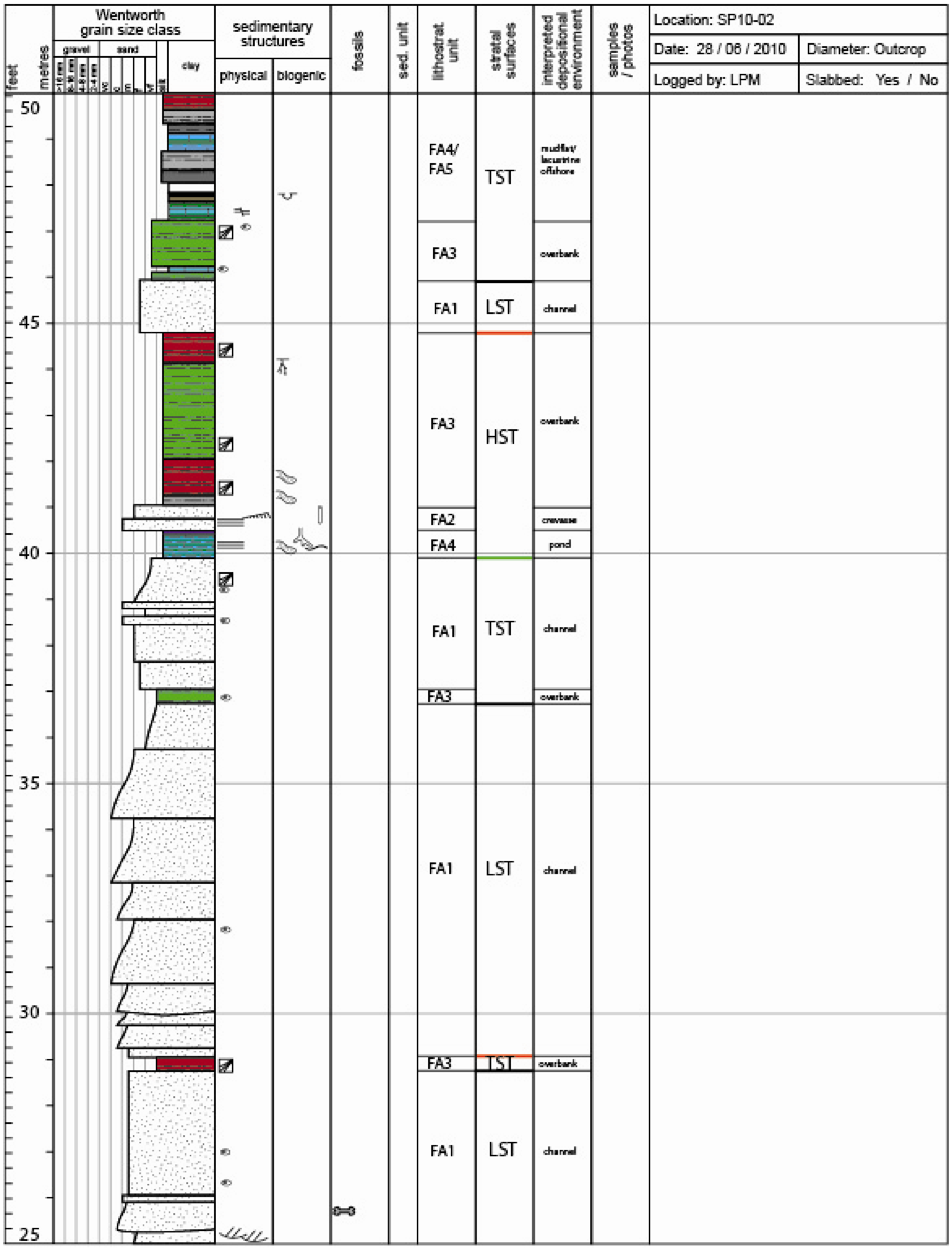

Location: SP10-02
Date: 28 / 06 / 2010
Diameter: Outcrop
Logged by: LPM
Slabbed: Yes / No
Wentworth grain size class
gravel
sand
clay
silt
feet
metres
sedimentary structures
physical
biogenic
fossils
sed. unit
lithostrat. unit
stratal surfaces
interpreted depositional environment
samples / photos
50
45
40
35
30
25
FA4/ FA5
TST
FA3
overbank
FA1
LST
channel
FA3
HST
overbank
FA2
crevasse
FA4
pond
FA1
TST
channel
FA3
overbank
FA1
LST
channel
FA3
TST
overbank
FA1
LST
channel

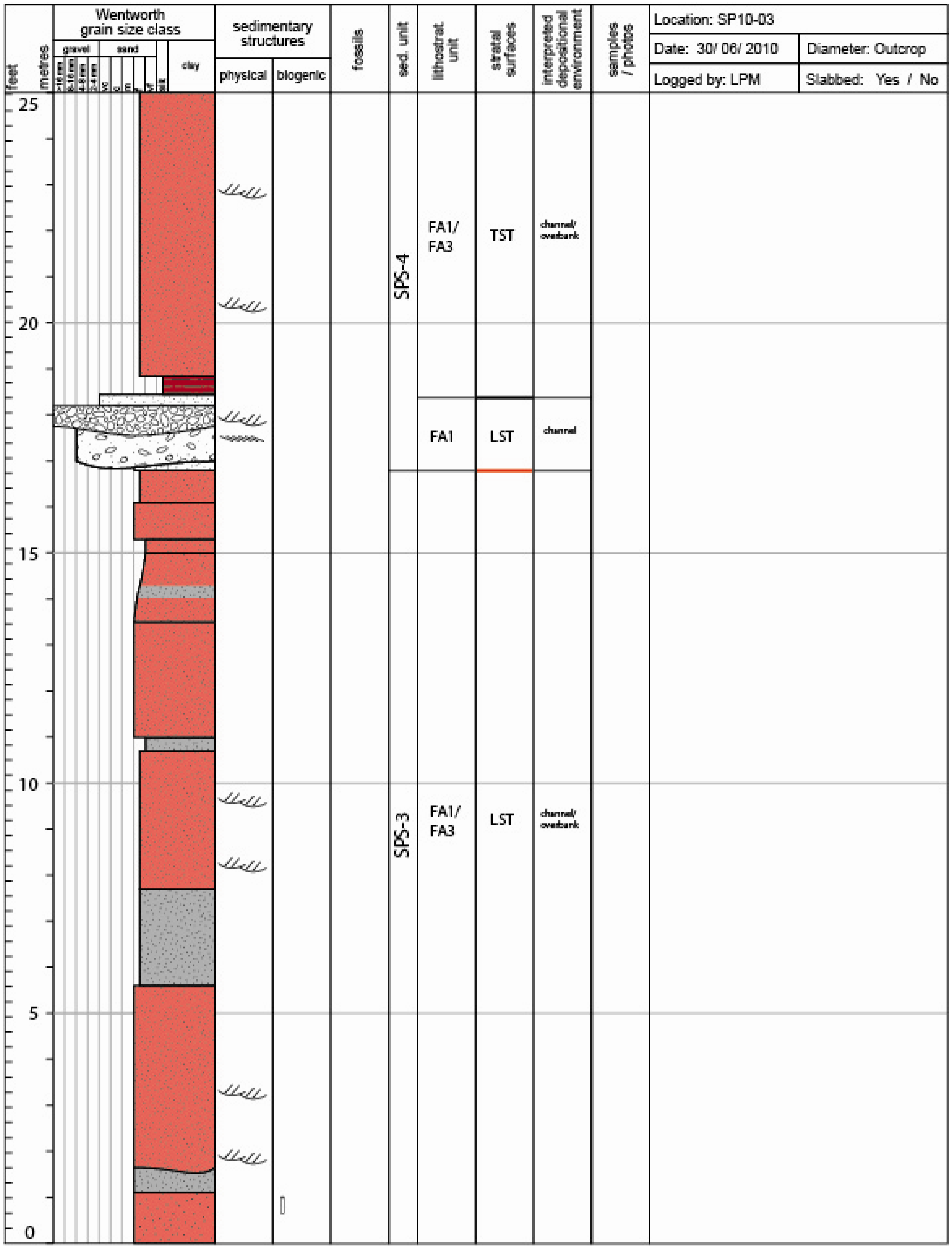

Wentworth grain size class
gravel
sand
clay
sedimentary structures
physical
biogenic
fossils
sed. unit
lithostrat. unit
stratal surfaces
interpreted depositional environment
samples / photos
Location: SP10-03
Date: 30/ 06/ 2010
Diameter: Outcrop
Logged by: LPM
Slabbed: Yes / No
feet
metres
25
20
15
10
5
0
SPS-4
FA1/ FA3
TST
channel/ overbank
FA1
LST
channel
SPS-3
FA1/ FA3
LST
channel/ overbank

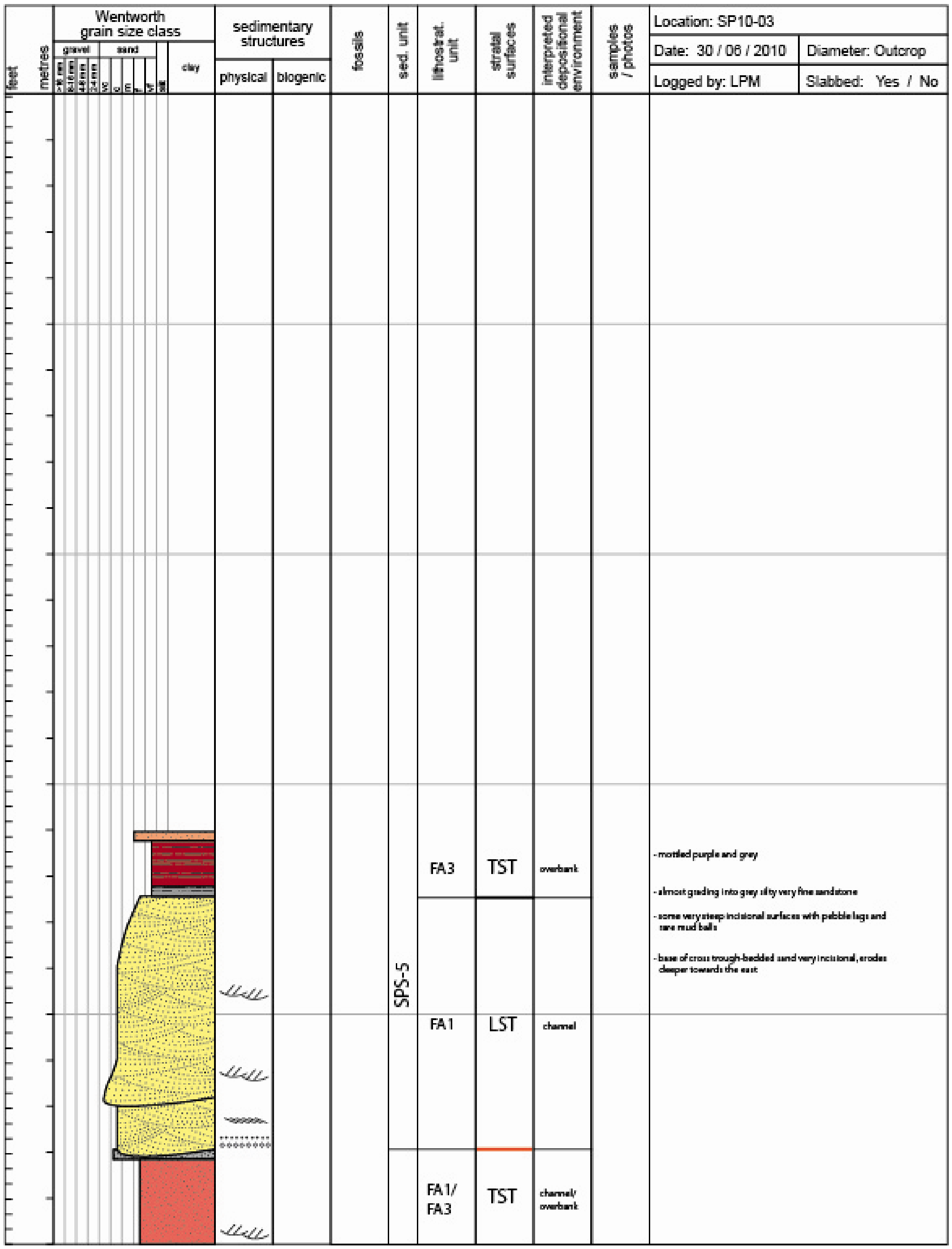

Wentworth grain size class
gravel
sand
clay
feet
metres
sedimentary structures
physical
biogenic
fossils
sed. unit
lithostrat. unit
stratal surfaces
interpreted depositional environment
samples / photos
Location: SP10-03
Date: 30 / 06 / 2010
Diameter: Outcrop
Logged by: LPM
Slabbed: Yes / No
SPS-5
FA3
TST
overbank
FA1
LST
channel
FA1/ FA3
TST
channel/ overbank
- mottled purple and grey
- almost grading into grey silty very fine sandstone
- some very steep incisional surfaces with pebble lags and rare mud balls
- base of cross trough-bedded sand very incisional, erodes deeper towards the east

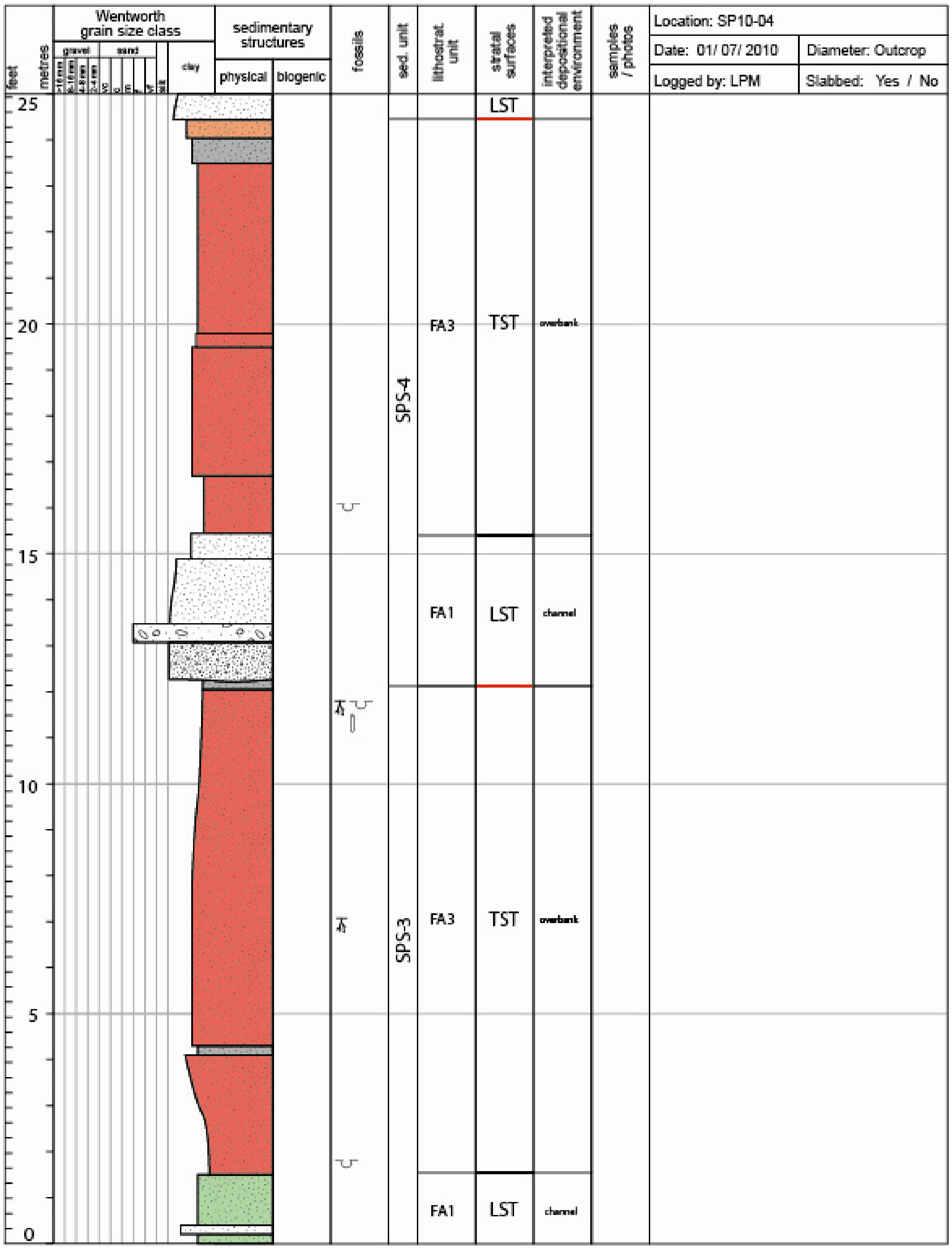

Location: SP10-04
Date: 01/ 07/ 2010
Diameter: Outcrop
Logged by: LPM
Slabbed: Yes / No
feet
metres
Wentworth grain size class
gravel
sand
clay
sedimentary structures
physical
biogenic
fossils
sed. unit
lithostrat. unit
stratal surfaces
interpreted depositional environment
samples / photos
25
20
15
10
5
0
SPS-4
SPS-3
FA3
FA1
LST
TST
overbank
channel

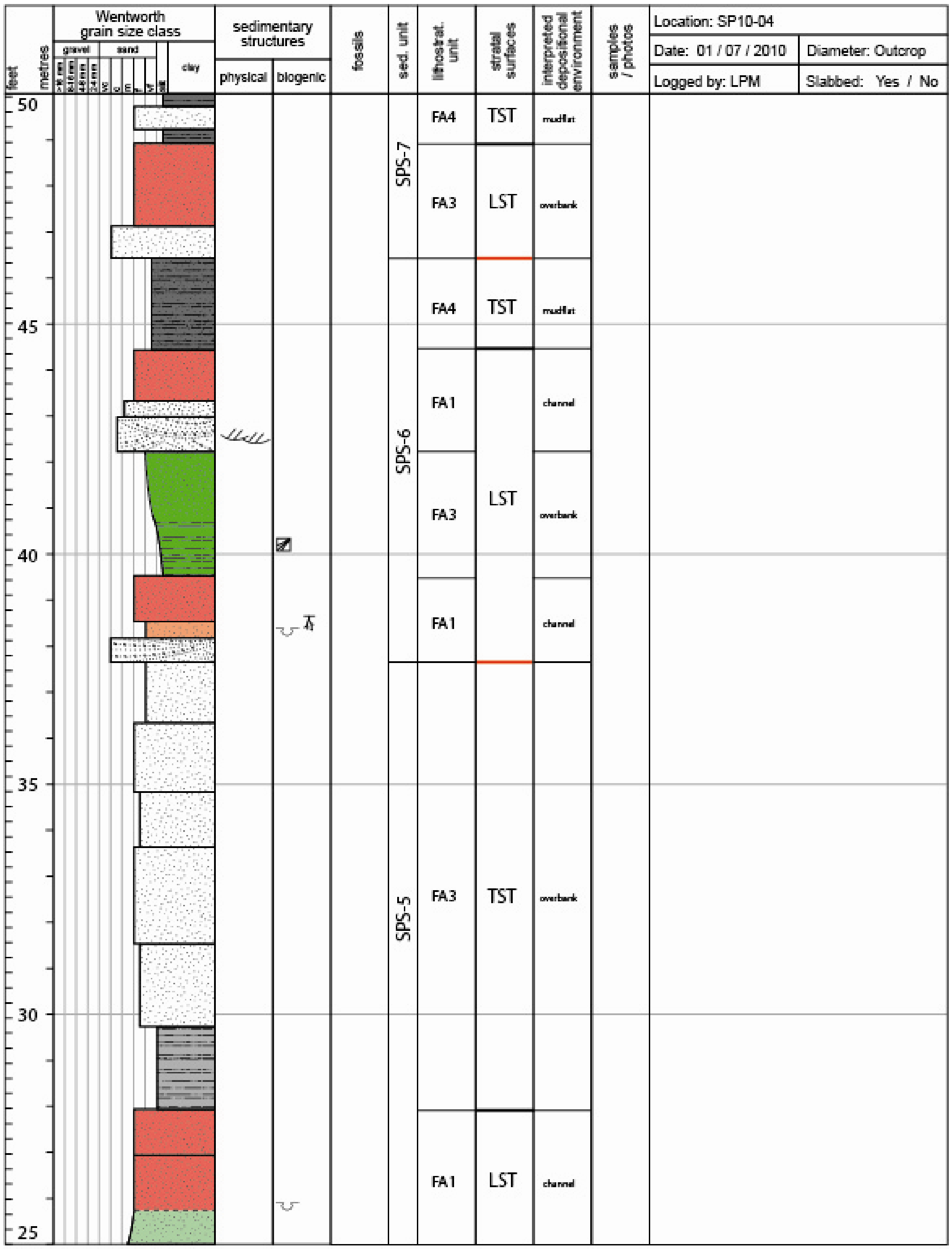
Wentworth grain size class
gravel
sand
clay
feet
metres
sedimentary structures
physical
biogenic
fossils
sed. unit
lithostrat. unit
stratal surfaces
interpreted depositional environment
samples / photos
Location: SP10-04
Date: 01 / 07 / 2010
Diameter: Outcrop
Logged by: LPM
Slabbed: Yes / No
50
45
40
35
30
25
SPS-7
SPS-6
SPS-5
FA4
FA3
FA4
FA1
FA3
FA1
FA3
FA1
TST
LST
TST
LST
TST
LST
mudflat
overbank
mudflat
channel
overbank
channel
overbank
channel

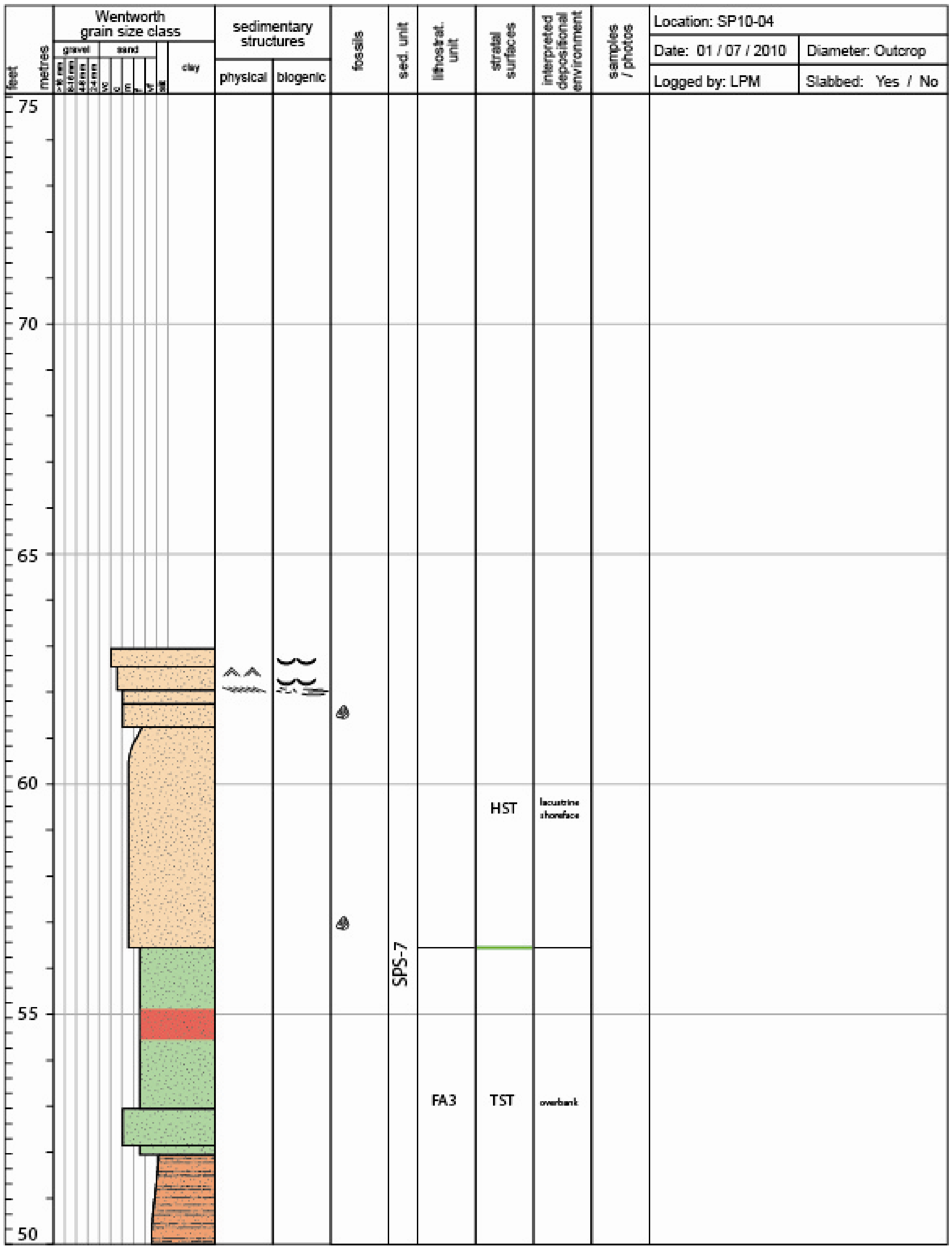

Wentworth grain size class
gravel
sand
clay
feet
metres
sedimentary structures
physical
biogenic
fossils
sed. unit
lithostrat. unit
stratal surfaces
interpreted depositional environment
samples / photos
Location: SP10-04
Date: 01 / 07 / 2010
Diameter: Outcrop
Logged by: LPM
Slabbed: Yes / No
75
70
65
60
55
50
SPS-7
HST
lacustrine shoreface
FA3
TST
overbank

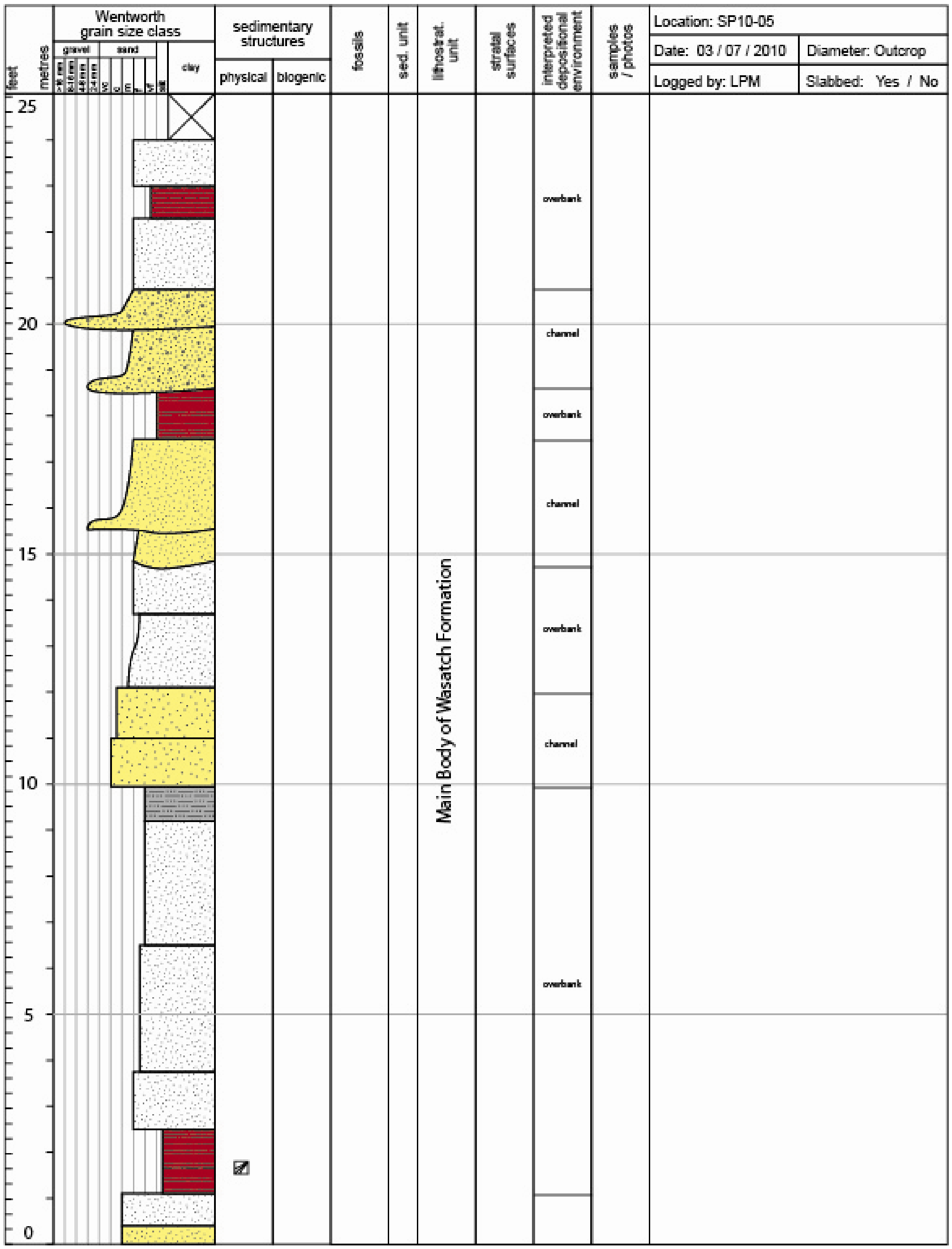
feet
metres
Wentworth grain size class
gravel
sand
clay
sedimentary structures
physical
biogenic
fossils
sed. unit
lithostrat. unit
stratal surfaces
interpreted depositional environment
samples / photos
Location: SP10-05
Date: 03 / 07 / 2010
Diameter: Outcrop
Logged by: LPM
Slabbed: Yes / No
25
20
15
10
5
0
overbank
channel
overbank
channel
overbank
channel
overbank
Main Body of Wasatch Formation

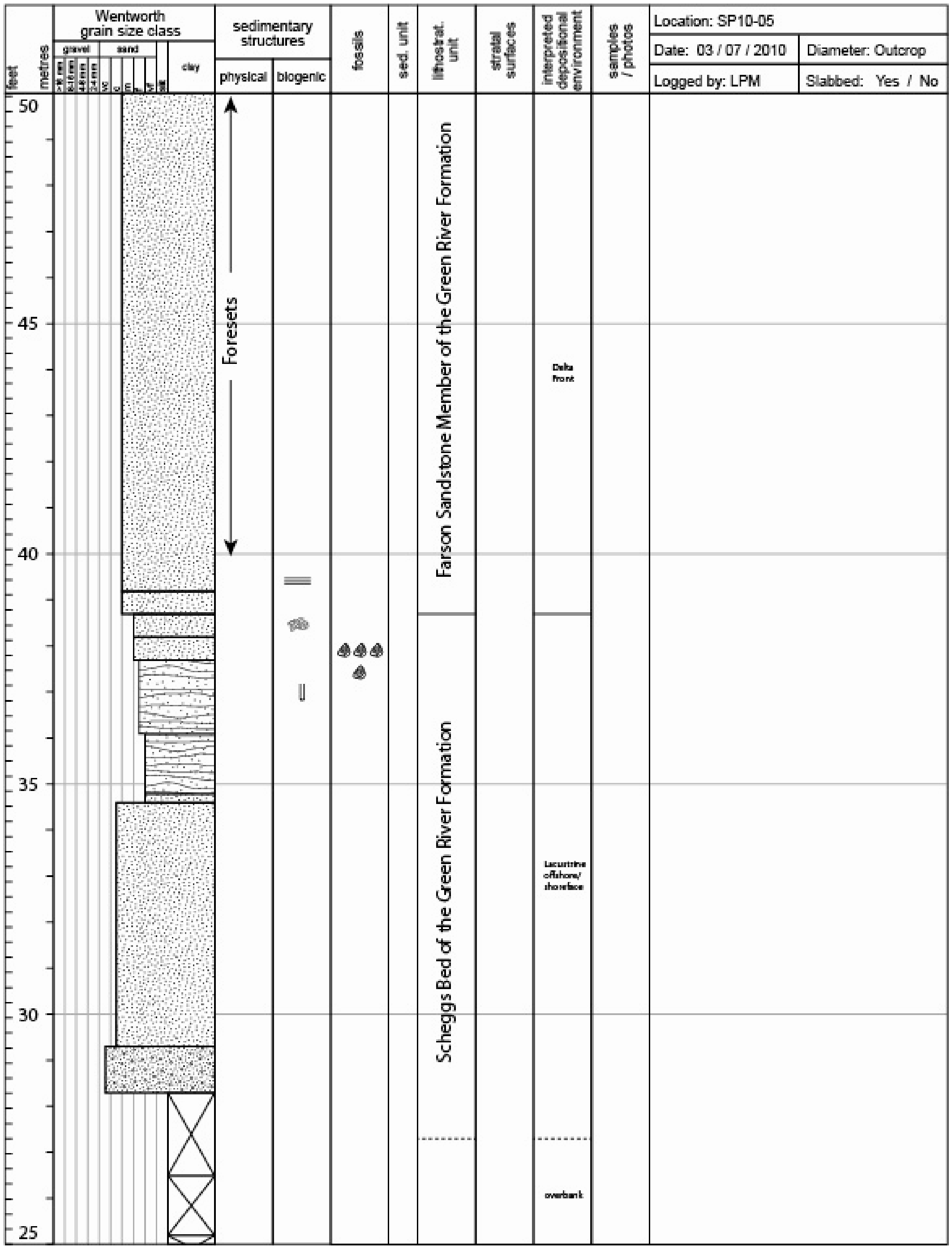
Location: SP10-05
Date: 03 / 07 / 2010
Diameter: Outcrop
Logged by: LPM
Slabbed: Yes / No
Wentworth grain size class
gravel
sand
clay
sedimentary structures
physical
biogenic
fossils
sed. unit
lithostrat. unit
stratal surfaces
interpreted depositional environment
samples / photos
feet
metres
50
45
40
35
30
25
Foresets
Farson Sandstone Member of the Green River Formation
Scheggs Bed of the Green River Formation
Delta front
Lacustrine offshore/ shoreface
overbank

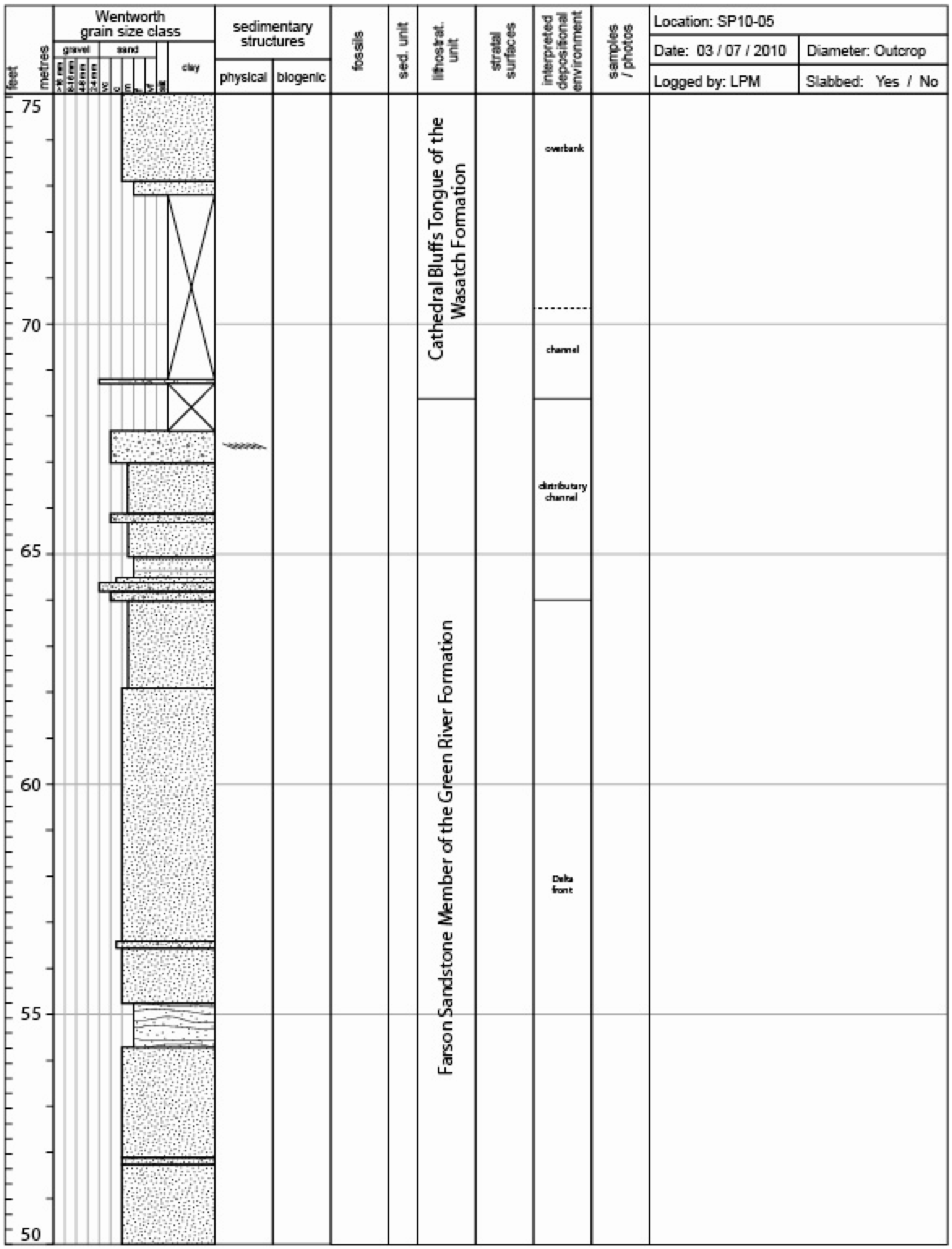

Wentworth grain size class
gravel
sand
clay
feet
metres
sedimentary structures
physical
biogenic
fossils
sed. unit
lithostrat. unit
stratal surfaces
interpreted depositional environment
samples / photos
Location: SP10-05
Date: 03 / 07 / 2010
Diameter: Outcrop
Logged by: LPM
Slabbed: Yes / No
75
70
65
60
55
50
Cathedral Bluffs Tongue of the Wasatch Formation
Farson Sandstone Member of the Green River Formation
overbank
channel
distributary channel
Delta front

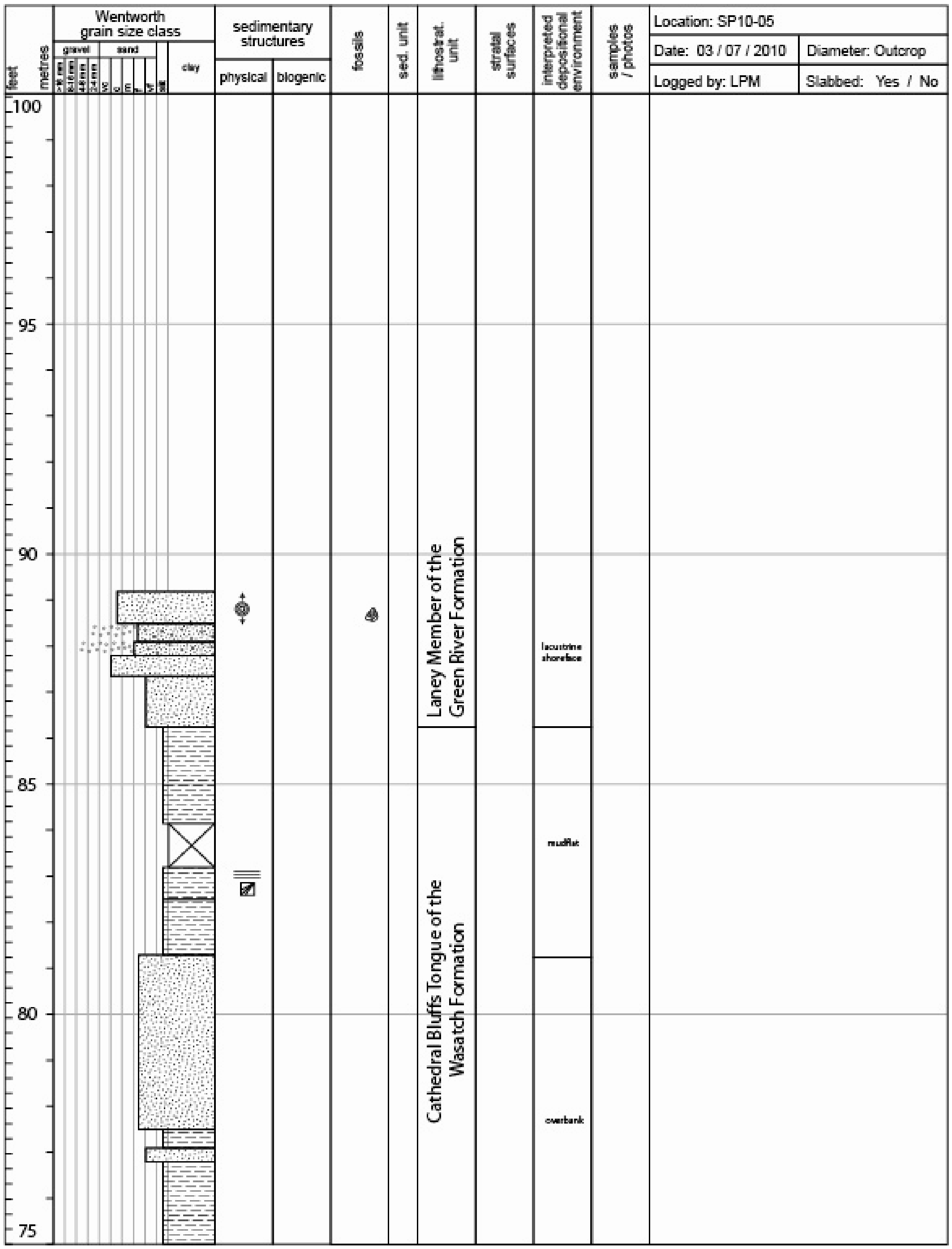

Location: SP10-05
Date: 03 / 07 / 2010
Diameter: Outcrop
Logged by: LPM
Slabbed: Yes / No
feet
metres
Wentworth grain size class
gravel
sand
clay
sedimentary structures
physical
biogenic
fossils
sed. unit
lithostrat. unit
stratal surfaces
interpreted depositional environment
samples / photos
100
95
90
85
80
75
Laney Member of the Green River Formation
Cathedral Bluffs Tongue of the Wasatch Formation
lacustrine shoreface
mudflat
overbank

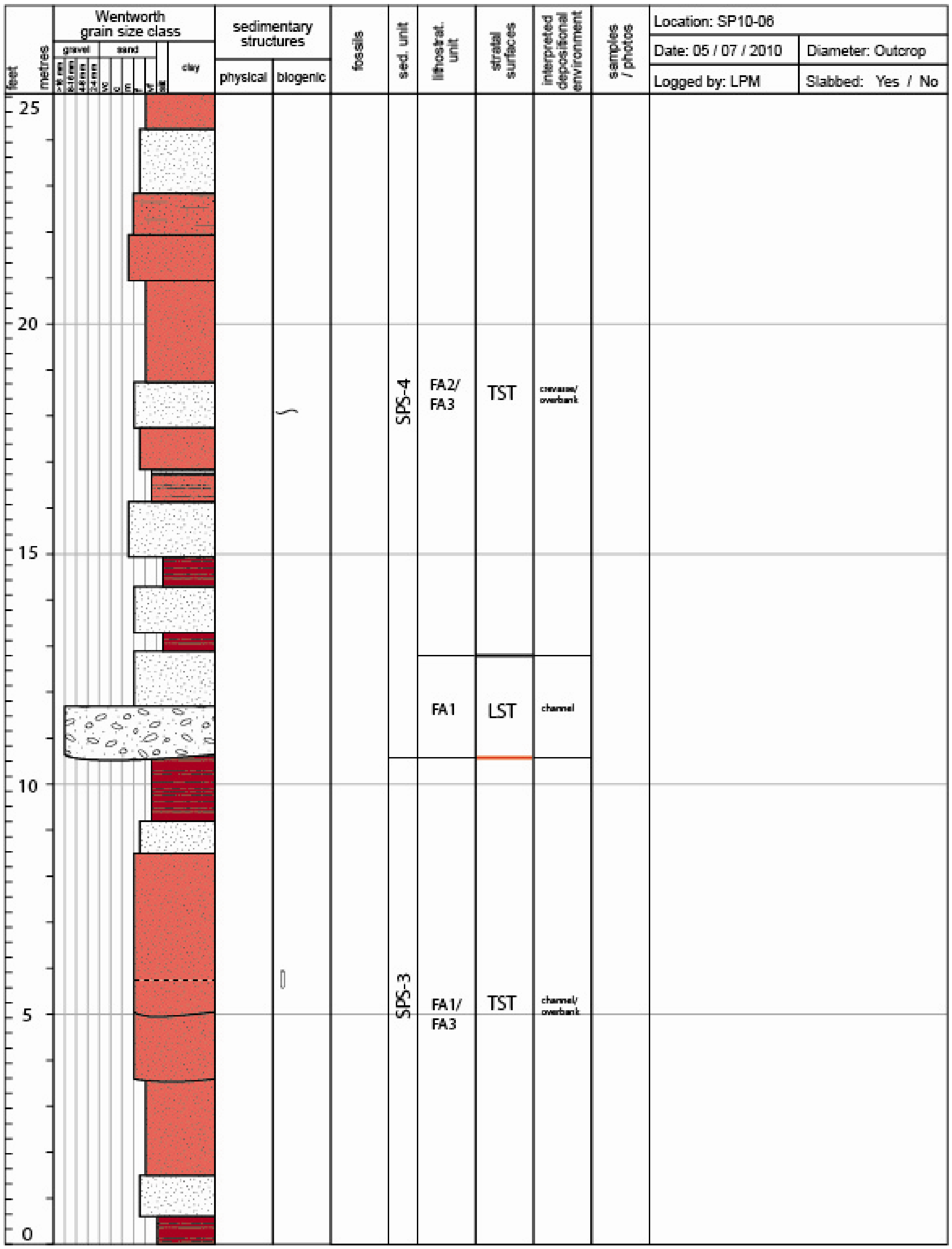

Wentworth grain size class
gravel
sand
clay
feet
metres
sedimentary structures
physical
biogenic
fossils
sed. unit
lithostrat. unit
stratal surfaces
interpreted depositional environment
samples / photos
Location: SP10-06
Date: 05 / 07 / 2010
Diameter: Outcrop
Logged by: LPM
Slabbed: Yes / No
25
20
15
10
5
0
SPS-4
FA2/ FA3
TST
FA1
LST
channel
SPS-3
FA1/ FA3
TST

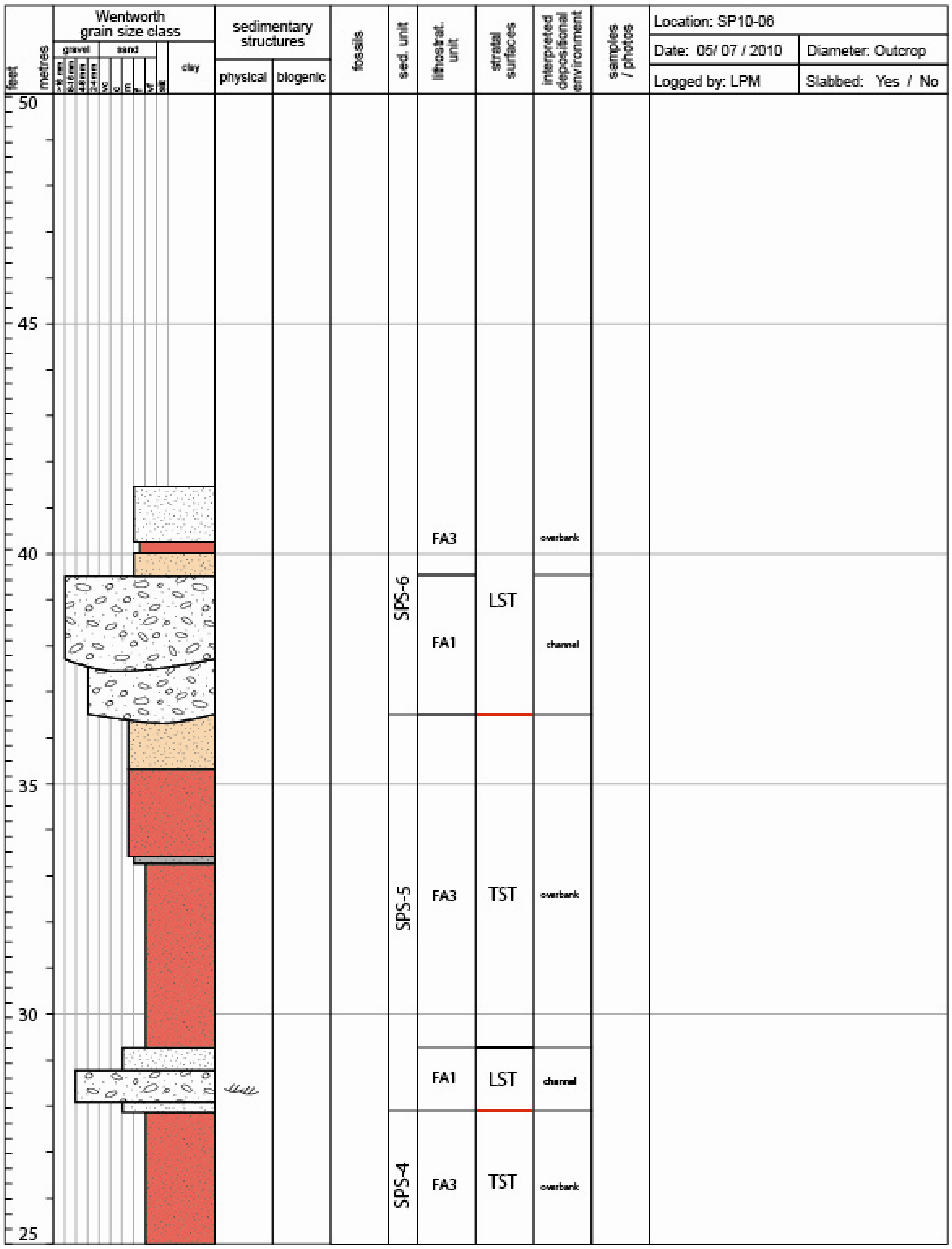

Location: SP10-06
Date: 05/ 07 / 2010
Diameter: Outcrop
Logged by: LPM
Slabbed: Yes / No
Wentworth grain size class
sedimentary structures
physical
biogenic
fossils
sed. unit
lithostrat. unit
stratal surfaces
interpreted depositional environment
samples / photos
feet
metres
gravel
sand
clay
50
45
40
35
30
25
FA3
overbank
SPS-6
LST
FA1
channel
SPS-5
FA3
TST
overbank
FA1
LST
channel
SPS-4
FA3
TST
overbank

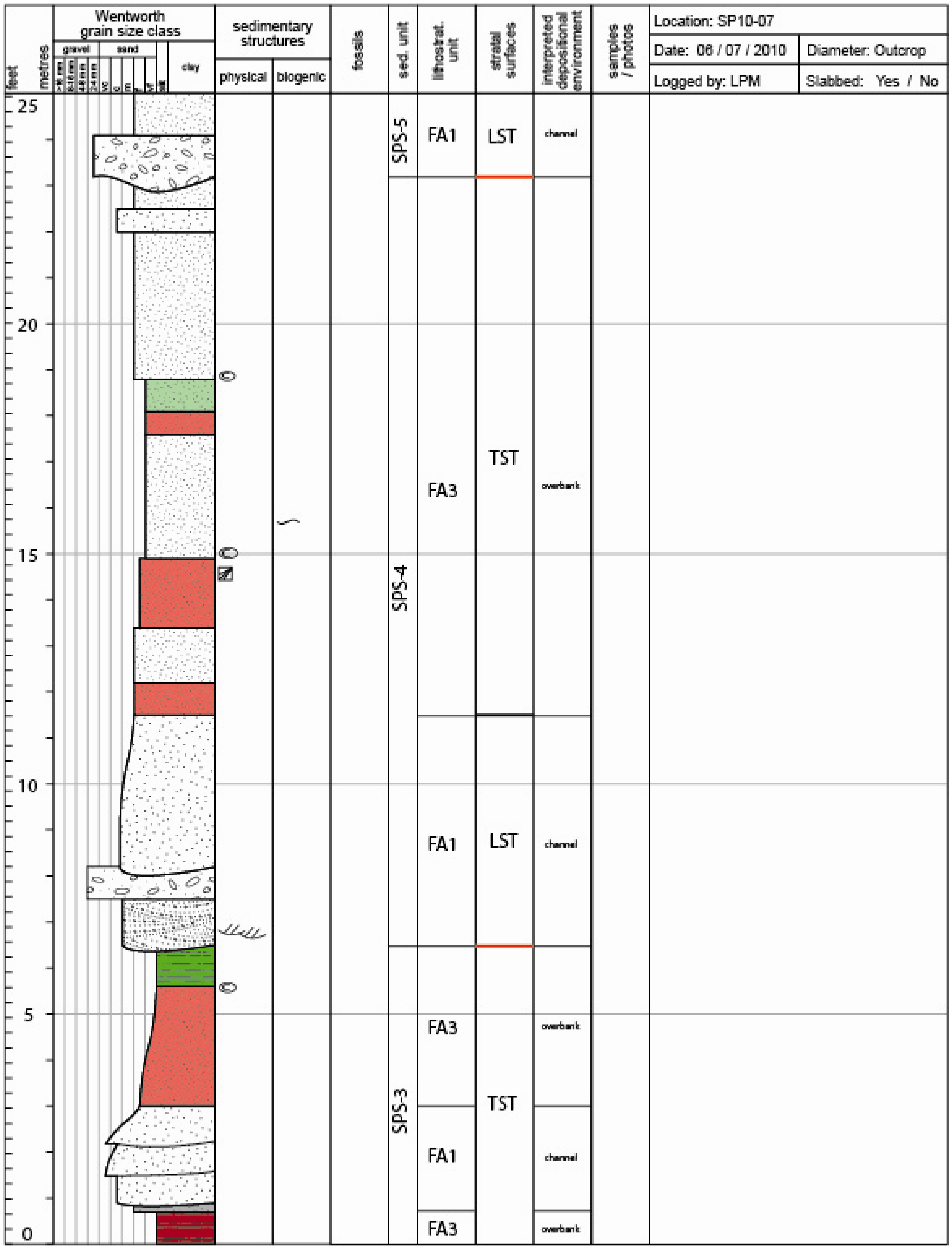

Wentworth grain size class
gravel
sand
clay
feet
metres
sedimentary structures
physical
biogenic
fossils
sed. unit
lithostrat. unit
stratal surfaces
interpreted depositional environment
samples / photos
Location: SP10-07
Date: 06 / 07 / 2010
Diameter: Outcrop
Logged by: LPM
Slabbed: Yes / No
25
20
15
10
5
0
SPS-5
SPS-4
SPS-3
FA1
LST
channel
FA3
TST
overbank
FA1
LST
channel
FA3
overbank
FA1
channel
FA3
overbank

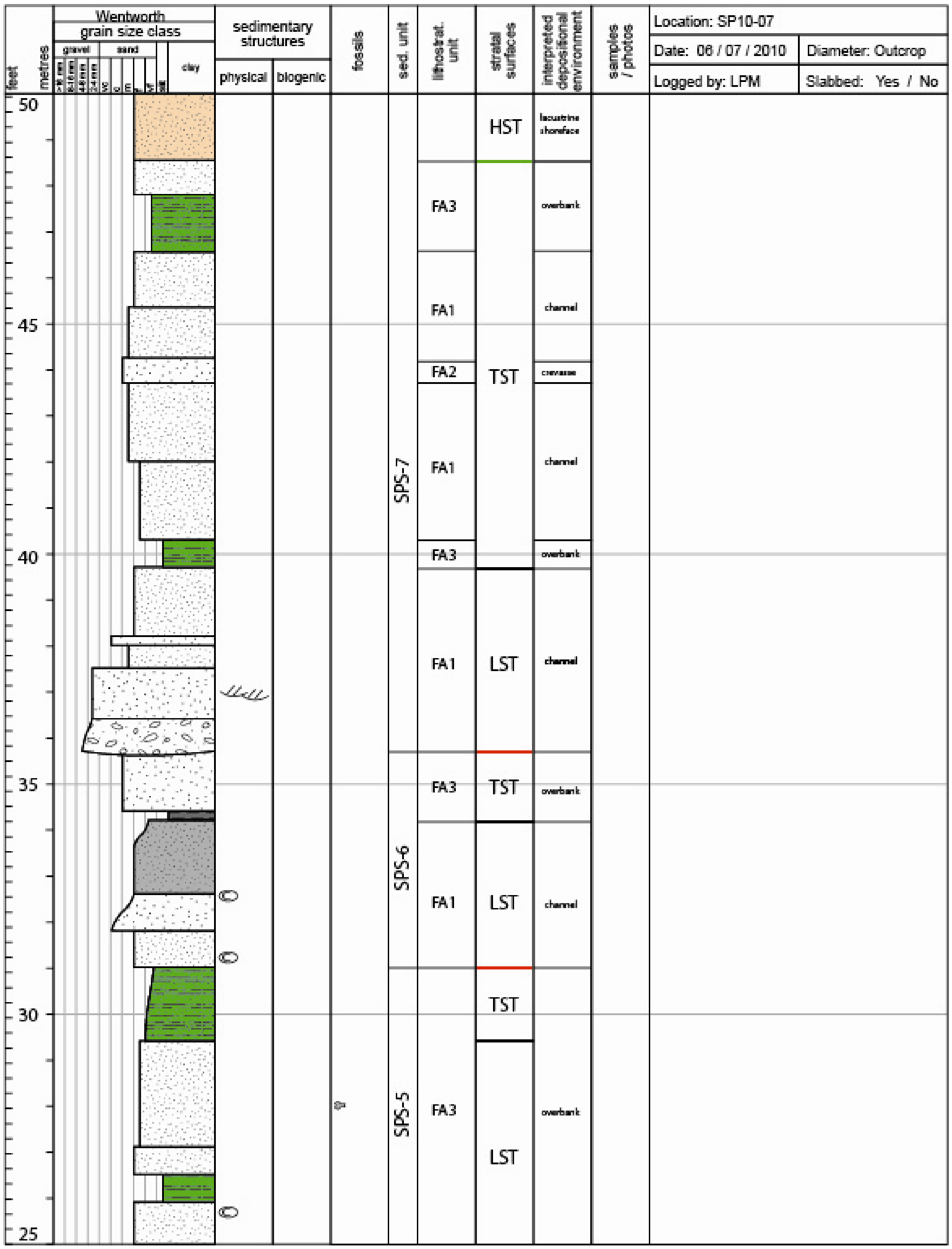
Location: SP10-07
Date: 06 / 07 / 2010
Diameter: Outcrop
Logged by: LPM
Slabbed: Yes / No
Wentworth grain size class
gravel
sand
clay
feet
metres
sedimentary structures
physical
biogenic
fossils
sed. unit
lithostrat. unit
stratal surfaces
interpreted depositional environment
samples / photos
50
45
40
35
30
25
SPS-7
SPS-6
SPS-5
FA3
FA1
FA2
FA1
FA3
FA1
FA3
FA1
FA3
HST
TST
LST
TST
LST
TST
LST
lacustrine shoreface
overbank
channel
crevasse
channel
overbank
channel
overbank
channel
overbank

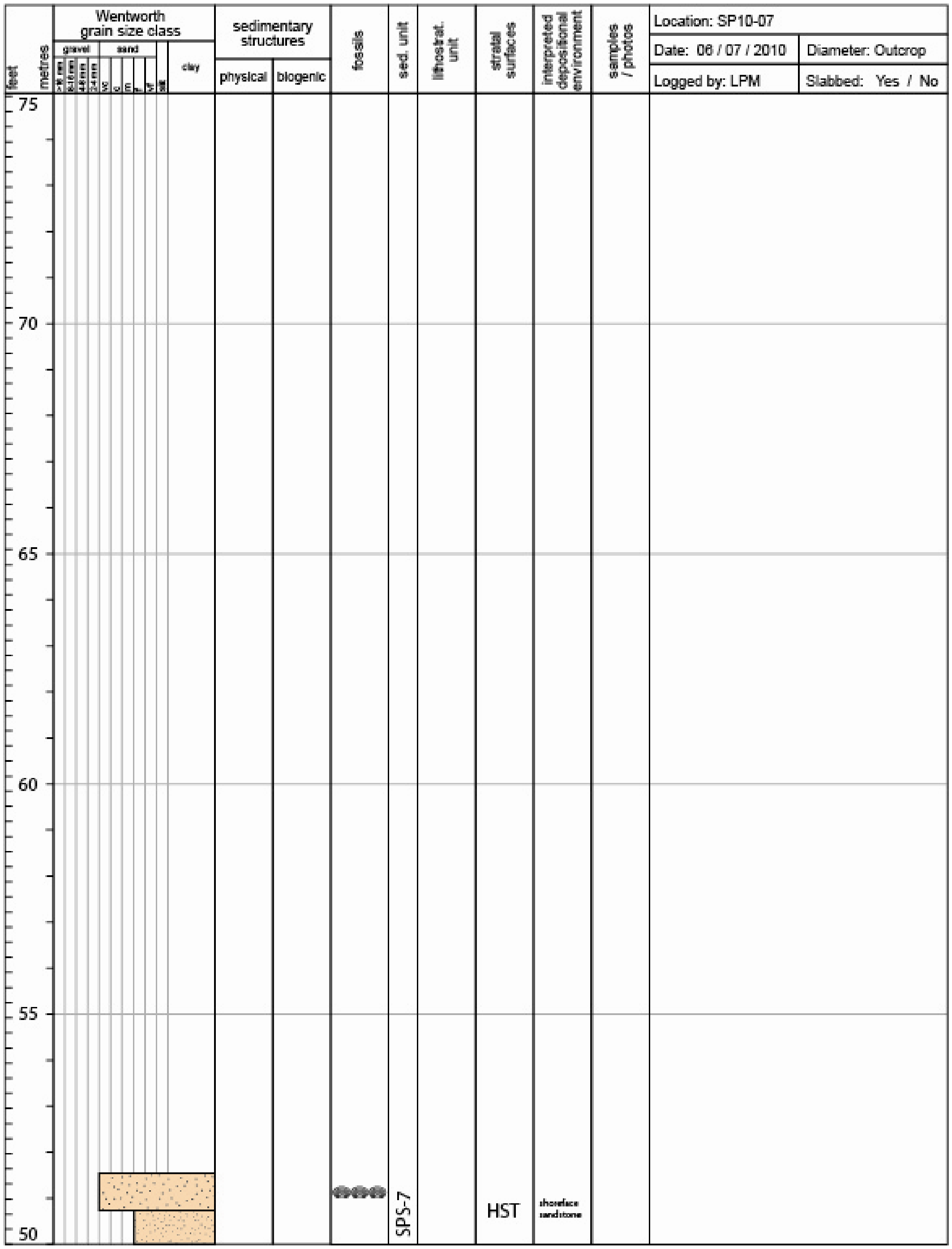

Wentworth grain size class
gravel
sand
clay
sedimentary structures
physical
biogenic
fossils
sed. unit
lithostrat. unit
stratal surfaces
interpreted depositional environment
samples / photos
Location: SP10-07
Date: 06 / 07 / 2010
Diameter: Outcrop
Logged by: LPM
Slabbed: Yes / No
feet
metres
75
70
65
60
55
50
SPS-7
HST
shoreface sandstone

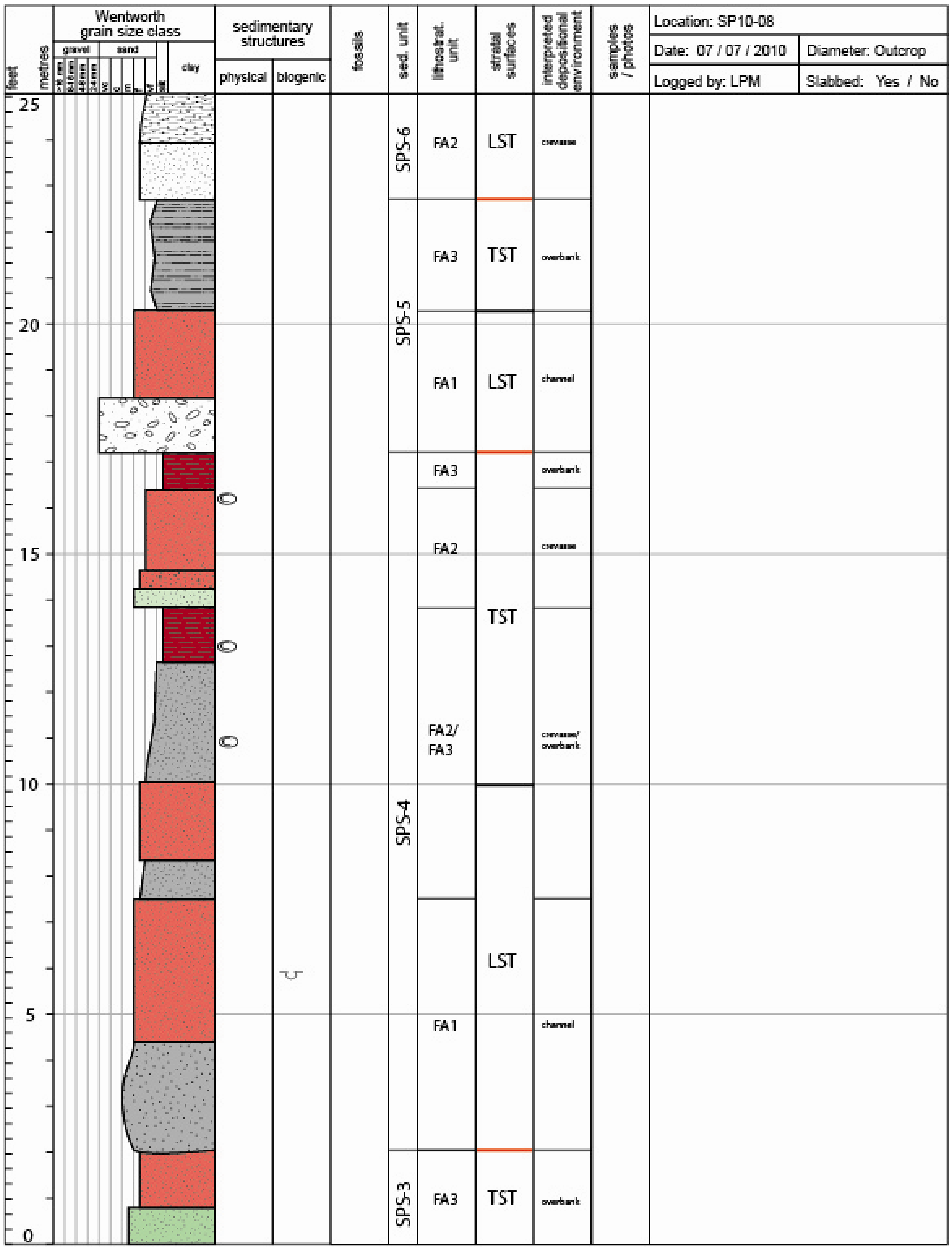
Location: SP10-08
Date: 07 / 07 / 2010
Diameter: Outcrop
Logged by: LPM
Slabbed: Yes / No
feet
metres
Wentworth grain size class
gravel
sand
clay
sedimentary structures
physical
biogenic
fossils
sed. unit
lithostrat. unit
stratal surfaces
interpreted depositional environment
samples / photos
25
20
15
10
5
0
SPS-6
SPS-5
SPS-4
SPS-3
FA2
FA3
FA1
FA3
FA2
FA2/ FA3
FA1
FA3
LST
TST
LST
TST
LST
TST
crevasse
overbank
channel
overbank
crevasse
crevasse/ overbank
channel
overbank

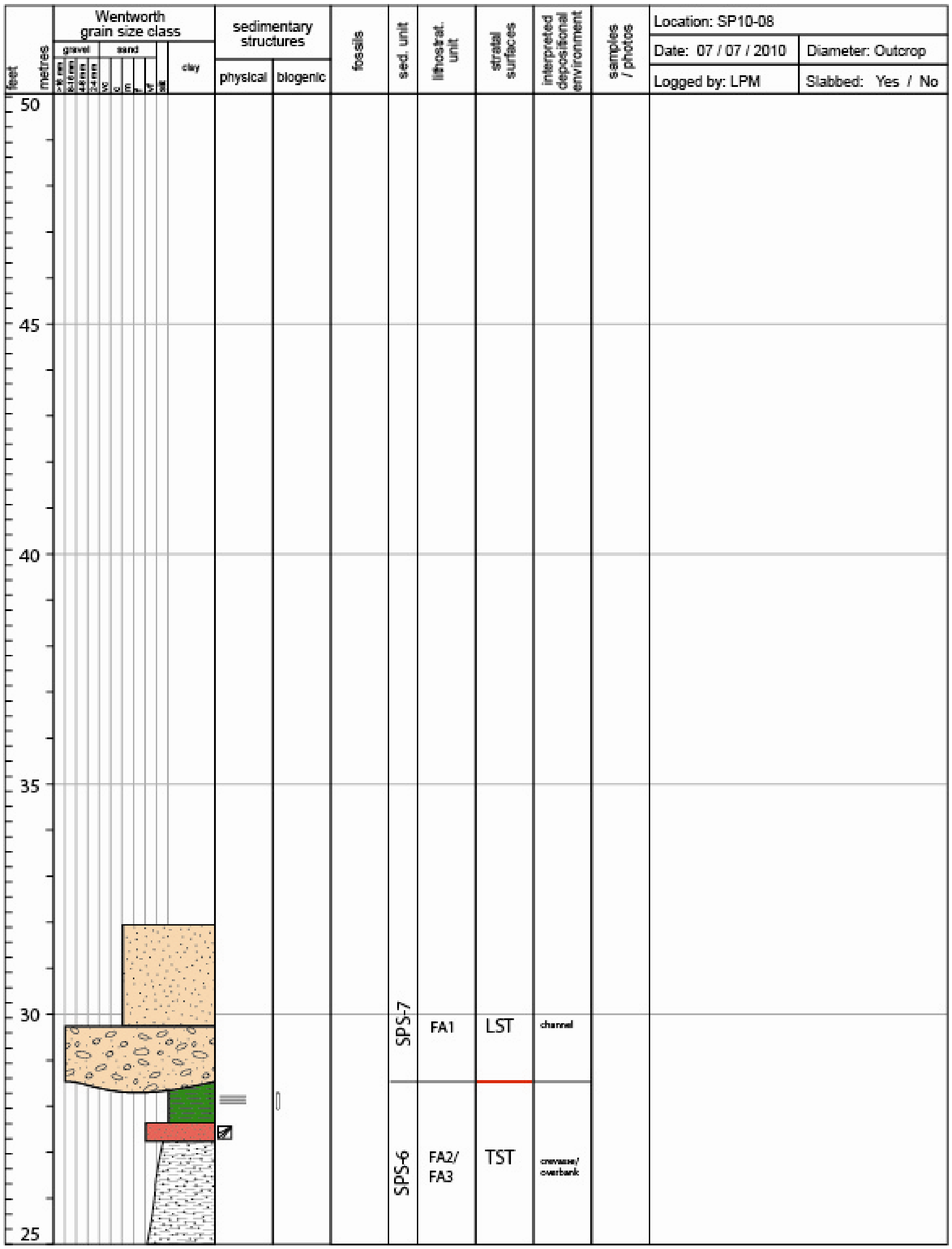
Location: SP10-08
Date: 07 / 07 / 2010
Diameter: Outcrop
Logged by: LPM
Slabbed: Yes / No
feet
metres
Wentworth grain size class
gravel
sand
clay
sedimentary structures
physical
biogenic
fossils
sed. unit
lithostrat. unit
stratal surfaces
interpreted depositional environment
samples / photos
50
45
40
35
30
25
SPS-7
FA1
LST
channel
SPS-6
FA2/ FA3
TST
crevasse/ overbank

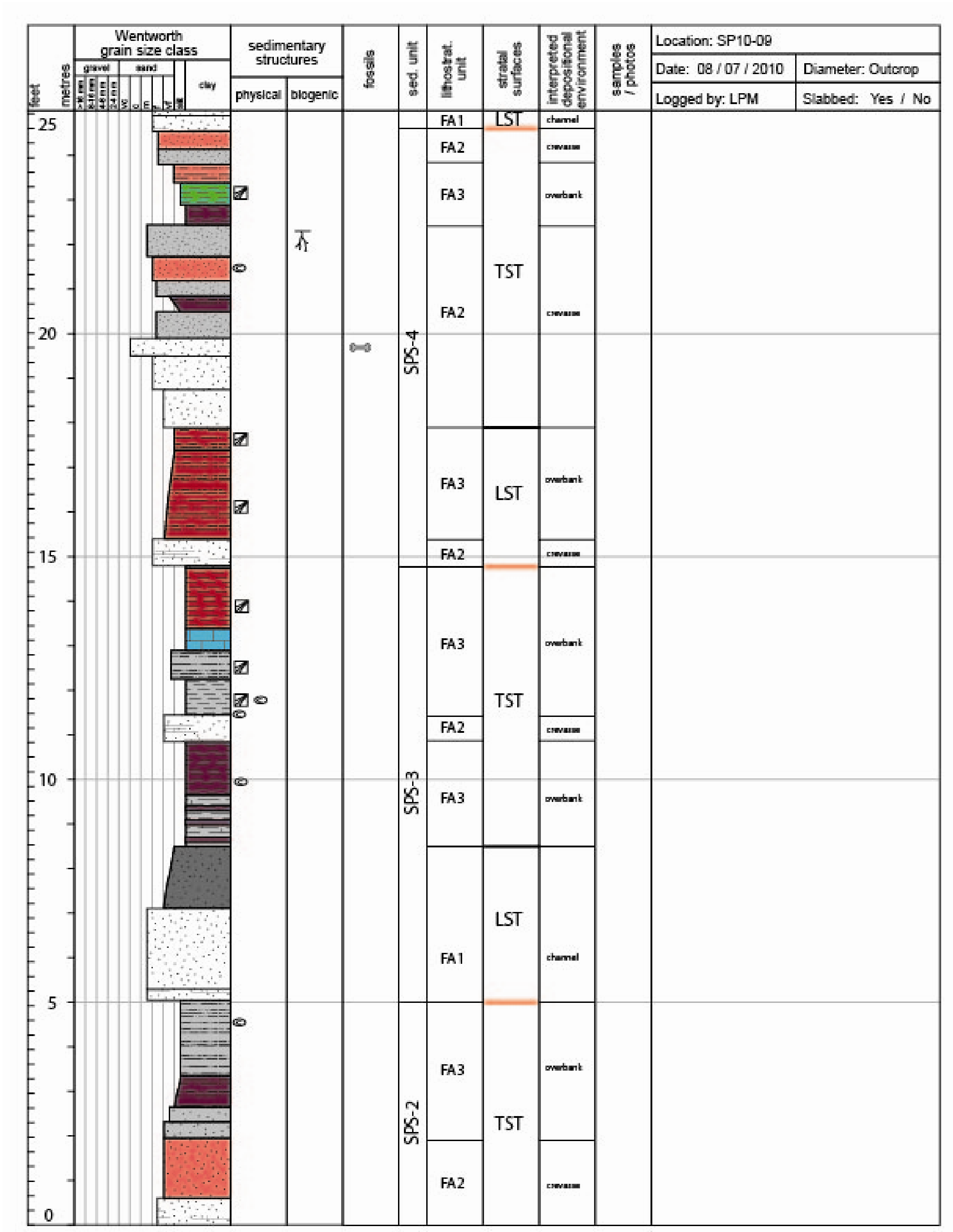

Wentworth grain size class
gravel
sand
clay
feet
metres
sedimentary structures
physical
biogenic
fossils
sed. unit
lithostrat. unit
stratal surfaces
interpreted depositional environment
samples / photos
Location: SP10-09
Date: 08 / 07 / 2010
Diameter: Outcrop
Logged by: LPM
Slabbed: Yes / No
25
20
15
10
5
0
SPS-4
SPS-3
SPS-2
FA1
FA2
FA3
FA2
FA3
FA2
FA3
FA2
FA3
FA1
FA3
FA2
LST
TST
LST
TST
LST
TST
channel
crevasse
overbank
crevasse
overbank
crevasse
overbank
crevasse
overbank
channel
overbank
crevasse

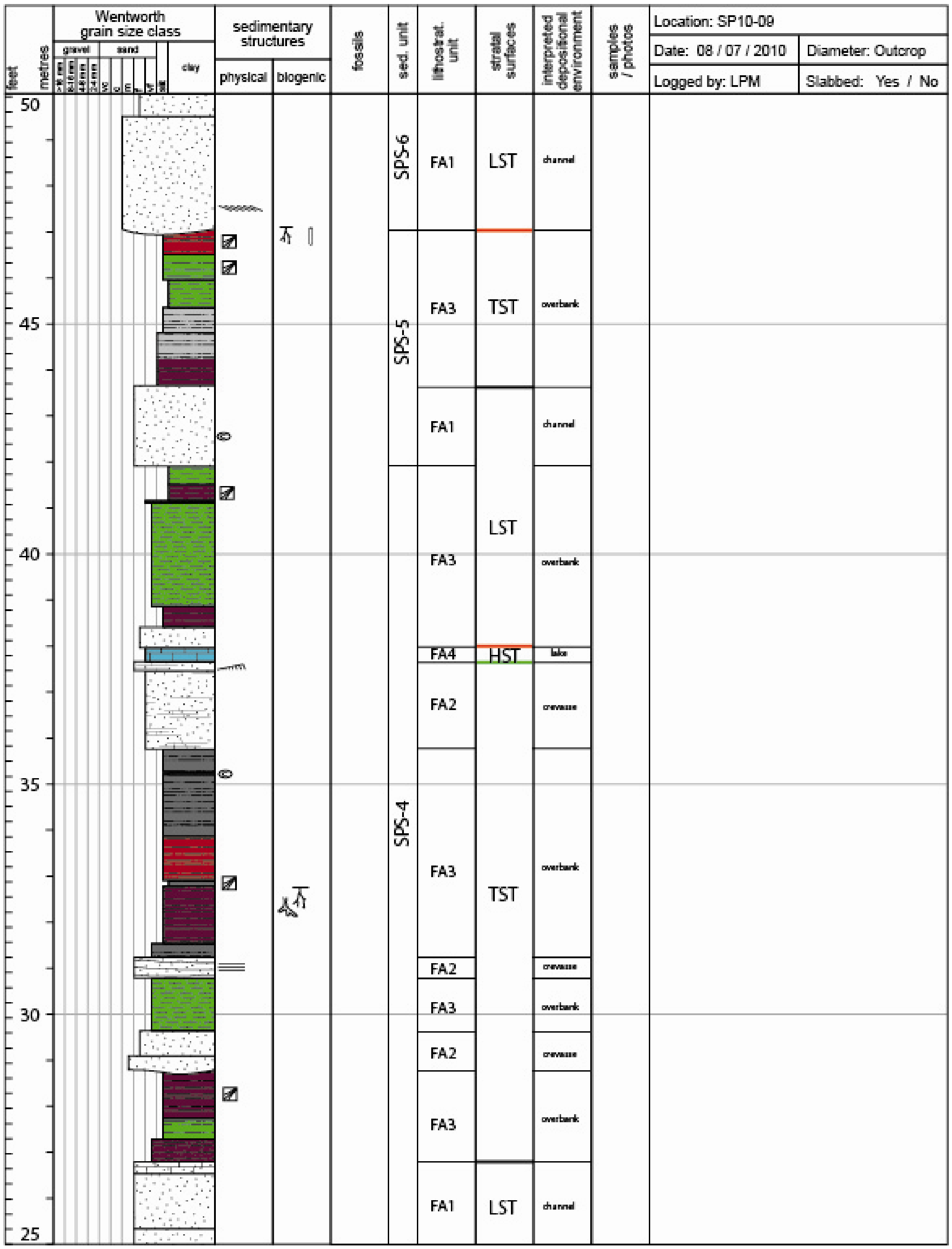
Location: SP10-09
Date: 08 / 07 / 2010
Diameter: Outcrop
Logged by: LPM
Slabbed: Yes / No
feet
metres
Wentworth grain size class
gravel
sand
clay
sedimentary structures
physical
biogenic
fossils
sed. unit
lithostrat. unit
stratal surfaces
interpreted depositional environment
samples / photos
50
45
40
35
30
25
SPS-6
SPS-5
SPS-4
FA1
FA3
FA1
FA3
FA4
FA2
FA3
FA2
FA3
FA2
FA3
FA1
LST
TST
LST
HST
TST
LST
channel
overbank
channel
overbank
lake
crevasse
overbank
crevasse
overbank
crevasse
overbank
channel

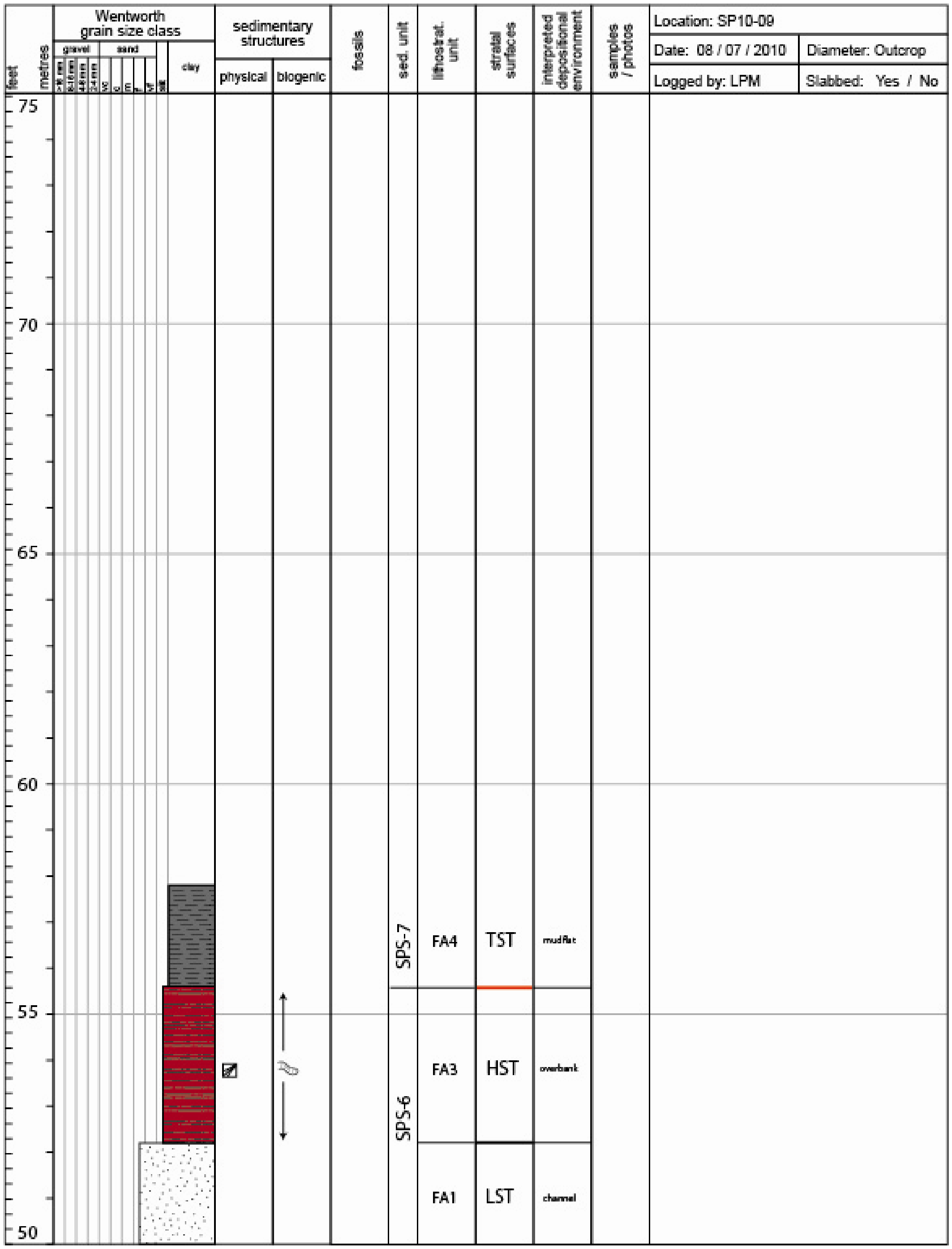

Wentworth grain size class
gravel
sand
clay
sedimentary structures
physical
biogenic
fossils
sed. unit
lithostrat. unit
stratal surfaces
interpreted depositional environment
samples / photos
Location: SP10-09
Date: 08 / 07 / 2010
Diameter: Outcrop
Logged by: LPM
Slabbed: Yes / No
feet
metres
75
70
65
60
55
50
SPS-7
FA4
TST
mudflat
SPS-6
FA3
HST
overbank
FA1
LST
channel

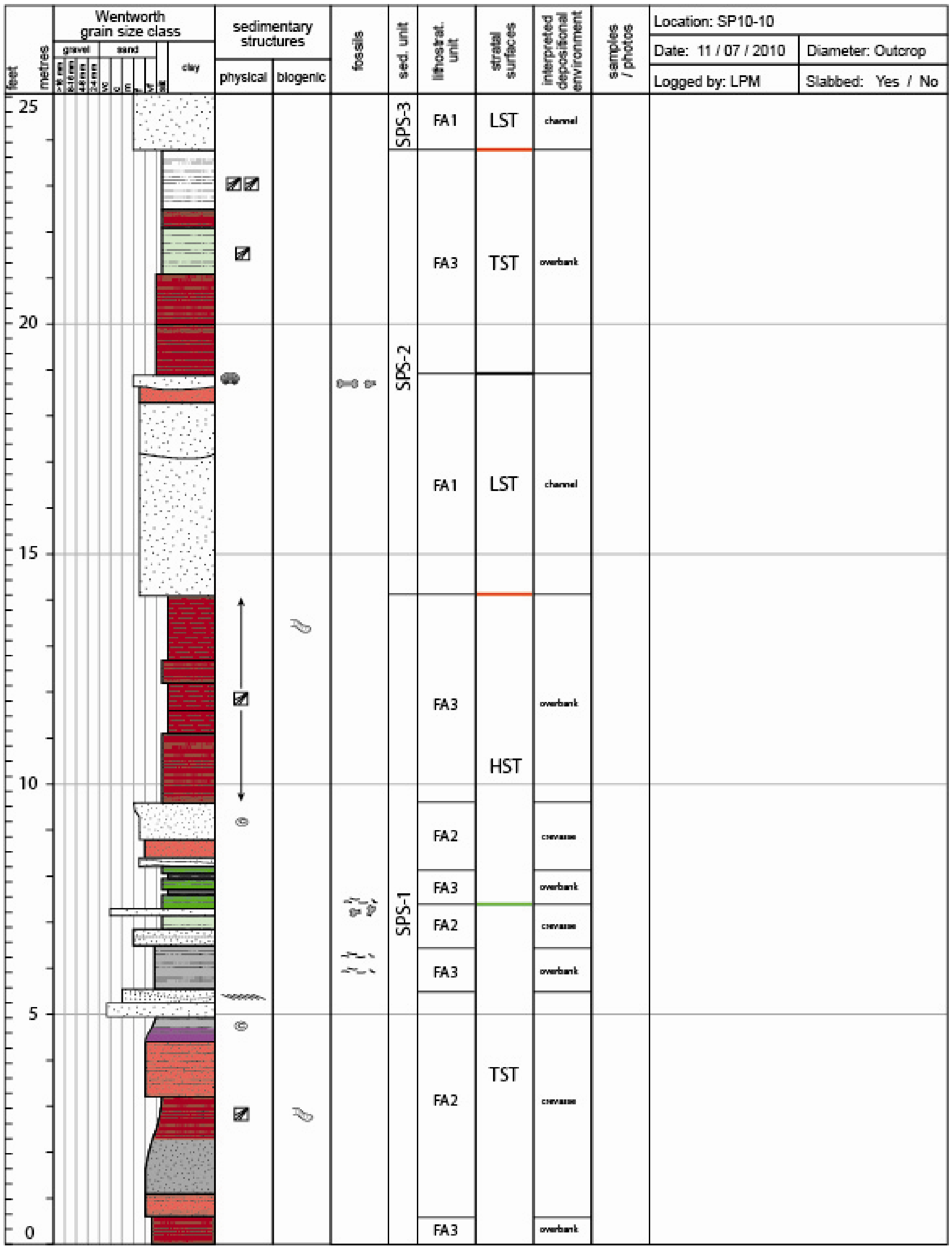
Location: SP10-10
Date: 11 / 07 / 2010
Diameter: Outcrop
Logged by: LPM
Slabbed: Yes / No
Wentworth grain size class
sedimentary structures
physical
biogenic
fossils
sed. unit
lithostrat. unit
stratal surfaces
interpreted depositional environment
samples / photos
metres
SPS-3
SPS-2
SPS-1
FA1
FA3
FA2
LST
TST
HST
channel
overbank
crevasse

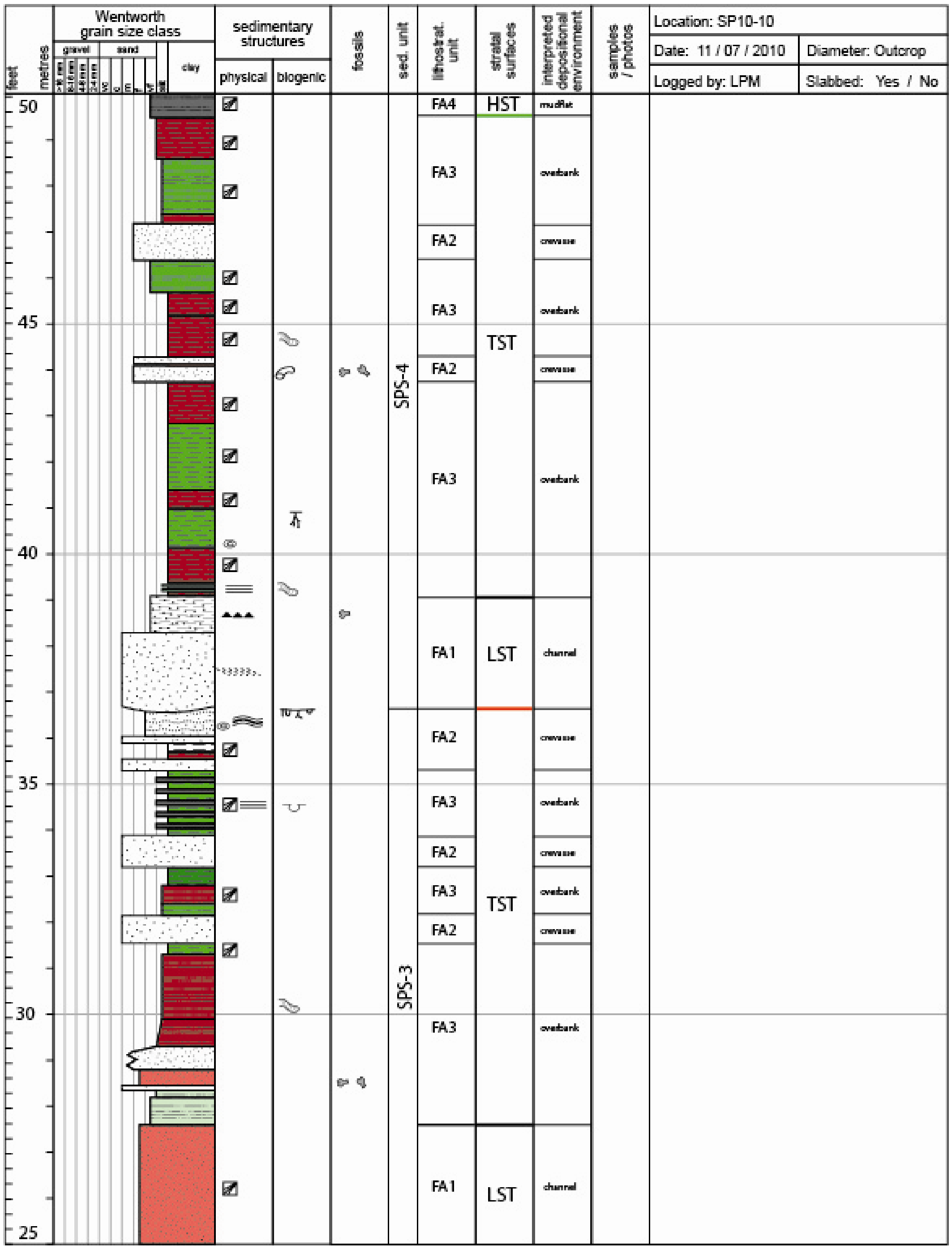
Location: SP10-10
Date: 11 / 07 / 2010
Diameter: Outcrop
Logged by: LPM
Slabbed: Yes / No
Wentworth grain size class
gravel
sand
clay
sedimentary structures
physical
biogenic
fossils
sed. unit
lithostrat. unit
stratal surfaces
interpreted depositional environment
samples / photos
feet
metres
50
45
40
35
30
25
FA4
HST
mudflat
FA3
overbank
FA2
crevasse
FA3
overbank
TST
FA2
crevasse
SPS-4
FA3
overbank
FA1
LST
channel
FA2
crevasse
FA3
overbank
FA2
crevasse
FA3
overbank
TST
FA2
crevasse
SPS-3
FA3
overbank
FA1
LST
channel

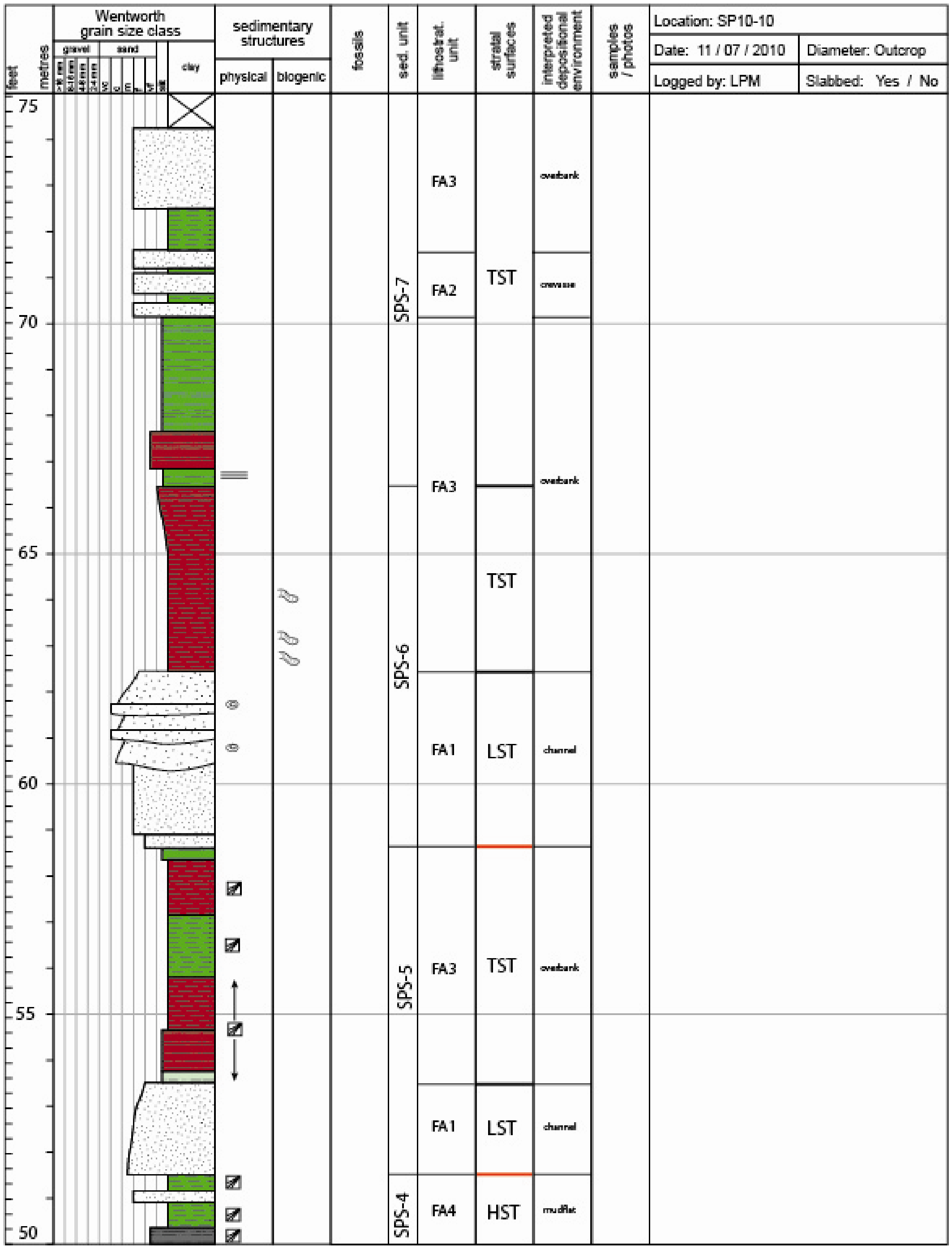
Wentworth grain size class
gravel
sand
clay
feet
metres
sedimentary structures
physical
biogenic
fossils
sed. unit
lithostrat. unit
stratal surfaces
interpreted depositional environment
samples / photos
Location: SP10-10
Date: 11 / 07 / 2010
Diameter: Outcrop
Logged by: LPM
Slabbed: Yes / No
75
70
65
60
55
50
SPS-7
SPS-6
SPS-5
SPS-4
FA3
FA2
FA3
FA1
FA3
FA1
FA4
TST
TST
LST
TST
LST
HST
overbank
crevasse
overbank
channel
overbank
channel
mudflat

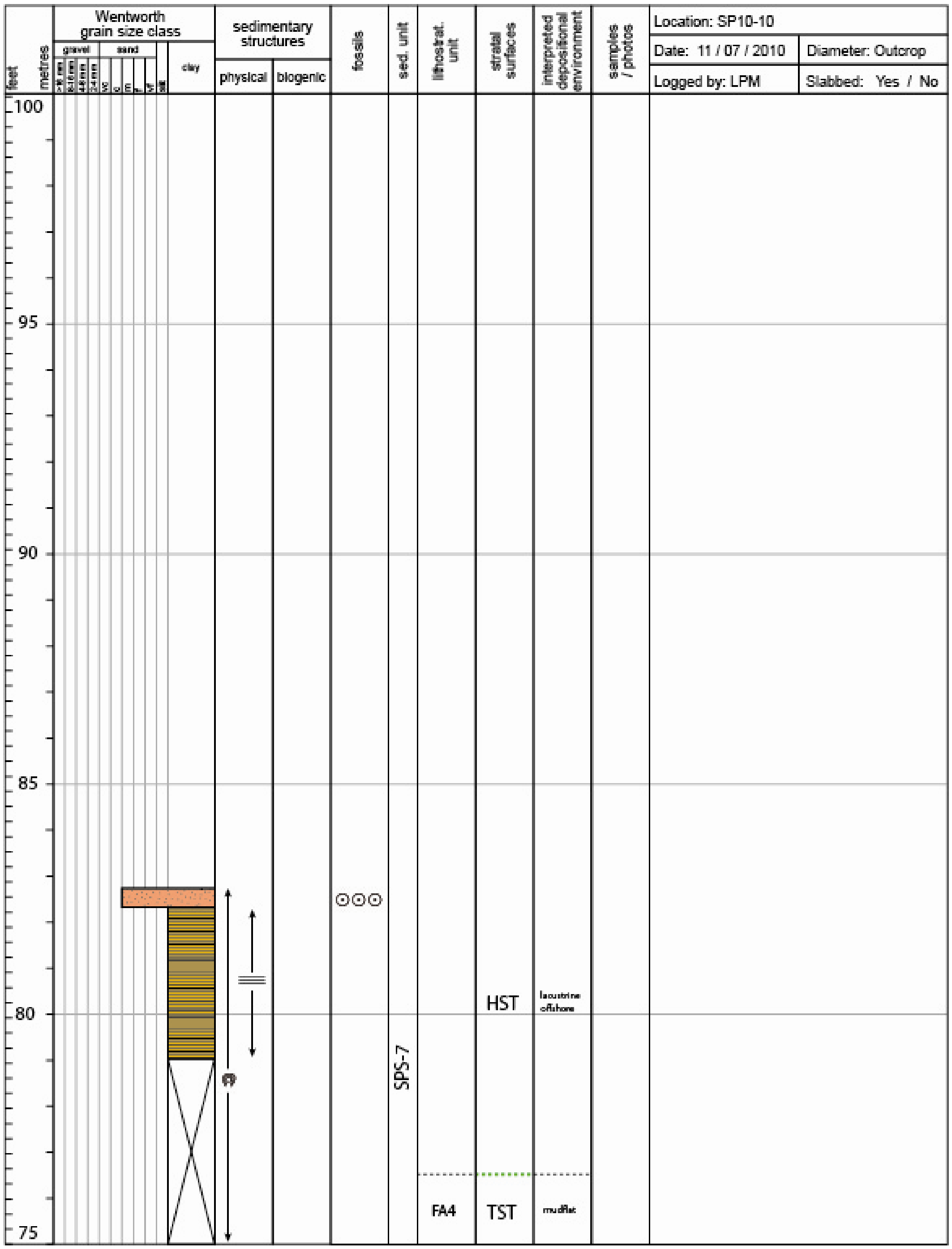
Wentworth grain size class
gravel
sand
clay
feet
metres
sedimentary structures
physical
biogenic
fossils
sed. unit
lithostrat. unit
stratal surfaces
interpreted depositional environment
samples / photos
Location: SP10-10
Date: 11 / 07 / 2010
Diameter: Outcrop
Logged by: LPM
Slabbed: Yes / No
100
95
90
85
80
75
SPS-7
HST
lacustrine offshore
FA4
TST
mudflat

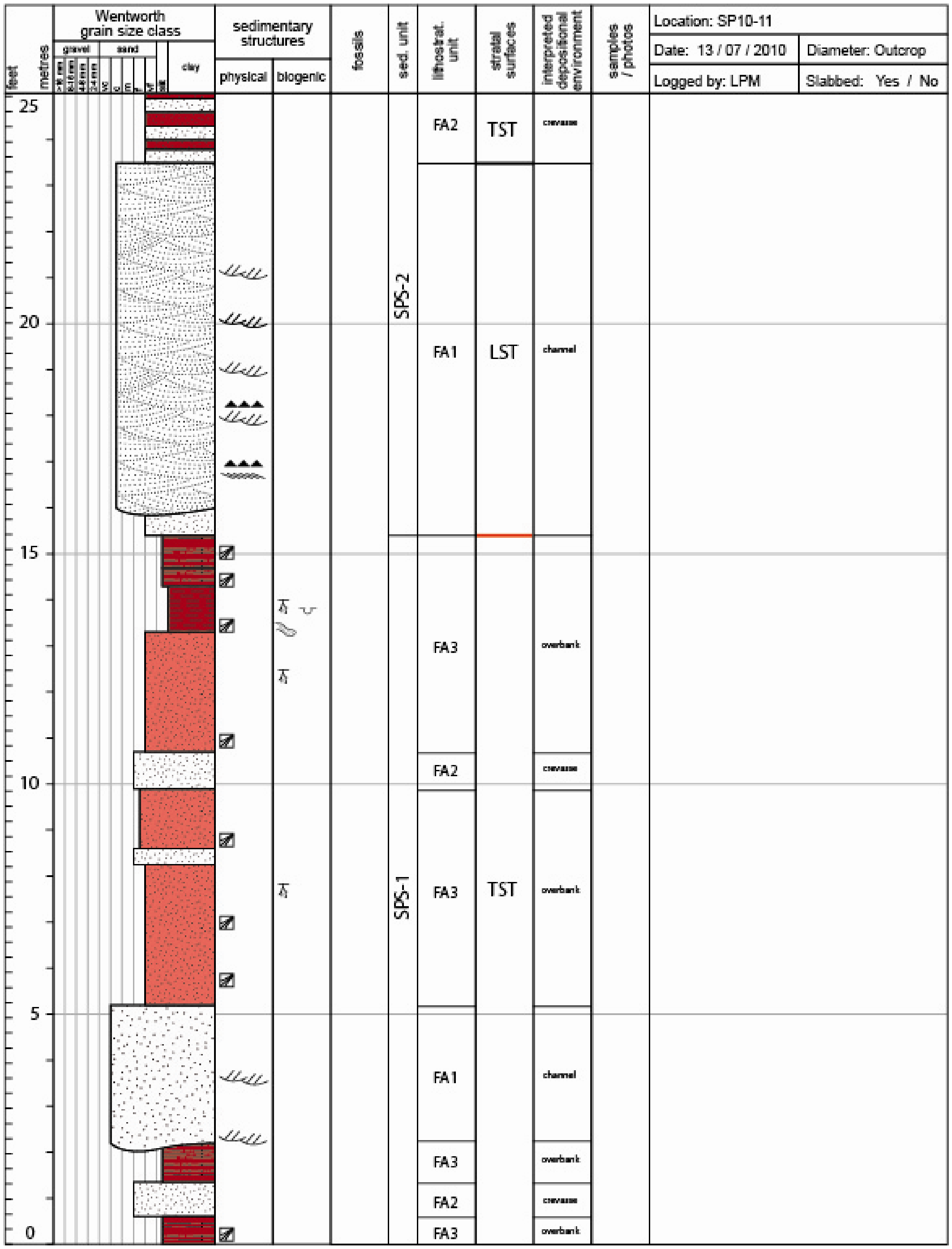

Location: SP10-11
Date: 13 / 07 / 2010
Diameter: Outcrop
Logged by: LPM
Slabbed: Yes / No
Wentworth grain size class
gravel
sand
clay
sedimentary structures
physical
biogenic
fossils
sed. unit
lithostrat. unit
stratal surfaces
interpreted depositional environment
samples / photos
feet
metres
25
20
15
10
5
0
SPS-2
SPS-1
FA2
FA1
FA3
FA2
FA3
FA1
FA3
FA2
FA3
TST
LST
TST
crevasse
channel
overbank
crevasse
overbank
channel
overbank
crevasse
overbank

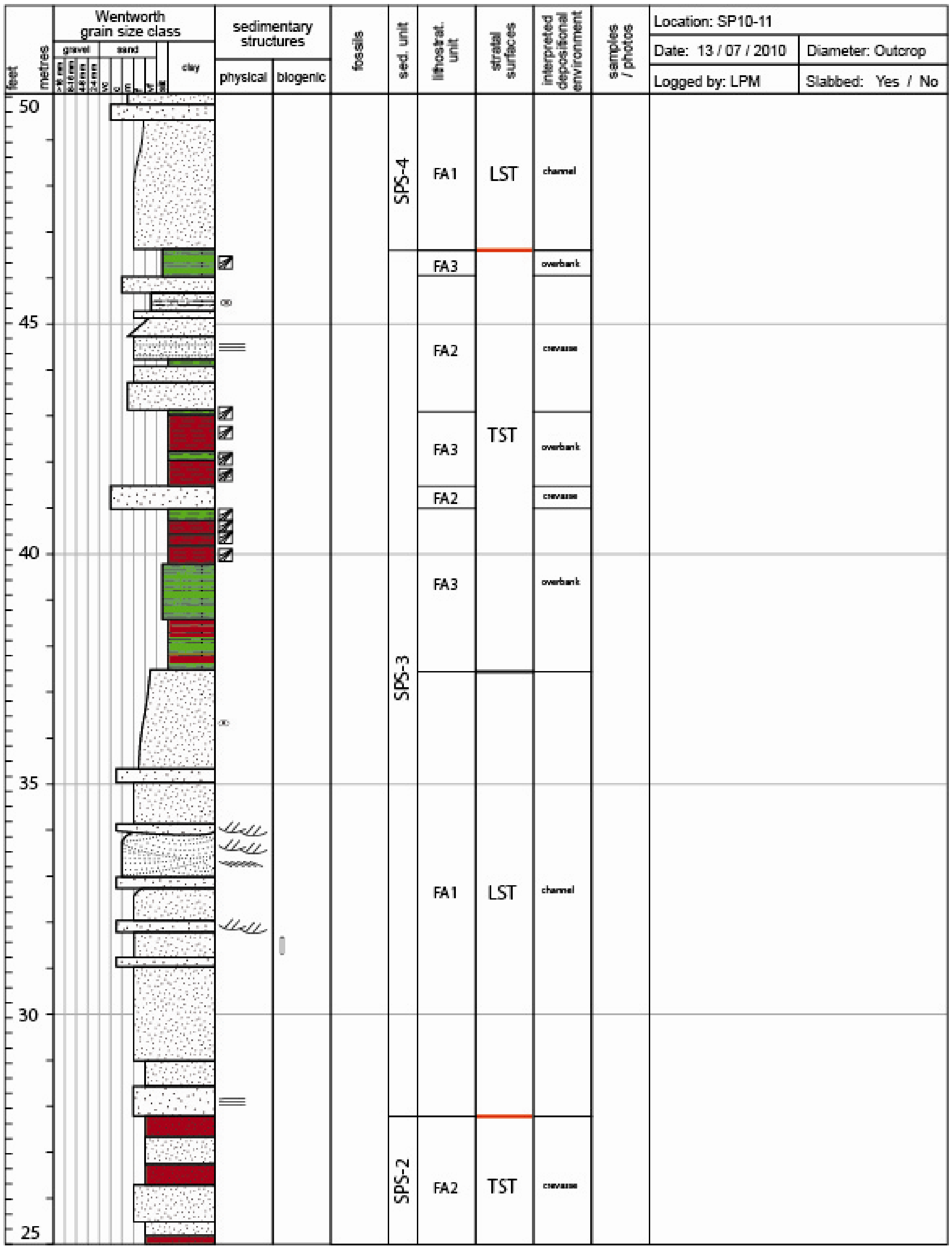
Wentworth grain size class
gravel
sand
clay
feet
metres
sedimentary structures
physical
biogenic
fossils
sed. unit
lithostrat. unit
stratal surfaces
interpreted depositional environment
samples / photos
Location: SP10-11
Date: 13 / 07 / 2010
Diameter: Outcrop
Logged by: LPM
Slabbed: Yes / No
50
45
40
35
30
25
SPS-4
SPS-3
SPS-2
FA1
FA3
FA2
FA3
FA2
FA3
FA1
FA2
LST
TST
LST
TST
channel
overbank
crevasse
overbank
crevasse
overbank
channel
crevasse

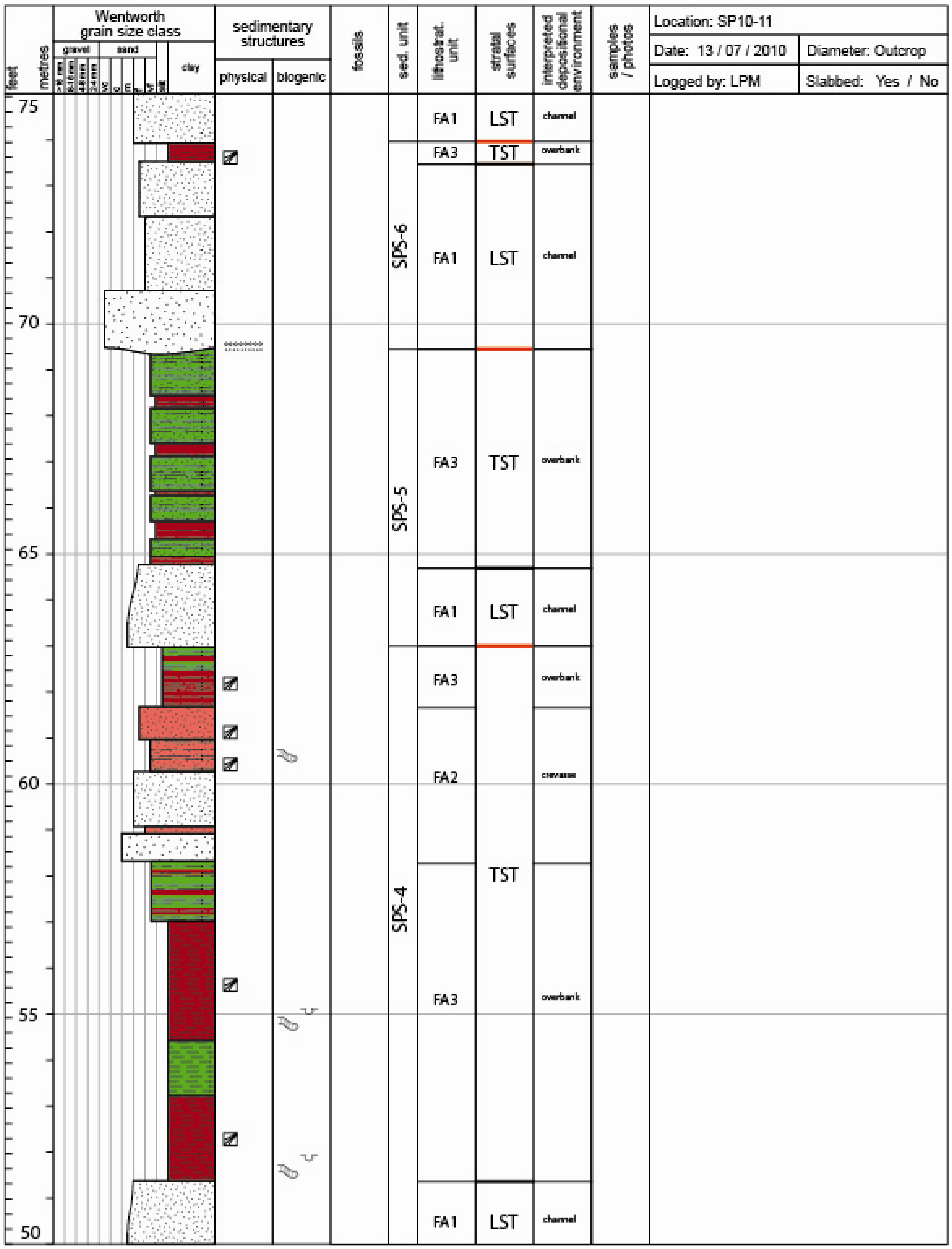

feet
metres
Wentworth grain size class
gravel
sand
clay
sedimentary structures
physical
biogenic
fossils
sed. unit
lithostrat. unit
stratal surfaces
interpreted depositional environment
samples / photos
Location: SP10-11
Date: 13 / 07 / 2010
Diameter: Outcrop
Logged by: LPM
Slabbed: Yes / No
75
70
65
60
55
50
SPS-6
SPS-5
SPS-4
FA1
FA3
FA1
FA3
FA1
FA3
FA2
FA3
FA1
LST
TST
LST
TST
LST
TST
LST
channel
overbank
channel
overbank
channel
overbank
crevasse
overbank
channel

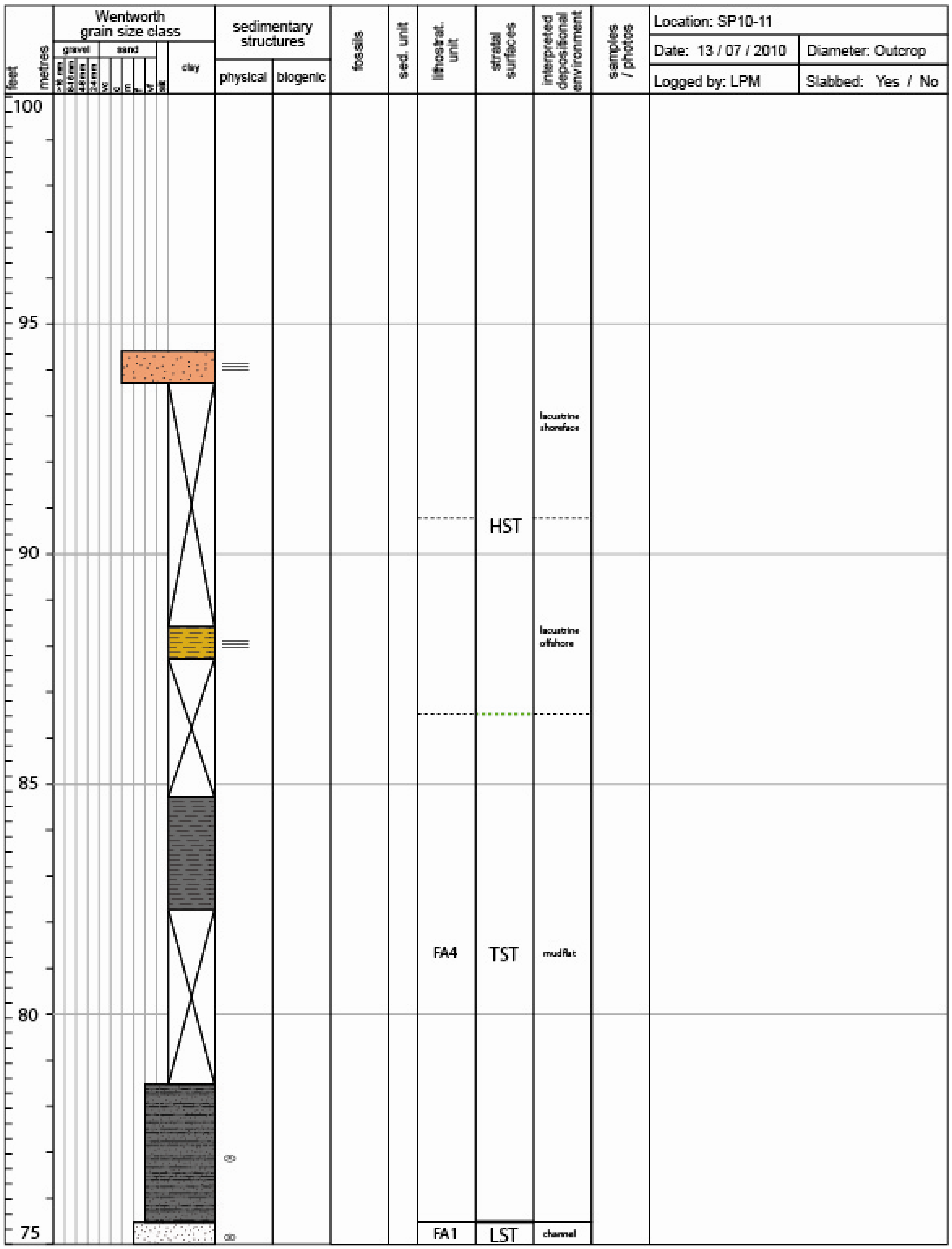
Location: SP10-11
Date: 13 / 07 / 2010
Diameter: Outcrop
Logged by: LPM
Slabbed: Yes / No
feet
metres
Wentworth grain size class
gravel
sand
clay
sedimentary structures
physical
biogenic
fossils
sed. unit
lithostrat. unit
stratal surfaces
interpreted depositional environment
samples / photos
100
95
90
85
80
75
lacustrine shoreface
HST
lacustrine offshore
FA4
TST
mudflat
FA1
LST
channel

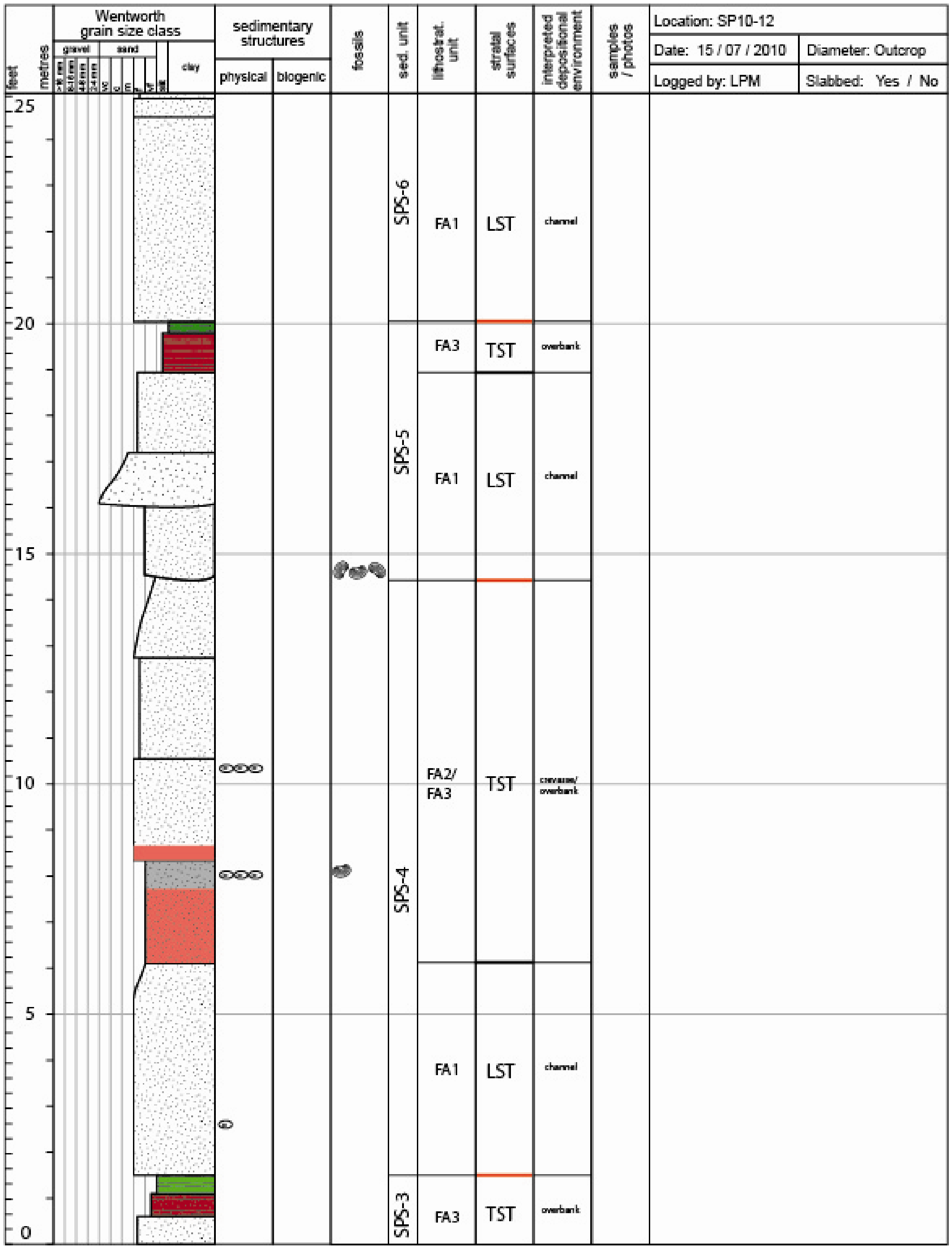

Location: SP10-12
Date: 15 / 07 / 2010
Diameter: Outcrop
Logged by: LPM
Slabbed: Yes / No
feet
metres
Wentworth grain size class
gravel
sand
clay
sedimentary structures
physical
biogenic
fossils
sed. unit
lithostrat. unit
stratal surfaces
interpreted depositional environment
samples / photos
25
20
15
10
5
0
SPS-6
FA1
LST
channel
FA3
TST
overbank
SPS-5
FA1
LST
channel
FA2/ FA3
TST
crevasse/ overbank
SPS-4
FA1
LST
channel
SPS-3
FA3
TST
overbank

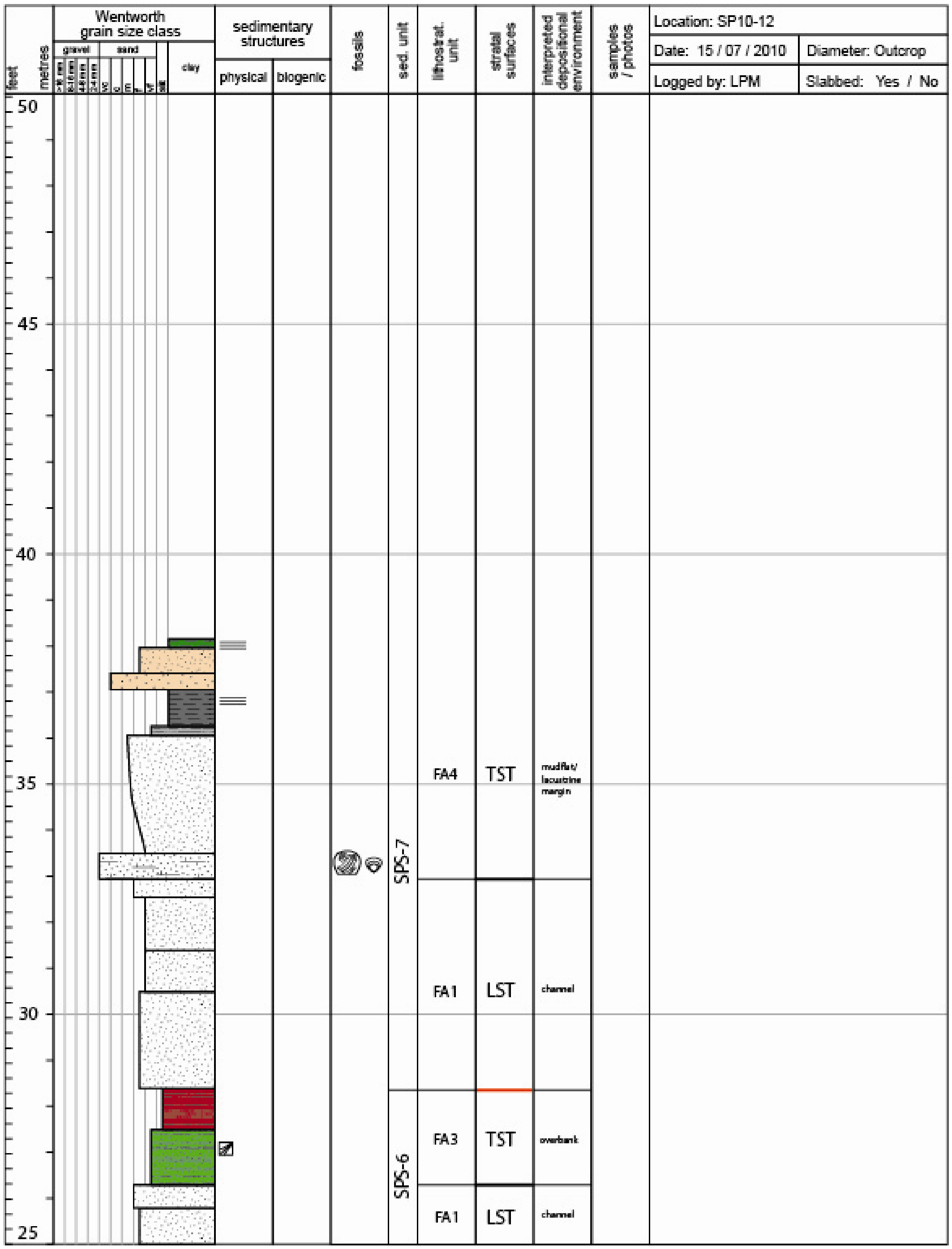
Location: SP10-12
Date: 15 / 07 / 2010
Diameter: Outcrop
Logged by: LPM
Slabbed: Yes / No
feet
metres
Wentworth grain size class
gravel
sand
clay
sedimentary structures
physical
biogenic
fossils
sed. unit
lithostrat. unit
stratal surfaces
interpreted depositional environment
samples / photos
50
45
40
35
30
25
SPS-7
SPS-6
FA4
TST
mudflat/ lacustrine margin
FA1
LST
channel
FA3
TST
overbank
FA1
LST
channel

APPENDIX B

Cross Sections

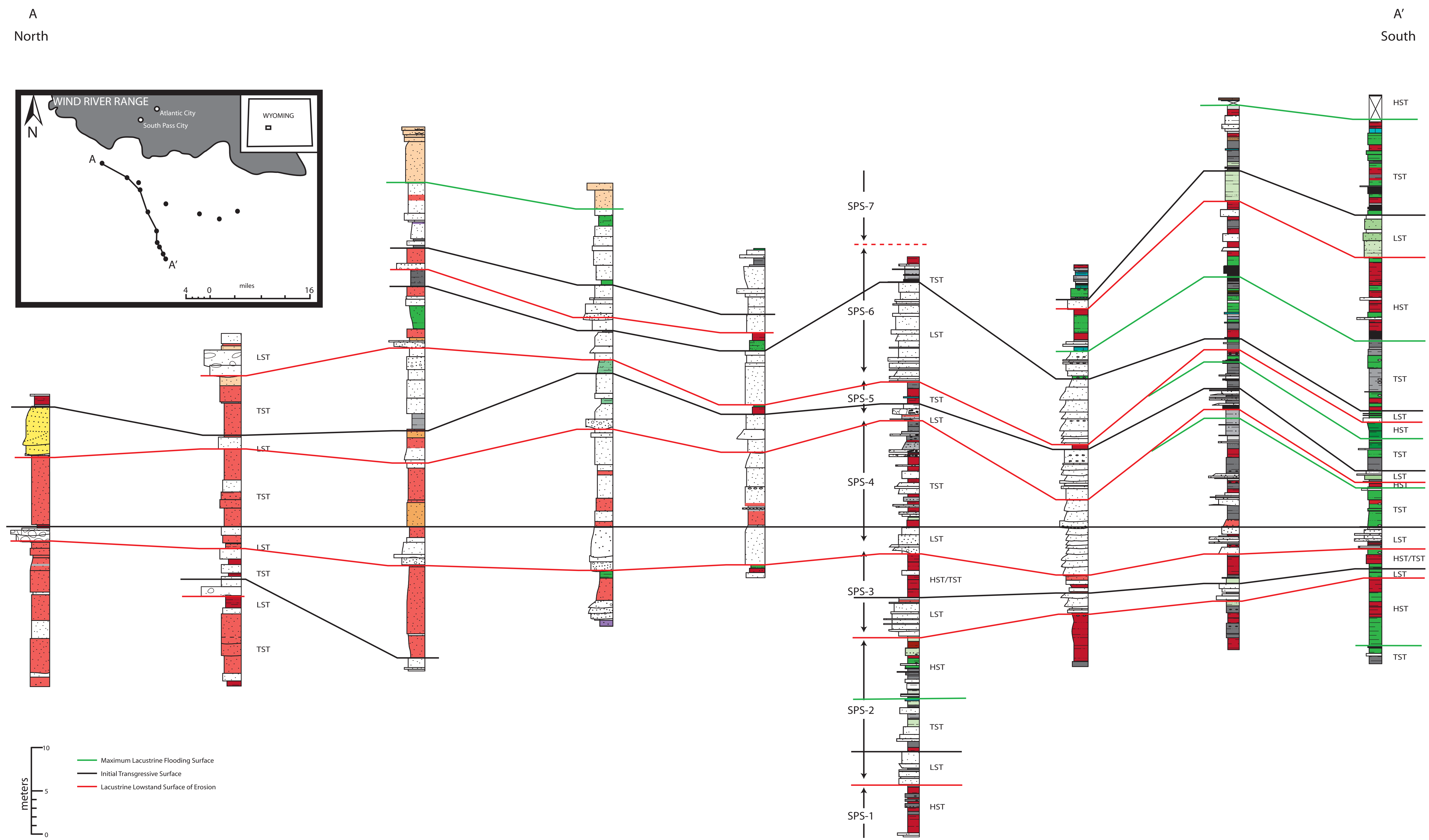

A
North
A'
South
WIND RIVER RANGE
Atlantic City
South Pass City
WYOMING
N
A
A'
4
0
miles
16
SPS-7
SPS-6
SPS-5
SPS-4
SPS-3
SPS-2
SPS-1
HST
TST
LST
HST/TST
meters
10
5
0
Maximum Lacustrine Flooding Surface
Initial Transgressive Surface
Lacustrine Lowstand Surface of Erosion

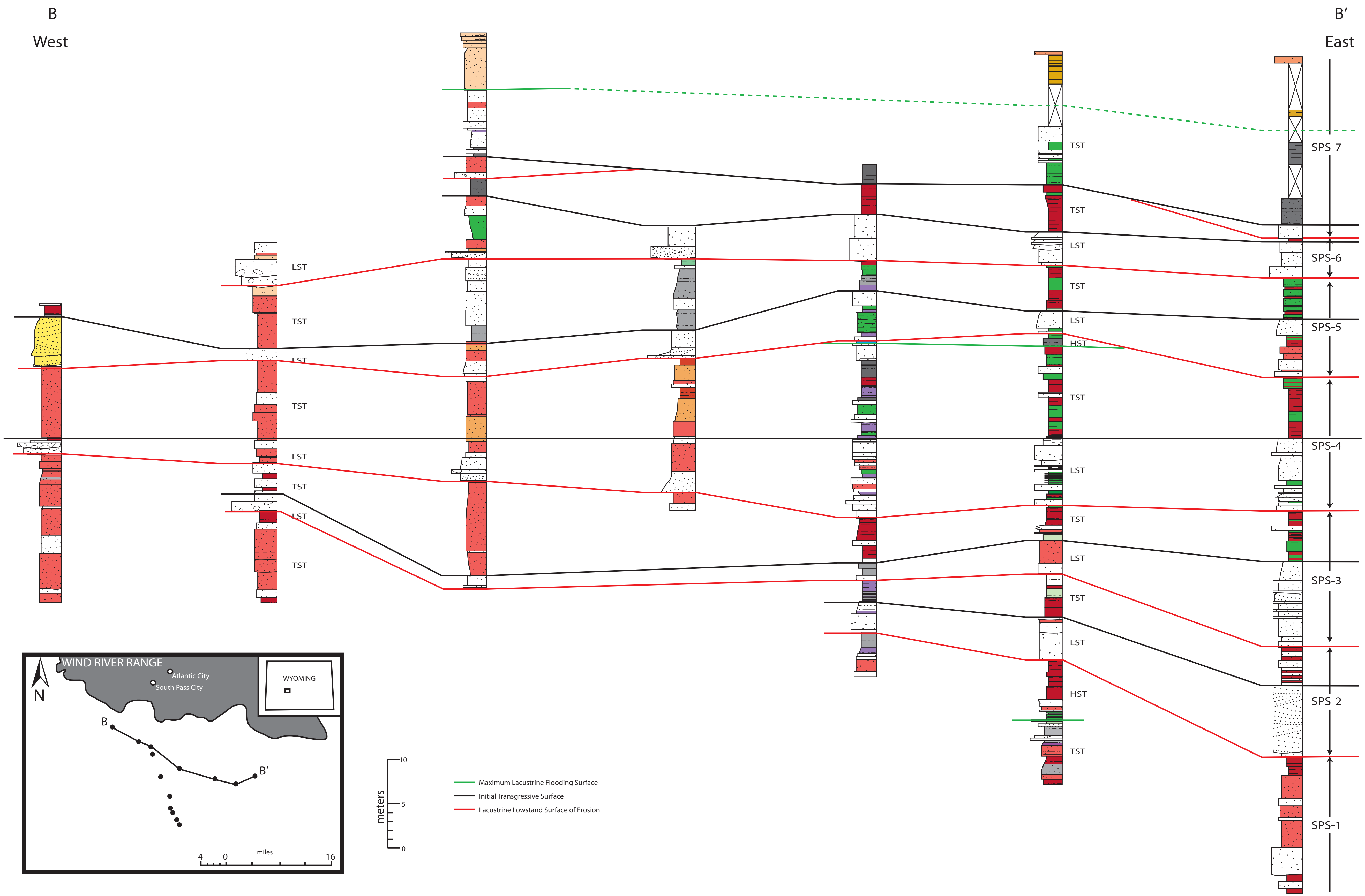
B
West
B'
East
LST
TST
HST
SPS-7
SPS-6
SPS-5
SPS-4
SPS-3
SPS-2
SPS-1
WIND RIVER RANGE
Atlantic City
South Pass City
N
WYOMING
B
B'
4 0 miles 16
meters
10
5
0
Maximum Lacustrine Flooding Surface
Initial Transgressive Surface
Lacustrine Lowstand Surface of Erosion

APPENDIX C

ICP-MS Geochemical Data

Sample	Li	Be	B	Mg	Al	P	K	Ca	Ti	V	Cr	Fe	Mn
SP09-01	ppm	ppm	ppm	ppm	ppm	ppm	ppm	ppm	ppm	ppm	ppm	ppm	ppm
0.5	61.7	1.7	<DL	16437	77105	720	22551	13288	4233	109	147	40968	327
1.5	81.2	3.5	<DL	18356	79897	574	23961	10808	4784	111	170	49563	320
2.7	86.7	2.6	<DL	17843	79546	602	22401	11298	4795	338	161	38974	336
3.6	79.8	1.6	<DL	18316	78320	674	20480	12458	4374	173	169	38173	350
4.45	50.0	2.9	<DL	16892	70500	610	21768	16534	3882	76.2	110	41682	381
5.75	64.1	2.4	<DL	22381	77161	805	22878	14374	4498	114	170	60461	554
7.05	38.0	1.3	<DL	13774	59036	828	16916	64888	2917	84.0	94.7	27670	1576
8.15	44.7	1.6	<DL	13574	63990	728	17492	45150	3325	91.3	93.2	30726	690
9.1	46.5	2.5	<DL	17727	69429	1064	21438	13824	3747	91.9	116	44110	317
9.8	30.6	2.1	<DL	23066	55817	968	16418	59664	3241	93.5	93.0	29044	899
10.2	71.3	1.3	<DL	18650	78700	471	23254	11890	3981	103	137	56360	289
10.8	52.4	2.2	<DL	11757	68277	328	20898	13946	2987	76.2	97.3	26714	235
11.9	40.7	1.8	<DL	10906	60907	377	18866	12214	2524	62.5	77.3	25273	214
12.85	16.3	1.6	<DL	10102	51593	676	16079	63537	1501	37.9	43.7	12738	865
14.05	22.1	1.5	<DL	7296	57183	220	20190	12778	1900	39.0	44.5	15037	127
14.75	28.0	1.4	<DL	8893	59526	358	21200	13926	2136	56.2	63.2	19632	190
15.65	45.7	1.2	<DL	18719	64159	986	20436	19321	3149	82.4	106	34670	352
16.6	23.8	1.5	<DL	10109	54408	330	19922	16969	2046	42.6	55.4	18129	275
17.3	62.2	1.9	<DL	15299	71942	591	17981	14754	3641	82.9	117	32940	335
18.55	88.6	2.3	<DL	21764	80776	575	21947	10048	4741	117	179.1	54072	448
19.65	36.6	0.8	<DL	16585	50903	703	15294	93922	2628	76.7	93.1	26823	1557
20.9	29.4	1.3	30	11401	63468	1178	18900	14882	3098	63.4	98.3	30968	123
22.1	59.4	1.8	8	18342	77446	279	25785	8865	4715	104	199	62539	319
22.7	43.3	2.7	<DL	15055	66135	435	21673	17957	3428	119	144	28517	202
24.45	15.8	1.6	<DL	6447	48168	174	25839	16977	1295	45.0	45.6	10687	152
25.5	13.9	1.8	<DL	4533	46919	122	27052	10824	1278	44.2	44.0	9998	98.4
27.95	30.5	2.2	9	9597	51707	307	22396	12816	2299	65.2	68.3	24786	81.5
28.95	46.1	2.2	10	13335	70138	1155	21914	15239	3501	66.2	115	36258	236

Sample	Co	Cu	Zn	Ga	Ge	As	Se	Rb	Sr	Y	Zr	Nb	Mo	Ru	Pd
SP09-01	ppm	ppm	ppm	ppm	ppm	ppm	ppm	ppm	ppm	ppm	ppm	ppm	ppm	ppm	ppm
0.5	36.0	59.8	131	23.3	1.77	11.6	1.2	107	342	26.8	141	11.4	1.43	0.03	5.62
1.5	36.7	74.6	133	25.6	2.15	34.6	3.0	129	272	23.9	127	12.1	1.04	<DL	4.74
2.7	38.9	48.5	150	27.8	1.59	9.67	2.3	119	311	21.8	134	11.6	1.10	<DL	5.17
3.6	34.3	50.5	133	26.2	1.53	4.77	1.1	114	317	18.4	147	11.5	0.68	<DL	5.45
4.45	30.5	36.0	98.1	22.0	1.88	5.54	1.9	116	347	17.8	127	11.4	0.68	0.03	4.87
5.75	46.6	50.4	118	24.9	1.76	23.7	0.8	123	484	25.1	99.3	10.9	0.97	<DL	4.27
7.05	37.4	28.2	79.8	17.6	1.02	6.55	<DL	83.9	405	17.7	68.1	7.10	0.86	0.09	3.09
8.15	24.9	25.2	82.7	18.9	1.16	8.63	<DL	85.8	391	16.9	85.1	9.08	0.66	0.11	3.53
9.1	33.1	36.8	116	23.3	1.59	62.6	0.7	105	312	20.5	134	13.5	2.89	0.07	5.29
9.8	27.2	33.8	106	16.8	1.09	9.74	0.6	78.6	502	18.8	133	9.93	1.31	0.25	5.72
10.2	34.0	39.3	104	24.1	1.94	55.9	0.4	132	299	17.2	102	12.1	1.09	0.02	4.38
10.8	41.6	22.5	76.5	19.8	1.29	12.2	<DL	94.3	399	11.7	85.7	8.91	1.19	0.03	3.67
11.9	28.5	19.4	66.2	18.0	1.14	8.61	<DL	83.4	326	10.8	84.0	5.82	0.62	<DL	3.41
12.85	29.6	11.0	83.6	13.0	0.92	14.4	<DL	58.3	514	10.7	90.5	5.98	1.42	0.17	3.60
14.05	22.3	10.1	36.1	15.5	1.06	25.1	0.4	70.2	390	6.38	89.4	4.94	1.01	<DL	3.34
14.75	37.3	13.3	49.5	17.0	1.03	8.85	<DL	81.9	400	6.75	80.2	5.81	1.20	0.02	2.97
15.65	39.6	31.8	76.3	19.3	1.07	23.0	2.4	87.9	402	18.9	101	7.98	0.95	0.01	3.78
16.6	40.4	12.7	42.9	14.8	1.00	9.00	5.9	73.3	365	12.6	102	5.11	1.21	<DL	3.80
17.3	35.1	30.8	83.6	20.4	1.31	13.7	0.3	86.9	361	16.5	130	8.50	0.47	<DL	5.00
18.55	41.0	52.1	128	27.4	1.56	31.8	0.9	117	247	16.0	119	10.7	0.56	<DL	4.57
19.65	29.7	25.3	68.2	15.4	0.95	110	1.1	70.3	484	18.5	88.4	6.47	0.82	0.25	3.46
20.9	24.7	19.8	70.0	19.8	1.52	9.84	<DL	85.7	358	27.7	131	9.04	2.39	<DL	5.54
22.1	30.5	48.3	145	28.7	2.81	18.9	0.9	140	245	21.5	124	12.0	1.18	<DL	5.25
22.7	23.3	30.4	99.8	23.0	1.38	23.9	<DL	107	428	19.1	111	8.24	0.89	<DL	4.56
24.45	46.5	9.77	36.3	15.5	1.13	9.07	<DL	110	355	9.43	53.9	4.27	2.02	<DL	2.10
25.5	34.8	7.15	47.9	16.1	1.07	11.2	1.1	107	300	9.38	47.3	3.64	1.57	<DL	1.85
27.95	37.0	16.8	56.2	18.6	1.66	5.97	<DL	94.5	339	12.0	109	6.72	1.40	<DL	4.47
28.95	29.7	30.3	87.5	22.5	1.89	44.0	<DL	107	386	23.5	156	8.75	0.92	<DL	6.13

Sample	Ag	Cd	Sn	Sb	Te	Cs	Ba	La	Ce	Pr	Nd	Sm	Eu	Gd	Tb	Dy
SP09-01	ppm	ppm	ppm	ppm	ppm	ppm	ppm	ppm	ppm	ppm	ppm	ppm	ppm	ppm	ppm	ppm
0.5	1.61	0.10	3.56	0.53	<DL	7.55	663	50.8	109	11.9	44.0	8.68	2.22	7.19	0.88	5.32
1.5	0.87	0.09	3.26	0.54	<DL	9.25	516	57.0	114	13.0	48.1	8.73	2.11	6.96	0.80	4.95
2.7	0.67	0.37	3.38	0.28	<DL	8.99	609	60.9	117	13.5	50.4	9.05	2.22	7.29	0.80	4.83
3.6	0.41	0.21	3.19	0.20	<DL	8.64	638	57.4	108	12.6	45.3	7.92	1.97	6.05	0.65	3.94
4.45	0.56	0.26	2.81	0.45	<DL	8.87	539	46.9	89.7	10.5	38.0	6.84	1.73	5.42	0.63	3.73
5.75	0.39	0.12	2.72	0.55	<DL	9.15	568	58.4	119.6	13.6	51.0	9.63	2.20	8.03	0.92	5.42
7.05	0.26	0.26	1.54	0.17	<DL	5.97	521	33.8	62.0	7.67	29.0	5.47	1.47	4.75	0.55	3.44
8.15	0.37	0.16	1.59	0.20	<DL	6.21	553	37.0	69.8	8.52	31.7	5.78	1.54	4.78	0.55	3.32
9.1	2.00	0.24	3.92	1.28	<DL	7.05	477	43.0	87.1	10.0	36.4	6.92	1.79	5.52	0.67	3.95
9.8	1.48	0.48	2.65	0.62	<DL	5.49	436	38.0	72.7	8.50	31.6	5.98	1.52	4.97	0.58	3.58
10.2	0.69	0.07	2.49	0.69	<DL	8.57	510	50.1	96.6	11.4	42.0	7.55	1.83	5.97	0.66	3.93
10.8	0.40	0.07	1.87	0.23	<DL	5.36	2366	34.6	59.3	7.28	28.1	4.92	1.87	3.84	0.41	2.49
11.9	0.27	<DL	1.56	0.15	<DL	4.58	669	26.0	47.5	5.64	21.1	3.72	1.14	3.06	0.35	2.17
12.85	0.54	0.40	1.49	0.62	<DL	2.14	633	17.7	32.6	3.76	14.0	2.67	0.91	2.19	0.29	1.79
14.05	0.36	0.07	1.45	0.48	<DL	2.49	738	18.4	34.1	4.06	14.2	2.57	0.91	1.95	0.24	1.38
14.75	0.30	0.16	1.81	0.39	<DL	3.60	990	22.4	37.6	4.59	16.3	2.86	1.06	2.21	0.24	1.42
15.65	0.42	0.18	2.06	0.41	<DL	5.85	632	35.4	71.0	8.32	30.7	5.86	1.58	4.83	0.58	3.60
16.6	0.24	0.16	1.49	0.28	<DL	2.92	892	25.0	46.3	5.60	20.3	3.71	1.17	3.15	0.40	2.40
17.3	0.26	0.12	1.95	0.30	<DL	6.30	508	35.3	70.3	8.11	30.9	5.67	1.61	4.91	0.57	3.52
18.55	0.29	0.14	3.06	0.42	<DL	10.6	534	49.7	91.5	10.9	39.8	7.13	1.75	5.24	0.60	3.55
19.65	0.24	0.61	1.59	0.38	<DL	5.49	441	33.8	65.1	7.42	27.9	5.20	1.36	4.43	0.55	3.38
20.9	1.21	0.15	2.99	1.24	<DL	5.53	443	33.6	54.2	7.69	29.4	5.91	1.68	5.98	0.76	4.59
22.1	0.71	0.13	3.95	0.84	<DL	10.9	504	62.1	113	13.8	51.3	9.00	2.20	7.50	0.85	4.78
22.7	0.50	0.14	3.35	0.34	<DL	7.37	600	36.2	37.8	7.72	29.3	5.78	1.66	5.15	0.62	3.77
24.45	0.27	0.08	1.65	0.26	<DL	2.88	753	18.4	23.6	3.51	13.1	2.40	0.85	2.12	0.27	1.83
25.5	0.23	0.10	1.27	0.22	<DL	2.68	824	20.1	34.5	4.23	15.1	3.01	0.86	2.39	0.30	1.91
27.95	0.29	0.15	2.64	0.36	<DL	4.17	705	28.4	48.7	6.20	22.6	3.97	1.18	3.36	0.39	2.48
28.95	0.33	<DL	2.28	0.38	<DL	6.36	699	42.7	82.2	9.51	36.2	6.89	1.78	5.91	0.71	4.37

Sample	Ho	Er	Tm	Yb	Lu	Hf	Ta	W	Re	Os	Pt	Au	Tl	Pb	Th	U
SP09-01	ppm	ppm	ppm	ppm	ppm	ppm	ppm	ppm	ppm	ppm	ppm	ppm	ppm	ppm	ppm	ppm
0.5	1.04	2.86	0.409	2.50	0.37	4.49	1.97	34.4	0.004	0.61	0.07	0.66	1.06	47.3	13.4	2.51
1.5	0.98	2.64	0.388	2.47	0.36	4.16	1.98	30.2	0.014	0.46	0.03	0.65	1.05	23.9	17.7	2.11
2.7	0.90	2.43	0.341	2.16	0.32	4.51	1.94	65.8	0.007	0.36	0.05	0.34	1.07	27.6	16.7	9.11
3.6	0.76	2.13	0.308	2.08	0.29	4.78	1.74	56.8	<DL	0.32	0.05	0.27	0.93	32.1	16.5	8.99
4.45	0.73	2.06	0.299	1.88	0.29	4.06	1.74	47.7	0.015	0.32	0.04	0.26	0.87	22.5	13.9	3.46
5.75	1.03	2.83	0.402	2.72	0.38	3.98	1.80	32.6	0.009	0.32	0.04	0.20	0.92	26.8	17.0	3.01
7.05	0.69	1.92	0.271	1.74	0.26	2.69	1.74	84.2	0.014	0.22	0.04	0.17	0.71	19.7	9.34	2.85
8.15	0.65	1.82	0.266	1.67	0.24	3.32	1.52	24.5	<DL	0.21	0.03	0.14	0.68	21.3	10.5	2.92
9.1	0.81	2.12	0.362	1.92	0.34	4.65	2.78	39.9	0.094	2.13	0.14	1.87	1.91	20.7	12.4	2.95
9.8	0.72	2.05	0.299	1.91	0.29	4.33	1.93	18.2	0.004	0.92	0.06	1.08	1.00	19.6	10.4	3.92
10.2	0.71	1.97	0.278	1.88	0.28	4.01	2.21	16.4	0.013	0.92	0.11	0.66	1.10	22.6	14.4	2.01
10.8	0.47	1.35	0.196	1.34	0.20	3.38	2.38	74.1	0.009	1.23	0.05	0.38	0.76	22.7	9.21	2.45
11.9	0.42	1.18	0.166	1.17	0.18	3.22	1.48	47.3	0.009	0.38	0.04	0.26	0.57	18.7	7.58	1.55
12.85	0.37	1.10	0.167	1.04	0.17	3.34	2.11	130	0.020	0.96	0.09	0.67	0.78	17.0	5.67	1.54
14.05	0.25	0.79	0.122	0.79	0.13	3.24	1.42	21.5	0.005	0.53	0.04	0.37	0.64	18.8	4.80	1.20
14.75	0.28	0.78	0.124	0.87	0.13	2.90	1.94	60.2	0.017	0.45	0.03	0.31	0.69	21.0	5.79	1.27
15.65	0.69	1.98	0.268	1.74	0.26	3.51	1.78	125	0.007	0.34	0.04	0.27	0.82	18.6	10.3	2.01
16.6	0.48	1.41	0.217	1.44	0.21	3.50	1.83	97.1	0.013	0.33	0.05	0.27	0.59	19.0	6.98	1.41
17.3	0.65	1.85	0.259	1.72	0.27	4.53	1.41	39.7	0.005	0.25	0.07	0.17	0.58	21.1	10.3	1.96
18.55	0.64	1.86	0.257	1.76	0.27	4.25	1.48	42.1	<DL	0.21	0.05	0.16	0.78	22.1	11.2	2.21
19.65	0.66	1.88	0.299	1.73	0.26	2.97	1.26	75.0	<DL	0.22	0.03	0.11	0.50	18.6	8.02	2.16
20.9	0.99	2.69	0.411	2.30	0.36	4.49	2.19	20.3	0.072	1.90	0.12	1.56	1.64	26.2	6.17	1.75
22.1	0.88	2.44	0.351	2.32	0.32	3.97	1.99	27.0	0.023	0.84	0.07	0.66	1.06	20.8	14.8	1.62
22.7	0.75	2.08	0.295	1.94	0.29	3.88	1.60	28.5	<DL	0.53	0.04	0.43	0.86	18.3	3.83	2.90
24.45	0.37	1.04	0.160	1.08	0.16	2.01	2.16	71.8	0.010	0.41	0.02	0.33	0.73	26.9	3.37	0.96
25.5	0.37	1.02	0.148	1.02	0.14	1.79	1.59	67.0	<DL	0.39	0.04	0.25	0.70	20.4	6.63	1.18
27.95	0.48	1.42	0.224	1.49	0.21	3.77	1.70	106	0.004	0.33	0.04	0.19	0.63	18.0	6.45	1.55
28.95	0.86	2.48	0.341	2.25	0.32	4.99	1.48	56.2	<DL	0.32	0.08	0.25	0.75	21.6	10.9	4.47

Sample	Li	Be	B	Mg	Al	P	K	Ca	Ti	V	Cr	Fe	Mn
SP09-01	ppm	ppm	ppm	ppm	ppm	ppm	ppm	ppm	ppm	ppm	ppm	ppm	ppm
29.95	37.0	1.7	8	11450	62114	393	17007	36375	2963	50.6	92.6	28647	396
30.9	36.0	2.4	6	13465	66085	1074	18701	18342	3215	80.2	109	30041	268
32.55	48.7	2.4	34	15933	76064	774	24031	12050	4357	111	178	52436	320
33.85	44.8	2.3	11	15428	70468	638	21431	15850	3635	96.2	144	38198	389
35.15	23.3	1.7	<DL	9730	47781	2053	13879	107926	2482	57.9	91.5	25866	2595
36.55	56.1	2.2	10	18123	74622	368	23644	12477	4279	97.0	173	57466	360
37.7	36.6	1.6	9	12822	65927	557	20007	13767	3326	93.8	126	36657	244
38.6	38.7	2.3	5	13488	73456	185	21993	12358	3874	99.5	145	48043	268
39.65	47.4	1.9	10	14809	76850	172	21814	10644	4424	106	163	57018	256
40.35	28.3	1.9	<DL	8048	63944	140	23127	12516	2390	74.1	86.5	22247	174
41.41	51.1	2.5	<DL	13635	72188	526	22707	12106	4031	86.7	140	51505	321
42.2	38.1	1.4	<DL	9358	60940	407	19997	14832	3047	75.9	85.4	23241	239
43.05	41.8	1.9	<DL	13675	60275	600	21699	20298	1903	68.5	94.6	31067	404
44.05	19.1	1.1	<DL	6676	46908	374	21390	74876	999	33.2	45.6	14058	1143
44.85	34.2	1.9	<DL	7302	57279	460	21381	12413	1802	63.6	75.4	20404	233
45.75	65.4	2.2	<DL	14700	70056	447	22104	11057	2875	93.9	146	46875	325
47.1	37.5	1.4	<DL	37278	50717	1212	20053	65337	2617	73.9	84.4	31440	784
48.55	25.5	1.6	<DL	7653	58689	315	25252	18621	1941	56.6	58.0	18259	272
49.55	41.0	2.0	<DL	10600	67324	503	23966	16421	2895	78.9	99.4	29136	332
49.95	29.9	2.1	<DL	8484	64136	433	23113	15280	2502	70.7	75.8	22710	213
51.65	37.7	1.7	<DL	9864	70399	356	23431	12264	3420	66.7	101	37042	220
52.7	36.8	2.2	<DL	8699	64580	351	23602	13142	2930	138	93.0	27029	267
54.1	16.7	1.8	<DL	4110	56318	155	25399	11140	1156	152	35.7	12367	112
55.85	62.5	2.7	<DL	13732	73770	184	26190	10853	3719	102	130	38408	307
56.95	26.7	1.8	<DL	7174	55799	274	20117	11366	2116	94.1	72.4	21880	230
62.05	14.8	1.3	<DL	4503	48396	193	20863	75988	1354	34.1	40.8	10760	1194
64.15	62.2	2.8	<DL	20051	72792	418	28674	17621	3340	107	108	36800	310
64.85	85.6	1.4	<DL	21692	81822	630	23042	11280	4146	119	163	40526	303

Sample	Co	Cu	Zn	Ga	Ge	As	Se	Rb	Sr	Y	Zr	Nb	Mo	Ru	Pd
SP09-01	ppm	ppm	ppm	ppm	ppm	ppm	ppm	ppm	ppm	ppm	ppm	ppm	ppm	ppm	ppm
29.95	27.7	33.1	72.7	18.9	1.52	21.4	<DL	78.0	417	17.9	133	7.33	0.89	<DL	5.09
30.9	35.1	28.1	80.9	20.2	1.44	12.3	1.4	86.3	470	22.0	132	7.37	0.86	<DL	5.01
32.55	35.9	50.0	117	25.3	1.91	23.4	0.8	118	358	23.8	142	11.3	2.04	<DL	5.94
33.85	32.0	37.3	105	22.7	1.61	22.1	3.4	105	369	19.6	108	8.70	1.02	<DL	4.64
35.15	22.7	20.9	56.8	14.2	1.00	44.9	<DL	60.4	506	19.4	111	4.06	0.87	0.16	4.74
36.55	34.3	50.7	123	26.0	2.03	20.4	0.6	118	316	18.1	123	10.8	0.87	0.06	4.94
37.7	37.5	25.1	78.9	21.1	1.57	17.2	8.8	90.7	539	16.1	124	8.12	2.83	<DL	5.86
38.6	30.9	31.4	163	23.2	2.09	13.4	2.4	102	348	17.8	127	9.32	0.79	<DL	4.97
39.65	33.6	37.0	106	25.1	2.49	17.2	1.1	103	345	19.9	131	10.9	0.69	<DL	5.23
40.35	25.8	15.0	60.4	18.8	1.12	6.04	2.9	91.5	355	10.3	90.0	6.12	1.12	<DL	3.64
41.41	32.5	34.4	106	24.5	2.24	15.1	2.9	105	332	19.2	157	12.2	2.98	<DL	5.45
42.2	30.0	19.1	72.7	20.5	1.32	8.82	2.7	90.9	419	14.2	133	6.95	1.58	<DL	5.00
43.05	32.7	24.5	77.6	20.9	1.36	11.0	1.2	94.2	457	15.4	107	6.39	1.05	<DL	3.95
44.05	28.3	12.3	36.7	13.8	0.92	3.76	<DL	76.2	445	8.84	49.2	3.33	0.90	<DL	1.82
44.85	33.0	19.4	59.7	18.8	1.23	5.81	0.6	86.6	386	10.8	110	5.41	0.94	<DL	4.08
45.75	33.4	35.0	95.9	24.1	1.49	11.4	29.0	104	310	13.9	134	7.83	0.67	<DL	5.01
47.1	20.9	28.3	76.2	16.5	2.63	7.82	11.1	80.2	750	14.8	113	6.66	0.47	<DL	4.20
48.55	44.2	16.2	50.0	17.4	1.29	8.51	3.9	97.4	389	11.5	100	5.99	1.53	<DL	3.82
49.55	33.8	25.6	82.7	21.2	1.44	11.4	1.6	102	356	16.6	124	7.37	0.89	<DL	4.69
49.95	29.3	24.0	62.1	19.3	1.29	6.22	0.6	87.8	417	13.2	134	8.66	2.57	<DL	5.39
51.65	26.4	30.7	71.9	21.6	1.64	11.0	29.7	100	353	19.1	137	9.43	1.14	<DL	5.59
52.7	36.7	20.1	71.0	19.9	1.30	19.5	3.6	90.7	400	17.0	114	7.55	1.23	<DL	4.48
54.1	75.1	10.2	30.8	15.7	0.94	6.37	5.8	84.4	372	6.62	49.0	4.46	2.13	<DL	1.95
55.85	32.8	31.1	91.0	23.6	1.47	11.3	8.3	98.0	330	15.3	119	9.59	0.63	<DL	4.71
56.95	35.6	16.9	53.3	16.0	1.04	14.0	3.6	77.6	334	15.2	96.2	5.63	0.98	<DL	3.81
62.05	33.1	10.1	32.2	13.3	0.85	5.78	0.7	76.1	379	10.4	68.5	4.50	1.00	<DL	2.78
64.15	27.5	55.2	111	24.4	1.58	7.22	6.5	129	271	16.7	95.0	12.4	1.02	<DL	4.01
64.85	28.6	36.9	188	27.1	1.79	5.81	2.0	142	277	12.0	132	14.2	2.57	0.06	4.94

Sample	Ag	Cd	Sn	Sb	Te	Cs	Ba	La	Ce	Pr	Nd	Sm	Eu	Gd	Tb	Dy
SP09-01	ppm	ppm	ppm	ppm	ppm	ppm	ppm	ppm	ppm	ppm	ppm	ppm	ppm	ppm	ppm	ppm
29.95	0.29	0.34	1.54	0.32	<DL	4.72	949	34.5	64.5	7.68	28.7	5.40	1.53	4.50	0.52	3.27
30.9	0.23	0.13	1.88	0.25	<DL	5.50	588	35.3	67.1	8.12	30.9	5.75	1.69	5.02	0.63	3.94
32.55	1.25	0.12	3.12	0.53	<DL	8.62	548	53.7	106	12.3	46.7	8.61	2.16	6.97	0.87	4.97
33.85	0.59	0.17	2.29	0.29	<DL	7.37	603	43.0	86.9	10.2	38.0	7.23	1.89	5.92	0.69	4.18
35.15	0.32	0.81	1.09	0.25	<DL	3.83	442	30.8	57.8	6.81	25.4	4.49	1.26	4.16	0.50	3.25
36.55	0.40	0.14	2.92	0.35	<DL	8.55	534	55.2	108	12.7	46.6	8.29	2.01	6.23	0.70	3.98
37.7	0.31	0.11	2.07	0.24	<DL	5.64	616	35.6	67.8	8.17	30.4	5.55	1.48	4.52	0.52	3.12
38.6	0.32	0.10	2.11	0.71	<DL	7.33	531	43.1	83.9	10.1	37.9	6.90	1.82	5.63	0.64	3.88
39.65	0.30	0.09	2.32	0.52	<DL	7.93	512	52.6	102	12.3	45.6	8.14	2.01	6.56	0.77	4.45
40.35	0.21	0.12	1.07	0.17	<DL	4.44	785	25.6	46.3	5.79	21.8	3.93	1.22	3.02	0.36	2.04
41.41	1.26	0.07	5.67	1.55	<DL	7.52	538	44.0	81.3	9.80	36.4	6.76	1.80	5.47	0.69	3.80
42.2	0.50	<DL	3.94	0.53	<DL	4.80	637	30.6	55.3	6.94	24.8	4.66	1.42	3.84	0.48	2.71
43.05	0.35	0.10	3.80	0.47	<DL	5.35	673	33.7	65.7	7.48	27.3	4.97	1.39	3.91	0.48	2.86
44.05	0.26	0.15	2.59	0.30	<DL	2.34	813	18.5	29.9	3.69	13.4	2.44	0.89	2.05	0.26	1.62
44.85	0.25	<DL	3.15	0.27	<DL	4.07	817	26.6	47.1	5.76	20.9	3.74	1.18	2.87	0.34	2.04
45.75	0.29	<DL	3.76	0.41	<DL	7.76	545	39.5	73.6	8.43	30.5	5.35	1.42	4.04	0.46	2.83
47.1	0.24	0.28	3.14	0.41	<DL	5.18	529	29.1	57.4	6.30	23.5	4.37	1.20	3.57	0.44	2.72
48.55	0.24	0.12	2.47	0.39	<DL	3.70	861	26.6	49.6	5.58	20.3	3.80	1.17	3.10	0.37	2.24
49.55	0.23	0.08	3.04	0.33	<DL	5.67	808	36.6	68.1	7.83	29.3	5.38	1.58	4.30	0.51	3.06
49.95	1.13	0.16	1.93	0.69	<DL	4.42	627	29.8	54.8	6.22	22.6	4.12	1.28	3.27	0.41	2.34
51.65	0.53	<DL	1.94	0.57	<DL	5.96	550	38.5	73.9	8.71	33.1	6.03	1.72	5.02	0.64	3.82
52.7	0.38	<DL	1.78	0.33	<DL	4.90	675	30.4	56.0	6.93	25.1	4.70	1.45	3.73	0.46	2.96
54.1	0.23	<DL	1.16	0.23	<DL	2.06	932	15.5	24.6	2.90	10.4	1.88	0.81	1.44	0.17	1.14
55.85	0.30	<DL	2.04	1.16	<DL	7.12	619	41.4	73.8	8.71	31.8	5.66	1.58	4.36	0.50	3.04
56.95	0.21	<DL	1.37	0.26	<DL	3.85	590	28.6	48.9	5.87	21.5	3.91	1.17	3.33	0.44	2.78
62.05	0.21	0.08	1.02	0.22	<DL	2.82	1004	17.8	30.4	3.59	13.0	2.31	0.91	1.98	0.25	1.70
64.15	0.34	0.17	2.58	0.76	<DL	7.46	473	55.5	115	11.9	43.2	7.67	1.78	5.76	0.62	3.66
64.85	1.50	0.87	4.67	1.82	<DL	11.0	661	44.0	85.2	9.29	31.5	5.22	1.32	3.74	0.45	2.43

Sample	Ho	Er	Tm	Yb	Lu	Hf	Ta	W	Re	Os	Pt	Au	Tl	Pb	Th	U
SP09-01	ppm	ppm	ppm	ppm	ppm	ppm	ppm	ppm	ppm	ppm	ppm	ppm	ppm	ppm	ppm	ppm
29.95	0.65	1.84	0.263	1.80	0.27	4.16	1.30	80.1	<DL	0.29	0.04	0.14	0.56	20.8	8.59	1.95
30.9	0.79	2.19	0.313	1.99	0.30	4.32	1.34	72.2	<DL	0.21	0.05	0.15	0.58	19.1	8.56	2.78
32.55	1.01	2.72	0.428	2.48	0.40	5.07	2.52	50.9	0.082	2.41	0.14	1.36	1.73	24.9	16.5	2.56
33.85	0.80	2.15	0.301	1.95	0.29	4.08	2.00	55.2	0.006	0.89	0.07	0.65	1.02	20.8	12.3	2.67
35.15	0.64	1.87	0.256	1.64	0.25	4.26	1.45	2.94	0.006	0.63	0.07	0.41	0.26	16.8	8.19	3.33
36.55	0.76	2.16	0.323	2.15	0.30	4.32	1.77	40.2	<DL	0.45	0.10	0.30	0.78	22.1	14.5	1.69
37.7	0.63	1.80	0.253	1.66	0.24	4.52	2.05	108	<DL	0.56	0.07	0.19	0.70	20.1	10.6	1.93
38.6	0.73	2.09	0.291	1.89	0.28	4.44	1.57	41.9	0.006	0.35	0.04	0.20	0.69	18.6	11.3	1.46
39.65	0.82	2.32	0.323	2.09	0.30	4.73	1.51	30.2	<DL	0.34	0.05	1.41	0.79	21.6	13.7	1.52
40.35	0.39	1.16	0.166	1.12	0.17	3.14	1.41	48.5	0.008	0.29	0.23	0.14	0.55	22.2	6.78	1.41
41.41	0.76	2.05	0.35	2.01	0.34	6.90	2.84	58.9	0.064	2.18	0.17	1.79	1.77	22.1	15.9	1.55
42.2	0.53	1.51	0.22	1.42	0.23	4.95	1.96	75.2	0.012	0.77	0.06	0.65	0.96	19.9	9.38	1.97
43.05	0.56	1.58	0.23	1.46	0.22	3.48	1.69	83.9	0.005	0.62	0.05	0.57	0.65	21.2	9.49	1.37
44.05	0.32	0.94	0.14	0.88	0.12	1.78	1.21	147	0.010	0.48	<DL	0.37	0.59	16.9	4.95	0.89
44.85	0.39	1.08	0.18	1.08	0.17	3.54	1.70	95.6	0.008	0.37	0.04	0.26	0.41	21.3	7.62	1.37
45.75	0.54	1.54	0.22	1.46	0.21	4.36	1.38	47.4	0.108	0.29	0.28	0.20	0.55	22.2	10.9	1.31
47.1	0.53	1.44	0.21	1.46	0.21	3.37	1.03	45.1	0.022	0.24	0.06	0.16	0.55	18.0	8.09	1.96
48.55	0.43	1.26	0.19	1.22	0.19	3.40	1.86	140	0.018	0.18	0.04	0.13	0.58	22.6	6.99	1.67
49.55	0.61	1.67	0.24	1.60	0.23	4.00	1.43	80.8	0.004	0.18	0.05	0.17	0.59	24.1	9.64	1.80
49.95	0.50	1.42	0.25	1.42	0.25	4.56	2.47	109	0.059	2.18	0.09	1.44	1.49	24.5	9.78	2.40
51.65	0.71	1.98	0.30	1.87	0.28	4.78	2.05	77.9	0.013	0.90	0.09	0.65	0.88	19.9	12.4	1.48
52.7	0.59	1.64	0.25	1.61	0.23	3.84	1.95	53.0	0.020	0.49	0.03	0.38	0.61	21.2	9.27	1.77
54.1	0.24	0.69	0.10	0.65	0.11	1.80	2.62	183	0.028	0.43	<DL	0.30	0.60	21.1	4.81	1.15
55.85	0.58	1.66	0.24	1.60	0.22	4.10	1.65	40.4	0.004	0.32	0.19	0.25	0.64	22.2	10.7	1.58
56.95	0.54	1.63	0.24	1.55	0.23	3.40	1.81	82.7	0.015	0.27	0.05	0.20	0.38	18.9	7.92	1.62
62.05	0.37	0.97	0.15	0.93	0.14	2.29	1.60	146	0.006	0.23	0.03	0.17	0.48	17.0	4.05	0.79
64.15	0.64	1.81	0.26	1.73	0.25	3.31	1.59	43.9	0.013	0.21	0.03	0.11	0.72	30.3	17.9	2.71
64.85	0.54	1.42	0.282	1.49	0.29	4.78	2.93	27.3	0.103	2.03	0.13	1.58	2.14	26.0	15.1	3.97

Sample	Li	Be	B	Mg	Al	P	K	Ca	Ti	V	Cr	Fe	Mn
SP09-02	ppm	ppm	ppm	ppm	ppm	ppm	ppm	ppm	ppm	ppm	ppm	ppm	ppm
0.1	38.0	1.9	<DL	17974	57121	1068	23837	65800	3202	124	100	41028	696
1.0	48.0	2.9	<DL	18938	65057	992	25358	42722	3800	108	126	47408	525
2.0	42.3	2.3	<DL	19536	58476	779	24969	67807	3283	109	113	42469	811
3.0	60.2	3.3	<DL	13425	65945	539	18722	36118	3858	210	127	59456	281
4.0	32.9	1.9	<DL	10768	61322	891	21180	14584	2409	74.5	77.5	32225	177
5.0	93.8	2.5	<DL	14884	85499	358	21069	18802	5127	160	180	50708	311
6.0	36.4	2.4	<DL	11449	62094	1143	18595	19332	2813	113	83.7	23873	250
7.0	27.8	1.7	<DL	9945	63545	241	20596	9220	2690	89.3	87.3	34085	138
8.0	50.7	2.0	552	23894	67875	790	17321	58192	3791	105	125	41760	548
8.8	58.1	2.5	502	13207	76617	1086	20505	4414	4075	157	140	55233	174
9.5	53.5	1.8	427	16034	76546	766	27591	6927	4690	104	154	62505	350
10.0	49.4	1.5	423	13381	64911	833	21589	108849	4009	168	136	51979	598
11.0	56.7	2.2	414	13218	71551	765	21309	65875	4236	173	156	54472	583
12.0	19.7	1.7	390	3826	53757	361	21997	41658	1528	27.0	41.3	9990	256
13.0	47.2	1.9	386	8911	68316	438	19132	10604	3317	84.3	103	26487	218
14.0	33.3	1.4	353	8563	51085	1729	16102	120538	2391	45.1	75.3	30049	758
15.1	76.2	2.1	331	14762	76218	330	21981	6987	4360	113	164	44368	299
16.0	45.0	2.4	382	10987	70208	1532	19200	14520	3729	79.8	113	31852	262
17.0	17.8	1.3	372	4242	45778	453	15488	138963	1707	28.7	43.1	11504	924
19.3	26.4	2.1	362	6405	57802	324	22810	8769	1685	33.9	55.6	14412	132
20.3	36.6	1.6	359	14730	60155	552	18849	41689	2673	55.3	75.7	25420	325
21.5	40.5	1.8	337	36677	53856	215	14851	97251	2771	56.4	79.2	37045	984
23.3	29.1	1.4	327	35897	46884	571	15822	109569	2282	69.2	50.5	20177	1054
24.6	28.7	1.7	306	15709	55527	434	26569	30891	1906	53.3	57.6	27459	355
25.3	17.0	1.5	283	9199	47804	585	13950	134176	1803	26.7	42.2	11539	529
26.8	60.8	2.1	<DL	14695	63795	539	22114	17344	3670	103	8.27	28938	199
27.6	9.4	1.6	<DL	2550	33981	245	18382	92867	624	13.5	0.88	5101	639
28.9	20.7	1.7	<DL	7418	49669	408	19951	18452	1870	36.9	2.25	12455	112
29.7	59.5	2.3	<DL	14969	63822	326	29913	8151	3916	124	6.93	44444	32
30.3	56.0	3.4	<DL	25615	55571	875	22195	56618	3037	99.5	10.8	34745	798

Sample	Co	Cu	Zn	Ga	Ge	As	Se	Rb	Sr	Y	Zr	Nb	Mo	Ru	Pd
SP09-02	ppm	ppm	ppm	ppm	ppm	ppm	ppm	ppm	ppm	ppm	ppm	ppm	ppm	ppm	ppm
0.1	24.4	29.7	97.1	18.8	1.44	17.2	9.1	111	389	18.1	73.3	9.93	3.52	0.17	2.85
1.0	30.1	53.3	115	23.1	1.84	29.0	2.8	120	311	26.5	91.4	14.3	5.57	0.22	3.82
2.0	28.2	36.9	98.1	19.4	1.43	28.9	31.8	108	324	22.6	84.6	11.2	6.28	0.17	3.29
3.0	29.7	48.6	111	22.8	1.78	132	30.7	108	276	25.2	106	12.2	12.1	0.04	4.23
4.0	106	60.3	65.7	17.6	1.53	24.9	<DL	92.7	353	25.0	99.1	7.68	3.08	0.02	4.10
5.0	31.1	41.7	138	28.8	1.71	38.0	4.1	123	197	15.5	102	13.8	3.61	<DL	4.09
6.0	42.1	20.4	71.4	17.7	1.18	4.43	4.5	84.4	337	15.9	105	7.57	2.50	<DL	4.21
7.0	35.7	21.4	75.2	18.8	1.28	48.9	4.0	93.1	242	16.0	87.6	8.22	5.30	<DL	3.41
8.0	27.3	69.2	56.9	24.0	1.54	49.5	<DL	107	307	26.4	85.5	13.6	6.48	0.14	3.76
8.8	26.0	52.9	62.0	26.7	1.99	109	<DL	134	318	25.6	94.9	12.6	3.86	<DL	3.92
9.5	28.2	43.3	67.4	28.2	2.12	65.8	<DL	149	192	26.7	97.8	13.4	5.41	<DL	4.15
10.0	23.3	71.0	60.1	23.7	1.68	11.4	<DL	117	237	26.7	99.0	10.8	5.06	0.03	4.26
11.0	31.8	87.0	75.3	24.9	1.45	18.1	<DL	116	288	24.8	120	10.7	6.11	<DL	5.13
12.0	30.5	14.0	13.8	14.6	0.96	10.2	<DL	89.0	350	14.8	73.2	4.57	5.02	<DL	2.82
13.0	31.8	23.1	34.0	21.0	1.23	4.94	<DL	96.7	322	13.8	136	7.70	5.77	<DL	5.20
14.0	27.6	23.7	33.3	15.0	1.00	6.92	<DL	74.5	372	17.2	115	5.77	5.60	<DL	4.81
15.1	40.1	41.2	57.3	26.0	1.53	6.15	<DL	116	288	17.9	141	10.5	2.32	<DL	5.76
16.0	39.8	30.1	41.3	21.8	1.37	3.65	<DL	98.4	354	20.4	151	11.1	3.57	<DL	6.21
17.0	31.9	11.3	16.5	13.3	0.91	1.72	<DL	66.4	420	15.1	85.5	6.15	2.29	<DL	3.47
19.3	45.2	12.2	17.0	17.4	1.18	0.78	<DL	101	313	7.54	66.0	5.63	2.27	<DL	2.74
20.3	21.7	22.9	28.2	17.5	1.28	4.49	<DL	88.2	548	15.2	130	7.17	1.44	<DL	5.26
21.5	23.4	26.5	45.0	18.0	1.26	4.04	<DL	82.4	632	16.9	103	8.69	1.31	0.09	4.19
23.3	20.2	27.6	44.1	14.9	1.15	2.13	<DL	67.3	1080	20.4	108	6.50	1.28	0.07	4.47
24.6	23.7	22.9	22.4	17.5	1.32	3.68	<DL	101	347	14.5	60.5	6.10	1.07	<DL	2.40
25.3	16.7	14.1	20.4	12.8	0.88	1.59	<DL	56.1	529	11.1	97.2	4.86	1.09	<DL	3.97
26.8	26.9	33.9	107	21.9	1.55	7.03	1.7	106	410	14.5	129	10.3	2.00	<DL	4.79
27.6	33.9	9.25	22.2	9.06	0.75	2.38	<DL	59.5	395	12.8	26.8	2.41	1.30	0.19	0.90
28.9	20.4	11.0	39.3	15.0	1.12	5.94	3.5	70.1	407	18.9	83.6	5.36	1.59	<DL	2.97
29.7	30.4	47.6	105	24.2	1.84	11.4	<DL	122	333	13.1	93.1	13.4	2.42	<DL	3.22
30.3	22.7	34.3	93.6	20.2	1.45	7.87	1.8	107	409	22.4	75.9	9.79	2.55	<DL	2.54

Sample	Ag	Cd	Sn	Sb	Te	Cs	Ba	La	Ce	Pr	Nd	Sm	Eu	Gd	Tb	Dy
SP09-02	ppm	ppm	ppm	ppm	ppm	ppm	ppm	ppm	ppm	ppm	ppm	ppm	ppm	ppm	ppm	ppm
0.1	0.35	0.44	2.32	0.67	<DL	6.57	399	46.9	105	10.4	37.4	6.98	1.46	5.29	0.61	3.74
1.0	1.34	0.47	3.16	0.84	<DL	7.59	633	67.2	134	14.7	53.7	9.70	2.23	8.12	0.92	5.43
2.0	0.57	0.59	2.53	0.61	<DL	6.52	451	58.4	117	12.7	45.6	8.20	1.86	6.60	0.72	4.46
3.0	0.58	0.20	2.23	1.07	<DL	7.50	436	64.0	145	14.5	52.7	9.31	2.05	7.58	0.86	5.28
4.0	0.41	0.08	1.64	0.35	<DL	4.66	776	35.3	85.8	8.86	34.1	6.91	1.82	6.33	0.82	5.05
5.0	0.41	0.18	2.85	0.63	<DL	10.1	441	77.8	152	16.4	57.3	9.38	2.00	6.59	0.65	3.68
6.0	0.39	0.12	1.33	0.19	<DL	4.91	582	30.6	61.5	6.98	26.4	4.83	1.38	4.13	0.46	2.99
7.0	0.28	0.17	1.28	0.43	<DL	5.32	701	45.2	96.4	10.5	37.2	6.99	1.74	5.63	0.63	3.82
8.0	2.95	0.63	3.95	0.82	<DL	8.07	362	49.9	85.3	11.3	43.2	8.26	1.97	7.12	0.92	5.38
8.8	1.14	0.19	3.69	0.60	<DL	8.72	392	65.9	89.4	12.8	43.5	7.37	1.67	5.89	0.69	4.30
9.5	1.31	0.38	4.36	0.41	<DL	9.70	355	61.2	68.5	12.4	46.1	8.52	1.97	7.12	0.85	5.19
10.0	3.65	0.43	3.27	0.32	<DL	8.09	354	62.7	118	13.9	51.8	9.38	2.15	7.59	0.86	5.07
11.0	1.35	0.35	3.53	0.35	<DL	8.48	482	66.6	149	15.7	59.6	10.6	2.48	8.09	0.91	5.34
12.0	0.27	0.15	1.52	0.71	<DL	2.55	941	21.2	39.7	4.58	18.0	3.60	1.25	3.37	0.43	2.96
13.0	0.43	0.14	2.53	0.12	<DL	5.77	668	33.9	60.7	7.59	29.3	5.58	1.59	4.59	0.52	3.06
14.0	0.58	0.47	1.71	0.14	<DL	4.07	548	25.9	47.3	5.69	22.1	3.86	1.17	3.38	0.40	2.54
15.1	0.71	0.26	3.27	0.20	<DL	8.50	572	48.5	94.2	11.0	41.5	7.42	1.91	5.84	0.68	4.01
16.0	1.38	0.25	2.60	0.35	<DL	6.75	617	36.7	69.4	8.47	32.2	5.97	1.69	5.19	0.66	3.81
17.0	0.42	0.09	1.44	0.16	<DL	2.38	647	21.0	34.4	4.13	15.1	2.86	0.94	2.63	0.39	2.62
19.3	0.17	0.14	1.42	0.15	<DL	3.54	896	19.2	33.1	4.00	14.4	2.49	0.89	2.00	0.23	1.41
20.3	0.13	0.24	1.93	0.35	<DL	4.62	692	30.9	59.5	6.86	25.6	4.52	1.31	3.99	0.48	2.89
21.5	0.16	0.28	1.85	0.45	<DL	5.65	374	36.0	66.3	7.57	28.0	5.11	1.22	4.39	0.55	3.24
23.3	0.11	0.51	1.30	0.31	<DL	3.73	654	30.9	61.0	7.06	27.4	5.27	1.45	4.70	0.61	3.71
24.6	0.09	0.39	1.46	0.48	<DL	4.16	864	32.7	63.3	7.23	26.7	4.78	1.32	4.28	0.51	2.96
25.3	0.09	0.27	1.04	0.22	<DL	2.50	611	23.0	44.0	5.00	18.6	3.38	1.04	3.04	0.35	2.15
26.8	0.71	0.35	3.61	1.54	<DL	7.37	587	34.3	66.0	7.83	28.7	5.06	1.49	4.03	0.48	2.80
27.6	0.31	0.24	1.07	0.72	<DL	1.33	768	14.7	30.7	3.28	12.4	2.52	0.95	2.70	0.38	2.31
28.9	0.28	<DL	1.83	0.56	<DL	2.70	656	25.5	36.0	5.42	20.4	4.25	1.28	3.79	0.52	3.29
29.7	0.47	0.66	3.35	1.50	<DL	7.03	434	65.1	126	13.1	44.4	7.18	1.55	5.20	0.54	3.07
30.3	0.47	0.72	2.51	0.97	<DL	6.24	507	52.9	107	10.9	39.5	7.54	1.68	6.01	0.72	4.31

Sample	Ho	Er	Tm	Yb	Lu	Hf	Ta	W	Re	Os	Pt	Au	Tl	Pb	Th	U
SP09-02	ppm	ppm	ppm	ppm	ppm	ppm	ppm	ppm	ppm	ppm	ppm	ppm	ppm	ppm	ppm	ppm
0.1	0.72	1.96	0.261	1.63	0.23	2.53	1.25	35.4	0.006	0.27	<DL	0.17	0.82	22.8	19.1	6.67
1.0	1.05	2.73	0.426	2.42	0.37	3.39	2.81	34.9	0.064	2.56	0.09	1.45	1.79	26.3	22.1	6.46
2.0	0.82	2.29	0.311	2.01	0.28	2.87	2.01	32.9	0.033	0.87	0.10	0.61	1.06	20.9	18.0	5.18
3.0	1.03	2.94	0.440	2.90	0.42	3.40	1.76	18.6	0.021	0.55	0.08	0.44	0.84	26.8	19.2	4.77
4.0	0.94	2.53	0.332	1.97	0.26	3.36	2.61	249	0.008	0.43	0.03	0.33	0.62	20.8	13.6	3.48
5.0	0.67	1.78	0.259	1.82	0.26	3.59	2.04	29.6	<DL	0.33	0.03	0.29	0.99	29.5	22.6	2.80
6.0	0.58	1.68	0.239	1.50	0.22	3.63	2.08	91.8	<DL	0.29	0.04	0.21	0.58	20.7	9.47	21.7
7.0	0.70	1.89	0.276	1.73	0.25	2.97	1.87	43.2	<DL	0.27	0.03	0.18	0.63	20.9	11.9	2.02
8.0	1.06	2.72	0.41	2.41	0.39	3.45	3.22	6.52	0.061	1.86	0.10	0.76	1.69	25.4	12.3	10.7
8.8	0.87	2.57	0.38	2.48	0.36	3.52	2.28	15.1	0.012	0.55	0.03	0.32	1.14	22.4	7.59	3.61
9.5	0.96	2.69	0.37	2.45	0.34	3.55	2.12	13.4	<DL	0.35	0.02	0.23	0.98	18.4	6.19	4.93
10.0	0.94	2.66	0.37	2.40	0.34	3.32	2.01	14.5	<DL	0.38	0.03	0.24	0.82	34.1	13.6	4.41
11.0	0.98	2.78	0.39	2.62	0.37	3.78	2.11	53.3	<DL	0.37	0.02	0.25	0.88	22.1	12.6	4.16
12.0	0.58	1.74	0.24	1.63	0.23	2.57	2.09	119	0.006	0.36	0.00	0.05	0.63	19.3	4.36	4.76
13.0	0.57	1.60	0.22	1.50	0.22	4.55	1.93	66.7	<DL	0.22	0.03	0.08	0.68	21.0	6.53	4.18
14.0	0.52	1.55	0.22	1.44	0.22	3.37	1.56	34.7	<DL	0.25	0.01	0.08	0.26	18.5	6.48	3.74
15.1	0.74	2.07	0.29	1.97	0.29	4.78	1.99	70.9	<DL	0.23	0.05	0.14	0.75	21.9	12.0	2.28
16.0	0.78	2.17	0.33	2.08	0.33	5.70	3.56	145	0.070	2.02	0.11	0.68	1.69	22.7	11.3	4.96
17.0	0.54	1.60	0.23	1.45	0.21	3.13	2.87	205	0.014	0.69	0.02	0.22	0.75	18.8	5.74	1.51
19.3	0.28	0.81	0.11	0.83	0.12	2.41	2.94	94.0	0.013	0.45	0.02	0.13	0.76	19.9	5.22	1.51
20.3	0.59	1.68	0.24	1.62	0.24	4.71	1.81	39.5	<DL	0.33	0.05	0.04	0.50	21.0	9.53	4.09
21.5	0.66	1.80	0.25	1.70	0.24	3.55	1.81	42.5	0.007	0.30	0.03	0.17	0.64	19.5	11.0	6.86
23.3	0.75	2.29	0.33	2.16	0.32	3.79	1.62	32.0	<DL	0.39	0.04	<DL	0.47	21.7	9.05	17.3
24.6	0.56	1.54	0.20	1.30	0.18	2.25	1.55	55.3	0.013	0.23	<DL	<DL	0.49	30.0	12.0	3.28
25.3	0.43	1.20	0.17	1.15	0.17	3.44	1.60	92.6	<DL	0.28	0.06	<DL	0.36	15.6	6.98	3.93
26.8	0.56	1.54	0.252	1.51	0.26	4.44	2.17	36.3	0.032	1.34	0.08	1.33	1.54	18.3	9.66	3.68
27.6	0.46	1.22	0.172	0.96	0.13	0.91	1.38	111	0.023	0.57	<DL	0.61	0.78	17.1	5.13	1.26
28.9	0.69	1.93	0.292	1.81	0.27	2.86	1.11	18.6	0.015	0.39	0.03	0.40	0.65	19.9	4.43	1.94
29.7	0.55	1.50	0.226	1.49	0.21	3.35	1.55	35.3	0.019	0.30	0.02	0.32	0.94	22.0	19.5	1.81
30.3	0.84	2.25	0.309	1.98	0.27	2.68	1.08	23.6	0.024	0.29	0.03	0.19	0.71	24.8	19.9	6.62

Sample	Li	Be	B	Mg	Al	P	K	Ca	Ti	V	Cr	Fe	Mn
SP09-02	ppm	ppm	ppm	ppm	ppm	ppm	ppm	ppm	ppm	ppm	ppm	ppm	ppm
31.3	110.5	2.1	<DL	20788	69980	365	24160	25487	4057	119	11.4	46427	491
32.8	50.6	2.9	<DL	10472	65305	1900	24369	16895	3320	97.2	5.01	26133	178
33.9	70.9	2.7	<DL	16940	66372	838	29119	30574	3783	120	10.4	42540	356
34.7	26.7	1.3	<DL	5959	44518	578	18466	76487	1868	45.7	4.61	12568	700
35.5	56.8	2.4	<DL	17514	62065	969	24657	35250	2916	146	6.20	42591	488
36.5	56.0	2.8	<DL	14761	71917	412	32057	5494	3982	148	14.6	48759	173
37.4	65.2	2.7	<DL	13186	74594	436	20368	8399	3768	128	8.70	39244	142
38.4	59.4	2.6	<DL	18208	68720	1558	19486	15760	3042	99.5	7.73	30110	302
39.3	74.8	2.0	<DL	13753	74723	400	20584	7683	3828	134	10.0	40259	156
40.1	64.4	2.4	<DL	14497	74254	409	24955	19082	4129	135	8.13	42561	232
40.8	85.7	3.0	<DL	13642	81024	483	24248	5179	4030	161	9.77	36343	155
41.5	58.4	2.4	<DL	13941	64965	1746	24272	23378	3495	98.5	7.80	33564	482
42.5	78.1	4.1	<DL	20446	55491	683	16752	25783	2542	163	22.1	25979	297
43.3	56.8	2.0	<DL	13620	63757	901	22950	17788	3207	113	5.81	35457	264
44.3	47.2	1.4	<DL	10972	54368	640	20761	27419	3175	79.3	4.97	27541	354
45.1	58.2	2.1	<DL	14423	60304	659	23567	21794	3233	104	5.12	34355	354
46.0	64.0	1.1	<DL	12521	63840	773	24113	21244	3338	114	5.85	40318	348
49.0	60.0	1.6	<DL	9914	66249	498	22193	10468	3336	125	4.45	36562	131
50.0	59.7	2.7	<DL	10854	67347	363	22947	4512	3497	124	5.17	35904	125
50.4	58.6	2.4	<DL	11713	67143	383	25803	4630	3714	115	6.27	33453	152
51.4	54.8	2.0	<DL	10392	69413	233	24321	4645	3737	108	4.53	31986	126
52.7	36.4	2.2	<DL	19004	45871	688	17958	82864	2248	88.0	5.69	27075	727
53.7	41.4	1.8	<DL	17541	52769	855	18918	63365	2767	105	6.05	31303	396
55.6	57.1	1.8	<DL	12380	61725	500	23983	6167	3051	121	6.99	30227	109
56.7	49.5	1.9	<DL	15443	62184	366	20379	4329	3052	128	7.80	47169	129
57.6	49.7	1.9	<DL	12689	62045	872	25824	10120	3360	110	7.10	40627	233
58.5	40.6	1.7	<DL	12372	59302	333	22933	7657	3220	95.7	6.95	33899	173
59.4	29.1	1.8	<DL	4636	52412	206	19612	7382	2811	62.9	4.19	15950	63.7
60.1	49.9	2.2	51	8174	57294	437	21077	6418	3022	72.2	64.5	23303	102
61.0	60.2	1.5	37	7603	66428	233	20079	6147	2936	87.0	70.2	30432	65.7

Sample	Co	Cu	Zn	Ga	Ge	As	Se	Rb	Sr	Y	Zr	Nb	Mo	Ru	Pd
SP09-02	ppm	ppm	ppm	ppm	ppm	ppm	ppm	ppm	ppm	ppm	ppm	ppm	ppm	ppm	ppm
31.3	35.4	39.8	122	25.0	1.79	9.04	3.5	138	252	12.3	107	10.8	2.58	<DL	3.60
32.8	24.9	37.4	107	22.3	1.53	27.2	<DL	107	344	30.9	125	10.9	2.41	<DL	4.54
33.9	27.7	53.8	109	23.0	1.77	10.9	<DL	130	289	24.8	93.9	12.5	4.22	<DL	3.27
34.7	35.4	20.8	53.5	13.7	0.95	7.79	<DL	72.1	402	22.2	86.4	5.58	2.40	<DL	2.90
35.5	18.4	35.0	117	21.9	1.83	8.34	31.2	136	231	27.7	66.0	13.9	2.94	<DL	2.49
36.5	24.3	52.3	134	28.1	2.30	20.1	5.1	146	139	22.4	90.8	13.2	2.82	<DL	3.33
37.4	19.9	35.3	129	28.1	1.58	13.6	18.6	128	285	20.1	84.7	16.9	3.00	<DL	3.16
38.4	17.5	31.6	95.6	24.0	1.36	7.92	18.6	116	217	26.2	87.6	14.7	1.52	<DL	3.32
39.3	17.6	52.6	134	27.3	1.51	9.00	16.0	135	290	22.1	102	15.2	3.35	<DL	3.68
40.1	23.9	50.5	118	27.1	1.51	7.36	9.9	132	194	25.8	86.3	14.2	1.99	<DL	3.11
40.8	22.1	52.0	135	28.6	2.17	6.85	4.8	150	174	20.8	99.5	13.7	3.59	<DL	3.60
41.5	23.9	34.9	109	22.7	1.38	25.8	1.6	135	269	33.6	103	11.9	6.19	<DL	3.70
42.5	36.1	81.5	164	19.9	2.29	114	24.1	102	308	32.7	81.2	13.7	129	<DL	3.27
43.3	15.7	27.0	119	22.1	1.40	6.37	4.3	135	221	23.2	83.9	13.0	2.70	<DL	3.15
44.3	16.9	22.4	85.8	18.2	1.39	4.59	3.0	104	226	19.5	118	11.5	1.20	<DL	4.29
45.1	42.7	32.4	105	20.7	1.45	8.97	0.7	117	237	18.0	95.0	11.7	1.00	<DL	3.31
46.0	16.0	27.6	110	21.3	1.81	8.94	2.9	123	173	21.4	94.4	12.3	1.11	<DL	3.34
49.0	21.0	24.3	104	22.7	1.65	7.90	<DL	129	272	26.4	84.4	13.4	0.93	<DL	3.04
50.0	17.8	26.1	102	22.4	1.68	5.23	1.3	129	124	23.5	94.1	13.7	0.94	<DL	3.20
50.4	21.9	42.8	119	23.9	1.45	10.5	<DL	132	221	14.8	103	12.6	1.43	<DL	3.54
51.4	19.9	22.8	96.3	23.9	1.26	8.90	2.0	135	144	15.9	97.1	15.3	2.31	<DL	3.35
52.7	13.3	21.6	74.5	16.3	0.92	10.1	3.8	100	229	16.7	53.8	10.9	2.73	<DL	2.30
53.7	19.4	33.1	78.8	18.3	1.09	17.8	6.9	114	256	21.4	69.2	11.5	2.01	<DL	2.71
55.6	12.8	22.2	126	22.2	1.46	3.15	5.3	147	151	15.3	73.7	15.0	0.84	<DL	2.80
56.7	17.4	35.7	117	22.5	1.11	7.19	13.6	121	134	27.5	79.7	12.7	1.29	<DL	3.21
57.6	26.1	26.9	109	21.6	1.71	9.11	2.3	119	151	19.8	111	11.6	1.12	<DL	4.08
58.5	22.0	26.4	99.8	20.1	1.45	8.18	4.0	108	167	16.6	107	10.5	0.91	<DL	3.94
59.4	26.8	8.31	51.1	18.3	1.03	14.9	2.4	87.6	203	14.2	106	10.0	2.40	<DL	4.05
60.1	18.6	17.6	89.4	20.6	1.33	4.06	10.7	121	120	26.6	111	11.9	0.19	<DL	4.94
61.0	15.2	19.2	82.9	23.0	1.64	2.63	3.38	122	142	16.2	61.1	12.3	0.19	<DL	2.77

Sample	Ag	Cd	Sn	Sb	Te	Cs	Ba	La	Ce	Pr	Nd	Sm	Eu	Gd	Tb	Dy
SP09-02	ppm	ppm	ppm	ppm	ppm	ppm	ppm	ppm	ppm	ppm	ppm	ppm	ppm	ppm	ppm	ppm
31.3	0.37	0.43	3.24	1.23	<DL	10.3	511	41.0	80.3	8.36	29.1	5.02	1.20	3.67	0.43	2.56
32.8	0.36	0.26	1.90	0.72	<DL	5.57	689	57.3	116	13.4	49.9	9.64	2.33	8.66	1.06	6.25
33.9	0.40	0.68	2.35	1.28	<DL	7.75	622	67.8	136	14.1	50.9	9.20	2.09	7.22	0.85	5.07
34.7	0.26	0.29	1.13	0.86	<DL	3.06	556	36.6	80.5	8.85	35.0	7.23	1.95	6.80	0.87	4.95
35.5	0.76	0.44	2.73	1.35	<DL	8.11	469	50.1	92.6	11.0	41.3	7.64	1.71	6.70	0.86	4.98
36.5	0.47	0.26	2.96	1.24	<DL	9.27	327	63.9	126	14.3	51.0	9.17	1.96	7.25	0.82	4.91
37.4	0.48	0.20	2.24	0.80	<DL	7.82	480	80.8	150	15.7	54.6	9.07	1.85	6.65	0.75	4.41
38.4	0.42	0.43	2.18	0.51	<DL	6.19	403	54.0	100	11.0	38.7	6.67	1.48	5.77	0.68	4.28
39.3	15.3	0.36	2.65	0.77	<DL	8.92	556	66.3	127	14.1	50.7	8.94	1.94	7.05	0.82	4.84
40.1	0.52	0.48	2.25	0.62	<DL	7.70	481	78.1	161	17.4	63.1	11.3	2.51	8.90	1.02	5.80
40.8	0.47	0.35	2.58	0.74	<DL	10.2	487	64.2	124	13.2	47.8	8.70	1.93	6.79	0.82	4.88
41.5	0.41	0.48	1.64	0.62	<DL	7.82	521	61.1	120	13.1	48.8	8.98	2.10	7.57	0.93	5.65
42.5	1.29	3.75	3.71	3.70	<DL	5.80	329	45.1	46.2	9.48	36.2	7.01	1.63	6.85	0.88	5.44
43.3	0.55	0.47	3.17	0.70	<DL	7.96	424	39.1	46.1	8.39	30.3	5.62	1.35	4.85	0.60	3.95
44.3	0.46	0.30	2.61	0.49	<DL	6.43	607	36.4	50.8	7.90	29.3	5.58	1.46	4.64	0.56	3.80
45.1	0.39	0.57	2.66	0.59	<DL	7.61	416	38.7	63.2	8.31	30.6	5.58	1.35	4.63	0.55	3.41
46.0	0.35	0.46	2.83	0.81	<DL	10.4	335	46.3	77.9	9.79	35.9	6.71	1.51	5.52	0.67	4.08
49.0	0.32	0.19	2.51	0.84	<DL	7.73	402	55.0	104	11.6	41.5	7.63	1.65	6.62	0.83	5.17
50.0	0.32	0.15	2.98	0.70	<DL	8.06	393	52.2	90.1	11.0	38.8	7.10	1.53	5.81	0.72	4.47
50.4	0.32	0.20	2.81	0.48	<DL	7.42	425	53.3	97.9	10.6	37.0	6.32	1.25	4.18	0.49	2.93
51.4	0.36	0.25	2.85	0.55	<DL	6.72	431	62.0	115	12.6	43.0	7.18	1.42	5.17	0.58	3.47
52.7	0.56	0.46	2.33	0.64	<DL	5.36	258	39.7	75.0	8.37	30.0	5.36	1.18	4.35	0.51	3.08
53.7	0.41	0.42	2.32	1.00	<DL	6.34	303	44.0	85.3	9.50	34.6	6.15	1.41	5.38	0.68	4.13
55.6	0.40	0.21	2.64	0.61	<DL	8.69	325	40.3	74.0	8.48	30.3	5.32	1.06	4.13	0.50	2.99
56.7	0.37	0.28	2.48	0.73	<DL	7.08	238	55.7	110	12.3	45.7	8.33	1.82	6.96	0.82	5.09
57.6	0.31	0.33	2.18	0.78	<DL	8.40	418	44.0	83.8	9.81	36.5	6.60	1.54	5.24	0.63	3.85
58.5	0.31	0.28	2.12	0.57	<DL	6.83	402	43.7	84.8	9.35	33.8	6.09	1.36	4.69	0.54	3.31
59.4	0.33	0.28	1.06	0.61	<DL	3.60	715	39.1	70.9	8.12	28.3	4.97	1.17	3.98	0.47	2.92
60.1	0.33	0.36	2.11	0.49	<DL	5.55	394	45.8	84.0	9.47	34.2	6.28	1.38	5.66	0.71	4.47
61.0	0.32	0.31	2.15	0.73	<DL	6.39	372	50.5	90.0	10.1	34.9	6.10	1.19	4.64	0.57	3.45

Sample	Ho	Er	Tm	Yb	Lu	Hf	Ta	W	Re	Os	Pt	Au	Tl	Pb	Th	U
SP09-02	ppm	ppm	ppm	ppm	ppm	ppm	ppm	ppm	ppm	ppm	ppm	ppm	ppm	ppm	ppm	ppm
31.3	0.48	1.39	0.201	1.38	0.22	3.58	1.16	20.1	0.018	0.26	0.04	0.17	0.75	16.7	16.1	3.72
32.8	1.15	3.03	0.410	2.48	0.35	4.07	1.19	46.6	0.011	0.22	0.03	0.14	0.77	32.6	18.1	25.6
33.9	0.94	2.59	0.357	2.31	0.31	3.20	1.25	26.2	0.012	0.19	<DL	0.11	0.80	34.6	22.5	3.84
34.7	0.89	2.28	0.298	1.75	0.24	2.99	1.24	48.3	0.012	0.15	0.02	0.08	0.20	19.0	11.8	8.32
35.5	0.99	2.58	0.385	2.12	0.32	2.89	2.16	8.09	0.133	1.67	0.08	1.27	1.64	23.4	17.8	4.01
36.5	0.91	2.45	0.347	2.16	0.32	3.47	1.66	11.5	0.073	0.62	0.04	0.56	1.21	27.4	20.4	2.91
37.4	0.83	2.25	0.333	2.15	0.31	3.47	2.06	10.1	0.130	0.36	0.03	0.42	1.04	37.8	29.6	3.54
38.4	0.84	2.35	0.338	2.09	0.30	3.60	1.54	9.01	0.170	0.25	0.04	0.24	0.81	21.5	21.6	10.0
39.3	0.91	2.49	0.354	2.28	0.33	3.99	1.59	8.82	0.446	0.18	0.03	0.18	0.85	35.0	22.7	5.29
40.1	1.08	2.87	0.392	2.51	0.33	3.33	1.49	9.88	0.495	0.26	0.01	0.15	0.89	40.7	21.7	9.38
40.8	0.91	2.55	0.364	2.46	0.35	3.83	1.45	9.11	0.117	0.15	0.02	0.13	0.99	36.3	19.0	26.4
41.5	1.12	3.12	0.419	2.60	0.37	3.72	1.31	12.6	0.063	0.13	0.01	0.08	0.74	25.9	20.1	14.7
42.5	1.13	3.09	0.422	2.47	0.39	2.86	2.47	7.98	0.444	1.68	0.10	1.32	1.60	40.8	5.98	95.0
43.3	0.77	2.16	0.311	1.95	0.30	3.12	1.58	3.53	0.023	0.58	0.04	0.63	0.96	16.1	5.08	2.95
44.3	0.74	2.09	0.300	1.92	0.29	3.97	1.37	9.19	0.009	0.37	0.05	0.45	0.77	16.4	4.70	2.97
45.1	0.67	1.82	0.248	1.67	0.25	3.26	1.40	23.6	0.015	0.33	0.04	0.39	0.78	17.0	7.27	3.30
46.0	0.81	2.22	0.318	2.09	0.30	3.43	1.33	4.70	0.019	0.26	0.06	0.31	0.76	21.2	8.42	2.42
49.0	1.00	2.73	0.375	2.31	0.36	3.13	1.56	10.6	0.008	0.19	0.04	0.23	0.76	28.1	23.9	4.27
50.0	0.88	2.39	0.336	2.14	0.32	3.22	1.44	4.95	0.021	0.17	0.04	0.17	0.83	24.7	17.2	3.45
50.4	0.56	1.63	0.243	1.66	0.25	3.47	1.29	9.80	0.048	0.16	0.05	0.21	0.85	31.7	19.5	12.3
51.4	0.62	1.75	0.240	1.63	0.23	3.32	1.43	13.1	0.024	0.14	0.05	0.18	0.88	20.6	28.5	3.94
52.7	0.62	1.62	0.239	1.44	0.22	2.34	1.94	13.7	0.082	1.71	0.08	1.24	1.30	16.3	14.2	10.7
53.7	0.80	2.19	0.319	1.95	0.28	2.82	1.67	13.1	0.135	0.65	0.02	0.59	1.01	20.5	14.7	6.77
55.6	0.60	1.62	0.240	1.53	0.21	3.07	1.61	9.84	0.082	0.25	0.04	0.26	0.79	16.7	14.2	3.00
56.7	1.00	2.72	0.380	2.38	0.34	3.19	1.47	7.37	0.035	0.17	0.03	0.21	0.67	14.4	18.3	2.66
57.6	0.76	2.08	0.295	1.97	0.29	4.05	1.42	24.2	0.016	0.15	0.05	0.20	0.70	19.7	12.5	2.30
58.5	0.68	1.97	0.279	1.95	0.27	3.98	1.32	25.0	0.023	0.13	0.04	0.17	0.64	21.5	14.7	2.34
59.4	0.55	1.55	0.231	1.49	0.22	4.00	1.63	38.9	0.019	0.12	0.06	0.14	0.53	21.3	15.4	4.22
60.1	0.89	2.55	0.345	2.20	0.32	4.55	1.21	19.2	0.052	<DL	0.06	0.13	0.72	21.2	21.3	3.04
61.0	0.64	1.80	0.254	1.64	0.23	2.64	1.22	15.4	0.020	<DL	0.05	0.17	0.85	24.4	26.9	2.67

Sample	Li	Be	B	Mg	Al	P	K	Ca	Ti	V	Cr	Fe	Mn
SP10-01	ppm	ppm	ppm	ppm	ppm	ppm	ppm	ppm	ppm	ppm	ppm	ppm	ppm
1.0	28.0	2.27	39	25722	49582	1313	21483	64265	2642	95.5	10.7	32250	797
2.0	17.3	2.21	23	23849	45451	1381	22920	75951	2532	77.7	8.54	27686	687
3.0	19.3	2.08	24	17508	58018	684	23306	22644	3242	102	7.13	37186	287
4.0	9.6	1.12	5	17494	34208	746	16638	134167	2005	72.9	10.0	25087	807
5.0	39.4	2.78	26	15696	63476	928	26358	8600	3867	164	10.7	73288	262
6.0	21.7	2.78	<DL	17270	55054	1669	23173	53664	3260	98.2	7.76	41861	725
7.0	29.9	2.30	6	15432	61223	1003	21965	12564	3766	156	12.6	53580	255
8.0	29.0	3.06	6	13159	61784	1238	18579	11073	3784	297	9.41	81833	246
9.0	39.2	2.22	70	19890	58167	1245	22910	29922	3917	135	9.63	43968	625
10.0	44.7	2.75	51	19332	64400	955	25851	21753	4362	127	9.40	49956	619
11.0	54.3	2.48	42	13139	68729	391	23772	7043	4721	176	10.5	51869	218
12.0	67.7	2.19	34	13449	68767	784	21648	8395	4675	173	13.7	46922	253
13.0	55.0	2.15	34	16899	60379	1228	20959	19891	4051	126	11.7	42033	418
14.0	45.1	2.56	59	22481	54899	715	21686	34688	2861	133	7.95	44456	420
15.0	30.6	1.46	8	8083	51712	461	17889	13454	2839	74.0	4.58	21479	191
16.0	21.3	1.56	22	17209	31082	913	13552	142242	1740	89.4	11.0	19341	772
17.0	53.5	1.74	42	13524	67527	319	23982	10198	4183	162	9.70	47379	196
18.0	59.7	3.00	76	11280	69887	459	23680	5115	3988	190	10.7	50481	143
19.0	37.6	2.41	59	15686	53401	1549	20856	58250	3089	115	7.80	41014	386
20.0	33.5	2.50	85	12084	60789	517	27075	25113	3247	135	7.89	42459	252
21.0	54.6	1.98	65	12226	64400	556	27688	11370	3615	127	8.21	45546	197
22.0	-7.1	1.39	15	1874	32455	259	9305	114122	1466	14.1	2.58	4623	1004
23.0	61.1	3.03	73	15837	63718	685	27758	16965	3889	143	7.53	40482	255
24.0	20.6	1.61	69	25176	45167	638	20530	85610	2578	88.0	9.63	27516	677
25.0	32.7	1.92	75	19592	54025	799	22765	39061	2758	100	6.06	30110	383
26.0	116	3.3	112	11986	85822	539	20711	6216	4736	166	11.0	30428	98.4
27.0	61.4	1.7	26	32658	55020	1085	19390	54491	2958	100	14.4	28965	467
28.0	41.5	1.6	50	12283	52393	1108	25736	55212	3141	82.1	5.49	29954	621
29.0	48.6	1.5	37	35809	45046	924	18017	69975	2519	145	10.3	27266	892
30.0	63.5	2.2	10	11542	73259	391	22029	4773	4057	173	8.74	42729	119
31.0	27.9	2.1	<DL	7053	32726	510	11711	174265	1841	109	10.9	18273	488
32.0	57.6	2.1	15	11950	71787	411	19877	6846	3687	134	7.38	41889	113

Sample	Co	Cu	Zn	Ga	Ge	As	Se	Rb	Sr	Y	Zr	Nb	Mo	Ru	Pd
SP10-01	ppm	ppm	ppm	ppm	ppm	ppm	ppm	ppm	ppm	ppm	ppm	ppm	ppm	ppm	ppm
1.0	26.1	28.4	86.4	18.6	1.79	12.6	1.77	118	454	14.9	68.0	9.81	5.07	0.50	2.75
2.0	26.1	25.5	74.5	16.8	1.58	19.1	2.35	106	479	16.7	66.4	8.81	6.27	0.64	2.67
3.0	26.1	33.6	85.9	21.6	1.93	71.3	1.92	114	309	18.9	95.6	11.6	13.0	0.06	3.67
4.0	26.6	25.8	53.7	12.8	1.39	49.2	2.48	68.9	325	18.0	57.3	5.63	5.64	0.92	2.34
5.0	37.9	47.0	110	22.8	2.58	69.3	2.99	132	340	19.3	127	11.2	13.1	0.07	4.87
6.0	30.3	31.5	76.3	19.7	1.72	26.2	2.75	109	319	26.2	103	10.2	4.01	0.34	3.84
7.0	33.6	55.1	91.5	22.4	1.67	183	4.03	108	319	27.4	99.2	11.6	12.9	0.05	3.71
8.0	50.5	74.9	106	22.6	2.44	433	3.79	96.9	411	35.6	107	12.2	37.4	0.06	4.21
9.0	41.2	63.1	108	22.2	1.61	59.5	13.6	94.9	515	31.7	98.7	13.7	4.32	0.15	3.39
10.0	46.3	53.0	123	25.1	1.78	55.8	25.5	118	245	31.3	99.6	12.5	3.27	0.06	3.31
11.0	39.0	60.4	135	27.1	1.67	74.7	11.3	124	202	24.7	109	12.1	4.30	<DL	3.76
12.0	42.7	64.7	136	28.5	1.81	91.6	24.3	129	252	28.7	132	11.6	3.99	<DL	4.40
13.0	41.1	63.3	107	25.6	1.68	18.1	33.1	117	307	25.2	140	10.4	4.18	0.04	4.50
14.0	25.0	29.8	89.9	22.1	2.05	7.66	7.9	138	277	17.0	80.2	11.7	6.39	0.17	2.63
15.0	38.7	19.9	62.6	20.0	1.20	9.53	3.8	92.6	296	11.1	126	6.81	54.5	0.04	4.06
16.0	24.2	43.1	56.5	13.1	0.87	5.83	14.3	74.7	317	16.8	56.5	5.79	5.40	0.99	2.02
17.0	29.5	60.5	130	29.3	1.86	38.1	46.7	144	220	18.7	108	11.9	9.48	<DL	3.69
18.0	31.9	82.0	135	28.4	1.87	129	40.4	142	188	17.1	94.7	14.0	15.4	0.05	3.31
19.0	18.9	39.8	94.1	21.1	1.49	36.4	24.9	114	302	29.3	67.4	10.3	3.26	0.32	2.49
20.0	26.7	104	106	24.0	1.95	39.9	5.3	133	304	19.1	86.8	11.2	4.56	0.04	3.16
21.0	36.7	31.1	111	24.8	1.72	9.90	10.1	141	357	13.3	94.9	11.6	3.71	0.06	3.21
22.0	29.5	9.44	6.33	8.2	0.65	3.46	0.5	30.6	447	11.1	127	3.88	1.90	0.41	4.26
23.0	28.7	53.1	117	26.9	2.15	9.11	31.4	135	196	17.4	89.1	11.2	3.32	<DL	3.10
24.0	27.9	25.1	68.4	17.9	1.07	15.4	19.5	102	440	17.3	59.4	8.47	3.87	0.55	2.18
25.0	25.9	29.0	84.5	20.6	1.17	42.5	5.7	115	326	18.7	61.0	9.75	9.00	0.16	2.18
26.0	36.4	154	171	31.3	1.95	18.5	3.3	101	243	27.7	110	14.5	13.3	0.05	3.55
27.0	21.6	23.7	90.2	19.9	1.19	2.36	11.3	112	411	20.8	73.5	11.8	10.1	0.33	2.58
28.0	30.5	21.1	77.3	18.9	1.16	9.47	22.0	122	210	26.3	97.2	10.7	7.44	0.19	3.14
29.0	38.9	27.5	133	18.1	1.15	27.4	86.8	99	420	24.1	64.3	5.68	16.2	0.50	2.42
30.0	23.3	66.1	125	27.8	1.50	8.41	40.4	128	217	23.7	100.5	11.7	4.18	<DL	3.33
31.0	25.5	46.9	72.8	13.6	0.69	13.0	25.5	59.4	269	62.9	42.9	3.00	1.74	0.79	1.81
32.0	19.7	38.6	119	27.8	1.53	5.75	25.5	126	153	23.2	86.3	14.6	3.91	<DL	3.02

Sample	Ag	Cd	Sn	Sb	Te	Cs	Ba	La	Ce	Pr	Nd	Sm	Eu	Gd	Tb	Dy
SP10-01	ppm	ppm	ppm	ppm	ppm	ppm	ppm	ppm	ppm	ppm	ppm	ppm	ppm	ppm	ppm	ppm
1.0	0.53	0.75	2.76	0.63	<DL	6.30	420	29.3	67.3	7.36	26.6	4.95	1.15	4.38	0.52	2.91
2.0	0.35	0.53	2.26	0.47	<DL	5.39	564	33.1	74.6	8.50	30.6	5.44	1.34	4.92	0.55	3.15
3.0	0.38	0.28	2.77	0.64	<DL	6.29	1462	50.2	111	12.3	43.3	7.41	2.07	6.56	0.69	3.83
4.0	0.24	0.80	1.69	0.37	<DL	3.84	605	36.4	84.1	9.10	32.3	5.79	1.42	5.46	0.59	3.47
5.0	0.51	0.16	2.86	1.16	<DL	8.89	468	48.0	109	11.7	41.5	6.71	1.60	5.92	0.61	3.83
6.0	0.36	0.60	2.22	0.73	<DL	6.28	719	52.1	126	13.7	50.0	8.70	2.11	7.81	0.84	4.85
7.0	0.40	0.24	2.30	0.78	<DL	6.88	392	65.4	157	15.9	55.7	9.77	2.19	8.91	1.00	5.44
8.0	0.44	0.33	2.36	1.33	<DL	6.69	516	77.9	186	18.3	65.0	11.3	2.48	10.6	1.23	7.59
9.0	0.52	0.96	3.27	0.59	<DL	5.82	423	81.0	190	19.1	68.2	11.9	2.74	9.49	1.05	5.70
10.0	0.44	0.76	2.93	0.49	<DL	7.35	336	67.7	158	16.8	61.6	11.0	2.44	9.33	1.05	5.83
11.0	0.42	0.37	2.87	0.49	<DL	8.37	451	67.7	159	17.5	65.3	11.7	2.66	9.56	1.00	5.58
12.0	0.38	0.31	3.01	0.41	<DL	9.45	464	61.0	143	15.8	58.4	10.5	2.48	8.58	0.94	5.43
13.0	0.42	0.39	2.60	0.42	<DL	7.97	415	47.7	113	12.8	48.0	8.55	2.20	7.34	0.79	4.61
14.0	0.35	0.40	2.56	0.51	<DL	7.91	406	36.0	74.3	8.26	29.1	5.10	1.14	4.12	0.49	2.89
15.0	0.22	0.27	1.47	0.12	<DL	4.90	500	25.6	50.9	6.27	22.8	3.84	1.21	3.43	0.37	2.06
16.0	0.45	2.19	1.54	0.16	<DL	4.27	272	28.6	62.1	6.88	25.7	4.50	1.05	3.97	0.44	2.75
17.0	0.54	0.34	2.48	0.58	<DL	8.83	410	61.1	140	15.6	57.3	9.69	2.25	7.72	0.81	4.33
18.0	0.58	0.40	2.74	1.14	<DL	7.84	428	77.2	173	17.5	60.6	9.95	2.08	7.65	0.77	4.24
19.0	0.39	0.64	2.04	0.57	<DL	6.10	321	54.3	126	13.8	51.5	9.29	1.99	8.20	0.90	5.34
20.0	0.49	0.58	1.90	0.66	<DL	6.73	742	52.2	110	12.4	43.9	7.28	1.75	6.42	0.66	3.90
21.0	0.35	0.44	1.97	0.35	<DL	7.87	556	59.9	127	13.2	44.7	6.51	1.37	4.82	0.47	2.81
22.0	0.16	0.36	0.93	0.10	<DL	0.80	386	12.8	28.0	3.03	10.8	2.05	0.79	1.84	0.28	1.83
23.0	0.35	0.54	2.21	0.49	<DL	7.55	440	48.7	111	12.1	44.5	7.72	1.86	6.49	0.67	3.82
24.0	0.45	0.76	1.42	0.42	<DL	5.19	411	41.0	88.0	9.94	36.1	6.31	1.41	5.24	0.57	3.28
25.0	0.39	0.68	1.56	0.58	<DL	5.20	453	44.7	95.6	10.7	38.9	6.98	1.52	5.76	0.64	3.66
26.0	0.63	2.02	3.00	1.42	<DL	7.87	416	82.9	199	22.2	79.4	13.8	2.99	10.9	1.22	6.51
27.0	0.42	0.34	2.00	0.51	<DL	6.19	346	48.0	101	11.1	40.1	7.10	1.53	6.26	0.75	4.19
28.0	0.34	0.78	1.89	0.85	<DL	5.44	437	46.2	105	11.3	42.0	7.72	1.85	7.16	0.84	5.07
29.0	0.24	1.16	1.63	0.98	<DL	5.69	357	37.5	84.4	10.1	38.4	7.30	1.70	6.95	0.82	4.77
30.0	0.37	0.33	2.49	0.79	<DL	8.74	405	64.3	136	14.6	52.8	9.21	2.03	7.62	0.83	4.95
31.0	0.24	4.07	1.03	0.27	<DL	3.73	365	35.5	85.6	9.85	38.5	8.01	1.89	9.01	1.21	8.23
32.0	0.39	0.21	2.51	0.87	<DL	7.70	287	60.7	130	14.4	51.4	8.80	1.83	7.50	0.84	4.74

Sample	Ho	Er	Tm	Yb	Lu	Hf	Ta	W	Re	Os	Pt	Au	Tl	Pb	Th	U
SP10-01	ppm	ppm	ppm	ppm	ppm	ppm	ppm	ppm	ppm	ppm	ppm	ppm	ppm	ppm	ppm	ppm
1.0	0.56	1.63	0.24	1.49	0.25	2.21	0.97	12.9	0.063	1.90	0.07	1.14	1.55	17.3	15.4	6.79
2.0	0.63	1.76	0.24	1.53	0.23	2.09	0.90	39.5	0.159	0.77	0.05	0.53	0.85	17.7	15.2	12.9
3.0	0.70	2.04	0.29	1.81	0.26	2.94	1.00	32.8	0.066	0.44	0.05	0.34	0.97	23.6	28.0	11.5
4.0	0.65	1.79	0.24	1.49	0.21	1.66	0.66	32.8	0.041	0.27	0.03	0.20	0.18	17.7	15.4	14.3
5.0	0.75	2.26	0.34	2.27	0.32	3.77	1.13	28.7	0.052	0.26	0.07	0.22	0.90	26.0	20.5	4.71
6.0	0.93	2.59	0.35	2.10	0.31	3.00	1.04	55.7	0.022	0.22	0.05	0.21	0.75	24.9	22.2	6.52
7.0	1.02	2.96	0.41	2.57	0.37	3.00	1.01	12.4	0.035	0.21	0.06	0.19	0.69	28.1	25.5	5.13
8.0	1.54	4.65	0.69	4.56	0.64	3.14	1.22	62.6	0.052	0.20	0.04	0.19	0.69	31.2	27.9	6.76
9.0	1.12	3.06	0.417	2.60	0.39	2.80	1.30	32.3	0.101	1.54	<DL	0.91	1.29	32.7	27.6	5.43
10.0	1.15	3.11	0.415	2.70	0.37	2.94	1.25	29.1	0.098	0.72	<DL	0.49	0.94	30.6	24.1	4.65
11.0	1.01	2.79	0.386	2.58	0.34	3.12	1.26	32.0	0.081	0.41	<DL	0.39	0.75	29.2	21.9	3.01
12.0	1.04	2.95	0.419	2.64	0.37	3.83	1.40	114	0.052	0.31	<DL	0.45	0.82	29.0	18.6	2.67
13.0	0.90	2.52	0.345	2.20	0.30	3.95	1.36	117	0.138	0.27	<DL	0.22	0.72	22.5	15.6	5.53
14.0	0.58	1.69	0.232	1.59	0.23	2.47	0.92	24.7	0.056	0.23	<DL	0.19	0.65	23.1	17.8	4.76
15.0	0.42	1.25	0.183	1.22	0.19	3.69	1.22	171	0.042	0.24	<DL	0.18	0.60	19.3	8.4	3.57
16.0	0.54	1.58	0.207	1.38	0.20	1.65	0.72	56.6	0.033	0.20	<DL	0.20	0.23	18.2	8.3	9.31
17.0	0.78	2.19	0.301	1.96	0.27	3.19	1.09	37.1	0.140	0.21	<DL	0.34	0.67	30.1	21.4	3.48
18.0	0.77	2.24	0.342	2.06	0.32	2.97	1.28	21.8	0.239	1.65	<DL	1.01	1.35	37.0	28.0	3.73
19.0	1.04	2.87	0.387	2.44	0.31	2.15	0.86	8.20	0.174	0.68	<DL	0.48	0.80	32.3	20.4	7.71
20.0	0.76	2.28	0.313	2.06	0.30	2.67	1.14	57.0	0.061	0.43	<DL	0.33	0.76	34.1	25.3	3.85
21.0	0.55	1.70	0.246	1.76	0.26	3.01	1.08	47.2	0.148	0.36	<DL	0.24	0.71	31.0	26.2	3.01
22.0	0.41	1.26	0.193	1.28	0.18	3.65	1.75	427	0.011	0.26	<DL	0.21	0.34	14.7	4.7	9.99
23.0	0.68	1.91	0.253	1.77	0.23	2.88	1.12	42.6	0.568	0.23	<DL	0.19	0.64	81.8	17.6	17.0
24.0	0.61	1.81	0.241	1.47	0.21	1.82	0.81	38.9	0.325	0.22	<DL	0.16	0.46	25.1	16.8	9.72
25.0	0.69	1.87	0.264	1.62	0.23	2.08	0.87	50.2	0.056	0.24	<DL	0.13	0.64	27.6	18.6	8.84
26.0	1.18	3.03	0.45	2.62	0.41	3.25	1.44	53.2	0.093	1.22	<DL	1.06	1.34	38.7	39.5	11.5
27.0	0.80	2.13	0.30	1.76	0.25	2.26	1.08	34.8	0.046	0.58	<DL	0.49	1.00	40.7	23.0	11.1
28.0	0.96	2.71	0.35	2.28	0.30	2.98	1.37	146	0.052	0.34	<DL	0.32	0.78	23.2	16.9	2.92
29.0	0.88	2.44	0.32	2.08	0.28	2.09	0.78	27.8	0.430	0.33	<DL	0.17	0.22	25.3	15.7	8.22
30.0	0.95	2.69	0.38	2.45	0.36	3.28	1.08	30.0	0.183	0.24	<DL	0.21	0.82	30.7	24.3	3.50
31.0	1.92	6.16	0.90	6.32	0.96	1.43	0.61	24.3	0.099	0.22	<DL	0.16	0.07	29.5	11.3	112
32.0	0.91	2.50	0.35	2.30	0.32	2.86	1.24	26.3	0.133	0.21	<DL	0.13	0.78	31.2	34.4	4.55

Sample	Li	Be	B	Mg	Al	P	K	Ca	Ti	V	Cr	Fe	Mn
SP10-01	ppm	ppm	ppm	ppm	ppm	ppm	ppm	ppm	ppm	ppm	ppm	ppm	ppm
33.0	51.1	1.9	<DL	17553	60169	488	19269	16242	3194	124	6.83	35887	219
34.0	23.6	1.4	<DL	17464	69203	193	9942	5448	2469	66.8	3.44	24903	79.1
35.0	55.3	1.8	15	12490	68467	499	20266	11104	3858	126	8.03	35793	206
36.0	56.3	1.9	33	14099	64807	549	24902	6364	3462	112	6.24	48067	194
37.0	53.5	2.8	14	13050	68785	387	23258	7647	3609	133	6.05	37658	141
38.0	44.6	2.2	11	26742	58127	523	19579	37783	2833	152	10.6	27731	375
39.0	56.9	2.4	<DL	13571	67651	1372	22452	14149	3591	128	8.41	44447	224
40.0	9.70	0.6	<DL	3000	27610	265	12969	112807	1361	27.7	3.12	6849	996
41.0	46.9	1.5	<DL	11456	57227	634	22150	23227	3234	102	6.80	34791	405
42.0	58.3	1.9	<DL	12344	60555	788	22873	22181	3137	114	8.77	41093	389
43.0	52.5	2.5	54	11712	62325	899	26709	16202	3439	119	7.01	41205	268
44.0	65.0	1.9	49	10481	75784	592	23819	7247	3664	136	6.08	41264	123
45.0	65.0	2.2	40	10892	71951	503	25227	6156	3775	128	7.22	40153	119
46.0	54.3	2.5	42	12590	68720	480	29168	8026	3688	120	6.58	41814	188
47.0	57.5	1.9	24	8892	71554	327	25058	6457	3831	129	6.29	37367	118
48.0	30.4	2.3	5	7900	51868	436	22282	9433	2748	60.6	3.84	19057	105
49.0	46.4	2.4	50	12741	61953	509	26538	12477	3354	92.7	6.01	34535	215
50.0	48.8	2.0	25	12845	67340	371	21379	16612	3260	130	7.21	44185	231
51.0	12.9	0.5	<DL	20379	15698	1861	5365	217670	805	28.5	7.49	12625	1155
52.0	47.0	2.4	59	11016	70650	489	22383	6725	3650	148	6.55	36008	75.1
53.0	47.1	2.6	49	12705	67116	259	24925	5399	3331	152	5.14	36596	84.9
54.0	53.5	1.7	37	16123	60242	709	22333	15631	2665	140	5.60	36065	195
55.0	59.4	2.0	33	15304	64363	787	20408	52400	3363	115	6.59	41746	324
56.0	55.3	5.3	70	8678	85039	2432	18765	6113	3923	217	10.6	29706	55.1
57.0	58.7	2.1	10	7765	69391	511	21051	6227	3225	104	5.88	37358	93.5
58.0	44.4	2.1	52	7273	81863	1010	18848	5114	3770	188	8.98	31853	54.3
59.0	38.1	1.3	<DL	6616	55027	381	18707	5560	2672	75.7	5.11	22067	74.0
60.0	48.4	1.8	15	8181	61356	557	20595	7384	3218	92.0	7.21	36407	98.8
61.0	72.1	1.8	47	12006	70782	433	24195	10123	3685	103	8.71	33219	217
62.0	51.4	2.3	37	11224	63662	378	26657	5793	3084	129	5.46	44117	93.4
62.5	57.7	2.9	46	11635	68000	492	28176	4973	3328	138	8.94	49549	104

Sample	Co	Cu	Zn	Ga	Ge	As	Se	Rb	Sr	Y	Zr	Nb	Mo	Ru	Pd
SP10-01	ppm	ppm	ppm	ppm	ppm	ppm	ppm	ppm	ppm	ppm	ppm	ppm	ppm	ppm	ppm
33.0	23.1	55.3	102	23.7	1.29	5.27	20.6	123	336	24.6	85.8	12.5	4.73	<DL	2.86
34.0	20.4	25.2	126	32.3	1.22	3.94	14.6	67.1	108	50.8	219	16.2	1.89	<DL	7.09
35.0	32.5	37.7	107	26.6	1.32	21.8	9.0	131	186	25.5	88.2	12.1	4.80	0.07	3.13
36.0	24.9	29.8	122	25.4	1.41	41.2	0.8	152	179	14.6	76.0	10.4	3.45	0.02	2.57
37.0	27.0	31.2	121	26.2	1.47	12.4	0.9	145	253	21.5	86.6	13.5	2.46	0.03	2.92
38.0	22.7	45.9	143	21.5	0.99	8.54	3.6	131	343	16.6	64.2	12.8	1.36	0.17	2.28
39.0	24.6	42.1	112	24.8	1.33	3.71	1.1	142	203	32.2	81.3	11.6	2.96	<DL	2.69
40.0	27.8	9.86	25.5	7.63	0.53	5.58	<DL	42.9	296	10.4	72.4	4.22	7.95	0.41	2.46
41.0	29.0	27.4	93.1	19.5	1.38	8.92	16.6	112	284	21.3	93.1	9.19	1.41	0.09	3.15
42.0	26.2	27.0	105	21.9	1.57	12.3	8.0	122	171	20.8	68.5	8.30	13.5	0.05	2.33
43.0	34.5	34.1	108	22.4	1.69	11.3	4.92	126	172	29.2	114	12.7	1.97	<DL	4.20
44.0	24.7	27.1	123	28.1	1.64	10.2	4.19	143	206	21.0	106	13.3	1.55	<DL	3.98
45.0	21.4	27.3	108	25.8	1.72	7.51	6.19	148	121	21.1	108	14.3	1.22	<DL	3.86
46.0	24.7	25.1	112	24.3	1.84	4.06	5.32	139	117	25.2	108	14.2	1.16	<DL	3.97
47.0	31.4	64.9	99.4	26.0	1.51	5.33	2.79	157	151	18.0	105	15.4	1.83	<DL	3.68
48.0	48.7	14.2	50.5	17.9	1.08	8.23	4.98	113	131	20.7	151	10.4	3.15	<DL	5.46
49.0	29.1	21.9	92.9	23.8	1.32	18.7	4.05	148	156	15.5	89.4	11.0	1.76	<DL	3.24
50.0	19.2	30.8	99.0	24.9	1.11	18.4	3.03	136	116	22.5	70.5	12.5	3.58	<DL	2.51
51.0	13.8	12.0	34.0	5.80	0.34	1.17	7.46	30.7	342	20.3	28.2	3.45	0.54	1.14	1.20
52.0	19.0	26.7	102	24.9	1.53	31.8	2.68	149	186	16.7	97.8	14.8	3.49	<DL	3.71
53.0	16.0	27.5	97.4	24.6	1.04	11.0	3.70	154	123	14.5	73.7	14.5	4.58	<DL	2.86
54.0	23.7	30.3	95.5	20.6	1.52	8.17	5.54	137	140	13.9	54.9	10.5	2.03	<DL	2.04
55.0	26.3	32.9	99.5	22.8	1.32	8.21	11.0	128	203	23.7	78.0	13.5	1.71	<DL	2.75
56.0	21.9	81.2	103	35.4	1.96	16.3	7.29	92.7	1343	46.5	96.8	16.8	8.05	<DL	3.79
57.0	31.4	19.3	88.8	24.3	1.63	8.29	5.25	139	123	24.0	66.2	12.1	1.70	<DL	2.45
58.0	39.6	60.2	107	30.4	1.50	8.09	5.16	106	582	30.3	78.9	14.7	6.32	<DL	3.03
59.0	43.9	14.4	75.5	18.5	1.13	3.73	3.67	102	205	15.4	66.5	8.35	1.97	<DL	2.51
60.0	45.6	27.4	92.3	21.0	1.52	2.81	5.10	116	311	20.3	82.6	12.3	2.54	<DL	3.18
61.0	29.7	31.3	139	25.3	1.64	25.4	5.40	145	160	18.6	87.6	14.5	3.50	<DL	3.40
62.0	24.9	26.1	107	22.3	1.74	2.14	6.65	164	135	19.0	71.2	14.3	1.19	<DL	2.78
62.5	22.8	25.5	116	24.8	2.06	2.85	4.71	177	135	28.7	81.7	15.7	1.15	<DL	3.30

Sample	Ag	Cd	Sn	Sb	Te	Cs	Ba	La	Ce	Pr	Nd	Sm	Eu	Gd	Tb	Dy
SP10-01	ppm	ppm	ppm	ppm	ppm	ppm	ppm	ppm	ppm	ppm	ppm	ppm	ppm	ppm	ppm	ppm
33.0	0.44	0.57	1.97	0.52	<DL	6.10	512	48.9	108	11.8	43.2	7.59	1.72	6.97	0.78	4.64
34.0	0.45	0.63	3.62	0.51	<DL	4.32	353	50.8	116	13.3	51.3	10.6	1.69	10.6	1.52	9.74
35.0	0.58	0.34	2.04	0.65	<DL	7.64	397	53.6	124	13.3	49.2	8.57	2.05	7.40	0.89	4.93
36.0	0.41	0.28	2.06	0.73	<DL	8.53	384	41.9	86.7	9.71	34.4	5.79	1.25	4.69	0.50	2.93
37.0	0.39	0.44	1.84	0.76	<DL	7.59	511	65.6	127	13.4	46.3	7.83	1.76	6.96	0.74	4.49
38.0	0.66	0.75	1.89	0.88	<DL	7.37	393	37.5	78.3	8.84	31.8	5.34	1.17	4.55	0.53	3.20
39.0	0.47	0.30	1.53	0.52	<DL	7.68	413	56.0	137	15.4	59.9	10.7	2.62	9.89	1.15	6.52
40.0	0.29	0.35	0.73	0.30	<DL	1.30	404	14.3	29.9	3.38	12.3	2.10	0.66	2.13	0.27	1.69
41.0	0.29	0.46	1.34	0.54	<DL	7.13	460	39.8	86.4	10.0	36.6	6.45	1.58	5.98	0.68	4.15
42.0	0.22	0.39	1.31	0.58	<DL	12.2	340	43.5	91.3	10.5	38.9	6.93	1.59	6.03	0.71	4.12
43.0	0.54	0.32	1.96	0.77	<DL	8.59	359	44.0	96.4	11.1	41.3	7.38	1.78	7.16	0.83	5.10
44.0	0.51	0.21	2.82	0.82	<DL	8.96	409	55.8	119	13.5	47.8	8.30	1.84	6.96	0.80	4.50
45.0	0.43	0.13	2.91	0.78	<DL	8.91	373	50.9	107	12.2	42.9	7.57	1.62	6.65	0.74	4.37
46.0	0.42	0.22	2.36	0.66	<DL	8.25	346	49.4	107	12.1	44.1	7.78	1.74	6.98	0.81	4.89
47.0	0.44	0.18	2.61	0.71	<DL	7.65	501	56.3	121	13.5	46.8	7.94	1.66	6.50	0.70	3.99
48.0	0.32	0.13	1.51	0.50	<DL	3.88	445	40.8	85.5	9.61	34.4	6.03	1.33	5.51	0.65	3.96
49.0	0.40	0.36	1.67	0.59	<DL	6.12	335	48.5	105	11.6	40.6	6.58	1.42	5.49	0.57	3.30
50.0	0.42	0.29	1.62	0.61	<DL	6.97	282	53.3	115	12.8	45.4	8.05	1.67	6.66	0.75	4.39
51.0	0.18	0.59	1.59	0.13	<DL	1.65	148	26.3	57.9	6.07	23.0	4.02	0.99	4.50	0.54	3.06
52.0	0.60	0.11	2.21	1.15	<DL	8.12	369	45.3	96.7	10.6	36.5	6.11	1.28	4.98	0.56	3.37
53.0	0.56	0.13	2.22	0.92	<DL	8.71	319	40.5	81.2	9.57	32.3	5.56	1.09	4.30	0.49	2.94
54.0	0.61	0.29	1.73	0.86	<DL	7.38	313	33.5	66.4	7.55	26.2	4.45	0.92	3.63	0.43	2.48
55.0	0.45	0.76	2.15	0.81	<DL	6.52	398	51.3	119	12.6	45.4	8.14	1.90	6.49	0.73	4.25
56.0	0.51	0.29	2.89	1.09	<DL	7.98	1709	243	406	40.3	123	19.1	4.04	16.0	1.65	10.0
57.0	0.39	0.20	1.57	0.68	<DL	6.27	351	60.6	140	15.6	53.6	9.40	1.85	8.03	0.88	5.06
58.0	0.58	0.24	1.94	0.71	<DL	6.76	687	100	206	21.8	73.6	12.6	2.40	9.89	1.07	6.39
59.0	0.32	0.21	0.87	0.47	<DL	4.61	380	44.2	87.8	9.79	33.8	5.60	1.23	4.93	0.54	3.14
60.0	0.51	0.13	1.57	0.61	<DL	6.13	469	54.7	123	13.5	47.5	7.96	1.73	6.87	0.71	4.14
61.0	0.48	0.97	2.14	0.82	<DL	7.78	381	53.3	116	12.6	44.3	7.37	1.56	5.97	0.65	3.73
62.0	0.51	0.23	2.39	0.72	<DL	8.82	364	40.7	87.7	10.1	35.8	6.11	1.24	5.18	0.58	3.52
62.5	0.49	0.13	3.18	1.01	<DL	10.3	319	54.7	123	13.7	50.0	8.59	1.81	8.22	0.92	5.28

Sample	Ho	Er	Tm	Yb	Lu	Hf	Ta	W	Re	Os	Pt	Au	Tl	Pb	Th	U
SP10-01	ppm	ppm	ppm	ppm	ppm	ppm	ppm	ppm	ppm	ppm	ppm	ppm	ppm	ppm	ppm	ppm
33.0	0.91	2.59	0.36	2.32	0.32	3.07	1.19	48.5	0.076	0.21	<DL	0.10	0.71	28.8	22.2	8.97
34.0	2.03	6.26	0.91	6.25	0.89	8.06	1.45	33.5	0.145	0.19	<DL	0.10	0.46	28.9	18.1	21.9
35.0	0.99	2.77	0.42	2.55	0.40	3.16	1.39	77.8	0.335	1.39	<DL	1.26	1.62	27.0	18.8	6.91
36.0	0.55	1.59	0.23	1.51	0.24	2.63	1.06	49.3	0.022	0.51	<DL	0.47	1.16	26.8	16.9	3.20
37.0	0.86	2.44	0.35	2.33	0.33	2.82	1.17	48.1	0.021	0.33	<DL	0.25	1.07	37.3	28.3	4.83
38.0	0.60	1.86	0.25	1.67	0.23	2.19	1.00	20.0	0.033	0.30	<DL	0.16	0.96	28.8	13.9	14.9
39.0	1.25	3.42	0.46	2.89	0.39	2.83	1.05	35.7	0.015	0.20	<DL	0.11	0.79	21.3	18.2	2.45
40.0	0.36	1.09	0.15	1.00	0.15	2.32	1.76	483	0.009	0.22	<DL	0.12	0.12	12.1	4.4	4.17
41.0	0.80	2.31	0.32	2.08	0.30	3.02	1.12	103	0.153	0.21	<DL	0.08	0.68	20.5	14.8	2.24
42.0	0.81	2.22	0.31	2.02	0.30	2.52	1.06	70.4	0.059	0.20	<DL	0.03	0.68	23.8	15.3	2.32
43.0	1.06	3.08	0.410	2.64	0.38	3.73	1.46	37.5	0.087	1.24	<DL	1.25	1.45	24.8	16.7	2.78
44.0	0.87	2.50	0.356	2.29	0.35	3.47	1.39	25.6	0.086	0.47	<DL	0.53	1.11	33.4	25.0	3.05
45.0	0.85	2.51	0.341	2.27	0.34	3.53	1.38	25.4	0.039	0.32	<DL	0.39	1.06	32.0	22.3	3.76
46.0	0.96	2.77	0.379	2.45	0.35	3.43	1.39	25.5	0.035	0.25	<DL	0.26	0.79	26.6	22.1	3.64
47.0	0.76	2.17	0.296	2.03	0.29	3.23	1.51	32.9	0.031	0.19	<DL	0.26	1.00	29.1	29.0	10.4
48.0	0.79	2.24	0.315	2.01	0.29	4.85	2.31	137	0.081	0.14	<DL	0.24	0.63	29.3	19.9	8.62
49.0	0.63	1.85	0.248	1.68	0.23	2.98	1.27	25.1	0.100	0.17	<DL	0.16	0.80	30.8	19.7	6.88
50.0	0.87	2.45	0.320	2.11	0.31	2.57	1.06	7.61	0.042	0.14	<DL	0.15	0.91	34.4	23.7	5.60
51.0	0.62	1.80	0.221	1.32	0.19	0.70	0.37	14.9	0.251	0.24	<DL	0.12	0.23	6.36	5.03	10.0
52.0	0.66	1.97	0.293	1.96	0.29	3.33	1.51	28.7	0.035	1.35	<DL	1.10	1.68	20.1	16.9	4.22
53.0	0.56	1.60	0.236	1.60	0.24	2.34	1.20	12.6	0.052	0.47	<DL	0.51	1.30	30.2	17.1	9.58
54.0	0.51	1.42	0.204	1.34	0.19	2.03	1.14	16.4	0.028	0.32	<DL	0.32	0.95	18.6	16.1	4.44
55.0	0.86	2.45	0.327	2.14	0.29	2.57	1.21	22.3	0.007	0.23	<DL	0.25	0.82	26.8	18.5	5.19
56.0	1.84	5.14	0.654	4.23	0.57	3.42	1.43	14.0	0.099	0.26	<DL	0.24	0.70	81.8	54.1	41.3
57.0	0.93	2.55	0.330	2.15	0.29	2.30	1.34	28.1	0.031	0.20	<DL	0.20	0.94	32.2	31.6	13.4
58.0	1.19	3.47	0.473	3.09	0.43	2.66	1.43	18.1	0.030	0.17	<DL	0.15	0.63	63.8	51.7	9.36
59.0	0.61	1.73	0.239	1.53	0.22	2.41	1.42	44.2	0.042	0.13	<DL	0.16	0.59	33.5	21.6	2.73
60.0	0.82	2.24	0.314	1.99	0.29	2.88	1.81	59.8	0.039	1.34	<DL	1.18	1.51	41.5	27.0	3.01
61.0	0.71	1.97	0.275	1.88	0.27	3.10	1.59	39.7	0.014	0.50	<DL	0.50	1.17	31.7	27.8	4.48
62.0	0.71	2.10	0.305	2.00	0.29	2.56	1.35	38.5	0.009	0.40	<DL	0.36	1.01	18.4	14.2	3.67
62.5	1.06	3.05	0.408	2.67	0.40	2.80	1.35	50.7	0.012	0.27	<DL	0.25	1.00	16.4	14.7	4.41

APPENDIX D

Spectral Gamma Data

SP10-01	Total		K		U		Th	
Height	ppm	cpm	wt %	cpm	ppm	cpm	ppm	cpm
0	2735.2	11558	1.85	731.8	11.79	320.9	71.4	569.6
0.5	1778	7513.3	1.71	574.2	10.67	236.6	37.13	300.3
1	1363.3	5760.7	2.26	597.9	9.45	178.8	16.6	140
1.5	1348.7	5699.2	2.17	574.6	9.25	173.9	15.68	132.5
2	1865.6	7883.7	2.01	626.1	15.89	279.1	18.23	155.9
2.5	1730.3	7311.9	2.23	625.2	9.44	198	26.42	216.9
3	2290.3	9678.2	2.57	748.7	13.22	265	31.23	257.3
3.5	2244	9482.5	2.08	616.2	12.34	235.1	23.18	192.7
4	1872.3	7911.8	1.85	523.6	9.15	178.2	18.88	156.8
5	1625.4	6868.3	1.86	471.2	4.03	102.2	19.58	159.5
5.5	1644.8	6950.4	1.35	376.5	5.36	115.2	16.32	133.7
6.5	1521.2	6428	1.23	330	4.57	95.4	12.48	102.9
7	1483.1	6267.2	1.13	300.3	4.23	86.1	10.41	86.2
8	1405.2	5937.9	0.72	211.5	6.04	96.5	2.03	20.7
8.5	1787.8	7554.6	2.49	695.8	7.47	192.3	38.53	311.1
9.5	1674.5	7076	2.97	772.1	7.46	183.2	33.58	273.4
10	1560.9	6595.8	3.24	790.3	6.05	152.5	28.54	233.6
11	1541.8	6515.1	3.29	783.9	3.82	123.5	30.96	251.5
11.5	1422.1	6009.3	2.99	720.3	4.16	122.4	27.97	227.6
12.5	1300	5493.5	2.84	668.9	3.9	107.7	22.62	185.2
13.5	1167.3	4932.5	2.09	544.4	7.6	150.6	16.54	138.2
14.5	1493.6	6311.3	2.46	656.6	10.42	199	19.26	161.8
15	1072.6	4532.4	2.2	539.3	6.32	124.8	13.2	111.5
16.5	1592.8	6730.8	3.1	769.7	6.17	156.3	29.73	242.7
17.5	1447.4	6116.4	2.79	691.4	5.18	136.8	27.65	225.2
19	1460.4	6171.2	1.44	380.1	6.72	119.7	8.13	70.4
20	1808.9	7643.9	3.47	855.8	5.5	159.3	36.1	293
21.5	1725.5	7291.4	2.9	772.8	10.49	218.2	28.09	231.9
22.5	1511	6385	2.83	720.7	9.17	184.1	21	175.5
23.5	1583.2	6690.3	3.27	810.1	8.83	184.3	23.32	194.4
24.5	1431.1	6047.3	3.1	747.6	7	151.7	20.93	174.3
25	2258.5	9543.7	1.58	397.8	8.22	127.9	0.59	12.5
25.5	1742.2	7361.9	2.84	758.1	10.43	216.3	27.68	228.5
26	1881.5	7950.6	2.91	775.5	9.23	207.8	32.52	265.9
27	2566.4	10845	3.55	1021.3	16.84	346	43.87	360.3
27.5	1605.4	6783.9	3.75	882.8	5.39	143.1	28.52	234.2
29	1682.3	7108.8	3.75	895.1	6.93	164	27.29	225.4
30	1598.2	6753.4	3.44	833.4	5.2	147.8	32.59	265.3
30.5	1638.3	6923	3.02	786.6	7.13	183.8	36.42	295.5
31	1635.3	6910.4	0.87	283.8	10.51	161	0.35	10.4
32	1668.9	7052.1	0.52	231.9	12.08	183.4	0	7.8
32.5	1378.9	5826.8	0.48	191.2	8.85	134.9	0.17	7.3
33	1476.9	6241	0.71	235.4	8.75	134.5	0.59	11
33.5	2031.2	8583.2	2.42	746.4	16.02	304.8	30.04	249.3
34	2851.4	12049.2	2.61	905.9	25.34	457.4	35.87	300.5
34.5	1696.6	7169.2	3.11	788.1	8.45	186.5	27.49	226.5
35	1572.8	6646.3	2.58	679.4	8.82	185.2	24.41	201.5

SP10-01	Total		K		U		Th	
Height	ppm	cpm	wt %	cpm	ppm	cpm	ppm	cpm
36	1447.7	6117.6	2.47	646.1	6.34	156.5	28.99	235.7
37	1489.9	6295.8	2.85	719.9	6.44	157.6	28.51	232.8
37.5	2264.2	9567.8	2.04	711.9	13.63	305.8	49.31	398.1
39	1290.5	5453.5	2.62	646.6	6.22	139.1	20.92	172.7
40	1008.1	4259.7	2.42	577.6	6.3	122.2	11.81	101.1
41	1254.5	5301	3.06	708.8	4.94	115.5	18.41	153.3
42	1199.9	5070.4	3.15	715.6	3.83	100	18.97	157.3
42.5	1003	4238.5	0.25	100	4.57	70.8	0.66	8.3
43	1170.2	4945	0.38	146.6	6.47	99.3	0.44	7.8
43.5	1305.8	5518	0.4	150.1	6.34	98	0.76	10.4
44.5	1419.9	6000	0.33	151.5	7.67	118.8	1.17	14.1
45	1612.2	6812.5	0.46	203.7	10.48	158.8	0	5.2
45.5	1494.4	6314.7	0.37	166.2	8.3	127.7	0.85	12
46	1409.4	5955.7	0.59	179.3	5.79	89.9	0.77	10.5
47	1728.1	7302.3	1.05	282.4	7.15	110.1	0.14	7.2
47.5	2134	9017.8	1.28	349.3	9.21	141.4	0.06	8.3
48.5	1980.8	8370.4	2.83	765.6	11.83	233.8	25.8	214.6
49.5	1539.1	6503.6	2.8	714.3	7.43	169.2	26.78	219.7
50	1397.3	5904.6	1.8	546	10.94	212.6	22.66	187.4
51.5	1500.2	6339.2	2.54	674.3	7.92	178.3	27.91	228.3
52.5	1951	8244.2	2.47	733.7	10.95	247.3	39.79	322.9
53.5	1486.3	6280.8	2.31	637.7	9.95	200.5	23.76	196.5
54.5	1582.5	6687.3	2.66	697.4	5.96	161.5	34.34	277.8
55	1388.1	5865.6	2.53	651.4	7.2	160.7	24.46	200.8
56.5	2667.1	11270.6	2.7	891.3	16.78	363.8	54.08	438.5
57.5	1779	7517.6	2.58	716.6	7.28	192.6	40.06	323.2
58.5	2097.4	8862.9	2.33	749.5	10.22	265.4	54.8	439.8
59.5	1606.5	6788.4	2.44	672.2	7.64	185.7	33.86	274.6
60	1581.3	6682	2.48	662	6.44	164.9	32.56	263.8
61.5	1396.6	5901.5	2.47	619.4	4.54	125	26.76	217.2
62.5	1357.6	5736.9	3.03	720.4	4.28	119.7	25.66	209.7

SP10-03	Total		K		U		Th	
Height	ppm	cpm	wt %	cpm	ppm	cpm	ppm	cpm
0	1006.4	4252.8	0.58	154	2.79	49.6	3.35	29
0.5	1276.6	5394.7	2.2	570.6	9.26	168	12.52	107.8
1	981.1	4145.9	2.83	627.9	2.91	76.3	14.21	118.8
2	988.8	4178.5	2.59	595.5	4.11	94.6	14.52	121.4
2.5	885.4	3741.5	2.35	528	2.83	71.1	12.54	104.7
3	968	4090.5	2.81	623.1	2.96	75.5	13.45	112.9
3.5	1116.8	4719.4	2.93	676.4	4.83	109.9	16.48	137.9
4.5	1103.8	4664.2	3.21	701.1	2.99	77.6	14.04	118.3
5	959.9	4056.4	2.47	558.7	2.81	75	14.63	121.3
5.5	963	4069.2	2.3	533.4	3.78	87.1	13.47	112.4
6	1000	4225.7	2.3	540.8	5.03	103	11.95	101.2
6.5	799.8	3379.7	1.67	405.2	4.61	90.1	9.09	77.2
7	692.5	2926.4	1.45	344.6	3.23	67.9	8.59	72.1
7.5	805.5	3403.8	1.57	387	4.78	92.3	9.02	76.6
8	914.6	3864.7	1.88	451.3	4.86	96.3	10.15	86.1
8.5	774.8	3274	1.82	412.1	2.36	58.4	10.16	84.7
9	796.6	3366	1.69	395.4	2.5	63.5	11.77	97.1
9.5	778.8	3291.1	1.72	396.4	2.64	63	10.4	86.5
10	797.5	3370.2	1.62	384.3	3.87	77.5	8.42	71.4
10.5	819.3	3462.3	1.55	369.2	2.83	66.7	11	90.9
11	918.8	3882.7	2.01	459.9	2.76	68.1	11.9	98.9
11.5	874.8	3696.6	1.78	418.8	2.99	71.5	11.99	99.3
12	1064.2	4497	2.48	579.3	5.06	105.3	12.71	107.5
12.5	1031	4356.7	2.64	612.8	4.14	98.8	16.42	136.4
13	982.4	4151.4	2.5	575.1	3.62	88.1	15.03	124.9
13.5	982.6	4152.3	2.52	576.1	3.71	87.8	14.18	118.4
14	957.1	4044.4	2.52	571.2	3.61	83.7	12.88	108.1
14.5	977.5	4130.8	2.6	579.6	2.56	70.2	14.03	116.7
15	1026.9	4339.5	2.77	624.3	3.42	84.6	14.59	121.9
15.5	920.4	3889.2	2.4	546.7	3.03	78	14.56	120.7
16	890.1	3761.5	2.46	548.5	2.6	68.8	13.11	109.3
16.5	963.9	4073.3	2.63	596.4	4.05	89.6	12.38	104.7
17	896.9	3790.2	2.45	553.8	3.14	77.7	13.48	112.4
17.5	854.2	3609.4	2.43	543.2	3.02	72.6	11.79	99.1
18	835.3	3529.8	2.08	486.6	4.54	91.6	10.03	85.4
18.5	799.5	3378.4	2.09	475	3.23	72.3	10.32	87
19	876.8	3704.9	2.07	466.8	2.5	63	11.24	93.8
19.5	922.9	3899.7	2.69	607.5	3.98	89.2	12.68	107.1
20	861.8	3641.7	2.38	537.7	3.35	77.6	11.84	99.5
20.5	922.7	3899	2.75	609.9	3.61	80.5	11.02	94.1
21	937.7	3962.3	2.59	585.7	3.5	83.7	13.66	114.3
21.5	934.1	3947.1	2.62	594.5	4.02	90.1	12.85	108.4
22	922.3	3897.5	2.66	598.4	3.02	78.2	14.51	120.9
22.5	970.5	4101	2.73	612.5	3.21	81.2	14.55	121.4
23	910.7	3848.2	2.64	589	3.07	76	13.04	109.4
23.5	921.5	3893.9	2.63	583.6	3.4	76.9	10.94	93
24	912.8	3857	2.31	525.5	3.25	77.2	12.46	104.2

SP10-03	Total		K		U		Th	
Height	ppm	cpm	wt %	cpm	ppm	cpm	ppm	cpm
24.5	892.7	3772.5	2.17	497.7	2.76	72.7	14.07	116.3
25	849	3587.7	2.08	482.4	3.75	82.7	11.61	97.4
25.5	905.2	3825.3	2.07	491.5	4.17	91.8	13.03	108.7
26	988.8	4178.2	2.31	542.3	4.53	98.7	13.58	113.7
26.5	1066.4	4506.3	2.5	577.5	4.43	96.5	13.04	109.8
27	959.3	4053.6	2.12	493.8	4.13	88	11.39	95.9
27.5	830	3507.1	1.89	428.8	2.72	63.5	9.91	83.1
28	832.8	3519.4	1.94	439	3.08	66.6	8.7	73.9
28.5	822.9	3477.4	1.91	431.8	2.53	61.4	10.34	86.4
29	864.1	3651.6	1.83	417.7	2.23	58.4	11.17	92.5
29.5	764.6	3230.9	1.68	379.2	1.93	50.8	9.75	80.9
30	892.3	3770.6	0.36	103.1	2.76	43.9	0.83	8.8
30.5	879	3714.4	1	233.2	2.48	46.3	3.76	32.9
31	865.6	3657.8	3.09	656.2	2.83	63.6	8.17	72
31.5	785.4	3318.8	2.88	611.9	2.33	56.4	8.49	73.8
32	835.4	3530.2	2.98	634.1	2.44	58.9	8.83	76.7
32.5	654.2	2764.4	0.26	79	2.57	40.1	0.41	5.2
33	579.7	2449.6	0.18	55.3	1.66	27	0.86	8
33.5	692.5	2926.4	0.23	65.6	1.65	26.5	0.63	6.4
34	678	2865.1	0.2	61.9	1.84	29.3	0.64	6.5
34.5	598.1	2527.3	0.15	47.2	1.45	23.7	0.83	7.6
35	866.6	3662.2	0.34	101	2.82	45.4	1.16	11.4

SP10-04	Total		K		U		Th	
Height	ppm	cpm	wt %	cpm	ppm	cpm	ppm	cpm
0	1266.6	5352.2	0.67	296.7	12.52	207.8	8.93	78.3
0.5	1261	5328.7	2.62	646.1	9.28	166.3	11.21	98.4
1	1095.4	4628.7	2.53	606.7	6.79	131.1	12.46	106.7
1.5	1090.3	4607.1	2.71	623.4	5.01	105.5	12.99	110.2
2	1009.3	4265.2	2.81	624.1	3.51	81.6	12.27	103.9
2.5	960.7	4059.6	2.61	590	3.53	83.8	13.48	113
3	953.8	4030.4	2.44	551.8	3.44	80.4	12.53	105.1
3.5	951.2	4019.5	2.41	547.7	3.4	80.7	13.09	109.4
4	925	3908.9	2.21	499.9	2.79	69.7	12.34	102.8
4.5	930.1	3930.4	2.04	463.4	2.39	63.6	12.44	103
5	1076.1	4547.4	2.34	522.6	2.2	63.1	13.38	110.9
5.5	973.2	4112.3	1.8	406.9	2.04	54.2	10.51	87.2
6.5	958.5	4050.4	1.1	263.7	1.88	46.9	8.58	70.6
7	946.6	3999.8	0.99	232.3	1.65	39.4	6.56	54.3
7.5	1051.1	4441.7	0.9	228.1	2.43	53.7	7.99	65.8
8	1002.7	4237.1	0.84	207.2	2.27	46.9	5.76	48.1
8.5	1012.8	4280	0.68	173	2.38	46	4.6	38.8
9	909.5	3843.1	0.49	131.2	2.52	43.9	2.6	22.8
9.5	896.1	3786.8	0.48	121.4	2.13	35.9	1.52	14.1
10	902.4	3813.5	0.49	125.9	2.45	40.8	1.55	14.5
10.5	962.3	4066.5	0.51	131.2	2.77	44.4	0.92	9.8
11	934	3946.8	0.44	115.6	2.44	40	1.23	11.9
11.5	1091.2	4610.9	3.2	711.8	4.07	93.6	13.82	117.2
12	1124.8	4753.2	3.49	770.5	4.3	98.1	14.07	119.9
12.5	1254.6	5301.6	3.04	719	7.67	147.1	13.48	116.2
13	1055.9	4462.1	3.26	723.7	5.53	107.6	9.69	85.8
13.5	1105	4669.5	3.41	749.3	5.3	103.4	9.14	81.6
14	1049.7	4435.7	3.35	736.8	5.29	103.2	9.18	81.8
14.5	1139	4812.9	3.05	699.5	6.47	124.4	11.08	96.7
15	1270.5	5368.7	2.77	666	7.85	147.9	12.66	109.3
15.5	1048.2	4429.3	2.01	449.3	2.42	58.9	9.77	82.1
16.5	1089.3	4602.9	3.1	693.5	2.93	84.2	17.88	148.1
17	1029.1	4348.5	2.96	663.2	3.93	91.1	13.81	116.6
17.5	1021.8	4317.9	3.11	686.4	3.32	82.2	13.89	117.1
18	1073.9	4538	3.11	693.9	3.51	88.2	15.49	129.7
18.5	1048.6	4431	2.9	654.2	4.07	94.2	14.37	120.9
19	998	4217.3	1.07	254.8	2.01	46.9	7.58	62.7
19.5	986.2	4167.3	0.98	233.3	2.17	45.6	5.76	48.3
20	1000.7	4228.5	0.76	188.7	2.62	48.5	3.98	34.2
20.5	1037.5	4384	0.61	161.2	3.18	54.2	2.68	24
21	1164.1	4919.1	2.03	457.8	3.18	68.3	8.66	73.9
21.5	1048.8	4431.8	3.21	705.1	3.35	82.3	13.61	115.1
22	1205.9	5095.8	3.33	755	5.13	113.6	15.76	133.2
22.5	1137.6	4807.3	3.12	716.6	5.23	115.9	16.34	137.4
23	1074.2	4539.3	3.07	687.5	3.13	86.1	17.4	144.4
23.5	1217.9	5146.4	3.08	718.5	6.91	136	13.62	116.9
24.5	1117.1	4720.5	2.83	655.6	5.59	115.5	13.62	115.7

SP10-04	Total		K		U		Th	
Height	ppm	cpm	wt %	cpm	ppm	cpm	ppm	cpm
25	1090.9	4609.7	3.13	702.6	5.47	109.2	11.02	95.9
25.5	1172.5	4954.8	2.85	674.2	7.55	141.4	11.68	101.6
26.5	1017.7	4300.3	2.97	660.6	3.3	83.3	14.7	123.2
27.5	1002.7	4237.3	2.9	649.1	3.42	84.8	14.6	122.3
28	1049.1	4433.3	2.72	618.6	3.87	91.1	14.42	120.8
28.5	927.9	3921.2	2.64	595	3.68	85	12.92	108.7
29	935.9	3955	2.67	600.6	4.14	88.6	11.1	94.8
29.5	889.2	3757.6	2.51	564.7	3.77	82.7	11.1	94.3
30	906.5	3830.6	2.7	604.9	2.9	77.5	15.09	125.4
30.5	928	3921.6	2.34	532.4	3.32	78.8	12.76	106.7
31	1053.2	4450.7	2.28	545.2	3.87	97.7	18.23	149.6
32	1000.4	4227.3	2.62	594	3.55	85.4	14.12	118
32.5	966.5	4084.1	2.49	561.1	3.12	76.9	13.23	110.6
33	898.4	3796.3	2.09	479.6	3.58	78.3	10.67	89.9
33.5	963.4	4071.1	2.25	509.1	3.24	74.8	11.35	95.4
34.5	1042.7	4406.4	2.21	500.2	3.14	72.5	10.98	92.3
35	1002.9	4238.2	2.17	495.1	2.93	72.9	12.85	106.8
35.5	1000.5	4227.7	1.89	434.7	3.25	71.5	9.88	83.1
36	1059.3	4476.2	1.63	395.7	3.93	83.2	10.85	90.5
37	950.8	4017.9	1.42	339.2	3.02	66.2	9.34	77.8
37.5	995.7	4207.5	1.57	384.4	3.99	83.8	10.75	89.7
38	1000.8	4229	1.71	400.7	2.68	66.3	11.74	97
38.5	1116.7	4718.8	3.25	726.2	3.79	94.8	16.59	138.8
39.5	1108.8	4685.6	3.16	704.8	3.19	87.1	17.31	143.9
40	1075.9	4546.4	3	667.8	3.55	85.9	14.04	118.2
41	993.1	4196.7	2.92	644.4	3.15	77.8	13.02	109.8
41.5	1066.5	4506.6	2.89	657.3	4.13	97.3	15.49	129.6
42.5	1050.3	4438.3	2.9	648	3.97	89.6	12.79	108.4
43.5	1009.5	4265.8	2.5	569.5	4.33	91.8	11.47	97.4
44.5	925.6	3911.2	2.22	499.4	2.83	68.8	11.56	96.7
45.5	1003.6	4241	2.01	477.5	3.42	83.8	14.77	121.8
46	1043.3	4408.5	2.97	670.8	4.33	98.2	14.38	121.2
47	1051	4441.4	3.08	695.8	5.26	108.6	12.43	106.7
47.5	982.1	4150.2	2.6	595.2	4.75	98.7	11.65	99.3
48.5	975.5	4122.3	2.87	646.9	4.63	98.1	12.05	102.9
49	940.2	3973	2.71	599.2	2.87	72.9	12.9	108.3
50	1026.4	4337.1	2.33	566.3	6.55	127.4	12.6	107.2
51	1358.9	5742.1	2.16	578.7	10.1	185.2	14.89	126.7
52	1195.3	5050.9	2.05	513.5	5.93	122.3	15.06	125.6
53	2116.4	8943.4	2.76	755.1	15.6	269.5	14.97	131.7
54	1516.6	6408.6	1.95	523.8	9.5	170.9	12.4	106.4
55	1429.7	6041.5	1.42	416.9	9.06	163.6	12.45	105.5
55.5	1755.1	7416.6	1.29	343.2	6.77	115.2	5.54	49.9
56	1985.9	8391.7	1.45	377	7.42	122.7	4.2	40.1

SP10-05	Total		K		U		Th	
Height	ppm	cpm	wt %	cpm	ppm	cpm	ppm	cpm
0	1246.1	5265.7	0	218.8	35.76	558.8	10.18	97.5
0.5	1332.3	5629.8	0	234.1	35.56	553.2	8.72	86.1
1	1345.3	5684.8	0	242.9	28.4	448.9	10.4	96.1
1.5	1208.8	5108.1	0.25	326.4	22.5	358.3	9.06	84
2	1093.7	4621.5	3	678.1	4.07	96	15.2	127.6
2.5	1189.3	5025.5	3.15	717.5	5.25	112.7	14.5	123
3	1091.8	4613.5	2.93	663.8	4.12	96.7	15.21	127.5
3.5	1118.8	4727.6	2.86	665.7	5.7	118.8	14.35	121.5
4	1092.9	4618.1	2.68	634.6	6.65	129.8	12.81	109.6
4.5	1127.4	4764	2.7	636.7	6.78	129.4	11.53	99.7
5	1028.5	4346.2	2.25	539.7	5.46	111.3	12.84	108.3
5.5	1039	4390.3	2.41	571	5.75	114.9	12.38	105.2
6	1018.6	4304.4	2.29	537.4	4.45	96.8	13.21	110.7
6.5	1143.1	4830.5	2.11	523.7	5.7	119.3	15.26	127.1
7	1165.1	4923.6	2.29	554.4	5.77	118.2	13.96	117.3
7.5	1167.5	4933.4	2.21	531.6	4.09	99.5	17.48	143.8
8	1084.1	4581.1	1.92	473.4	4.72	103.2	14.74	122.1
8.5	1089.2	4602.7	1.91	456.1	3.56	83.7	13.74	113.6
9	1106.6	4676.1	2.08	485	3.42	80.6	13.12	109
9.5	1087.2	4594.1	1.91	455.6	4.45	91.4	10.81	91.1
10	1234.5	5216.4	1.9	440	4.35	82.8	7.2	62.7
10.5	1685	7120.5	1.93	492.5	9.12	151.9	5.6	52.9
11	1601.7	6768.4	1.42	377.6	7.06	123	7.21	63.3
11.5	1512.8	6392.8	2	495.5	7.62	132.5	7.27	65.3
12	1347.3	5693.4	3.28	780.2	8.7	165.3	14.62	126.2
13	1080.3	4565	2.91	668.3	5.48	113.3	13.2	112.5
13.5	1064.9	4499.8	3.11	695.1	4.9	101.8	11.72	101
14	1022.1	4319	2.86	648.5	4.83	101.8	12.44	106.1
14.5	1079.9	4563.2	2.5	596.5	5.84	120.2	14.29	120.4
15	1092.6	4617	2.64	615.5	5.27	110.8	13.75	116.1
15.5	1102.2	4657.8	2.64	610.8	4.14	97.7	15.84	131.9
16	1032.5	4363.2	2.63	602.6	4.98	101.8	11.45	97.9
16.5	1063.8	4495.4	2.29	550.7	6.03	118.7	12.23	103.9
17	1032.5	4363.2	2.38	571.4	5.62	117.4	14.68	123
17.5	1068.9	4516.8	2.78	630.8	4.41	97	13.27	112.1
18	1016	4293.1	2.49	579.1	4.23	97.2	15.05	125.4
18.5	1062.3	4489.2	2.8	633.9	4.09	93.4	13.84	116.5
19	937.1	3959.8	2.84	625.9	2.51	69.9	14.02	117.1
19.5	958	4048.3	3.16	680.9	2.94	70.5	10.8	92.8
20	992.2	4192.6	3.21	700.4	3.07	77	13.09	110.9
20.5	1020.2	4311.2	2.95	652.3	3.38	80.9	12.86	108.8
21	1207.1	5100.8	2.8	660.9	5.83	124.2	16.19	135.8
21.5	1121.3	4738.2	2.84	660.5	5.84	119.1	13.46	114.6
22	1241.5	5246.1	3.29	768.1	6.61	139.1	17.4	146.8
22.5	787.1	3325.9	0.22	84.7	3.69	56.8	0.34	5.2
23	831.1	3512	0.33	106.7	3.58	57	1.22	12.3
23.5	1070.7	4524.4	0.51	154.9	4.93	76.5	0.63	8.7

SP10-05	Total		K		U		Th	
Height	ppm	cpm	wt %	cpm	ppm	cpm	ppm	cpm
24	1011.7	4275.3	0.5	145.2	4.35	67.2	0.35	6.2
Cover								
35	709.6	2998.7	0.13	49.7	1.91	30.6	0.83	7.8
35.5	691.1	2920.4	0.14	48.7	1.87	29.4	0.42	4.6
36	735.3	3107	0.2	61	2.03	31.1	0.05	2
36.5	786.2	3322.3	0.15	55.4	2.23	34.7	0.37	4.5
37	797	3367.7	0.09	45.8	2.55	38.9	0.11	2.4
37.5	783.9	3312.5	0.18	58	2.17	33.2	0.06	2
38	1100.9	4651.9	0.24	89.7	4	61	0.08	3.3
38.5	1069.6	4519.7	0.24	79.5	2.94	45.2	0.18	3.5
39	1218.2	5147.6	0.29	102.4	4.19	64.5	0.37	5.9
39.5	1245.8	5264.5	3.89	868.1	7.77	140.3	8.53	79.2
40	1167.2	4932.4	4.02	862.8	5.21	100.9	8.09	74.6
40.5	1108.4	4683.9	1.37	368.1	8.13	133.6	4.35	41.4
41	967.1	4086.8	1.29	337.6	6.78	112.3	4	37.8
41.5	856.8	3620.6	1.04	280.6	6.16	101.4	3.41	32.3
42	865.3	3656.7	1.07	291	6.55	107.8	3.64	34.4
42.5	920.6	3890.4	1.42	350.9	5.77	96.9	3.79	35.9
43	896.9	3790	1.39	341	5.33	90.1	3.73	35.1
43.5	910.1	3845.9	1.31	319.1	5.12	85.5	3.06	29.5
44	950.1	4014.9	1.46	358	5.46	93.9	4.64	42.4
44.5	918.9	3882.9	1.54	379	5.71	98.8	5.14	46.6
45	908.7	3840.1	1.31	333.2	5.52	96.7	5.74	50.7
45.5	905.6	3826.9	1.34	326.7	4.58	81.2	5.01	44.6
46	927.2	3918.3	1.48	353.7	4.54	80.7	5.01	44.9
46.5	918.8	3882.6	1.58	372.7	4.65	82.4	4.91	44.3
47	979	4136.8	1.71	400.3	4.57	83.3	5.9	52.3
47.5	899.2	3799.6	1.44	351.5	4.81	86.1	5.67	50.1
48	886.6	3746.3	1.62	380.6	5.26	87.1	2.58	26.5
48.5	885.2	3740.6	1.52	366.6	5.19	90.3	4.8	43.7
49	1186.8	5015	1.9	458.9	6.79	115.4	5	46.9
49.5	905.6	3827	1.8	407.6	4.02	72.4	4.46	40.9
50	918	3879.3	2.08	461.7	3.73	70.3	5.4	48.7
50.5	1029.4	4349.8	3.72	797.9	4.95	94	6.81	63.8
51	923.9	3904.2	1.79	407.9	4.64	79.3	3.26	31.9
51.5	1049.8	4436.3	1.98	453	4.81	86	5.19	47.4
52	932.7	3941.2	1.57	377.6	4.92	87.8	5.64	50.2
52.5	969.6	4097	1.61	388.9	4.97	90.8	6.71	58.6
53	856.8	3620.8	3.04	650.5	4.17	77.7	5.1	48.6
53.5	862.2	3643.4	3.02	649.4	4.07	77.7	5.81	54.1
54	733.8	3101	2.4	529.9	4.19	78.9	5.99	54.2
54.5	1266.7	5352.9	3.46	790.7	7.5	141.3	11.46	101.1
55	1527.8	6455.9	3.75	884.1	9.92	184.6	14.73	128.7
55.5	1169.1	4940.4	3.63	801.9	6.09	116	9.29	83.7
56	1456.2	6153.3	4.94	1073	7.08	137.1	11.45	103.9
56.5	876.3	3703	2.84	619.1	4.3	82	6.43	58.7
57	886.9	3747.9	2.53	579.4	5.76	106.1	7.69	68.7

SP10-05	Total		K		U		Th	
Height	ppm	cpm	wt %	cpm	ppm	cpm	ppm	cpm
57.5	1012.8	4280	2.88	650.6	5.43	105.5	9.63	84.4
58	904.5	3822.1	2.51	568.8	5.26	98.3	7.6	67.7
58.5	1180.6	4988.9	2.82	667.5	8.57	150	8.13	74.3
59	1207.4	5102	2.83	683	10.02	171.1	7.77	72.3
59.5	933.2	3943.4	2.75	616.2	5.81	103.8	5.95	55.6
60	786.8	3324.8	2.31	512.3	4.24	78	5.23	48.1
60.5	949.3	4011.6	2.79	622.4	5.07	96.1	7.64	68.5
61	834.5	3526.3	2.82	604.1	3.78	71.5	5.07	47.7
61.5	779.8	3295.4	2.66	577.2	3.63	72.2	6.71	60.1
62	797.2	3368.6	3.07	645.3	2.83	59.4	6.03	55.2
62.5	956.5	4041.9	3.32	719	4.58	89.1	7.44	67.7
63	769.5	3251.7	2.45	531.5	2.93	63	7.6	66.2
63.5	681	2877.5	2.52	532.8	2.47	51.8	5.33	48.4
64	680.9	2877.4	2.15	472.9	3.93	70.8	4.04	38.3
64.5	1152.7	4870.9	3.35	749.5	5.65	113.4	11.6	101
65	1134.8	4795.2	3.09	706.7	6.66	126.3	10.63	93.4
65.5	1221.2	5160.3	3.2	744.3	7.84	145.5	11.21	98.8
66	897.9	3794.4	2.94	640.9	4.08	81.7	7.9	70.3
66.5	871.6	3683.2	3.04	660.9	4.67	87.5	6.21	57.6
67	998.7	4220	3.36	729.1	4.68	91.3	7.85	71.1
67.5	890.1	3761.3	2.89	637.8	5.51	98.8	5.59	52.8
68	1454.8	6147.5	3.4	811.3	11.42	193.9	8.15	77.3
72	1218.9	5150.5	3.48	784.7	6.81	129.6	10.82	95.8
72.5	1126.5	4760.1	2.66	645	8.82	157.3	10.1	89.5
73	1098.6	4642.4	2.66	626.9	6.95	129.4	10.31	90.2
73.5	987.5	4172.9	2.78	626.7	5.11	100.3	9.51	83.1
74	996.2	4209.8	2.73	607.1	3.46	80.4	12.19	103.1
74.5	1273.9	5383.2	3.14	718.5	3.91	103.2	20	165.3
75	1394.3	5891.8	3.39	775.2	4.43	113	20.78	172.3
75.5	1223.2	5168.8	2.9	657.6	4.82	102.9	13.01	110.6
76	1177.6	4976.3	2.86	652.4	4.83	104	13.59	115.1
76.5	1268.3	5359.3	3.07	697.8	4.76	106.6	15.29	128.7
77	1331.1	5624.7	2.92	682.7	5.87	123.8	15.59	131.4
77.5	1240.5	5241.9	3.21	708.9	3.97	89.9	12.7	108.3
78	1221.5	5161.7	2.78	631.8	4.26	95.8	13.8	116.3
78.5	1225.2	5177.2	2.45	573.7	4.92	104.6	13.5	113.6
79	1178.9	4981.8	2.27	536.6	4.95	103.5	12.81	107.8
79.5	1110.4	4692.4	2.7	619.7	5.22	106.3	11.82	101.1
80.5	1247.8	5272.8	3.64	809.5	4.48	105.6	16.45	138.9
81	1220.8	5158.7	3.58	796.9	4.84	108.5	15.19	129.1
81.5	1102.5	4658.9	3.01	690.6	5.33	113.4	14.31	121.3
82	1199	5066.5	3.25	749.6	7.08	137	12.66	109.9
83.5	1274.3	5384.8	3.88	871	6.55	133.1	14.33	123.9
84	1361.9	5755.2	3.83	861.3	5.75	125.5	16.62	141.3
84.5	1302.9	5505.8	3.33	790.2	8	159.4	17.01	144.6
85	1223.7	5170.8	3.43	776.3	5.62	119.7	14.99	127.7
85.5	1193.8	5044.6	3.59	807.7	5.66	120.2	14.81	126.6

SP10-05	Total		K		U		Th	
Height	ppm	cpm	wt %	cpm	ppm	cpm	ppm	cpm
86	1307.5	5525	3.75	842.1	6.41	129.5	13.65	118.3
86.5	971.2	4104.1	2.72	623	6.05	113.3	8.99	79.5
87	863.5	3648.9	2.48	566.4	5.64	103.6	7.39	66.2
87.5	1251.6	5288.7	3.5	804	8.83	156.3	8.86	81.6
88	1207.1	5100.9	0.86	356.9	15.59	248.9	6.01	57.6

SP10-06	Total		K		U		Th	
Height	ppm	cpm	wt %	cpm	ppm	cpm	ppm	cpm
0	1149.1	4855.8	3.13	716.6	6.08	122.7	13.23	113.5
0.5	1259.1	5320.8	3.41	770.6	5.55	117.3	14.34	122.5
1	1694.4	7160.2	3.11	820.2	16.29	274.6	11.97	109.3
1.5	1400.9	5919.9	2.91	730.5	11.28	200	12.73	112
2	1336.3	5647	2.8	704.4	11.2	196.2	11.52	102.3
2.5	1388.4	5867	2.97	742.2	11.14	198.6	13.06	114.7
3	1520.3	6424.4	3.25	794.1	10.88	195.6	13.3	117
3.5	1351.5	5711	3.12	733.6	7.04	141.3	15.36	130.8
4	1118.2	4725.1	2.86	660	5.64	115.7	13.23	112.7
4.5	1075.5	4544.8	2.78	629	4.16	93.2	13.28	112.1
5	1185.7	5010.6	2.73	638.4	5.39	115.5	15.18	127.5
5.5	1092.9	4618.1	2.52	580.6	4.14	94.2	14.14	118.3
6	1285.6	5432.5	2.63	639.4	7.25	142.4	14.69	124.6
6.5	1269.1	5363	2.56	594.7	5.18	106.8	12.54	106.4
7	1228.8	5192.5	3.38	772.4	5.9	125.6	15.92	135
7.5	1121.3	4738.5	3.21	716.1	4.45	98.8	13.59	115.6
8	1030.8	4355.7	2.42	579.6	6.04	120.7	13.04	110.5
8.5	1145.4	4840	2.62	636.5	7.83	147.4	12.68	109.2
9	1296.2	5477.4	2.85	696.8	8.76	164.7	14.18	121.9
9.5	1549.5	6547.6	2.95	756.4	13.08	226.3	12.24	109.3
10	1467.3	6200.6	2.8	721.1	12.42	217.3	12.88	113.7
10.5	1010.6	4270.6	2.81	640.7	4.22	97.6	15.02	125.8
11	1051.1	4441.4	2.77	624.2	3.33	84.4	15.19	126.6
11.5	1068	4512.9	2.8	630.5	3.45	85.6	14.85	124.1
12	1058	4471	2.77	618.8	3.33	80.9	13.42	112.7
12.5	1138.4	4810.5	2.68	622.7	5.81	114.9	11.71	100.6
13	973.3	4113.1	2.26	509.6	3.32	73.9	10.33	87.5
13.5	1187.3	5017.1	1.99	492.5	6.37	120.7	10.91	93.1
14	957.9	4047.7	1.47	345.7	2.13	56.5	11.25	92.4
14.5	921.6	3894.3	1.39	330.5	2.71	61.3	9.27	77
15	994.8	4203.8	1.43	337.5	2.6	60.5	9.69	80.3
15.5	885.8	3743.2	2.21	513.1	4.72	93.6	9.59	82.4
16	826	3490.3	2.12	485.7	3.27	76	11.88	99.3
16.5	894.8	3781	2.35	530.5	3.44	77.1	10.93	92.5
17	928.4	3923	2.55	560.6	2.14	61.7	12.93	107.7
17.5	827.6	3497.3	0.44	111.4	1.93	32.8	1.48	13.6
18	795.4	3361.3	0.37	104.4	2.2	38.3	2.28	19.8
18.5	815.2	3444.8	0.39	109.1	2.65	43.3	1.4	13.2
19	794.8	3358.5	0.4	104.7	2.11	34.9	1.16	11.1
19.5	849.6	3590	0.36	100.3	2.47	40	1.02	10.1
20	596.2	2519.4	0.34	83.9	1.61	25.7	0.39	4.6
20.5	851.7	3599.1	0.39	103.7	2.49	39	0.38	5.2
21	890.9	3764.5	0.28	95.4	3.71	57.2	0.33	5.2
21.5	925.4	3910.4	0.35	102.4	2.8	44.6	0.9	9.4
22	936	3955.4	2.58	586	4.16	90.3	11.92	101.1
22.5	674.5	2850	1.68	381.2	2.2	54.2	9.31	77.7
23	913.3	3859.4	2.62	583.6	3.1	75.4	12.49	105

SP10-06	Total		K		U		Th	
Height	**ppm**	**cpm**	**wt %**	**cpm**	**ppm**	**cpm**	**ppm**	**cpm**
23.5	964	4073.7	3.03	663.3	2.74	72.9	13.65	114.7
24	922.8	3899.6	2.67	598.8	3.51	82.1	12.74	107.3
24.5	966.5	4084	2.54	585.6	4.59	98.4	12.78	107.9
25	680.1	2873.9	1.9	426.8	3.29	66.1	6.86	59.5
25.5	909	3841.3	0.44	117	2.76	43.2	0.44	5.9
26	803.3	3394.6	0.27	86.9	3	47.3	0.76	8.2
26.5	773.1	3267.1	0.33	96.3	2.69	42.6	0.69	7.6
27	785	3317.3	0.3	93.2	2.98	46.7	0.61	7.1
27.5	749.3	3166.5	0.17	77.1	3.74	58.3	0.74	8.2
28	762.4	3221.8	0.26	89.1	3.2	50.9	1.08	10.8
28.5	771.8	3261.5	0.2	73.4	2.9	45.7	0.79	8.2
29	792.9	3350.6	0.28	94	3.23	51.5	1.17	11.6
29.5	818.9	3460.6	0.25	89.3	3.43	53.6	0.73	8.2
30	815.7	3447.1	0.19	84.9	4.12	64.6	0.97	10.3
30.5	758.8	3206.5	0.29	91.9	2.95	46.7	0.82	8.7
31	773.8	3269.9	0.24	84.2	3.36	52	0.44	5.8
31.5	779.9	3295.6	0.32	94.5	2.68	42.5	0.77	8.2
32	745.9	3152.1	0.32	98.2	3.14	49.3	0.73	8.1
32.5	765.3	3233.9	0.2	79.7	3.52	54.7	0.62	7.2
33	768.1	3245.6	0.21	84.2	3.9	59.9	0.33	5.2
33.5	865.7	3658.4	2.15	478.7	3.02	65.7	8.48	72.6
34	855	3612.9	2.58	567.4	2.68	66.7	11.34	95.7
34.5	963.5	4071.4	2.62	597.7	4.78	98.6	11.31	96.7
35	917.4	3876.7	2.78	614	3.47	78	10.85	92.7
35.5	1057.7	4469.6	3.42	741.9	3.28	80.2	12.88	109.8
36	1049.6	4435.3	3.3	716.3	2.88	75.3	13.57	114.8
36.5	1087.2	4594.3	3.03	684.9	4.38	100.5	15.05	126.6
37	1136.7	4803.3	3.36	751	4.85	106.2	14.13	120.4
37.5	1029	4348.2	3.04	675.5	3.8	87.9	13.15	111.4
38	1095.4	4629	2.96	666	3.84	92.1	15.01	125.9
38.5	1032.3	4362	2.91	652.2	3.57	86.9	14.49	121.5
39	969.2	4095.4	3.27	695.4	2.92	66.7	8.92	78.3
39.5	847.9	3583.2	2.87	609.5	2.38	56.9	8.43	73.3
40	820.6	3467.5	2.76	581.2	2.18	50.6	6.78	60.1
40.5	831.1	3511.8	2.39	529.7	3.27	71.1	9.14	78.4
41	891.7	3768.1	2.62	565.6	2.73	61.8	8.42	72.9
41.5	868.9	3671.8	2.44	523.2	1.53	46.2	9.79	82.6
42	845.6	3573.2	2.28	503	3.04	65.4	8.13	70.1
42.5	830.9	3511.1	2.47	527.8	2.23	52.1	7.45	64.7
43	846.6	3577.4	2.18	485.7	2.75	64.1	9.77	82.6

SP10-09	Total		K		U		Th	
Height	ppm	cpm	wt %	cpm	ppm	cpm	ppm	cpm
0	878.8	3713.6	2.74	610.3	3.93	84.8	10.76	92.2
0.5	932.6	3941	2.53	578.4	4.19	92.4	12.78	107.7
1	876.3	3703.1	2.49	553.8	2.57	68	12.91	107.7
1.5	848.2	3584.1	2.38	534.1	2.7	69.6	12.8	106.7
2	846.7	3577.7	2.43	541	3.01	71.3	11.24	94.8
2.5	851.5	3598.3	2.29	520.5	3.8	81	10.21	86.9
3	831.2	3512.3	2	460.7	3.66	77.7	9.8	82.9
3.5	931.8	3937.6	2.14	482.7	2.85	67.4	10.73	90.1
4	981.4	4146.9	0.48	131.7	2.63	46	2.79	24.3
4.5	820.9	3468.9	1.02	235.5	2.17	42.7	4.28	36.9
5	656	2772.2	0.31	78.2	1.31	22.6	1.14	10.3
5.5	846.8	3578.4	1	226.4	2.25	40.6	2.57	23.5
6	968.1	4091.1	3.52	743.1	2.53	63.1	9.9	86.2
6.5	1067.5	4511.1	3.21	714.4	3.96	93.2	14.43	121.9
7	1048	4428.6	3.1	682.7	3.66	84.4	12.39	105.5
7.5	968.3	4091.6	2.91	635.5	3.26	74.7	10.71	91.8
8	898.1	3795.1	2.68	595.3	3.83	82.2	10.3	88.3
8.5	914.9	3866	3.01	648.4	3.59	74.6	7.98	70.8
9	754.4	3187.7	2.02	453.1	3.26	68	7.95	68.2
9.5	866	3659.6	2.53	560.9	2.49	66.6	12.76	106.6
10	890.1	3761.1	2.6	574.1	2.81	69.2	11.61	97.9
10.5	876.4	3703.4	2.67	587.2	3.14	72	10.41	88.9
11	834.9	3528	2.48	541.1	2.36	59.9	10.41	88
11.5	721.4	3048.5	1.6	388.3	4.25	85.2	9.41	79.4
12.5	872.3	3686.2	2.56	560.9	3.18	69.1	8.73	75.4
13	737.2	3115.1	0.26	83.2	2.85	44.3	0.39	5.2
13.5	579.6	2449.1	0.29	83.2	2.24	35.6	0.66	7
14	785.4	3318.8	0.21	82.2	3.85	58.4	0	2
14.5	812.1	3431.6	0.22	84.5	3.44	54.4	1.1	11
15	630.7	2665	0.19	75.1	3.32	51.1	0.3	4.6
15.5	761.9	3219.7	0.18	76.4	3.41	54.2	1.17	11.5
16	934	3946.7	0.27	106	4.93	75.1	0.09	4
16.5	849.6	3590.4	0.24	87.8	3.67	56.9	0.57	7
17	802.7	3392	0.21	91.5	4.37	68.5	1.03	11
17.5	896.5	3788.2	0.19	89.9	4.68	72.3	0.66	8.2
18.5	952.3	4024	2.4	555.9	4.29	94.5	13.21	110.8
19	908.3	3838.1	2.41	550.3	4.1	88.6	11.62	98.3
19.5	852.4	3601.9	2.31	536.6	5.13	99.9	9.54	82.4
20	996.4	4210.7	2.58	581.2	3.53	81.7	12.43	104.7
20.5	895.2	3782.9	2.15	480.6	2.35	61.5	11.54	96.2
21	892.6	3771.8	2.65	591.7	3.65	81.8	11.46	97.3
21.5	940.5	3974.2	2.81	621.2	2.61	71.4	14.02	117.2
22	997.4	4214.9	3.09	674.9	3.28	77.7	11.86	101.2
22.5	809.2	3419.4	1.42	357.4	2.94	75.8	14.84	120.8
23	959.5	4054.6	2.45	569.5	3.94	92.8	15.02	124.9
23.5	951.1	4019	2.45	568	4.38	96.9	13.7	114.8
24	936.5	3957.2	2.52	576.8	4.34	93.6	12.3	104

SP10-09	Total		K		U		Th	
Height	ppm	cpm	wt %	cpm	ppm	cpm	ppm	cpm
24.5	880.5	3720.8	2.11	481.3	3.01	71.7	11.66	97.4
25	826	3490.5	1.82	431	3.15	75.9	13.05	107.7
25.5	845.7	3573.7	2.17	487.9	2.94	68.8	10.69	89.9
26	895	3782.2	2.11	498.9	4.63	96.7	11.93	100.4
26.5	876.2	3702.6	2.2	499.2	3.16	73.1	11.2	94.1
27	1136.2	4801.1	2.65	618.6	4.82	107.7	15.69	131.1
27.5	916.5	3872.9	0.16	64.4	2.75	43.2	0.69	7.3
28.5	923.6	3902.7	0.14	69.5	3.55	55.5	0.79	8.5
29	853.6	3607.2	0.16	60.9	2.55	39.8	0.5	5.6
29.5	776.2	3280.1	0.15	56.4	2.32	36.7	0.69	7
30	863	3646.6	0.08	55.4	3.52	54.2	0.45	5.7
30.5	906.3	3829.6	0.16	62.3	2.75	42.7	0.43	5.2
31	794.7	3358.1	0.18	64.5	2.62	41	0.56	6.2
31.5	689.9	2915.2	0.15	52.3	1.83	29.4	0.75	7.2
32	785.7	3320.1	0.11	49.3	2.25	36.2	1.03	9.6
32.5	783.9	3312.5	0.18	63	2.41	37.9	0.55	6
33	817.7	3455.4	0.16	61	2.51	40.1	0.95	9.1
33.5	752.5	3179.9	0.2	64.5	2.44	37.2	0.03	2
34	813.7	3438.6	0.14	66.1	3.53	54.3	0.36	5
34.5	791.5	3344.6	0.09	54.3	3.13	48.5	0.59	6.5
35	791.4	3344.2	0.12	60.6	3.2	49.6	0.53	6.2
36	825.7	3489.2	0.16	66.4	3.03	47	0.46	5.7
36.5	702.7	2969.3	0.13	50.8	2.21	34.9	0.63	6.5
37	667.9	2822.1	0.08	46.4	2.67	41.1	0.34	4.3
37.5	711.2	3005.5	0.11	50.2	2.42	37.6	0.45	5.1
38	1090.5	4608.2	2.46	595.8	6.53	129.9	13.97	118.2
38.5	1208.6	5107	3.16	722.7	4.93	111.8	16.51	138.6
39	1227	5185.1	3.43	771.1	4.91	110.5	15.76	133.3
39.5	1083.2	4577.1	2.86	651.8	5.55	109.7	10.9	94.4
40	1022.3	4319.9	2.68	610.9	4.72	99.3	12.11	103.1
40.5	1011.2	4273.1	2.8	628.1	4.48	93.2	10.72	92.3
41	951.6	4021.1	2.56	577.1	4.27	88.8	10.31	88.4
41.5	1089.4	4603.5	2.94	655.6	4.04	89.9	12.37	105.3
42	1075.2	4543.4	2.68	598.9	3.42	80.3	12.42	104.8
42.5	962.7	4068.2	2.03	480.2	4.23	91.1	12.23	102.4
43	862.4	3644.2	1.7	396.7	3.36	70.7	8.81	74.4
43.5	872.9	3688.4	1.77	400.3	2.53	57.9	8.59	72.4
44	970.2	4099.6	2.52	570.2	3.83	85.1	11.88	100.4
44.5	977.2	4129.5	2.47	561.6	4.37	90.3	10.4	89
45	1059.4	4476.9	2.54	567.2	2.88	72.4	12.69	106.3
45.5	972.3	4108.5	2.01	453.5	2.57	62.6	10.5	87.8
46	1018.4	4303.4	1.62	388	3.77	78.7	9.75	81.8
46.5	942.5	3982.8	1.33	323.9	3.32	69.7	8.92	74.5
47	1017.9	4301.5	0.78	228.7	5.74	96.1	4.12	37.1
47.5	1102.1	4657.2	2.76	650.1	4.7	112	18.74	155.1
48	1138.2	4809.9	2.55	617.1	5.63	124.4	18.04	149.8
48.5	846.6	3577.6	3.56	733.9	2.66	54.9	4.67	45.5

SP10-09	Total		K		U		Th	
Height	ppm	cpm	wt %	cpm	ppm	cpm	ppm	cpm
49	835.4	3530	3.57	729.8	2.25	47.7	4.16	41.3
49.5	768.9	3249.2	2.99	619	1.69	42.6	6.31	56.6
50	722.9	3054.6	0.22	64.7	2.02	31.4	0.26	3.6
50.5	823.6	3480.1	0.65	156.4	1.81	34.3	3.03	26.1
51	883.4	3732.9	0.49	124.6	2.12	36.9	2.08	18.5
51.5	773.6	3268.9	0.09	48.7	2.7	41.6	0.38	4.7
52	802.9	3392.9	0.11	48	2.29	35.6	0.46	5.1
52.5	1067.2	4509.5	0.24	83.8	3.27	50.9	0.54	6.5
53	1026.8	4339.1	0.23	83.3	3.37	51.9	0.34	5
54	981.9	4149.1	0.16	69	3.37	52	0.41	5.5
54.5	1188.8	5023.4	0.18	92.7	5.16	79.1	0.41	6.5
55	1143.9	4833.7	0.15	92.9	5.73	87	0.08	4.1
55.5	1117.7	4723.1	0.18	90.8	5.13	77.7	0	2.6
56	1018.9	4305.7	0.18	82.3	4.43	67.1	0	2
56.5	882.1	3727.3	0.2	77	3.49	53.5	0.2	3.9
57	842.7	3561.1	0.12	59.6	2.96	47	1.08	10.3